

**ABSTRACTS FROM THE
22ND NORTH AMERICAN ISSX MEETING**

**July 15 - 19, 2018
Montréal, Canada**



22nd North American ISSX Meeting
July 15 - 19, 2018
 Montréal, Canada
 Contents

Sunday, July 15, 2018

Short Course 1: Model Systems and Methods for Assessing Uptake and Efflux of Small Molecules	3
Abstracts: SC1.1 - S1.4	
Short Course 2: Enzyme Induction and Regulatory Guidance	4
Abstracts: S2.1 - SC2.4	
Short Course 3: <i>In silico</i> Modeling of <i>in vitro</i> Metabolism, Transport, and Toxicity Data	5
Abstracts: SC3.1 - SC3.6	
Short Course 4: Immunotoxicology	8
Abstracts: SC4.1 - SC4.4	
Keynote Lecture: Immuno Oncology State-of-the-Field and How it Helps Understand the Immune System and Mechanisms for Drug Efficacy and Toxicity	9
Abstract: S1	

Monday, July 16, 2018

Plenary Lecture 1: Intracellular Drug Concentrations: Theory, Practice, and Promise	9
Abstract: S2	
Parallel Symposium 1: Transporters as Determinants of Target Organ Toxicities	10
Abstracts: S3 - S6	
Parallel Symposium 2: Development of Guidelines to Implement Pharmacogenomics-based Clinical Decision	11
Abstracts: S7 - S10	
Selected New Investigator Abstract Presentations	43, 46, 47, 95, 97, 107, 114, 129
Abstracts: P5, P12, P13, P110, P114, P135, P150, and P180	
Pre-doctoral/Graduate Poster Awards Finalist Poster Presentations	34
Abstracts: A1 - A6	
Poster Presentation Session 1	42
Abstracts: P1 - P62	

Tuesday, July 17, 2018

Plenary Lecture 2: Novel Synthetic and Computational Approaches to the Discovery of Drugs Targeting ...	12
Abstract: S11	
Parallel Symposium 3: The Impact of Pregnancy on Xenobiotic Disposition	12
Abstracts: S12 - S15	
Parallel Symposium 4: Genomic Approaches for Revealing Mechanisms of Cancer Drug Efficacy and Toxicity	14, 110, 111
Abstracts: S16 - S18, P142, and P143	
Postdoctoral Poster Awards Finalist Poster Presentations	37
Abstracts: A7 - A12	
Poster Presentation Session 2	72
Abstracts: P63 - P117	

Wednesday, July 18, 2018

Plenary Lecture 3: Site-specific Deuterium Labeling: A Viable Approach in Drug Discovery and Development	15
Abstract: S19	

Parallel Symposium 5: Antibody Drug Conjugates (ADCs) Disposition and Modeling	15
Abstracts: S20 - S23	
Parallel Symposium 6: Microphysiological Systems/Organs on a Chip	16
Abstracts: S24 - S27	
Plenary Session: The Role of the Microbiome in Drug Metabolism and How this Influences Drug Toxicity	18
Abstracts: S28 - S30	
Parallel Symposium 7: Revisiting the Regulatory Guidelines (EMA, FDA and PMDA) for Induction Studies and Regulatory DMPK	19
Abstracts: S31 - S35	
Parallel Symposium 8: Endogenous Biomarkers for Drug Metabolism and Transporter Activity. Predicting Drug Interactions in Clinical Development and for Application in Precision Medicine	20
Abstracts: S36 - S39	
Pre-doctoral/Graduate and Postdoctoral Poster Awards Finalist Poster Presentations	34
Abstracts: A1 - A12	
Poster Presentation Session 3	98
Abstracts: P118 - P187	
Thursday, July 19, 2018	
Plenary Lecture 4: Opportunities and Challenges in the Discovery of Novel Agents for the Treatment of Malaria	21
Abstract: S40	
Parallel Symposium 9: Addressing ADME Challenges with High Performance Analytical Capabilities	22
Abstracts: S41 – S44	
Parallel Symposium 10: Designed Covalent Inhibitors, ADME Aspects of Design, Characterization and Risk Assessment	23
Abstracts: 45 - S48	
Poster Details	25
Finalists for the Pre-doctoral/Graduate Poster Awards Competition (Monday, July 16 - Wednesday, July 18, 2018)	34
Abstracts: A1 - A6	
Finalists for the Postdoctoral Poster Awards Competition (Monday, July 16 - Wednesday, July 18, 2018)	37
Abstracts: A7 - A12	
Poster Presentations (Monday, July 16 - Wednesday, July 18, 2018)	42
Abstracts: P1 - P187	
Author Index	133
Keyword Index	139
Notes Pages	140

SC1.1 - NOVEL *IN VITRO* MODELS TO STUDY TRANSPORTERS**Yurong Lai**

Gilead Sciences

Drug transporters are involved in the uptake or efflux of drugs across barriers such as the intestine, liver, kidney and brain, and play a key role in drug ADME/Tox. Disruption of drug transporter functions leads to changes in the pharmacokinetics and, as a result, possibly to impact efficacy and toxicity profiles. Hence, regulatory agencies such as US FDA or European Medicines Agency (EMA) provide guidelines to characterize transporter drug interactions. *In vitro* transporter assays are usually carried out with either intact cells or cell fractions over expressing transporter proteins. Although an increasing number of experimental methods and models are developed to study drug-transporter interactions and the tools appear to be useful to address transporter-related questions, it still remains challenge to translate results from *in vitro* transporter models to the human situation. The method selected is based on the physicochemical features of a drug, as well as the specific question one would like to address. The short course presentation will introduce the *in vitro* tools that are commonly used for transporter characterization, and describe the pros and cons of the tools for characterizing transporter interactions.

SC1.2 - ANIMAL MODELS FOR DRUG TRANSPORTERS**Daniel Bow**

AbbVie

In addition to the use of *in vitro* tools to study drug transport, animal models can also be used to facilitate our understanding of the role uptake and efflux drug transporters play in compound disposition and elimination. These models can be used at various stages in drug discovery and development. The application, timing, and translation of data generated from multiple models will be discussed. Models that will be covered include transporter knockout animals, humanized transporter models, and the use of chemical inhibition studies. Daniel Bow is an employee of AbbVie. The design, study conduct, and financial support for this research was provided by AbbVie. AbbVie participated in the interpretation of data, review, and approval of the publication.

SC1.3 - PET IMAGING TO UNDERSTAND HEPATOBILIARY TRANSPORTERS**Yuichi Sugiyama**

Sugiyama Laboratory, RIKEN Innovation Center, RIKEN Research Cluster for Innovation, RIKEN

The changes in pharmacokinetics due to genetic polymorphisms and drug-drug interactions involving transporters can often have an adverse effect on the therapeutic safety and efficacy of many drugs. For drugs, the target molecule of which is inside the cells, the efflux transporter is the determinant for their pharmacological effect or adverse reactions even though it had negligible impact in the plasma concentrations. Because of difficulty in quantitative evaluation of the subsequent efflux process (both basolateral and apical side), the transporters playing key roles in the efflux process remains unclear in humans. Development of probe substrates applicable to the PET imaging will elucidate the quantitative relationship between the transport activities and drug response. Labeled PET probes are being developed for specific transporters. Here in this presentation, I will show you our recent progress in the use of the analysis of plasma clearance of drugs and PET imaging to evaluate the transporter function *in vivo* including PET probes for hepatic uptake transporters (OATP1B1, OATP1B3) and biliary excretion transporters (MRP2, BCRP) both in experimental animals and in human.

Acknowledgments I would like to thank Drs. Y.Watanabe, K.Maeda and H.Kusuhara for their great contribution to these PET studies.

References:

1. Takashima T et al., PET imaging-based evaluation of hepatobiliary transport in humans with (15R)-11C-TIC-Me.J Nucl Med, 53: 741-8 (2012)
2. Takashima T et al., Evaluation of Breast Cancer Resistance Protein Function in Hepatobiliary and Renal Excretion Using PET with 11C-SC-62807.Nucl Me Jd, 54: 267-76 (2013)
3. Kaneko K et al. A clinical quantitative evaluation of hepatobiliary transport of [11C]Dehydropravastatin in humans using positron emission tomography. Drug Metab Dispos in press Drug Metab Dispos. 46 719-728 (2018)

SC1.4 - PROBE DRUGS FOR CLINICAL TRANSPORTER DDI EVALUATION**Maciej J. Zamek-Gliszczyński,**

GlaxoSmithKline

This presentation will highlight the state-of-the-art in transporter clinical probes based on upcoming 2018 ITC whitepapers (Clin Pharmacol Ther 104, November 2018). Special emphasis will be placed on emerging transporters of clinical relevance and transporters with recent advances in their clinical evaluation approaches. For example, OCT1 was shown recently to be the rate-determining step in the clearance of several drugs in humans (e.g., sumatriptan, ondansetron, tropisetron, fenoterol, etc.), and thereby a mechanism of pharmacogenetic variability and DDIs. OCT1 modulation impacts metformin response, but not pharmacokinetics, and therefore OCT1 inhibition is a driver for the conduct of a metformin DDI study, but metformin is not a preferred clinical OCT1 probe drug. Similarly, P-gp inhibition can trigger a digoxin safety study, but digoxin is neither a specific nor sensitive P-gp probe. Dabigatran etexilate has been proposed as a specific intestinal P-gp probe, and is particularly sensitive when administered as a microdose. Clinical investigation of BCRP DDIs has been controversial in part due to a lack of consensus on clinical probes and inhibitors, which has now been reached. Oral sulfasalazine (immediate release) is the best available clinical probe for intestinal BCRP, oral rosuvastatin for both intestinal and hepatic BCRP, and intravenous rosuvastatin for hepatic BCRP. Ultimately, selection of clinical probes depends on co-medication relevance and the specific questions being addressed (e.g. direct characterization of a DDI with a likely co-medication or description of a DDI via a specific mechanism for extrapolation to other drugs). For example, pitavastatin is not commonly used but is the most selective clinical OATP1B1 probe. In contrast, atorvastatin and rosuvastatin are the most commonly used statins but are less selective for OATP1B1/3 and these DDIs must at a minimum consider CYP3A4 and BCRP/OATP2B1 modulation, respectively. Finally, emerging transporter biomarkers, and their future potential use in drug development will be discussed.

SC2.1 - INTRODUCTION TO THE FUNDAMENTALS OF INDUCTION**Michael Sinz**

Bristol-Myers Squibb

Induction of drug metabolizing enzymes can result in clinically significant adverse effects due to changes in the pharmacokinetics, efficacy and safety profile of drugs. Nuclear hormone receptors such as the pregnane X receptor (PXR) and constitutive androstane receptor play a significant role in the induction of major cytochrome P450 (CYP) enzymes, such as CYP3A4 and CYP2B6, respectively. The presentation will describe the basic mechanisms of induction with an emphasis on PXR and CAR-mediated induction of enzymes, the tools that are used to predict human drug-drug interactions, and the correlation between *in vitro* assays and *in vivo* induction related drug-drug interactions. Moreover, a brief description of the draft FDA guidance associated with predicting enzyme induction will be described.

SC2.2 - PHOSPHORYLATED NUCLEAR RECEPTORS AS DRUG-TARGETS**Masahiko Negishi**

NIEHS, NIH

Phenobarbital (PB) is the classic drug that induces hepatic drug metabolism, for which nuclear receptor CAR mediates this induction. Studies of the induction mechanism found that CAR is, in principle, a cell signal-regulated nuclear receptor, repressing its constitutive activity to acquire drug response capability by phosphorylation at Thr38 within the DNA binding domain (DBD). Drugs target Thr38 to regulate CAR by directly binding CAR or indirectly through cell membrane receptor signals such as insulin. This phosphorylation motif constituted by Thr38 is conserved in 42 out of 46 human nuclear receptors and their corresponding mouse counterparts. Through phosphorylation of this motif as a language tool, nuclear receptors communicate to integrate their actions, presenting "unlimited" drug targets. Nuclear receptor PXR becomes phosphorylated at Ser350 within the ligand binding domain (LBD) in response to low glucose in HepG2 cells or fasting in mouse livers. Phosphorylated PXR is unable to form a heterodimer with RXR, disabling direct DNA binding and trans-activation activities. Instead, it functions as a cell signal transducer regulating a set of biological responses different from that by none-phosphorylated PXR. Thus, drugs can be developed to target these two forms of PXR differently. This LBD motif is also conserved in CAR as well as 30 other human nuclear receptors. In addition to communications through either the motif within the DBD or LBD, these two motifs can also communicate to integrate nuclear receptors to which drugs/xenobiotics can target.

SC2.3 - TECHNICAL CONSIDERATIONS FOR EVALUATING HUMAN LIVER ENZYME INDUCTION POTENTIAL**Stephen Ferguson**

National Institute of Environmental Health Sciences (NIEHS)

The failure of animal models to predict human drug-drug interactions and liver enzyme induction led to an explosion of *in vitro* approaches to better predict the likelihood of human response to xenobiotic exposures. Primary cultures of human hepatocytes emerged as the most effective model system for evaluating the potential for liver enzyme induction, and serve a key role within the drug development process. In this presentation, an overview of critical factors important for experimental modeling of human liver enzyme induction with *in vitro* models will be provided and include: cell source selection, culture configuration (cell-matrix interactions, cell-cell interactions, sandwich cultures, and emerging 3D models), assay selections/integration, compound exposure considerations, and data analysis/integration. A series of case examples will be presented which reveal the characteristics of liver enzyme inducers with *in vitro* liver models, examples of metabolically-activated inducers, modeling of auto-induction, dual-acting inducers/inhibitors, and examples of confounding biological-response effects on liver enzyme pathways in response to cellular stress/suppression. The primary objectives are to convey the most critical factors for effectively modeling liver enzyme induction with *in vitro* models, and the importance of understanding the context of observed responses that include the relative potencies of induction, inhibition, and cellular stress.

SC2.4 - IN VITRO DATA FITTING AND INTERPRETATION**Jane Kenny**

Genentech

The International Consortium of Innovation and Quality in Pharmaceutical Development (IQ) Induction Working Group (IWG) recently highlighted several areas of regulatory recommendations that would benefit from further evaluation¹. One focus area was *in vitro* data interpretation, specifically, what constitutes a positive *in vitro* induction signal and how to assess whether this induction signal is clinically relevant. As part of that investigation there were extensive discussions on *in vitro* induction data fitting and interpretation that would benefit scientist that either process or interpret *in vitro* CYP induction studies in primary human hepatocytes. This workshop presentation will start with recommendations from the IWG on what constitutes a positive and negative *in vitro* CYP3A4 mRNA induction response. A suggested best practice for fitting *in vitro* induction data and generating EC50 and Emax values will be discussed along with guidance on how to handle unusual concentration-induction response curves (such as those that arise when solubility or cytotoxicity is limiting or when there are competing mechanisms of CYP induction and suppression). Finally, approaches to objectively define concentration dependence when *in vitro* induction signal is weak and/or variable will be discussed.

Reference:

1. Hariparsad et al., (2017). Drug Metab Dispos 45:1049-1059

SC3.1 - WHY IS MODELLING OF IN VITRO EXPERIMENTAL DATA IMPORTANT?**Iain Gardner**

Certara UK - Simcyp Division

Over the last 25 years there has been an increased use of *in vitro* data to understand the metabolism, transport, interaction potential and toxicity of drugs and other xenobiotics. A number of *in vitro-in vivo* extrapolation approaches have been described to utilise this type of *in vitro* information to parameterise physiologically based pharmacokinetic (PBPK) models (Rostami-Hodjegan, 2012) and also to try and understand the *in vivo* toxicity potential of drugs and other xenobiotics (e.g., Hamon et al., 2014). With this increased utility of *in vitro* data to predict the *in vivo* effects of xenobiotics it has become apparent that in many cases it is necessary to use mathematical modelling approaches to accurately describe the processes that are occurring in the *in vitro* systems. This is particularly apparent in the more complex *in vitro* systems that are currently being developed such as multi organ micro-physiological systems. Some of the key things to understand in the *in vitro* system are the unbound concentration of the xenobiotic that is available for passive and active cellular uptake and the unbound intracellular concentration available for metabolism, transport or to exert toxicological effects. The different experimental and computational approaches that can be used to determine these concentrations will be discussed in detail during this session. As an example of the impact of understanding the intracellular concentration, markedly different conclusions about the behaviour of the efflux transporter P-glycoprotein (P-gp) were drawn depending on whether the action of the transporter was related to the applied, nominal (extracellular) concentration of a xenobiotic or to the intracellular concentration (Tachibana et al., 2010). The Michaelis constant for the transport of quinidine by P-gp was more than 30-fold lower when calculated based on the intracellular rather than the applied, nominal concentration. This difference would lead to very different conclusions about the saturability of quinidine transport and drug interaction potential if the *in vitro* data based on either the extracellular or intracellular data was used as an input into a PBPK model.

There are also some challenges in trying to predict the interaction potential of compounds from *in vitro* data when multiple processes e.g. transport, mechanism-based inhibition and induction are occurring simultaneously. The utility of different modelling approaches to tease apart the complex interplay of these various processes will also be discussed during the session.

References:

1. Hamon J., Jennings P. and Bois F. (2014), BMC Syst-Biol., 8, 76.
2. Rostami-Hodjegan A. (2012), Clin Pharmacol. Ther, 92, 50.
3. Tachibana T., Kitamura S., Kato M., Shirasaka Y., Yamashita S. and Sugiyama, Y. (2010), Pharm. Res., 27, 442.

SC3.2 - EXPERIMENTAL APPROACHES TO UNDERSTAND INTRACELLULAR BASED DRUG BIOAVAILABILITY

Per Artursson

Uppsala University

Exposure at the site of action has been identified as one of the three most important factors for success in drug discovery and the design of chemical probes. Modern drug discovery programs have, to a great extent, shifted to intracellular targets, but methods for efficient determination of intracellular drug concentrations have been lacking. We therefore developed a methodology for predicting intracellular exposure of small-molecule drugs to understand their potency toward intracellular targets and off targets (including intracellular drug metabolizing enzymes) based on measurements of the free intracellular drug concentration. For this purpose, we introduced the concept of intracellular bioavailability (Fic), i.e., the ratio between the intracellular unbound concentration—that is available to elicit pharmacological effects inside the cell—and the extracellularly applied free concentration. We then assessed how cellular drug disposition processes affect Fic and observed how the intracellular drug exposure is influenced by cell- and tissue-dependent expression of drug-transporting proteins and metabolizing enzymes, tissue lipid content and type, intracellular drug binding proteins and subcellular distribution as exemplified by low pH organelles such as the endo-lysosomal compartment. For the latter case, the concept of lysosomal bioavailability was developed. Finally, we determined Fic in multiple cellular assays and cell types representing different targets from a number of therapeutic areas, including cancer, inflammation and dementia. We found Fic predicts drug access to intracellular targets and hence pharmacological effect. Further, Fic gives new insights on membrane permeable compounds in terms of cellular potency and intracellular target engagement compared to biochemical potency measurements alone. We conclude that Fic provides a measurement of the net impact of all cellular drug disposition processes on bioavailable drug levels inside cells. Importantly, no prior knowledge of the involved drug distribution pathways is required, allowing for high-throughput determination of drug access to intracellular targets in complex cell systems (including primary human cells). Knowledge of the amount of drug that is locally available to bind intracellular targets provides a powerful new tool for compound selection in early drug discovery.

SC3.3 - *IN SILICO* APPROACHES TO MODELING TRANSPORTER DATA

Manthena Varma

Pfizer Inc.

A number of *in vitro* cell-based systems are used to characterize transport function and further estimate transport kinetics of drugs and metabolites. Generally, there are two types of experiments that are routinely conducted to characterize passive diffusion and transporter-mediated processes. These include permeability assessments across cell monolayers in the apical to basolateral (A-B) and/or basolateral to apical (B-A) directions, and cell or vesicle accumulation measurements. Kinetic studies may also be conducted at multiple drug concentrations to determine *in vitro* parameters such as the Km (Michaelis constant) or KI (inhibition constant). Several approaches can be used to estimate transporter kinetics from these *in vitro* experiments. Here, the importance of modelling transport data to ensure that accurate kinetic parameters (CLint, Jmax, Km and Ki) are obtained for subsequent use in *in vitro-in vivo* extrapolation will be discussed. Basic and mechanistic dynamic fitting approaches to characterize uptake and efflux kinetics will be presented with case examples.

SC3.4 - MECHANISTIC MODELING OF *IN VITRO* ASSAYS TO IMPROVE *IN VITRO/ IN VIVO* EXTRAPOLATION

Grazyna Fraczkwicz, Viera Lukacova, Jim Mullin, and Michael Bolger

Simulations Plus, Inc.

In vitro assays using cell monolayers (Caco-2, MDCK, etc.), sandwich or suspended hepatocyte cultures are routinely run to assess passive and active transport and/or metabolism of drug molecules. These are important to aid in the evaluation of critical mechanisms affecting drug absorption, clearance and metabolism pathways, and the extraction of *in vitro* parameters from these systems inform physiologically-based pharmacokinetic (PBPK) models to predict *in vivo* absorption, hepatobiliary transport, drug-drug interactions, and the relative importance between active transport and

metabolism in the liver tissue. To that end, a fully mechanistic simulation of drug transport in cell monolayers (Caco-2, MDCK), sandwich and suspended hepatocytes has been developed in MembranePlus™ (Simulations Plus, Inc.) that allows for the simultaneous determination of kinetic parameters (K_m and V_{max}) for metabolic enzymes and active influx/efflux transporters. The sandwich hepatocyte model also includes the simulation of active and passive transport into the bile canaliculus. All models account for additional processes affecting the drug behavior in the *in vitro* assay, such as passive transcellular permeation, diffusion in the unstirred boundary layer, protein binding in both media and cytosol, lysosomal trapping, and drug partitioning into lipid bilayers. Case studies will be presented to demonstrate the model's capabilities, including active uptake and biliary excretion, the interplay between active uptake and metabolism of small drug molecules, *in vitro/in vivo* extrapolation of metabolism, and the evaluation of the effect of lysosomal trapping on drug absorption. Collectively, the examples will show that mechanistic simulations of *in vitro* assays can be valuable to aid in the extraction of critical parameters from *in vitro* assays for further use in PBPK models.

SC3.5 - SIMULTANEOUS MODELING OF METABOLISM, COMPETITIVE AND MECHANISM BASED INHIBITION

Howard Burt

Certara UK - Simcyp Division

Mechanism-based enzyme inhibition (MBI), whereby an inhibitor causes a time-dependent and irreversible loss of enzyme activity, often leads to strong drug-drug interactions (DDIs). The currently established methods for the prediction DDIs from MBI rely on the experimental determination of k_{inact} (the maximum inactivation rate constant) and K_i (the irreversible inhibition constant) for an inhibitor. However, both static and PBPK models have a tendency to over-predict DDI magnitude.

The conventional 'two-step' *in vitro* assay involves pre-incubation of the inhibitor with enzyme, prior to a final incubation with a specific probe substrate. The analysis of such experiments typically assumes that the inhibitor is not significantly metabolised during the preincubation and that competitive inhibition is not significant during the final incubation, despite these often being inherent properties of the enzyme-inhibitor interaction.

In order to address this, two methods were developed for the determination of k_{inact} and K_i . The mechanistic experimental protocol (MEP) involves the simultaneous analysis of substrate depletion and competitive inhibition assays alongside the two-step assay, whereas progress curve approach (PCA) aims to simultaneously model a simple experiment whereby all components (enzyme, inhibitor and substrate) are co-incubated.

The PCA method has shown potential for providing an improved mechanistic insight when determining MBI parameters; however a clear improvement in DDI predictability is yet to be shown and the method has not been widely adopted (Burt *et al.* 2012). Conversely, a protocol based on the use of plasma suspended hepatocytes, has shown improved predictability (Mao *et al.* 2011). More recently, investigators have challenged the assumption of a conventional MBI reaction scheme for all such inhibitors (Nagar *et al.* 2014, Korzekwa *et al.* 2014) and a 'numerical approach' to the analysis of conventional experiments has shown a potential improvement in prediction accuracy (Yadav *et al.* 2018).

This talk will provide an appraisal of these methods with respect to both *in vitro* data analysis and DDI prediction and will discuss the potential advantage of a combination of modelling approaches, whereby both inhibitor depletion is accounted for and the conventional MBI reaction scheme is not assumed in all cases.

References:

1. Burt HJ, Pertinez H, Säll C, Collins C, Hyland R, Houston JB, Galetin A. Progress curve mechanistic modeling approach for assessing time-dependent inhibition of CYP3A4. *Drug Metab Dispos.* 2012; 40(9): 1658-67
2. Mao J, Mohutsky MA, Harrelson JP, Wrighton SA, Hall SD. Prediction of CYP3A-mediated drug-drug interactions using human hepatocytes suspended in human plasma. *Drug Metab Dispos.* 2011 Apr; 39(4): 591-602.
3. Nagar S, Jones JP, Korzekwa K. A numerical method for analysis of *in vitro* time-dependent inhibition data. Part 1. Theoretical considerations. *Drug Metab Dispos.* 2014; 42(9): 1575-86.
4. Korzekwa K, Tweedie D, Argikar UA, Whitcher-Johnstone A, Bell L, Bickford S, Nagar S. A numerical method for analysis of *in vitro* time-dependent inhibition data. Part 2. Application to experimental data. *Drug Metab Dispos.* 2014; 42(9): 1587-95.
5. Yadav J, Korzekwa K, Nagar S. Improved Predictions of Drug-Drug Interactions Mediated by Time-Dependent Inhibition of CYP3A. *Mol Pharm.* 2018.

SC3.6 - VIRTUAL CELL MODELS TO PREDICT BINDING AND DISTRIBUTION OF CHEMICALS IN *IN VITRO* TOXICITY ASSAYS

Ciarán Fisher

Certara UK - Simcyp Division

Toxicity endpoints quantified in *in vitro* assays are routinely related to the nominal treatment concentration. However, this nominal treatment concentration is not necessarily equal to the operational concentration at the target site mediating the observed effect. Unless mediated by targets on the cell surface, the intracellular, or even intraorganelle, concentration will

be the relevant effect concentration driving toxicity. This concentration can also be considered to be the more appropriate in extrapolating *in vitro* endpoints to *in vivo*. The processes that determine the *in vitro* distribution of compounds, and so the intracellular exposure, are dependent on the assay format, cell type, and physicochemical properties of the test compound. Together these will dictate, for instance, the partitioning of compound into the air (headspace) above the culture media, binding to media components, binding to the culture vessel, and partitioning into the cultured cells. Additionally, the *in vitro* kinetics will be impacted upon by metabolic activity of the cultured cells, the activity of transport proteins expressed in the cell membrane, cell turnover and cytotoxicity. To experimentally quantify each of these processes routinely would be resource intensive and does not represent a pragmatic approach to high-throughput safety assessment. As a result, a number of *in silico* modelling tools have been developed, and published, in recent years to predict the intracellular concentration accounting for the processes outlined above (Armitage, Wania and Arnot, 2014; Comenges et al., 2016; Fischer et al., 2017). Here we will discuss some of the models developed, their assumptions, applicability, and performance. Finally, we will look at how such models may be used in conjunction with physiologically based pharmacokinetic models as part of an integrated approach to testing and assessment (IATA). This synergistic use of *in vitro* and *in silico* tools will be a key component of toxicity testing in the 21st century.

References:

1. Armitage, J. M., Wania, F. and Arnot, J. a (2014) 'Application of mass balance models and the chemical activity concept to facilitate the use of *in vitro* toxicity data for risk assessment.', *Environmental science & technology*, 48(16), pp. 9770-9. doi: 10.1021/es501955g.
2. Comenges, J. M. Z. et al. (2016) 'Theoretical and mathematical foundation of the Virtual Cell Based Assay - A review', *Toxicology in Vitro*. Elsevier B.V. doi: 10.1016/j.tiv.2016.07.013.
3. Fischer, F. C. et al. (2017) 'Modeling exposure in the Tox21 *in vitro* bioassays', *Chemical Research in Toxicology*, p. acs.chemrestox.7b00023. doi: 10.1021/acs.chemrestox.7b00023.

SC4.1 - DEVELOPMENTAL IMMUNOTOXICITY

Mark Collinge

Pfizer Inc.

There are significant differences with respect to immune system development when comparisons are made across species. For instance, humans and NHP are generally born with functional immune systems, although antigen driven maturation and immune memory continues beyond birth. Conversely, in rodents, significant post-partum immune system development is required. These species differences can complicate the assessment of the effects of xenobiotics on the developing immune system, which is generally considered to be more susceptible to insult (chemical/pharmaceutical) than that of the adult.

This presentation will address the following: (i) An overview of the immune system in the context of system development, with an emphasis on key species differences with respect timing of key developmental landmarks; (ii) Factors to consider, including species differences in critical immune developmental windows, and approaches for the evaluation of developmental immunotoxicity (DIT) testing; (iii) Case studies outlining approaches to DIT testing will be included.

SC4.2 - ON-TARGET RELATED IMMUNOTOXICITY

Dong Lee

Revolution Medicines

The adaptive and innate immune system is a double-edged sword. When molecular and cellular functions proceed properly, the immune system can provide defense to infectious pathogens and surveillance to potentially arising tumor cells. However, too much of a good thing can lead to autoimmune diseases such as arthritis and lupus, and too little can lead to opportunistic infections and possibly cancer. These adverse events stemming from the dysfunction and imbalance of the immune system underlie the basis of immunotoxicity. In this presentation, I will focus on the safety risks and implications resulting from the immunotoxicity of on-target modulation for established and experimental drug targets.

SC4.3 - IMMUNOLOGICAL COMPONENTS OF LIVER INJURY

Cynthia Ju

University of Texas Health Science Center at Houston

The liver is continuously exposed to bacterial products, environmental toxins, and food antigens through portal and systemic circulations. To effectively and quickly defend against infectious pathogens and toxic agents, the liver is equipped with abundant number and types of innate immune cells, such as macrophages, natural killer (NK), NK T cells, and gd T cells. On the contrary, the liver develops immune tolerance to the innocuous antigens derived from the gastrointestinal tract, such as dietary antigens. This challenge is met by the adaptive immune responses in the liver

favoring immune tolerance. In this presentation, I will discuss the hepatic innate and adaptive immune systems in the context of acute and chronic liver injuries. Lastly, I will focus on the immune mechanisms of drug-induced liver injury by discussing what we have learned from animal models.

SC4.4 - NONCLINICAL IMMUNOTOXICITY TESTING ASSESSMENT

Jennifer Wheeler

Bristol-Myers Squibb

The recommendations outlined in the ICH S6, S8, and S9 guidances regarding immunotoxicity testing for pharmaceuticals include non-functional and functional assessments of critical components of the immune system. Common assessments of immune parameters included on standard toxicology studies include weights of immune organs (e.g. spleen and lymph nodes), hematology, and microscopic evaluation of target organs. Other immune endpoints that should be considered for evaluation on toxicology studies include immunophenotyping of immune cell populations, cytokine profiling, antibody and cellular responses to specific antigens, and anti-drug antibody formation. However, in cases of unanticipated immunomodulation by a drug, follow up studies, *in vitro* and/or *in vivo*, should be considered that include specialized or mechanism-based assessments (e.g. *ex vivo* recall responses, cytokine release assays, and NK cell/T cell activation assays). It is also critical that for compounds in which the goal is immunomodulation, for example immuno-oncology products, intended immunomodulation or pharmacology of the compound is demonstrated. These studies require a different approach than what is expected for assessing unintended immunosuppression or enhancement, and should focus on assessing immunomodulation on a case-by-case basis, tailored for each program. In all approaches, customized immunotoxicology testing is key to providing sound assessments of pharmaceuticals on the immune system.

S1 - IMMUNO ONCOLOGY STATE-OF-THE-FIELD AND HOW IT HELPS UNDERSTAND THE IMMUNE SYSTEM AND MECHANISMS FOR DRUG EFFICACY AND TOXICITY

Diane Hollenbaugh

AbbVie

The evasion of an immune response is a hallmark of cancer. The immune system is highly regulated through a complex interplay of control mechanisms to respond to threats and protect normal tissues. These same mechanisms are reflected in the diverse and complex mechanisms of immunoevasion in cancer. They range from intrinsic tumor-cell resistance through systemic immune suppression, with many variations. For the benefit of patients, the field of immuno-oncology seeks to harness the power of the immune system to treat cancer. In doing so, however, we are changing that balance of the up and down of immune cells, often leading to unforeseen toxicities. Here, I will review the mechanisms of immune suppression, known and emerging, the successes and failures in the diverse therapeutic approaches, and directions and needs in the field.

S2 - INTRACELLULAR DRUG CONCENTRATIONS: THEORY, PRACTICE, AND PROMISE

Dennis Smith

Retired from Pfizer, now advisor to a number of organisations

The distribution of a drug in the body can be considered from the viewpoint of various barriers to the movement of free drug into the aqueous compartments of the body. From the circulation extravascular fluid is readily accessible except where the vasculature has become tight and only transmembrane access occurs such as the CNS. The same transmembrane access applies to intracellular water. It can be assumed that at a true steady state, even for a compound of restricted lipoidal permeability, unbound concentrations in any aqueous compartment (blood, extracellular, intracellular) would be identical, unless that compartment had a clearance / uptake process. In contrast total drug concentrations would reflect unbound concentrations corrected for binding to constituents of each compartment. Unionised drug is the prevalent form that crosses membranes so correction needs to be made for ionisation influenced by different pH values in the compartments. For most high lipoidal permeability drugs, with rapid membrane transit this uniform concentration still applies even when steady state is not achieved. However many compounds have restricted lipoidal permeability and are (or) are subjected to transport / clearance processes causing dissociation between intracellular, CNS and extracellular unbound concentrations. Additional concerns arise where the drug target resides in a site of limited vascularity. Poor perfusion and the absence or presence of fluid flow may also be a factor in unbound circulation concentrations versus "water intimate to target" concentration dissociation. This dissociation raises many uncertainties about a drug's efficacy and safety profile: are the absence or presence of the effects of primary and secondary pharmacology influenced by unbound drug concentration gradients? The need to understand unbound concentrations in every compartment seems obvious, but the technology and understandings are an area of concern. Many measurements rely on total drug, which is often highly misleading. Correction if made is usually made by measuring tissue binding, but this is usually limited by the homogeneity of the organ or compartment. Some techniques such as microdialysis can sample extracellular

concentrations and give some direct information. Displacement of an appropriate ligand or measurement of a biomarker (target engagement) can give information on intracellular unbound drug concentration by back-extrapolation from measures of compound affinity performed *in vitro*. Techniques (NMR etc.) which could provide direct measurement of intracellular concentrations are underdeveloped.

S3 - KIDNEY TRANSPORTERS AND NEPHROTOXICITY

Rosalinde Masereeuw

Utrecht Institute for Pharmaceutical Sciences

The relevance of membrane transporters gained momentum in recent years and it is now widely appreciated that transporters are key players in xenobiotic disposition. In the kidney, transporters play an important role in the elimination of endogenous waste products and drugs, many of which are potentially harmful for the organism. Among them are the Solute Carriers, organic anion transporters 1 and 3 (OAT1/3), organic cation transporter 2 (OCT2) and the ATP Binding Cassette (ABC) transporters, breast cancer resistance protein (BCRP), multidrug resistance proteins 2 and 4 (MRP2/4) and P-glycoprotein (P-gp). These transporters facilitate renal tubular excretion by a concerted action in uptake and efflux mechanisms. The transport systems are notable for their high transport capacity and wide variety of substrates accepted, but may also be important determinants of nephrotoxicity. Recently novel *in vitro* renal physiological systems, including a bioengineered proximal tubule and 3D organoid cultures, have been developed that allow studying renal drug excretion and associated adverse effects with improved human predictivity. This presentation will give an overview of important drug transporters in renal proximal tubules and focuses on the currently available models to study the therapeutic implications associated with renal drug handling.

S4 - TRANSPORTERS AND DRUG-INDUCED LIVER INJURY

Kim Brouwer

University of North Carolina, Chapel Hill

Drug-induced liver injury (DILI) is a major challenge in drug development and one of the primary reasons for compound attrition during preclinical and clinical evaluation, and for the withdrawal of approved drugs from the market. One mechanism of hepatocyte injury is the accumulation of toxic bile acids due to inhibition of hepatic transport proteins that are critical in bile acid disposition and maintenance of bile acid homeostasis. These proteins include the canalicular bile salt export pump (BSEP), the multidrug resistance proteins (MRP2, MRP3 and MRP4), and the basolateral organic solute transporter (OST α/β). Preclinical species do not reliably predict bile-acid mediated DILI in humans. *In vitro* and *in silico* approaches that can facilitate the identification of compounds with cholestatic potential a priori during the early stages of drug development will be discussed. A novel, human cell-based system has been developed to identify inhibitors of OST α/β -mediated bile acid transport, including compounds associated with cholestatic DILI. Mechanistic modeling of human sandwich-cultured hepatocyte data can be used to evaluate the impact of drug-bile acid transporter interactions (induction or inhibition) on hepatocellular bile acid exposure. The interplay between bile acid exposure, hepatic transporter dynamics, and the regulation of these proteins to protect the hepatocyte from bile acid-mediated hepatotoxicity will be highlighted. Quantitative systems pharmacology (QSP) models can accurately predict the hepatotoxic potential of drugs and identify susceptibility factors (e.g., disease) that may predispose some patients to DILI. Tolvaptan-mediated DILI in patients with autosomal dominant polycystic kidney disease will be used as one example to demonstrate the application of *in vitro* tools and QSP modeling to provide a mechanistic understanding of the observed clinical hepatotoxicity. These innovative approaches in transporter science enable identification of drug-mediated alterations in hepatic bile acid transport, and provide a framework for more accurate predictions of DILI risk in humans.

Supported by NIH R35 GM122576

S5 - TRANSPORTERS AND ARSENIC TOXICITY

Elaine Leslie

University of Alberta

Millions of people world-wide are chronically exposed to the environmental toxicant arsenic in drinking water. This has created a public health crisis because arsenic is a proven human carcinogen, and causes a myriad of other adverse health effects. In addition to unintentional exposures, arsenic trioxide (As₂O₃) is used clinically to treat acute promyelocytic leukemia, and is in clinical trials for the treatment of other tumour types. Cellular transport pathways potentially have an important influence on regulating the cellular/tissue levels, epithelial passage, and ultimately elimination of arsenic. Thus, transport pathways are likely important regulators of the overall body burden of arsenic, and genetic differences in such pathways could influence arsenic-induced disease susceptibility and the effectiveness of arsenic-based therapeutics. Arsenic is extensively methylated in human hepatocytes forming four major products monomethylarsonous acid (MMAIII), monomethylarsonic acid (MMAV), dimethylarsinous acid (DMAIII), and

dimethylarsinic acid (DMAV). Arsenic elimination from the body occurs primarily through urinary excretion of dimethylated species. Recent progress in the understanding of arsenic transport pathways, using relevant human cell models, will be presented.

S6 - ABC EFFLUX TRANSPORTERS AND DRUG TOXICITY

John Schuetz

St. Jude Children's Research Hospital

Abstract not available.

S7 - PHARMACOGENOMICS IN DRUG RESPONSE AND SAFETY ASSESSMENT

Ann Daly

Newcastle University

There is an abundance of data concerning the effect of pharmacogenomics on drug response and safety assessment but to date implementation of testing for most associations has been limited. With increasing availability of pharmacogenomic data from genome sequencing studies, preemptive genotyping projects and commercial providers offering testing direct to the public, this is likely to change in the near future. Examples of pharmacogenomic tests currently in routine use such as TPMT and HLA-B*57:01 genotyping will be compared with others showing promise for implementation, including genotyping for polymorphisms relevant to warfarin dosing including CYP2C9 and VKORC1 and for HLA alleles predictive of adverse drug reactions.

S8 - ACADEMIC AND INDUSTRY PERSPECTIVES ON PHARMACOGENOMICS: DRUG OPTIMIZATION

Alan Shuldiner

Regeneron Genetics Center and the University of Maryland School of Medicine

Advances in high-throughput DNA sequencing technologies now provide an opportunity to exploit human genetic "experiments of nature" to discover novel drug targets more likely to be safe and effective, identify new indications for existing drug targets, and develop biomarkers to select patient subpopulations more likely to respond or less likely to experience adverse effects. The Regeneron Genetics Center works closely with more than 60 academic collaborators world-wide to sequence large patient cohorts linked to deidentified electronic health record data, case-control collections for diseases of unmet medical need, founder and consanguineous populations, and probands and families segregating rare undiagnosed Mendelian diseases. Sequencing of over 250,000 exomes to date has identified rare and common variants associated with a host of human traits that have informed human biology, and identified new drug targets for hyperlipidemia, cardiovascular disease, diabetes, pulmonary artery hypertension, inflammatory bowel disease, among others. Enabled by close collaboration between industry and academia in a precompetitive model, this work has mutually benefited both parties and most importantly has rapidly advanced discovery and translation to benefit research participants and patients. This lecture will review our progress to date, using as examples some of our most productive collaborations. Synergy created by partnership between industry and academia in human genomics represents a most promising path to our common goal of improving human health through precision medicine.

S9 - USING ELECTRONIC MEDICAL RECORDS TO ADVANCE GENOMIC MEDICINE - NOVEL APPROACHES FOR FINDING ACTIONABLE PHARMACOGENOMICS

Joshua Denny

Vanderbilt University Medical Center

Precision medicine offers the promise of improved diagnosis and for more effective, patientspecific therapies. Typically, such studies have been pursued using research cohorts. At Vanderbilt, we have linked de-identified electronic health records (EHRs), to a DNA repository, called BioVU, which has nearly 250,000 samples. Through BioVU and a NHGRIfunded network using EHRs for discovery, the Electronic Medical Records and Genomics (eMERGE) network, we have used clinical data of genomic basis of disease and drug response using real-world clinical data. These studies have demonstrated drug effects and actionable pharmacogenomic findings, some of which have been implemented into practice. Use of phenome-wide association studies highlight potential drug indications and side effects. In addition, by looking for clusters of diseases and symptoms occurring together, we find unrecognized genetic variants associated with common disease that may lead to novel treatments for subsets of the population. The coming era of huge international cohorts such as the UK Biobank, Million Veteran Program, and the newly launced All of Us Research Program - all with electronic health record data linked to molecular measurements - portends a rich future of drug discovery through electronic health data.

S10 - BIOINFORMATICS: ACCUMULATING AND IMPLEMENTING PHARMACOGENOMICS INFORMATION**Michelle Whirl-Carrillo**

Stanford University

This talk provides an introduction to two of the leading pharmacogenomics (PGx) resources: the Pharmacogenomics Knowledge Base (PharmGKB; <https://www.pharmgkb.org>) and the Clinical Pharmacogenetics Implementation Consortium (CPIC; <https://cpicpgx.org>). Both resources aggregate published peer-reviewed PGx articles, evaluate the evidence for gene- and variant-drug associations, and use standardized terminologies to aid in the interpretation of these associations for clinical applications, but each resource has a different focus area. CPIC brings clinical and research experts together to focus on providing genotype-based recommendations for drug prescribing/dosing based on gene-drug associations reported in the literature. PharmGKB annotates PGx knowledge from drug labels and international prescribing recommendations (eg. CPIC, the Dutch Pharmacogenetics Working Group, the Canadian Pharmacogenomics Network for Drug Safety) in addition to the published literature, and compiles drug-centered pathways, very important pharmacogene summaries and clinical annotations which summarize variant-drug associations. PharmGKB and CPIC work together to cover the field from basic PGx knowledge to clinical implementation.

S11 - NOVEL SYNTHETIC AND COMPUTATIONAL APPROACHES TO THE DISCOVERY OF DRUGS TARGETING NONALCOHOLIC FATTY LIVER DISEASE**William Westlin**

Nimbus Therapeutics

The global rise in obesity has produced an increase in incidence and severity of metabolic diseases including non-alcoholic steatohepatitis (NASH). NASH is characterized by accumulation of liver fat droplets, inflammation, hepatocyte ballooning, and fibrosis and may lead to increased mortality due to cirrhosis and hepatocellular carcinoma. The acetyl-CoA carboxylase isozymes, ACC1 and ACC2, are critical enzymes in de novo fatty acid synthesis and fatty acid oxidation, respectively. Due to the unique position in intermediary metabolism, pharmacologic inhibition of ACC presents an attractive approach to limit fatty acid synthesis in lipogenic tissues while simultaneously stimulating fatty acid oxidation in oxidative tissues. Advanced computational approaches identified an allosteric site in the biotin carboxylase (BC) subunit of ACC that was modulated by an endogenous metabolic regulator, AMPK, and a natural product macromolecule, Soraphen A. GS-0976 (formerly NDI-010976) was designed to occupy this allosteric binding site and prevents activation of both human ACC1 and ACC2 by acting at the protein dimerization interface on the BC domain to prevent enzyme dimerization. GS-0976 is a highly potent and selective inhibitor of both ACC1 and ACC2 in biochemical and cellular assays, and possesses favorable physicochemical and pharmacokinetic properties including chemically-designed liver-specific biodistribution. GS-0976 was designed to be a substrate for hepatic transporter proteins, namely the organic anion transporting polypeptides (OATPs), resulting in favorable liver-directed biodistribution that ensures that the pharmacological effects are focused on the key target tissue for NASH. The results of nonclinical pharmacodynamic and efficacy studies indicate that GS-0976 favorably affects the dyslipidemia, hepatic steatosis, inflammation, and subsequent fibrosis in mechanistic models of NASH. De novo lipogenesis (DNL), the synthesis of fatty acids such as palmitate from carbohydrates or amino acids, occurs primarily in the liver and adipose tissue. Direct measurements of lipid flux have demonstrated that elevated lipogenesis provides a significant source of the fatty acids accumulating in the liver of individuals with NASH. A reproducible method for assessing hepatic DNL has been developed and validated by measuring the appearance of de novo synthesized palmitate in very-low density lipoproteins (VLDL) in response to oral fructose using [1-13C]acetate and mass isotopomer distribution analysis (MIDA). Overnight infusion of 13C-acetate led to incorporation of the 13C label into the endogenous pool of acetyl CoA. Periodic oral fructose administration over a 10 hr period led to stimulation of mean hepatic fractional DNL that increased in placebo treated subjects over baseline. An assessment of the data for fractional DNL in a Phase 1b study in obese male subjects demonstrated that all subjects administered GS-0976 had substantial inhibition of de novo lipogenesis. In addition, Phase 2 studies have demonstrated a decrease in liver fat following administration of GS-0976 using MRI proton density fat fraction analysis. Clinical pharmacodynamic studies have demonstrated that ACC engagement by GS-0976 results in substantial inhibition of de novo lipogenesis in the liver. Therefore, GS-0976 has the potential to contribute considerable value to the treatment algorithm of NASH.

S12 - PHARMACOKINETIC CHANGES IN PREGNANCY: CLINICAL IMPLICATIONS**Shinya Ito**

Hospital for Sick Children

Pregnancy is characterized by significant changes in body compartment sizes, hemodynamics, organ function and hepatic expressions of drug metabolizing enzymes. These changes influence ADME processes, leading to altered pharmacokinetic (PK) parameters for many drugs compared to non-pregnant state. First, gastric pH is elevated and gastro-intestinal transit time is prolonged in pregnancy, which increase bioavailability of drugs such as amoxicillin.

Second, extracellular fluid compartment is expanded, leading to larger volume of distribution (Vd) for hydrophilic compounds, which include many antimicrobials. Third, cardiac output and glomerular filtration rate increase by nearly 50%, contributing to higher renal clearance in pregnancy. Increased requirement of lithium in pregnancy is one of the examples. Fourth, expression of hepatic drug metabolizing enzymes changes during pregnancy. Evidence is strong for increased liver expression with functional consequences of CYP3A4 (substrate drugs: indinavir, midazolam, nifedipine), CYP2C9 (phenytoin), CYP2D6 (selective serotonin reuptake inhibitors), CYP2A6 (nicotine), CYP2B6 (efavirenz) and UGT1A4 (lamotrigine). In contrast, CYP1A2 (caffeine) and CYP2C19 (activation of clopidogrel) expression appear to be reduced during pregnancy. These PK parameter changes in pregnancy are reflected in changes of drug concentrations in serum. Particularly, alterations in drug clearance (CL) lead to corresponding changes in average serum concentrations at steady state. Although it is often said that Vd increase in pregnancy is the cause of decreased drug concentrations in serum, average concentrations at steady state are dependent on CL by definition, but not Vd. In fact, increased Vd may reduce peak concentrations but trough concentrations increase due to prolonged half-life, offsetting the impact on average concentrations. Given the importance of CL to define average drug concentrations at steady state, mechanistic understanding of pregnancy-induced expression changes of drug metabolizing enzymes is important. While PK changes are significant during pregnancy, whether pharmacodynamics remains the same or not is poorly understood. For example, CYP3A4-dependent CL of anti-HIV protease inhibitors is significantly increased in pregnant patients, causing substantial reduction in average serum concentrations at steady state. Some other anti-HIV drugs show similar trends. However, if this leads to therapeutic failure is not obvious, and concerns on fetal safety further complicate the issue. In summary, pregnancy-associated PK changes are evident for many drugs, but if PK-PD relationship in pregnancy remains the same or not requires further research.

S13 - DYSREGULATION OF TRANSPORTERS IN MATERNAL DISEASE; POTENTIAL IMPACT ON FETAL DRUG EXPOSURE

Micheline Piquette-Miller

Leslie Dan Faculty of Pharmacy, University of Toronto

During intrauterine life, the placenta is involved in nutrient uptake and serves as a barrier against potentially harmful substances. The ATP-binding-cassette (ABC) efflux transporters as well as solute carrier (SLC) uptake transporters are highly expressed in placenta and are believed to control fetal exposure to numerous endogenous and exogenous substances. While many prevalent obstetric complications are associated with an inflammatory response, numerous studies in our laboratory in pregnant animal models of acute (viral, bacterial and protozoal infections) inflammatory conditions observed significant changes in the expression of many ABC efflux and SLC uptake transporters in both maternal and fetal tissues. These changes were also associated with altered drug accumulation in maternal and fetal tissues. More recently, dysregulation of transporters has been seen in placenta obtained from women with acute and chronic inflammatory disease. As drug transporters are involved in the distribution and elimination of a large number of chemically diverse and clinically important drugs as well as potentially toxic agents, our studies suggest that prevalent co-existing inflammatory conditions could potentially impact maternal and fetal exposure to these agents which could put them both at increased risk for adverse outcomes or therapeutic failure.

S14 - PREDICTING AND VERIFYING MATERNAL-FETAL EXPOSURE TO DRUGS DURING PREGNANCY

Jashvant Unadkat

University of Washington

Pregnant women take multiple medications during pregnancy. However, due to ethical concerns, determining fetal exposure to drugs and therefore fetal efficacy/toxicity of drugs is not possible. Therefore, alternative approaches are required to determine fetal (and maternal) exposure to drugs throughout gestation. To do so, we have developed a Physiologically-Based Pharmacokinetic (PBPK) model to predict maternal-fetal exposure to drugs throughout gestation. We have verified this model at term, using umbilical cord drug concentrations, for drugs that passively cross the placenta and are not metabolized there (Zhang et al., 2017; Zhang & Unadkat, 2017). Next, we are expanding this model to predict and verify maternal-fetal exposure to drugs that are actively transported by the placenta (e.g. by P-glycoprotein). To do so we have quantified the expression of a number of transporters in human placentae of varying gestational age using targeted quantitative proteomics. My talk will cover the research progress we have made to date. Supported by NIH P01DA032507.

S15 - USE OF ANTIEPILEPTICS DURING PREGNANCY: CLINICIAN'S VIEW**Tadeu Fantaneanu**

The Ottawa Hospital, University of Ottawa

This talk will outline the clinical management of epilepsy during pregnancy using an illustrative case as an example. Focus will be given to preconception antiseizure drug selection and rationale, therapeutic drug monitoring during pregnancy and delivery and postpartum considerations.

S16 - GENETIC PREDICTORS AND UNDERLYING MECHANISM OF TREATMENT-RELATED COMPLICATIONS IN CHILDHOOD ACUTE LYMPHOBLASTIC LEUKEMIA**Maja Krajcinovic**, R. Abaji, M. Plesa, V. Gagné, C. Laverdière, J.M. Leclerc, S.E. Sallan, and D. Sallan

University of Montréal

Acute lymphoblastic leukemia (ALL) is the most common cancer in children and it accounts for 25% of all childhood malignancies. Survival rates have improved significantly over time with the progressive intensification of ALL treatment and the implementation of multi-agent risk-adapted protocols. However, a subset of patients experience short-term treatment-related toxicities, which might result in the interruption or discontinuation of chemotherapy or can have severe, fatal, or lifelong consequences that challenge their ability to lead a normal life as future adults. Using genetic markers for prospective stratification of patients at high risk of developing treatment complications has the potential to improve ALL treatment by identifying a patient subgroup, which might benefit more from an alternative regimen. Pharmacogenetic studies of ALL evolved over the time from candidate gene approach to genome and exome wide association studies. Here we present identification of genetic component, derived from both approaches, that predicts development of osteonecrosis (ON) and pancreatitis, common side effects of childhood ALL treatment associated respectively with the use of corticosteroids (CS) and asparaginase (ASNase). The results that were obtained through association studies in discovery cohort and were further confirmed in replication patient group. The example of candidate gene approach is depicted by *BCL2L11* gene, which encodes pro-apoptotic Bim protein. Particular polymorphisms of this gene were associated with ON in clinical setting and influenced in vitro sensitivity to dexamethasone and Bim gamma isoform mRNA levels. For exome wide association study, we focused the analysis on predicted functional germline variants obtained through whole-exome sequencing. Following adjustment for multiple testing, several SNPs underlying asparaginase-related pancreatitis were identified. The risk was further increased through combined SNPs effect suggesting synergistic interactions between the SNPs. The discriminatory ability of the model to predict ASNase-induced pancreatitis was also explored by weighted genetic risk score (wGRS). From the functional point of view, particularly interesting are SNPs in *MYBBP1A* and *IL16* genes. *MYBBP1A* encodes MYB Binding Protein 1a which is important for many cellular processes including its role as a co-repressor of the nuclear factor kappaB, whereas interleukin-16 is a multifactorial cytokine involved in inflammatory and autoimmune diseases as well as cancer risk. We also produced knock-outs of these genes in PANC1 (pancreatic) cancer cell-lines using CRISPR-CAS9 technology and tested the difference in viability between the knockouts & wild-type cells following ASNase treatment. The screening demonstrated that both SNPs incurred a significant modulation of drug sensitivity in LCLs. In the PANC1 cells, $\Delta MYBBP1A$ & $\Delta IL16$ cells were associated with resistance to ASNase reflected by a significantly higher IC₅₀ 48h after drug challenge. Furthermore, both knockouts showed differences in the morphology but $\Delta IL16$ -PANC1 cells seem to reflect a more malignant and drug resistant phenotype. Using different pharmacogenetic strategies, we identified several genetic predictors of treatment-related complications in ALL patients and explored their functional role.

S17 - GENOME-GUIDED MEDICATIONS FOR SAFER AND MORE EFFECTIVE TREATMENT OF DISEASE.**Colin Ross**

University of British Columbia

The treatment of childhood cancer is particularly impacted by adverse drug reactions (ADRs). ADRs in children are 3-fold more likely to be life-threatening and a staggering 73% of childhood cancer patients develop chronic health conditions and 42% develop disabling or life-threatening ADRs from cancer treatment. It is increasingly evident that genetic differences can influence a patient's likelihood of experiencing an ADR. Anthracyclines, such as doxorubicin, are an effective chemotherapy for childhood and adult cancers; however, treatment is limited by the development of cardiotoxicity in some patients. Recent studies suggest a pharmacogenomic component to this severe ADR. A genome-wide study of 730,000 SNPs in 280 pediatric oncology patients of European ancestry identified a significant association with rs2229774, a non-synonymous variant (Ser427Leu) in the RARG gene with replication in two independent cohorts (n=176), including various worldwide ancestries. Functional analyses demonstrated significantly reduced RARG activity for this variant. Based on these findings we are exploring novel strategies to mitigate this toxicity using cardioprotective strategies and/or combining pharmacogenomic variants with clinical risk factors to prospectively identify patients at high risk of anthracycline-induced cardiotoxicity. Moving forward, we are working to expand the discovery and validation of ADR -

associated pharmacogenomic biomarkers in pediatric oncology for additional drugs, and lay the foundation for accessible pharmacogenomic testing in Canada.

S18 - TOXICOGENOMICS AND SYSTEMS TOXICOLOGY APPROACHES TO UNDERSTANDING ADVERSE OUTCOMES

Jeffrey Willy, Jiabin Qiu, Evan Wang, and Yue Webster
Eli Lilly & Co.

Drug Induced Liver Injury (DILI) is a major contributor to the overall clinical occurrence of acute liver failure (ALF), often leading to early termination of clinical trials, post-marketing drug withdrawals, and the need for liver transplantation, and compound-specific causality is not always clear. Despite a recent pivot toward utilization of *in vitro* tools for early safety assessment, nonclinical safety studies are still utilized to predict clinical liabilities for new drugs. However, recent advancements in genome editing coupled with network-based approaches in toxicogenomics allow new insight to explore relationships from molecular/cellular level to pathological changes occurring at the organ in preclinical studies. Here, we will focus on recent investigations utilizing an integrated systems biology toolkit consisting of CRISPR/Cas9 and toxicogenomics to reduce uncertainty for both adaptive and progressive changes in the liver during early safety assessment.

S19 - SITE-SPECIFIC DEUTERIUM SUBSTITUTION: A VIABLE APPROACH IN DRUG DISCOVERY AND DEVELOPMENT

Margaret Bradbury¹, Edward Hellriegel², Yael Marantz², Tom Baillie³, and David Stamler⁴

¹Consultant for Teva Pharmaceuticals, ²Teva Pharmaceuticals, ³University of Washington, ⁴Prana Biotechnology

Drug developers have long sought to improve medications by optimizing concentrations of the active moiety in plasma and target tissues. Formulation strategies can slow and /or or target the site of absorption, but do not address underlying metabolic liabilities that might be responsible for short half-lives, drug-drug interactions, or exposure to undesired metabolites; they also may reduce the extent of absorption. Site-specific deuterium substitution is a drug development tool that can slow bond cleavage by Phase 1 metabolic enzymes such as cytochrome P450s (CYP)s and oxidases. If deuterium is substituted for hydrogen in a bond that is the rate-limiting for a drug's metabolism, and if different metabolic reactions do not compensate, then the slower bond cleavage rate can be detected as a change in the inherent half-life of the compound *in vitro*. Such changes have the potential to translate into reduced systemic clearance. With a slower metabolic rate, deuteration can improve the pharmacokinetic profile of medications by increasing substrate half-lives, lowering peak concentrations, reducing peak to trough fluctuations, and reducing exposure to undesired or inactive metabolites. For patients, these changes have the potential to provide more convenient dosing, reduce the burden of CYP-based drug interactions or genotyping, provide more sustained pharmacodynamic action, and improve tolerability. The pharmacodynamics of deuterated drugs will generally reflect changes in plasma concentrations to the extent that deuterium substitution preserves the pharmacological binding of the molecule at the target or off-target sites. In some instances, optimization of existing approved medications can lead to faster regulatory approval through the referencing of the original medication's label. This presentation will describe the process by which deuterium impacts drug metabolism, review the history of deuterium labeling in drug development, and will survey the recent applications of deuterium for potential commercial applications. This presentation will also summarize highlights from the development of deutetrabenazine (Austedo®), a deuterium-substituted form of tetrabenazine, including an innovative comparative [14C]-labeled mass balance and metabolite profiling study. Austedo® is the first deuterated drug approved by the US FDA (in 2017) and is indicated for treatment of chorea associated with Huntington's disease and tardive dyskinesia.

S20 - SYSTEMS PHARMACOKINETIC MODELING OF ADCS

Dhaval Shah
SUNY Buffalo

This presentation will highlight state-of-the-art mathematical models that are developed to understand and predict cellular, whole body, and tumor specific disposition of ADCs. The following case studies will be presented to highlight the application of these models. Development of cell-level systems PK-PD model to characterize and predict the bystander effect of ADCs. Development of tumor disposition model for ADCs to facilitate preclinical-to-clinical translation of their efficacy. Development of a PBPK model for ADCs to a priori predict their tissue PK and the PK in the clinic.

S21 - INTRA-TISSUE CATABOLITE CHARACTERIZATION IS A MISSING LINK IN DISCOVERY OF ADCS

Donglu Zhang, Yong Ma, Shang-Fan Yu, Thomas H. Pillow, Jack D. Sadowsky, Dian Su, Andrew G. Polson, and Peter S. Dragovich, Cornelis ECA Hop, and S. Cyrus Khojasteh
Genentech

Antibody drug conjugates (ADCs) have a complex structure that combines an antibody with a small molecule drug through a chemical linker. The convenient and practical sampling and analysis allows quantification of circulating ADC species such as total antibody, conjugated antibody, conjugated drug, and payload drug, however, challenges remain to correlate the exposures of these circulating species to efficacy. The major challenge is the disconnect between intra-tissue tumor concentration of the active component of the ADC and circulating concentration of analytes. In this study, studies with DM1, MMAE, and PBD linked ADCs in xenograft mouse models showed that the structures and concentrations of payloads in tumors correlate with tumor growth inhibition efficacy while ADC exposures in circulation could not predict the corresponding efficacy profiles. These are the cases where intratumor payload analysis explained the efficacy data in a way that was not possible by simply assessing total antibody and/or ADC stability and circulating exposures. Chemical structure and concentration of intra-tumor catabolites determine the ADC *in vivo* efficacy. Therefore, intra-tumor catabolites should be more routinely analyzed to support ADC to better understand the drivers for efficacy.

S22 - IN VITRO AND IN VIVO MECHANISMS OF ADC DISPOSITION AND ACTIVITY

Colin Phipps

AbbVie

The mechanisms that govern antibody-drug conjugate (ADC) pharmacology are multifactorial and complex. Significant efforts have been made to investigate these processes preclinically using *in vitro* and *in vivo* methods in conjunction with mathematical modelling. *In vitro* systems have been used to quantify various rate parameters that contribute to ADC efficacy including target kinetics (i.e. synthesis and basal internalization), ADC-target binding, complex internalization, ADC recycling, payload release and cell-killing. These systems can inform mathematical models, which are a useful tool to investigate the dynamic interactions between various ADC-related mechanisms and propose strategies for ADC optimization. The range of possible mathematical models is wide, and many underlying assumptions will be considered including those that govern targeted uptake, non-specific uptake, target kinetics, endosomal sorting and payload release. Examples of *in vitro/in vivo* PKPD models for ADCs that have proven useful will be presented including a mechanistic model for *in vitro* ADC internalization that was used to identify inefficient ADC processing steps. Colin Phipps is an employee of AbbVie. The design, study conduct, and financial support for this research was provided by AbbVie. AbbVie participated in the interpretation of data, review, and approval of the publication.

S23 - CHARACTERIZATION AND ADME PROPERTIES OF A NOVEL AURISTATIN PAYLOAD-BASED ADC

Mauricio Leal

Pfizer, Inc.

An ADC is composed of a small molecule cytotoxin conjugated to a monoclonal antibody via a chemical linker. These three components are varied and make up the numerous ADCs currently in development and in the clinic. Characterizing the ADC's ADME properties and that of the released and active species in particular, is complex given the nature of the small molecule and its properties, the linker and the conjugation process used and the targeting and internalizing capacity of the large molecule antibody. This presentation will walk through the steps and points to consider while evaluating the ADME properties of an ADC and specifically of the highly toxic small molecule payload.

S24 - A HUMAN LIVER MICROPHYSIOLOGY SYSTEM FOR DRUG DISCOVERY AND DEVELOPMENT

D. Lansing Taylor

University of Pittsburgh Drug Discovery Institute

A Human Liver Microphysiology System for Drug Discovery and Development. D. Lansing Taylor, Ph.D. Distinguished Professor & Allegheny Foundation Professor of Computational & Systems Biology, Director of the University of Pittsburgh Drug Discovery Institute. We have been evolving human, 3D, microfluidic, microphysiology systems to model liver disease progression for drug discovery and to model toxicology for drug development using quantitative systems pharmacology (QSP). We have evolved a human, 3D, 4 cell type, microfluidic, liver microphysiology system (MPS) as a key experimental component of our liver-targeted metastatic breast cancer and liver disease programs. The evolution of the liver MPS has been driven by the following principles: a) create a liver acinus biomimetic, including structure, oxygen zonation, and function for at least one month; b) evolve the complexity and functionality on a "fit for purpose" for efficacy testing and ADME-TOX; c) evolve the use of patient primary cells to iPSC-derived liver cells from patients to capture heterogeneity of genomic and disease backgrounds; d) create and implement real-time fluorescence-based biosensors,

together with measurement of drugs, metabolites and secreted molecules in the efflux media; f) implement a microphysiology database to manage, analyze and model the data; g) design the liver MPS as a stand-alone liver or coupled to other organ MPS such as the intestine and kidney; and h) the design should be scalable to create a human chip “farm”. I will discuss our recent development of a vascularized liver acinus MPS (vLAMPS) with the ability to quantify immune cell infiltration, the application of the liver MPS models to metastatic breast cancer and non-alcoholic steatohepatitis (NASH), as well as a platform to investigate chronic toxicology either alone or coupled to other organ systems.

S25 - LINKED ORGANS-ON-CHIPS FOR PROBING XENOBIOTIC BIOACTIVATION, TRANSPORT AND TOXICITY

Edward J. Kelly

University of Washington

Information from toxicity testing is critical for the evaluation of environmental risks from chemical and drug exposure, and serves as the basis for many public health and regulatory decisions. Aristolochic acids (AA) are naturally occurring toxins found in plants of the Aristolochiaceae family, many of which have been used for centuries for medicinal purposes. Relatively recently, it has been discovered that AA are etiologic agents in clinical syndromes previously known as Chinese Herbs Nephropathy and Balkan Endemic Nephropathy, and contribute to the global burden of both kidney failure and urothelial cancers. However, the precise mechanisms whereby hepatic and/or renal enzymes activate or detoxify AA remain unclear, because results from *in vitro* and *in vivo* studies have been inconsistent. To clarify these toxicological mechanisms and *in vivo* organ-organ interactions, we have linked a liver hepatocyte microphysiological system (MPS) to a human kidney tubule MPS, thereby demonstrating that first pass hepatic metabolism of AA is necessary and sufficient to induce acute kidney injury, and have delineated a multistep pathway for dose-dependent AA nephrotoxicity that requires hepatic bioactivation. Based on inhibitor studies, nitroreduction is the key initiating reaction pathway in the liver and an intermediate (AL-I-NOH) is sulfo-conjugated for export with uptake of this reactive compound, sulfonyloxyaristolactam (AL-I-NOSO₃), requiring active transport into the kidney MPS. Acute exposure to AA results in covalent DNA adducts but the most dramatic effects at the doses tested are acute cell injury and death. The establishment of a linked liver-kidney MPS will allow us to address the role of individual genetic variation in AA-associated enzymatic pathways and transport, and delineate mechanisms of chronic, low dose-induced genotoxicity. This is critical to addressing the observation that not all individuals exposed to AA develop nephropathy or upper urothelial tract carcinoma.

S26 - THE UTILITY OF LIVER SPHEROIDS IN ADDRESSING CURRENT ISSUES IN DRUG METABOLISM AND LIVER TOXICITY EVALUATIONS

Jinping Gan

Bristol-Myers Squibb

The study of the absorption, distribution, metabolism, and excretion (ADME) is essential part of drug discovery and development process as it is fundamentally integral to the efficacy and safety of experimental medicines. Over the last ten years, the rapidly evolving R&D landscape has presented new challenges for ADME science, and novel *in vitro* models are needed to help meet these challenges. Recent advances in 3D cell culture models hold promise in multiple disciplines including ADME/Tox, disease modeling, precision medicine, and regenerative tissue engineering. Despite the enormous potential of these models, it is still far away from the widespread adoption for biopharma industry applications. This talk analyzes this issue from the ADME perspective, and provides real world context of use in ADME discipline, fundamental requirements for the successful use of these models, and recent examples from the academia and industry. Three major organs, intestine, liver, and kidney, will be emphasized as pertinent to the absorption, metabolism, and excretion of therapeutics.

S27 - MICROPHYSIOLOGICAL SYSTEMS IN PHARMA: EVOLVING A PARADIGM

William Proctor

Genentech

Microphysiological systems (MPS or tissue-chips) are a rapidly emerging technology that has the potential to transform drug discovery and development by creating more predictive *in vitro* tools to model drug disposition, safety, and efficacy. As this technology matures, a significant beneficial effect will be to refine, reduce, or even replace traditional animal models with relevant human-derived MPS models. The public sector, including the National Institutes of Health (NIH) National Center for Advancing Translational Sciences (NCATS), Defense Advanced Research Projects Agency (DARPA), and the US Food and Drug Administration (FDA), has invested extensively in MPS technology. Notably, MPS is highlighted as a “promising new technolog[y] in predictive toxicology” and is a key area of focus in the recently released 2018 FDA Predictive Toxicology Roadmap. Considerable public investment has sped the maturation and industrialization of the technology and there is now an opportunity to test the suitability of these systems for end user applications. The

pharmaceutical and biotechnology industry has also invested heavily in MPS technology; which mainly involved companies working independently with MPS vendors on potentially redundant tissue chip development and proof-of-concepts efforts. The existing public and private efforts afford the possibility for collaborative efforts by the pharmaceutical industry to incubate and implement an integrated strategy for applying MPS to drug discovery and development. This talk will focus on emerging cross-industry consortia in this space with the goal of speeding up the development, qualification, and regulatory acceptance of MPS models.

S28 - PREDICTING AND PREVENTING THE INACTIVATION OF DRUGS BY HUMAN GUT BACTERIA

Peter Turnbaugh

University of California San Francisco

The unpredictable variation between patients in drug response is a major limitation to modern medicine. Considerable progress has been made in recent years to attribute these differences to environmental factors like dietary intake and polymorphisms in the human genome, but these studies ignore our “second genome”—that of the trillions of microbes that thrive in and on the human body: the microbiome. We now know that the human gut microbiome can metabolize at least 50 drugs; however, the microbial species, genes, and enzymes responsible are either unknown or poorly characterized. We discovered that the cardiac drug digoxin induces the expression of a 2-gene operon encoded by the type strain of *Eggerthella lenta*: the cardiac glycoside reductase (*cgr*) operon. The *cgr* operon is absent in *E. lenta* strains that do not metabolize digoxin; *cgr* operon presence and abundance predicts the extent of drug inactivation by human gut microbial communities. Analysis of the genomes of 25 *E. lenta* strains and close relatives revealed an expanded 8-gene *cgr*-associated gene cluster present in all digoxin metabolizers and absent in non-metabolizers. Using heterologous expression and *in vitro* biochemical characterization, we found that a single flavin- and [4Fe-4S] cluster-dependent reductase, Cgr2, is sufficient for digoxin inactivation. Unexpectedly, Cgr2 displays strict specificity for digoxin and other cardenolides. Quantification of *cgr2* in gut microbiomes revealed that this gene is widespread and conserved in the human population. Together, these results demonstrate that human-associated gut bacteria maintain specialized enzymes that protect against ingested plant toxins. Ongoing work in our lab is focused on establishing a generalizable toolkit to precisely edit the human gut microbiome. Endogenous CRISPR-Cas systems can be programmed to target their own genomic DNA using custom guide RNAs homologous to a gene of interest. As an initial proof-of-principle we are targeting the bacterial gene sufficient for the inactivation of the cardiac drug digoxin. *E. lenta* DSM 2243 encodes a Type I-C CRISPR-Cas system. RNA-seq during *in vitro* growth revealed that the *E. lenta* CRISPR-Cas system is transcribed, consistent with results using targeted analysis of *cas* gene expression and Northern blot probes for CRISPR RNA expression. Heterologous expression of the *E. lenta* system in a genetically tractable model bacterium resulted in sequence-specific targeting of foreign DNA. Self-targeting often led to cell death, while the survivors contained targeted chromosomal deletions. We are currently troubleshooting approaches for introducing foreign DNA into *E. lenta* using bacteriophage, conjugative plasmids, and electroporation using a natural cryptic plasmid identified in our strain collection. These results provide a critical step towards developing modular tools for engineering the gut microbiome to improve the treatment of human disease.

S29 - DRUG-MICROBE INTERACTIONS IN HIV TRANSMISSION

Nichole Klatt

Miller School of Medicine, University of Miami

More than one million women are infected with HIV annually. However, the biological mechanisms associated with transmission in women are not well understood. One factor that has consistently been associated with increased acquisition of HIV in women is imbalanced vaginal bacteria, i.e. vaginal microbiome dysbiosis. Lack of healthy *Lactobacillus* bacteria, but increased anaerobic bacteria and higher diversity of the microbiome in the female reproductive tract has been associated with clinical vaginosis, inflammation, and increased HIV infection. We recently demonstrated that dysbiotic vaginal bacteria can also alter the efficacy of topical pre-exposure prophylactic (PrEP) strategies. We found the mechanism by which dysbiotic bacteria decrease efficacy of topical antiretroviral-based PrEP is by direct metabolism of the drugs by bacteria. Here we will summarize what is currently known about vaginal microbial dysbiosis and HIV infection, and the potential mechanisms of how vaginal bacteria may influence HIV transmission in women.

S30 - DISENTANGLING HOST AND MICROBIOME CONTRIBUTIONS TO DRUG PHARMACOKINETICS AND TOXICITY

Andrew Goodman

Yale University School of Medicine

The gut microbiota is implicated in the metabolism of several medical drugs, which can have important consequences for efficacy, toxicity, and interpersonal variation in drug response. However, dissecting host and microbial contributions to

drug metabolism is challenging, particularly in cases where host and microbiome carry out the same metabolic transformation. I will describe our efforts to combine genetic manipulation of human gut commensal bacteria, gnotobiotics, and pharmacokinetic modeling to quantify the contribution of the microbiome to systemic drug and metabolite exposure and toxicity. This approach could improve our understanding of the environmental and genetic factors that influence drug response variability.

S31 - AZ1 - A CYP3A4 INDUCER WITH A COMPLEX DDI PREDICTION ANALYSIS

Ken Grime

AstraZeneca

From the 2017 updated FDA guidance on Drug-Drug Interaction Studies, the Relative Induction Score correlation method, the basic kinetic model and Simcyp PBPK model using the single reference drug rifampicin will be discussed in the context of AZ1, an AstraZeneca candidate drug. Difficulties encountered in assessing the potential for CYP3A4 induction dependent DDI included higher than clinically relevant induction of mRNA for AZ1 and control drugs including rifampicin, inability to completely describe the *in vitro* drug concentration-induction response curve for AZ1 and weak induction at predicted clinically relevant unbound drug concentrations but stronger than rifampicin induction at higher drug concentrations.

S32 - REGULATORY REQUIREMENTS TO ASSESS INDUCTION

Eva Gil Berglund

Medical Products Agency

The European Drug Interaction Guideline came into operation 2013. This was the first time the EMA asked for information on the induction potential in applications for all new investigational products. The guideline requirements and their rationale will be presented along with case examples showing interpretation of data, impact of recurrent problems and labelling consequences for different situations.

S33 - CONSIDERATIONS FROM THE IQ INDUCTION WORKING GROUP IN RESPONSE TO DRUG-DRUG INTERACTION GUIDANCES FROM REGULATORY AGENCIES

Niresh Hariparsad

Vertex Pharmaceuticals

Regulatory agencies, including the European Medicines Agency (EMA), the Food and Drug Administration (FDA), and the Pharmaceutical and Medical Devices Agency (PMDA), have issued guidelines for the conduct of drug-drug interaction studies. A team of scientists under the auspices of the Drug Metabolism Leadership Group of the Innovation and Quality (IQ) Consortium, formed the Induction Working Group (IWG) and reviewed guideline recommendations, focusing initially on the current EMA guidelines. Following feedback from IQ member companies, the IWG, principally representing the pharmaceutical industry (IQ member companies) and CROs, focused on getting a better understanding of regulatory requirements related to; 1) evaluation of downregulation, 2) *in vitro* assessment of CYP2C induction, 3) the use of CITCO as the positive control for CYP2B6 induction by CAR, 4) data interpretation (a 2-fold increase in mRNA as evidence of induction), and 5) the duration of incubation of hepatocytes with test article. In addition to collecting, collating and analyzing data obtained via a blinded survey, the IWG also generated additional data to strengthen our recommendations. With the intention of the EMA and FDA to finalize their respective DDI guidances in the near future, the IWG is looking to support and test current recommendations using a data driven approach. The results of the survey are presented, together with consensus recommendations on downregulation, CYP2C induction, CYP2B6 positive control and data interpretation.

S34 - FUTURE PERSPECTIVES RELATED TO HEPATIC ENZYME INDUCTION

Edward LeCluyse

LifeNet Health

In recent years, there has been an increased focus on the application of 3D organotypic culture systems for drug development and safety assessment. As part of these initiatives, there has been a growing appreciation for the contribution of the other non-parenchymal cell types (Kupffer cells, hepatic stellate cells, and sinusoidal endothelial cells) and other parameters, such as fluid flow, to more accurately model complex mechanisms of drug disposition and toxicity. This presentation will focus on some of the current trends in hepatic culture technologies as well as the impact they have on the restoration and maintenance of hepatocyte integrity, metabolic capacity and induction responses. The opportunities and challenges for adopting these novel systems for routine assessment of the enzyme induction potential of drug candidates will also be discussed.

S35 - PBPK MODELING OF INDUCTION**Ping Zhao**

Bill and Melinda Gates Foundation

PBPK analyses are routinely used by drug developers and regulators to evaluate and inform drug-drug interaction (DDI) liabilities for new molecular entities (NMEs). In 2017, the US FDA published draft clinical and *in vitro* DDI guidances, which encourage the use of PBPK as a type of DDI study that “can be used in lieu of some prospective DDI studies” with detailed recommendations. The lecture will review findings from regulatory science researches that support PBPK recommendations in the new draft DDI guidances. Predictive performance of PBPK to assess CYP induction for an NME as a victim and a perpetrator will be discussed.

S36 - DEVELOPMENT OF ENDOGENOUS BIOMARKERS FOR CYP3A TO BE USED IN DRUG INTERACTION STUDIES.**Tommy Andersson**

AstraZeneca

Drug-drug interactions (DDI) is a major concern in the development of new drugs. The vast majority of clinical DDI studies investigate the effect on cytochrome P450 (CYP 3A). A sensitive probe drug for CYP3A is midazolam, which is commonly used to assess inhibition or induction of this enzyme. Sensitive endogenous biomarkers, especially urinary biomarkers, if applicable, would have great utility, avoiding unnecessary drug exposure and invasive sampling. 4b-hydroxycholesterol (4b-HC) is considered as an emerging endogenous biomarker for CYP3A. 4b-HC is a blood biomarker that has successfully been used to study CYP3A induction. The long half-life of the biomarker and the dynamic range has however limited its use to investigate CYP inhibition. The endogenous bile acid metabolite 1b -hydroxy-deoxycholic acid (1b-OH-DCA) excreted in human urine was recently suggested as a sensitive CYP3A biomarker in drug development reflecting *in vivo* CYP3A activity. The major hydroxylated metabolite of deoxycholic acid (DCA) in human liver microsomal incubations was identified as 1b -OH-DCA by comparison with the synthesized reference analyzed by UPLC-HRMS. Its formation was strongly inhibited by CYP3A inhibitor ketoconazole. Screening of 21 recombinant human cytochrome P450 (P450) enzymes showed that the most abundant liver P450 subfamily CYP3A, including CYP3A4, 3A5, and 3A7, specifically catalyzed 1b -OH-DCA formation. This indicated that 1b -hydroxylation of DCA may be a useful marker reaction for CYP3A activity. The potential utility of 1b-hydroxylation of DCA as a urinary CYP3A biomarker was illustrated by comparing the ratio of 1b -OH-DCA:DCA in a pooled spot urine sample from six healthy control subjects to a sample from one patient treated with carbamazepine, a potent CYP3A inducer; 1b -OH-DCA:DCA was considerably higher in the patient versus controls (ratio 2.8 vs. 0.4). In an on-going DDI study the 1b -OH-DCA is currently validated as urinary biomarker for CYP3A inhibition.

S37 - ENDOGENOUS BIOMARKERS FOR DRUG METABOLISM AND TRANSPORTER ACTIVITY**Kathy Giacomini**

University of California-San Francisco

Transporters in the Solute Carrier Superfamily (SLC) are major determinants of the systemic and tissue specific levels of many endogenous metabolites and clinically used drugs. In this presentation, I will describe the use of genome wide association and metabolomic studies to uncover the endogenous substrates of transporters that play an important role in drug absorption and disposition. In particular, I will focus on transporters in the SLC22 and SLCO families. In addition, I will describe the inhibitory effects of endogenous compounds and compounds generally regarded as safe (GRAS) on transporters in the intestine, which are responsible for drug absorption. The focus here will be on natural products including endogenous metabolites, which are used as excipients in oral drug products. Interactions between the gut microbiome, specific excipients and transporter-mediated drug absorption will be described. Collectively, this presentation will highlight the complex interplay between endogenous metabolites and pharmacologic transporters responsible for drug absorption and disposition.

S38 - QUANTITATIVE INVESTIGATION OF OATP1B-MEDIATED DRUG-DRUG INTERACTIONS USING ENDOGENOUS SUBSTRATES**Hiroyuki Kusuvara**

The University of Tokyo

Organic anion transporting polypeptide 1B1 (OATP1B1) and OATP1B3 mediate the sinusoidal uptake of various anionic drugs in the liver. Their activities are significantly associated with the hepatic first pass effect of oral drugs, and hepatic clearance. To address drug safety in combinatorial use of drugs, evaluation of the OATP1B inhibition potential of new investigation drugs is mandatory in drug development. There is growing interest in using endogenous substrates as

surrogate probe for *in vivo* DDI assessment since it could free investigators from the restrictions of probe administration; evaluation of DDI risk using phase I samples, or even in patients (at bedside). The approach would potentially reduce the burden of probe drug administration, unnecessary DDI studies using recommended probes, and is also expected to reveal DDI risks that may be unfortunately overlooked at the preclinical stages. We challenged to demonstrate the performance of various endogenous OATP1B substrates in the assessment of OATP1B-mediated DDI using rifampicin as inhibitor. Among the substrates, rifampicin dose-dependently increased the AUC of direct bilirubin, glycochenodeoxycholate sulfate and coproporphyrin I the AUC of which showed reasonable correlation each other, and with that of atorvastatin. These data support that the AUC can be quantitative index of OATP1B-mediated DDI assessment. Another clinical study using an anticancer drug as perpetrator also suggests strength and duration of inhibition of OATP1B1 by the anticancer drug following administration for the first time in lung cancer patients. Furthermore, their plasma concentrations or AUC were influenced by OATP1B1 genotype, suggesting their application to OATP1B1 phenotyping in humans without administration of probe drug substrates. In addition to OATP1B, the endogenous substrates for other drug transporters such as OAT1, OAT3, OCT2&MATEs have been reported. Multiplexed analysis of the DDI potential of new investigational drugs for drug transporters can be performed in the same subjects using endogenous substrates as biomarker.

References:

1. Rodrigues, A.D., et al Clin Pharmacol Ther, 103(3), 434-448, 2018.
2. Takehara, I., et al Pharm Res, Accepted.
3. Takehara, I., et al Pharm Res, 34(8), 1601-1614, 2017.
4. Tsuruya Y., et al Drug Metab Dispos. 44(12):1925-1933, 2016.
5. Imamura Y., et al., Drug Metab Dispos. 42(4):685-94, 2014.
6. Kato K. et al., Pharm Res. 31(1):136-47, 2014.
7. Ito S. et al., Clin Pharmacol Ther, 92(5):635-41, 2012.

S39 - CLINICAL VALIDATION AND UTILITY OF COPROPORPHYRINS AS ENDOGENOUS PROBES TO PREDICT OATP1B-MEDIATED DRUG-DRUG INTERACTIONS

Hong Shen

Bristol-Myers Squibb

Hepatic uptake by OATP1B1 and OATP1B3 represents the rate-determining process for clearance of many drug substrates, and the transporters can serve as loci for drug-drug interaction (DDI). Monitoring endogenous biomarkers for OATP function in early phase clinical trials would be an attractive and cost-effective approach to assess OATP1B inhibition by new molecule entities, particularly those for which *in vitro* assays have shown borderline DDI magnitude. Therefore, we assessed the dynamic changes and usefulness of coproporphyrins (CPs) I and III as endogenous biomarkers for OATP1B inhibition in several clinical DDI studies. In the first study in South Asian Indian subjects (n=12), rifampin (600 mg PO) significantly increased C_{max} and AUC_{0-24h} of CPI and CPIII by 3.3- to 6.5-fold. It also increased C_{max} and AUC_{0-24h} of HDA and TDA by 2.2- to 3.2-fold. These changes are similar to the AUC_{0-24h} of rosuvastatin, a drug probe in the same subjects (5.0-fold). Based on the magnitude of effect sizes for the endogenous compounds that demonstrated changes from baseline over inter-individual variations, the overall rank order for the AUC change of endogenous compounds tested was found to be CPI > CPIII > HDA \approx TDA >> BAs \approx BILI \approx DHEAS. In an additional study conducted in populations of mixed ethnicities (n = 16), including black, white, and Hispanic subjects, the C_{max} and AUC_{0-24h} of CPI and CPIII were increased 2.8- to 5.5-fold by rifampin (600 mg PO), consistent with the values observed previously in Asian population. The sensitivity of endogenous biomarkers towards OATP1B inhibition was also investigated by evaluating changes of plasma CP levels in healthy volunteers in the presence of compounds that were predicted to have a minimal inhibitory effect on OATP1B. As expected, administration of diltiazem, itraconazole, BMS-A and BMS-B did not increase plasma CPI and CPIII concentrations relative to prestudy levels. Additionally, the basal CP concentrations in subjects with *SLCO1B1* c.388AG genotypes, i.e. increased OATP1B1 activity, had significantly lower concentrations of CPI than those with *SLCO1B1* c.388AA ($p < 0.05$). Collectively, these findings provide evidence supporting the translational value of CPI and CPIII as suitable endogenous clinical probes to gauge potential for OATP1B-mediated DDIs.

S40 - OPPORTUNITIES AND CHALLENGES IN THE DISCOVERY OF NOVEL AGENTS FOR THE TREATMENT OF MALARIA

Jeremy Burrows

Medicines for Malaria Venture

Malaria is a devastating disease affecting millions of people each year yet, surprisingly, apart from the Artemisinin Combination Therapies (ACTs) there are relatively few effective treatments for *Plasmodium falciparum* and only one complete treatment for *Plasmodium vivax*. This talk will briefly summarise the work of Medicines for Malaria Venture (MMV) and its mission to reduce the burden of malaria in disease-endemic countries by discovering, developing and

facilitating delivery of new, effective and affordable antimalarial drugs in collaboration with international partners. MMV manages a significant antimalarial pipeline with global Pharmaceutical companies as well as Universities and Research Institutes, and this has been strengthened in recent years with the delivery of new products, new clinical candidates and early stage discovery projects. The talk will explain both the challenges that need to be overcome and the strategy adopted to control and eradicate the disease, including definitions of target product and candidate profiles necessary for asexual blood stage cures (including single dose combination treatment), transmission blocking, vivax and chemoprotection. Given the particular challenges associated with new antimalarial treatments and chemoprotectants, namely the ideal of delivering a cure from an oral single dose of a fixed-dose combination, or achieving >1 month protective cover from an *intra-muscular* injection, the pharmacokinetic challenges and strategies adopted will be described.

S41 - DEVELOPING PEPTIDES THERAPEUTICS BY UNDERSTANDING THEIR METABOLISM AND TRAFFICKING

Mark Cancilla

Merck & Co. MSD

With the rapid growth of protein and peptide therapeutics there has been an increased need for understanding the impact of their biotransformation to support discovery and preclinical structure optimization. Current workflows for small molecule metabolite identification (MetID) are not suitable for large peptides and proteins because of their overwhelming complexity and alternative metabolic pathways. To better comprehend the trafficking and metabolism of peptide therapeutics we utilize high-resolution mass spectrometry in combination with innovative sample preparation, low flow ionization techniques and novel software applications to analyze complex *in vivo* metabolism profiles and assess *in vitro* to *in vivo* correlations of clearance and metabolic profiles. We have demonstrated the capability of our platforms using complex peptide therapeutics containing multiple disulfides and non-natural modifications to overcome the challenges of interrogating peptide biotransformation in different in-vitro and in-vivo biomatrices and provide detailed metabolite structures for peptide discovery programs. Examples will be reviewed where results of unambiguously identifying therapeutic peptide metabolism were used to pinpoint labile soft spots which potentially lead to decreased stability and increased in-vivo clearance. We have also incorporated the use of our workflows to streamline our DMPK studies for pre-clinical therapeutic peptide programs to rapidly enhance in-vitro in-vivo correlations. Examples will be demonstrated of both commercial peptide therapeutics as well as in-house pre-clinical peptide case studies.

S42 - DRUG TARGET QUANTITATION, TRANSLATIONAL PK/PD

Joe Palandra

Pfizer

The increase of new biotherapeutic modalities has almost increased the use of PK/PD modeling and systems pharmacology. This has subsequently increased the demand from bioanalytical and biomarker groups with respect to quantitative measurements of biologics, biomarkers and biomeasures in soluble matrices and tissues. These biomeasures can be critical as they can inform target validation, dose projections, occupancy, precision medicine for patient stratification, normal vs disease for target or biomarker measurements, membrane bound or intracellular proteins and finally drug levels. Obtaining accurate and robust measurements however can be quite challenging at times. These challenges can come from many factors, such as binding partners, soluble or shed receptors, splice variants, PTM's, just to name a few. The use of immunoaffinity coupled with nano LC\MS\MS (or hybrid LBA LC\MS) offers a unique way to meet these biological challenges associated with quantitative protein target measurements. This talk will introduce immunoaffinity LC\MS to protein target measurements, outline some of these biological challenges and how hybrid LBA LC\MS can assist in mitigating them using real world examples and how they are ultimately impacting our translational PK/PD models.

S43 - BIOTRANSFORMATION OF ADCS. PATHWAYS AND ENZYMES

Donglu Zhang, Thomas H. Pillow, Dian Su, Niña G. Caculitan, Joseha Chuh, Yong Ma, Shang-Fan Yu, and Shuai Yu
Genentech

Antibody drug conjugates (ADCs) are a complex structure that combines an antibody with a small molecule drug (often a cytotoxin) through a chemical linker. Depending on the nature of the linker and the payload, there are different biotransformation pathways operating on the small molecule payload. The major biotransformation pathways for the small molecule drug once it is cleaved include oxidation and conjugation that are catalyzed by CYP and UGT enzymes located in selected organs such as liver and kidney, but hydrolysis is the major biotransformation mechanism for the antibody portion in every tissue. Different from that for a small molecule or antibody, biotransformation of an ADC involves both hydrolysis of the protein portion and metabolism of payloads in addition to linker metabolism. Examples will be given to demonstrate biotransformation of commonly used peptide and disulfide linkers in which both cleavage and immolation are

important. Further biotransformation of payloads could be important as DNA alkylation of DNA alkylators should be considered as disposition pathways for these compounds. In addition, payload could be directly biotransformed while on the ADC conjugates. Examples will be discussed to show importance of identification of payload catabolites both *in vitro* and *in vivo*.

S44 - UNDERSTANDING DMPK OF BIOTHERAPEUTICS USING INTACT PROTEIN BIOANALYSIS

Wenyang Jian

Janssen Research & Development, Johnson & Johnson

As therapeutic proteins become more widely applicable for the treatment of various types of diseases, there is an increased demand for universal platforms for the determination of their DMPK properties. LC-MS, owing to its capability of providing both highly specific quantitation and qualitative structural elucidation, has emerged as one of the effective technologies to analyze protein therapeutics in biological samples. The mostly commonly used analytical approach for large protein therapeutics is “bottom-up”, by digesting protein using proteolytic enzyme, followed by LC-MS/MS analysis of selected signature peptides as surrogate of the targeted protein. With the improvement of sample preparation techniques and development of high resolution mass spectrometry (HRMS), it has become possible to analyze large molecular proteins in biological samples at intact level without digestion. Intact analysis can provide valuable information about the integrity of the molecules and their biotransformation *in vivo*, which is critical for designing and screening novel protein therapeutics and for understanding their pharmacokinetics and pharmacodynamics. We have established an LC-HRMS workflow to simultaneously identify catabolites and quantify the intact parent molecule for large molecular protein therapeutics. With the integrated LC-MS workflow, an insightful understanding of the *in vivo* fate of protein therapeutics and their DMPK properties can be gained. As therapeutic proteins become more widely applicable for the treatment of various types of diseases, there is an increased demand for universal platforms for the determination of their DMPK properties. LC-MS, owing to its capability of providing both highly specific quantitation and qualitative structural elucidation, has emerged as one of the effective technologies to analyze protein therapeutics in biological samples. The mostly commonly used analytical approach for large protein therapeutics is “bottom-up”, by digesting protein using proteolytic enzyme, followed by LC-MS/MS analysis of selected signature peptides as surrogate of the targeted protein. With the improvement of sample preparation techniques and development of high resolution mass spectrometry (HRMS), it has become possible to analyze large molecular proteins in biological samples at intact level without digestion. Intact analysis can provide valuable information about the integrity of the molecules and their biotransformation *in vivo*, which is critical for designing and screening novel protein therapeutics and for understanding their pharmacokinetics and pharmacodynamics. We have established an LC-HRMS workflow to simultaneously identify catabolites and quantify the intact parent molecule for large molecular protein therapeutics. With the integrated LC-MS workflow, an insightful understanding of the *in vivo* fate of protein therapeutics and their DMPK properties can be gained.

S45 - TARGETED COVALENT INHIBITORS FOR DRUG DESIGN

Thomas Baillie

University of Washington

In contrast to the traditional mechanism of drug action that relies on the reversible, non-covalent interaction of a ligand with its biological target, covalent drugs (also referred to as targeted covalent inhibitors) are designed a priori such that the initial, reversible association is followed by the formation of a covalent bond between a judiciously positioned electrophile on the ligand and a specific nucleophilic center on the protein. Although this approach offers a variety of potential benefits, including high potency and extended duration of action, concerns over the possible toxicological consequences of protein haptization have hindered development of the covalent mechanism in drug design. However, over the past decade, approaches to mitigate the risk of serious adverse reactions to this new class of agent have emerged, stimulating interest in the field and leading to marketing authorization of the first cadre of covalent drugs for applications in oncology. This presentation will provide an overview of the basic concepts behind covalent drug design, and will highlight the importance of target selectivity in minimizing the risk of adverse reactions often associated with covalent protein modification.

S46 - ACTIVITY-BASED PROTEOMICS - PROTEIN AND LIGAND DISCOVERY ON A GLOBAL SCALE

Benjamin Cravatt

The Scripps Research Institute

Advances in DNA sequencing have radically accelerated our understanding of the genetic basis of human disease. However, many of human genes encode proteins that remain uncharacterized and lack selective small-molecule probes. The functional annotation of these proteins should enrich our knowledge of the biochemical pathways that support human physiology and disease, as well as lead to the discovery of new therapeutic targets. To address these problems, we have

introduced chemical proteomic technologies that globally profile the functional state of proteins in native biological systems. Prominent among these methods is activity-based protein profiling (ABPP), which utilizes chemical probes to map the activity state of large numbers of proteins in parallel. In this lecture, I will describe the application of ABPP to discover and functionally annotate proteins in mammalian physiology and disease. I will also discuss the generation and implementation of advanced ABPP platforms for proteome-wide ligand discovery and how the integration of these global 'ligandability' maps with emergent human genetic information can expand the druggable fraction of the human proteome for basic and translational research objectives.

S47 - HOW TO BE SELECTIVELY PROMISCUOUS

Jack Taunton

University of California, San Francisco

Quantifying drug/target engagement in living cells is a challenging problem for which new chemical methods are needed. This is especially critical for kinase inhibitors, which may target any one of 500 closely related enzymes. In this talk, I will describe the development of chemoproteomic probes that enter live cells and rapidly form a covalent bond with the catalytic lysine of protein kinases. Using these probes and label-free mass spectrometry, we can quantify drug/target engagement for a broad swath of the endogenous human kinome. I will also discuss our recent efforts to apply this chemoproteomic approach to proteins with noncatalytic lysines.

S48 - COVALENT BINDING - FROM 20TH CENTURY LIABILITY TO 21ST CENTURY TARGETED THERAPIES

Greg Slatter

Kartos Therapeutics Inc.

Interest in covalent binding of drugs and metabolites surged in the mid 1970's, around the time Mitchell et al., (1) showed that acetaminophen (APAP) depleted hepatic glutathione in mice, shedding light on the mechanism of hepatotoxicity in clinical overdose. The number of papers with the search term "covalent binding" grew exponentially over ten years, spurred on by the application of GCMS and new LCMS technologies. Ultimately the structure of the reactive metabolite of acetaminophen, NAPQI, was elucidated in 1984 (2), and acetaminophen bioactivation became core curriculum in the education of drug metabolism scientists. In an ironic twist, it was not until 2011, that NAPQI's covalent interaction with spinal TRPA1 was shown to be the elusive mechanism of action for APAP analgesia (3). During an unprecedented spate of unforeseen product withdrawals in the 1980s and 90s, covalent binding became associated with rare instances of idiosyncratic hepatotoxicity (4), and the Danger Hypothesis emerged (5). Covalent binding measurements became a core tool for drug metabolism scientists in the 1990s, and thresholds were set that often precluded the development of compounds that were highly covalently bound *in vitro*. In the early 2000s, retrospective comparisons of covalent binding in hepatotoxic versus non-hepatotoxic compounds (6,7) resulted in deconstruction of some assumptions regarding causal links between covalent binding and idiosyncratic hepatotoxicity. Genetic factors that predisposed individuals to idiosyncratic liver injury were identified and Paracelsus' tenet, "the dose makes the poison" was discerned to be important in risk assessment. Coincidentally, the human genome project and advances in molecular modeling enabled a new wave of targeted agents that set new benchmarks for potency and selectivity. Covalent drugs, though initially viewed skeptically, emerged as safe and effective agents that no longer required target coverage through the dose interval (8). As such, target dynamics became important in setting dose and dose frequency. Reversibility of the covalent target interaction, and selectivity in covalent reactivity, emerged as factors in risk:benefit assessment (9). The same enzyme kinetics math used for time-dependent inactivation of P450s were applied and these learnings now drive the development of new PK/PD models for covalent agents. In conclusion, Older selective covalent agents such as Prilosec™ have established that a positive risk:benefit is possible for drugs with a covalent mechanism of action. Now, new targeted, selective, covalent anticancer agents such as the BTK inhibitor, Calquence™ (acalabrutinib, 10, 11), are taking their place in patient care.

References:

1. Mitchell JR et al., 1973 JPET 187 211-17
2. Dahlin DC et al., 1984 PNAS 81 1327-31
3. Andersson DA et al., 2011 Nature Commun 2:551-11
4. Kaplowitz N, 2005 Nat Rev Drug Discov. 4:489-99
5. Pirmohamed M et al., 2002 Toxicology 27;181-182, 55-63
6. Obach RS et al., 2008 CRT 21:1814-22
7. Nakayama S et al., 2009 DMD 37 1970-7
8. Barf T, Kaptein A, 2012 J Med Chem. 26 55:6243-62
9. Baillie T, 2017 Angw Chem 55 13408-21
10. Barf T et al., 2017 JPET 363:240-52
11. Wang M et al., 2018 Lancet 391:659-67

PRE-DOCTORAL/GRADUATE POSTER FINALISTS
(A1 – A6)**A1 - NOVEL INSIGHTS INTO PREDICTING HEPATIC DDI LIABILITIES WHEN TRANSPORTERS AND ENZYMES ARE INVOLVED***Gabriela Patilea-Vrana, University of Washington, Seattle, WA, USA***A2 - A MOUSE MODEL FOR INVESTIGATING HUMAN BRAIN CYP2D6***Edgor Cole Tolledo, University of Toronto, Toronto, ON, Canada***A3 - THE DEVELOPMENT OF A CRISPR/CAS-MEDIATED PD-1 KNOCKOUT RAT MODEL TO STUDY IDIOSYNCRATIC DRUG REACTIONS INCLUDING NEVIRAPINE-INDUCED LIVER INJURY***Tiffany Cho, University of Toronto, Toronto, ON, Canada***A4 - INTERINDIVIDUAL VARIABILITY IN HEPATIC EXPRESSION OF HUMAN SULFOTRANSFERASE 2A1: ABSOLUTE QUANTIFICATION BY LC-MS/MS PROTEOMICS AND EFFECT OF ETHNICITY, GENOTYPE, AGE AND GENDER***Mayurbhai Kathadbbhai Ladumor, National Institute of Pharmaceutical Education and Research, S.A.S. Nagar, India***A5 - DIFFERENT MEASURES OF VARENICLINE ADHERENCE, NICOTINE METABOLITE RATIO AND SMOKING ABSTINENCE***Annie R. Peng, University of Toronto, Toronto, ON, Canada***A6 - DOES PLASMA MEMBRANE AND TOTAL TRANSPORTER ABUNDANCE DIFFER BETWEEN SUSPENDED, PLATED, SANDWICH CULTURE HEPATOCYTES AND HUMAN LIVER TISSUE?***Vineet Kumar, University of Washington, Seattle, WA, USA***POSTDOCTORAL POSTER FINALISTS (A7 – A12)****A7 - N-ACETYLATION CAPACITY OF N-ACETYLTRANSFERASE 2 IN HUMAN PERIPHERAL BLOOD MONONUCLEAR CELLS REGULATED BY NAT2 GENOTYPE AND SIRTUIN 1***Raul A. Salazar-Gonzalez, University of Louisville, Louisville, KY, USA***A8 - STEROIDAL ANTI-ANDROGENS INHIBIT LITHOCHOLIC ACID SULFONATION AND INCREASE LITHOCHOLIC ACID-INDUCED TOXICITY IN A HUMAN HEPATOCELLULAR CARCINOMA CELL MODEL***Siew Ying Wong, National University of Singapore, Singapore, Singapore***A9 - COMPARATIVE CHANGES IN RENAL GENE EXPRESSIONS IN CHRONIC KIDNEY DISEASE AND VITAMIN D DEFICIENT MOUSE MODELS***Keumhan Noh, Department of Pharmaceutical Sciences, Leslie Dan Faculty of Pharmacy, University of Toronto, Toronto, ON, Canada***A10 - AMELIORATING EFFECT OF BAICALIN IN CADMIUM INDUCED KIDNEY FIBROSIS***Manushi Siddarth, University College of Medical Sciences (University of Delhi) & GTB Hospital, Delhi, India***A11 - A PHYSIOLOGICALLY BASED PHARMACOKINETIC MODEL (PBPK) UTILIZING SPECIFIC MUSCLE TISSUE FOR INTRAMUSCULAR INJECTION OF THERAPEUTIC PROTEINS***Timothy Chow, University of British Columbia, Vancouver, BC, Canada***A12 - RELATIVE ACTIVITY FACTOR (RAF)-BASED SCALING OF UPTAKE CLEARANCE OF OATP1B SUBSTRATES FROM TRANSFECTED CELL SYSTEMS TO HUMAN HEPATOCYTES AND TO *IN VIVO****Saki Izumi, Eisai Co., Ltd., Tsukuba, Japan***ADVERSE DRUG REACTIONS (P1)****P1 - COVALENT BINDING OF TRIMETHOPRIM: IMPLICATIONS FOR TRIMETHOPRIM-INDUCED ADVERSE REACTIONS***Yanshan Cao, University of Toronto, Toronto, ON, Canada***ANIMAL MODELS (P2)****P2 - ESTABLISHMENT OF ALBUMIN-DEFICIENT NOG MICE AS A USEFUL MODEL FOR DRUG DISCOVERY RESEARCH***Hiroshi Suemizu, Central Institute for Experimental Animals, Kawasaki, Japan***ANTIBODY-DRUG CONJUGATES (P3)****P3 - *IN VITRO* AND *IN VIVO* CATABOLISM OF TAK-164, A GCC-TARGETED ANTIBODY-DRUG CONJUGATE***Jayaprakasam Bolleddula, Takeda Pharmaceuticals International Co., Cambridge, MA, USA***P4 - ABSTRACT WITHDRAWN****BIOAVAILABILITY (P5 - P8)****P5 - ESTIMATING EFFLUX TRANSPORTER-MEDIATED DISPOSITION USING TRANSPORTER GENE KNOCKOUT RATS***Taiji Miyake, Chugai Pharmaceutical Co., Ltd., Shizuoka Pref., Japan***P6 - RESISTANCE MEDIATED BY LYSOSOMAL SEQUESTRATION OF ANTICANCER AGENTS *IN VITRO****Petr Mlejnek, Palacky University Olomouc, Olomouc, Czech Republic***P7 - ABSTRACT WITHDRAWN****P8 - RAPID ADME SCREENING FOR STREAMLINED FDA SUBMISSION; A CASE STUDY ASSESSING ORAL ABSORPTION VALIDATION AND TRANSPORTER SUBSTRATE ASSESSMENT OF NEW MOLECULAR ENTITIES IN WT CACO-2 CELLS (C2BBE1)***Kevin Thomas, Eurofins Panlabs, Saint Charles, MO, USA***BIOLOGICAL MONITORING (P9)****P9 - DETERMINING LEVELS OF METHYLENEDIANILINE AND TOLUENEDIAMINE AS BIOMARKERS FOR ISOCYANATE EXPOSURE IN HUMAN URINE BY UPLC-MS/MS***Maggy Lépine, UQAM - IRSST, Montréal, QC, Canada***CLEARANCE PREDICTION (P10 - P14)****P10 - *IN VITRO-*IN VIVO** CORRELATION OF CLEARANCE FOR H3B-5942, A NOVEL SELECTIVE ER α COVALENT ANTAGONIST (SERCA)***Federico Colombo, H3-BIOMEDICINE, Cambridge, Ma, Usa***P11 - CAN TRANSPORTER-EXPRESSING CELLS PREDICT ROSUVASTATIN UPTAKE CLEARANCE IN SUSPENDED OR PLATED HUMAN HEPATOCYTES?***Vineet Kumar, University of Washington, Seattle, WA, USA*

P12 - IMPACT OF HEPATIC DRUG DISTRIBUTION ON PREDICTIONS OF CLEARANCE

Jasleen K. Sodhi, University of California San Francisco, San Francisco, CA, USA

P13 - PREDICTION OF HUMAN HEPATIC CLEARANCE FOR CYTOCHROME P450 SUBSTRATES VIA A NEW CULTURE METHOD USING THE COLLAGEN VITRIGEL MEMBRANE CHAMBER AND PXB-CELLS

Ryuji Watari, Eisai Co., Ltd., Tsukuba-shi, Ibaraki, Japan

P14 - CHARACTERIZATION OF HUMAN HEPATOCYTES BY QUANTITATIVE DMET PROTEOMICS ADDRESSES LOT-TO-LOT VARIABILITY: RELEVANCE IN IN-VITRO TO IN-VIVO EXTRAPOLATION OF HEPATIC DRUG CLEARANCE

Bhagwat Prasad, University of Washington, Seattle, WA, USA

CONJUGATION REACTIONS AND ENZYMES

(P15 - P18)

P15 - IN VITRO CHARACTERIZATION OF ERTUGLIFLOZIN GLUCURONIDATION

Kimberly Lapham, Pfizer Worldwide Research and Development, Groton, CT, USA

P16 - POLYMORPHISMS IN CANINE GLUTATHIONE S-TRANSFERASE (GST) GENES: PREVALENCE AND FUNCTIONAL RELEVANCE

James Sacco, Drake University, Des Moines, IA, USA

P17 - SCREENING FOR PHASE I AND PHASE II DRUG METABOLISM USING SUPPLEMENTED LIVER AND INTESTINAL S9 FRACTIONS: A COCKTAIL APPROACH

Kevin Thomas, Eurofins Panlabs, Saint Charles, MO, USA

P18 - IDENTIFICATION OF DOPA-MODIFIED AMINO ACIDS USING HIGH-RESOLUTION TANDEM MASS SPECTROMETRY

Maxime Sansoucy, UQAM, Montreal, QC, Canada

CYTOCHROME P450 (P19 - P29)**P19 - METABOLISM OF 3,7-DIHYDROXYFLAVONE MEDIATED BY CYTOCHROME P450**

Mirza Bojic, University of Zagreb, Faculty of Pharmacy and Biochemistry, ZAGREB, Croatia

P20 - MICROSOMAL CYTOCHROME P450 ENZYME ACTIVITIES IN NONALCOHOLIC STEATOHEPATITIS LIVERS

Maciej Czerwinski, Sekisui XenoTech LLC, Kansas City, KS, USA

P21 - CHARACTERIZATION OF INDIVIDUAL DIFFERENCES IN CYP3A5 ACTIVITY USING A CYP3A5-SELECTIVE MARKER REACTION IN VITRO

Klarissa Jackson, Lipscomb University College of Pharmacy & Health Sciences, Nashville, TN, USA

P22 - PHENOBARBITAL IS AN AGONIST OF HUMAN BUT NOT MOUSE PREGNANE X RECEPTOR

Lin hao Li, University of Maryland, Baltimore, Baltimore, MD, USA

P23 - IN-SILICO TOOL TO PREDICT NEW CYP3A5 SILENSOMESTM USING T-5 SUBSTRATE AND LAPATINIB AS MECHANISM-BASED INHIBITOR

Solenne Martin, Eurosafe,, Saint-Grégoire, France

P24 - ARE CYP3A5 EXPRESSER SUBPOPULATIONS AT AN INCREASED RISK FOR ACETAMINOPHEN TOXICITY?

Kunihiko Mizuno, Takeda California Inc., San Diego, CA, USA

P25 - CYTOCHROME P450 3A ENZYME-DEPENDENT THALIDOMIDE TOXICITY AND INDUCIBILITY IN CULTURED HUMAN PLACENTAL CELLS

Norie Murayama, Showa Pharmaceutical University, Tokyo, Japan

P26 - RAPID CYP450 QUANTIFICATION BY IMMUNOAFFINITY-MASS SPECTROMETRY

Oliver Pötz, SIGNATOPE GmbH, Reutlingen, Germany

P27 - QUANTITATIVE DETERMINATION OF THE EFFECT OF DDT AND DDE TREATMENTS ON CYP1 ENZYME EXPRESSION IN MCF-7 CELLS

Brianne Raccor, Campbell University College of Pharmacy and Health Sciences, Buies Creek, NC, USA

P28 - A NEW CYP-SILENCED CELL-BASED ASSAY FOR DIRECT MEASUREMENT OF THE CONTRIBUTION OF MAJOR CYTOCHROME P450 ENZYMES TO DRUG CLEARANCE/ METABOLISM

Ashwani Sharma, Biopredic International,, Saint-Grégoire, France

P29 - OXIDATIVE METABOLISM OF SYNTHETIC CANNABINOID STS-135 BY RECOMBINANT P450S AND HUMAN LIVER MICROSOMES

Azure Yarbrough, University of Arkansas for Medical Sciences, Little Rock, AR, USA

DIFFERENCES IN METABOLISM (SPECIES, GENDER, AGE, DISEASES) (P30 - P37)**P30 - ASSOCIATION OF HIGH BLOOD LEAD LEVELS WITH FOK1, APA1 AND BSM1 VITAMIN D RECEPTOR GENE POLYMORPHISM IN OCCUPATIONALLY EXPOSED BATTERY WORKERS**

Himani, SGT Medical College Hospital & Research Institute, Gurugram, India

P31 - CIRCULATING HORMONES AND NUCLEAR HORMONE RECEPTOR EXPRESSION ARE ASSOCIATED WITH TREATMENT-FREE SURVIVAL IN PATIENTS WITH CHRONIC LYMPHOCYTIC LEUKEMIA

Eric Allain, Pharmacogenomics laboratory, CHU de Quebec Research Center and Faculty of Pharmacy - Laval University, Quebec, QC, Canada

P32 - SEX DIFFERENCES IN BRAIN OXYCODONE METABOLISM AND ANALGESIA

Nicole Arguelles, University of Toronto, Toronto, ON, Canada

P33 - IDENTIFICATION OF METABOLOMIC BIOMARKERS FOR ENDOMETRIAL CANCER AND ITS RECURRENCE AFTER SURGERY IN POSTMENOPAUSAL WOMEN

Yannick Audet-Delage, CHU de Quebec Research Center - Laval University, Quebec, QC, Canada

P34 - CONTRIBUTION OF HEPATIC FMO-1 IN THE METABOLISM OF COMPOUND 1. IMPLICATION OF CLEARANCE MECHANISM AND EXTRAPOLATION OF METABOLISM DATA FROM PRECLINICAL SPECIES TO HUMANS

Steve Bowlin, Takeda, San Diego, CA, USA

P35 - CHEMICAL-INDUCED TOXICITY IS AMELIORATED BY SWIMMING EXERCISE IN CAENORHABDITIS ELEGANS

Jessica Hartman, Duke University, Durham, NC, USA

P36 - ENVIRONMENTAL XENOBIOTICS SAFETY ASSESSMENT THROUGH COMPARATIVE METABOLISM STUDY IN FISH, SWINE, GOAT, CHICKEN, RAT AND HUMAN

Mingming Ma, Dow AgroSciences, Indianapolis, IN, USA

P37 - EFFECT OF AGE ON BRAIN EXPOSURE OF P-GP SUBSTRATES IN NEONATAL RATS*Michael Rooney, Biogen, Cambridge, MA, USA***DISPOSITION (P38 - P41)****P38 - ADVERSE EFFECTS OF PSYCHIATRIC DRUGS ON BONE: DOES DRUG DISTRIBUTION TO MARROW PLAY A ROLE?***Karen Houseknecht, University of New England, Biddeford, ME, USA***P39 - DISTRIBUTION AND EXCRETION OF A NEW ORAL FORMULATION OF DOCETAXEL IN MICE***Byoung Soo Kim, Korea Institute of Radiological and Medical Sciences, Seoul, Korea***P40 - DISTRIBUTION AND PHARMACOKINETICS OF 3H-GEMCITABINE AFTER SINGLE AND MULTIPLE INTRAPERITONEAL TREATMENT ALONE AND IN COMBINATION WITH INTRAVENOUS DOCETAXEL IN BXPC-3 TUMOR BEARING MICE***Elizabeth Spencer, Covance Laboratories, Madison, WI, USA***P41 - CELLULAR DISTRIBUTION OF BIOLOGICS: A COMPARISON OF MICROAUTORADIOGRAPHY TECHNIQUES***Stephen Harris, Pharmaron, Rushden, United Kingdom***DRUG DISCOVERY AND DEVELOPMENT (P42 - P62)****P42 - ENHANCED METABOLITE IDENTIFICATION USING ORBITRAP TRIBRID MASS SPECTROMETER***Kate Comstock, Thermofisher Scientific, San Jose, CA, USA***P43 - LIGNAN ENTEROLACTONE MODULATES CELLULAR LIPID AND CHOLESTEROL HOMEOSTASIS LINKING DIVERSE MOLECULAR MECHANISMS***Franklyn De Silva, University of Saskatchewan, Saskatoon, SK, Canada***P44 - PREDICTION OF ADVERSE DRUG REACTIONS OF BIASED DATA USING BOOTSTRAP AGGREGATING AND MACHINE LEARNING TECHNIQUES***Dipayan Ghosh, Tata Consultancy Services Ltd, Hyderabad, India***P45 - PREDICTION OF RESPIRATORY TOXICITY USING CHEMICAL INFORMATION AND MACHINE LEARNING TECHNIQUES***Dipayan Ghosh, Tata Consultancy Services Ltd, Hyderabad, India***P46 - DEVELOPMENT OF A NOVEL ORALLY ACTIVE INVERSE AGONIST OF ESTROGEN-RELATED RECEPTOR GAMMA (ERR γ), KH-NDTC AS AN ENHANCER FOR SODIUM IODIDE SYMPORTER: ITS PHARMACOLOGICAL EFFECTS IN ANAPLASTIC THYROID CANCER (ATC) IN VITRO AND IN VIVO***Yong Hyun Jeon, Daegu-Gyeongbuk Medical Innovation Foundation, Daegu, Korea***P47 - DESI-MS IMAGING TO OBSERVE THE DRUG AND DRUG-INDUCED EVENTS IN TUMOR TISSUE***Sang Kyoon Kim, Daegu Gyeongbuk Medical Innovation Foundation, Daegu, Korea***P48 - ZEBRAFISH AS A SCREENING MODEL FOR TESTING THE PERMEABILITY OF BLOOD-BRAIN BARRIER TO SMALL MOLECULES***Seong Soon Kim, Korea Research Institute of Chemical Technology, Daejeon, Korea***P49 - OPTIMIZED DECISION MAKING FROM EARLY DISCOVERY TO DEVELOPMENT PHASE FOR BETTER PREDICTION OF ADME BEHAVIOR***Heasook Kim-Kang, Q2 Solutions, Indianapolis, IN, USA***P50 - AN INTEGRATED *IN VITRO* SCREEN USING SANDWICH-CULTURED HUMAN HEPATOCYTES FOR PREDICTION OF CHOLESTATIC HEPATOTOXICITY***Jonathan Jackson, BioIVT, Durham, NC, USA***P51 - DEEP CONVOLUTION NEURAL NETWORKS ANALYSIS OF CHEMICAL IMAGES: APPLICATIONS IN DRUG DISCOVERY AND DEVELOPMENT***Geervani Koneti, Tata Consultancy Services Ltd, Hyderabad, India***P52 - GENERATION OF REPRODUCIBLE PREDICTIVE MODELS USING PARALLELIZED MODIFIED TEACHING LEARNING BASED SEARCH OPTIMIZATION METHOD AND ITS APPLICATIONS IN DRUG DISCOVERY AND DEVELOPMENT***Geervani Koneti, Tata Consultancy Services Ltd, Hyderabad, India***P53 - *IN VITRO* PRIMARY HUMAN HEPATOCYTE 3D SPHEROID MODEL FOR HEPATOTOXICITY STUDIES***Feng Li, Corning Incorporated-Life Sciences, Bedford, MA, USA***P54 - TRANSCRIPTOMIC BIOMARKERS TO ASSESS THE LIVER AND METABOLIC RESPONSES ASSOCIATED WITH BIOACTIVATION MECHANISMS OF DRUG INDUCED LIVER INJURY***James Monroe, Merck Research Laboratories, West Point, PA, USA***P55 - THE IMPACT OF PLASMA PROTEIN BINDING ON THE TISSUE DISTRIBUTION OF WARFARIN - INVESTIGATION IN NAGASE ANALBUMINEMIC RATS (NAR)***Jodie Pang, Genentech, South San Francisco, CA, USA***P56 - PRECLINICAL DEVELOPMENT OF THE PI3K ALPHA SELECTIVE AND PIK3CA MUTANT SELECTIVE INHIBITOR GDC-0077 AND PREDICTION OF ITS HUMAN PHARMACOKINETICS***Jodie Pang, Genentech, South San Francisco, CA, USA***P57 - EFFECTS OF THYROPARATHYROIDECTOMY ON CLINICAL PATHOLOGY AND BONE DENSITY IN THE RAT***Dominic Poulin, Charles River, Senneville, QC, Canada***P58 - APPLICATION OF NON-STANDARD APPROACHES TO INVESTIGATIONS OF HUMAN MASS BALANCE AND METABOLITE CHARACTERISATION***Iain Shaw, Quotient Sciences Ltd, Nottingham, United Kingdom***P59 - DEVELOPMENT OF A DISCOVERY CYP INHIBITION SCREEN FOR EARLY IDENTIFICATION OF DDI LIABILITIES***Teresa Sierra, Cyprotex, Watertown, MA, USA***P60 - DEVELOPMENT OF A QUANTITATIVE BIOANALYTICAL METHOD FOR THE ASSESSMENT OF BENSERAZIDE IN PRE-CLINICAL SAMPLES***Amy Q. Wang, National Center for Advancing Translational Sciences, National Institutes of Health, Rockville, MD, USA***P61 - OPTIMIZATION OF STEPPED COLLISION ENERGIES OF HCD IN ORBITRAP MASS SPECTROMETRY FOR METABOLITE STRUCTURE ELUCIDATION***Jianwei Zhao, WuXiApptec XenoBiotic Laboratories, Plainsboro, NJ, USA*

P62 - PRECLINIAL BIOPHARMACEUTICS AND PHARMACOKINETIC CHARACTERIZATION OF AN HIV-1 REPLICATION INHIBITOR DB213

Zhong Zuo, School of Pharmacy, The Chinese University of Hong Kong, Shatin, Hong Kong

DRUG INTERACTION (P63 - P71)**P63 - LACK OF PHARMACOKINETIC INTERACTION BETWEEN SINGLE ORAL DOSES OF LETEMOVIR (MK-8228) AND FLUCONAZOLE IN HEALTHY SUBJECTS**

Adedayo Adedoyin, Merck & Co., Inc., Kenilworth, NJ, USA

P64 - EFFECTS OF ESSENTIAL OILS OF CULINARY HERBS AND SPICES ON THE CYP3A4 EXPRESSION IN PRIMARY HUMAN HEPATOCYTES AND CELL LINES

Iveta Bartonkova, Palacky University Olomouc, Faculty of Science, Department of Cell Biology and Genetics, Olomouc, Czech Republic

P65 - EVALUATION OF THE TIME-COURSE OF CYP INDUCTION AND IMPACT ON DRUG INTERACTION RISK ASSESSMENT FROM THE IQ INDUCTION WORKING GROUP

Niresh Hariparsad, Vertex Pharmaceuticals, Boston, MA, USA

P66 - THE ROLE OF NUCLEOSIDE TRANSPORTERS IN ENTECAVIR TRANSPORT ACROSS PLACENTA

Sara Karbanova, Charles University, Faculty of Pharmacy, Hradec Kralove, Czech Republic

P67 - REACTIVE METABOLITE FORMATION BY IRREVERSIBLE AND QUASI-IRREVERSIBLE CYTOCHROME P450 INHIBITORS

Jennifer Thomas, Charles River Laboratories, Wilmington, MA, USA

P68 - ATP-BINDING CASSETTE TRANSPORTERS AND CYP450 ISOFORMS ARE POSSIBLE SITES OF RIBOCICLIB DRUG INTERACTIONS

Ales Sorf, Charles University, Faculty of Pharmacy in Hradec Kralove, Hradec Kralove, Czech Republic

P69 - METHYLINDOLES AND METHOXYINDOLES ARE AGONISTS AND ANTAGONISTS OF HUMAN ARYL HYDROCARBON RECEPTOR AHR

Zdenek Dvorak, Palacky University, Olomouc, Czech Republic

P70 - GENOTYPE-SENSITIVE REVERSIBLE AND TIME-DEPENDENT CYP2D6 INHIBITION IN HUMAN LIVER MICROSOMES

Flavia Storelli, Geneva University Hospitals, Geneva, Switzerland

P71 - ASSESSMENT OF INTERACTION WITH NUCLEOSIDAL TRANSPORTERS BETWEEN ENASIDENIB AND AZACYTIDINE

Usha Yerramilli, Celgene, Summit, NJ, USA

DRUG-INDUCED LIVER INJURY (P72)**P72 - QUALIFICATION AND APPLICATION OF AN *IN VITRO* LIVER MODEL EARLY IN PHARMACEUTICAL DEVELOPMENT TO HELP DERISK DRUG-INDUCED LIVER INJURY (DILI)**

Kaushik Mitra, Merck, West Point, PA, USA

ENZYME INDUCTION (P73 - P80)**P73 - A NOVEL STRATEGY FOR CYP3A4 INDUCTION SCREENING IN DRUG DISCOVERY: USE OF HEPARG CELLS AND SIMPLIFIED RELATIVE INDUCTION SCORE METHOD.**

Yusuke Aratsu, JAPAN TOBACCO INC, Takatsuki, Japan

P74 - QUANTITATIVE PREDICTION OF CYP3A4 INDUCTION USING SIMPLE RELATIVE FACTOR APPROACH

Shino Kuramoto, Chugai pharmaceutical Co. Ltd., Kamakura, Japan

P75 - CRYOPRESERVED HUMAN INTESTINAL MUCOSA: A NOVEL *IN VITRO* 3-D ORGAN CULTURE FOR THE EVALUATION OF P450 INDUCTION IN HUMAN INTESTINES

Albert P. Li, In Vitro ADMET Laboratories Inc., Columbia, MD, USA

P76 - CHARACTERIZATION OF CYP2C INDUCTION IN CRYOPRESERVED HUMAN HEPATOCYTES AND ITS APPLICATION IN THE PREDICTION OF THE CLINICAL CONSEQUENCES OF THE INDUCTION

Mika Nagai, Kaken Pharmaceutical Co., LTD., Kyoto, Japan

P77 - REVISITING EVALUATION OF CYP2C9 AND CYP2C19 INDUCTION *IN VITRO*: POTENTIAL FOR ROBUST INDUCTION RESPONSES WITH \geq 4-DAY HEPATOCYTE EXPOSURE TIMES

David Stresser, AbbVie, Inc., North Chicago, IL, USA

P78 - RECOMMENDATIONS FOR *IN VITRO* CYP3A4 MRNA DATA ANALYSIS FOR DRUG-DRUG INTERACTION RISK ASSESSMENT FROM THE IQ INDUCTION WORKING GROUP

Donald Tweedie, Merck, West Point, PA, USA

P79 - EXPRESSION AND INDUCTION ABILITY OF CYTOCHROME P450 IN HUMAN HEPATOCYTES ISOLATED FROM CHIMERIC MICE WITH HUMANIZED LIVERS

Shotaro Uehara, Central Institute for Experimental Animals, Kawasaki, Japan

P80 - EVALUATION OF A PRE-CONSTRUCTED RELATIVE INDUCTION SCORE (RIS) CURVE FOR PREDICTION OF CYP3A4 INDUCTION RESPONSE *IN VIVO*

George Zhang, Corning Life Sciences, Woburn, MA, USA

ENZYME INHIBITION/INACTIVATION (P81 - P84)**P81 - INHIBITION OF LITHOCHOLIC ACID 3-OXIDATION BY SELECTIVE ESTROGEN RECEPTOR MODULATORS**

Sumit Bansal, National University of Singapore, Singapore, Singapore

P82 - DEVELOPMENT OF UGT1A7 AND UGT1A8 INHIBITION ASSAYS USING RECOMBINANT ENZYMES AS A TEST SYSTEM

Ritu Singh, Corning Gentest Contract Research Services, Woburn, MA, USA

P83 - INHIBITION OF UGT ENZYMES USING RECOMBINANT UGT ENZYMES FOR DDI ASSESSMENT

Guy Webber, ENVIGO, Huntingdon, United Kingdom

P84 - CHARACTERIZATION OF ANTIHYPERTENSIVE DRUGS AS POTENT INHIBITORS OF CYP2J2

Satoshi Yamaori, Shinshu University Hospital, Matsumoto, Japan

EXTRAHEPATIC METABOLISM (P85 - P87)**P85 - CRYOPRESERVED HUMAN INTESTINAL MUCOSA AS A 3-DIMENSIONAL ORGANOID CULTURE FOR THE EVALUATION OF INESTINAL DRUG METABOLISM, DRUG-DRUG INTERACTIONS, ENTEROTOXICITY, AND ENTEROPHARMACOLOGY**

Albert P. Li, In Vitro ADMET Laboratories Inc., Columbia, MD, USA

P86 - INFLUENCE OF DICHLOROACETATE TREATMENT ON THE CONTRIBUTIONS OF RODENT BRAIN, HEART, LIVER AND KIDNEY IN THE ACTIVITY OF GSTZ1*Edwin Squirewell, University of Florida, Gainesville, FL, USA***P87 - TISSUE-SPECIFIC MECHANISMS OF IRINOTECAN METABOLISM***Marc Vrana, University of Washington, Seattle, WA, USA***GOLD NANOPARTICLES (P88)****P88 - PEGYLATED CRUSHED GOLD SHELL-RADIOLABELED CORE NANOBALLS FOR IN VIVO TUMOR IMAGING WITH DUAL POSITRON EMISSION TOMOGRAPHY AND CERENKOV LUMINESCENT IMAGING***Yong Hyun Jeon, Daegu-Gyeongbuk Medical Innovation Foundation, Daegu, Korea***HEPATIC UPTAKE (P89 - P91)****P89 - UNDERSTANDING THE TRANSLATIONAL CAPABILITY OF *IN VITRO* ACTIVE HEPATIC OATP UPTAKE DATA USING PBPK MODELING***Christine Bowman, University of California, San Francisco, San Francisco, CA, USA***P90 - AN EFFICIENT HIGH THROUGHPUT 96-WELL PLATED HUMAN HEPATOCYTES ASSAY FOR DRUG UPTAKE AND UPTAKE TRANSPORTER INHIBITION***Albert P. Li, In Vitro ADMET Laboratories Inc., Columbia, MD, USA***P91 - *EX VIVO* WHOLE LIVER PERFUSION MODEL FOR PREDICTION OF DRUG-DRUG INTERACTIONS AND BILIARY EXCRETION OF ROSUVASTATIN***Evita van de Steeg, TNO, Zeist, Netherlands***HEPATOCYTES (P92 - P99)****P92 - THE COMBINED APPLICATION OF LONG TERM HEPATIC CO-CULTURE AND RNA INTERFERENCE FOR REACTION PHENOTYPING: LESSONS LEARNED***Anthony Borel, Eil Lilly and Company, Indianapolis, IN, USA***P93 - HEPATIC 3D SPHEROIDS: AN *IN VITRO* TOOL FOR STUDYING HEPATIC FUNCTION AND DRUG TOXICITY***Sujoy Lahiri, Thermofisher Scientific, Frederick, MD, USA***P94 - EFFECTIVE INHIBITION OF CYP3A4-DEPENDENT DRUG OXIDATION BY ANTI-CYP3A4 ANTIBODIES IN METMAX CRYOPRESERVED HUMAN HEPATOCYTES***Albert P. Li, In Vitro ADMET Laboratories Inc., Columbia, MD, USA***P95 - METMAX HUMAN HEPATOCYTE/HEK293 CYTOTOXICITY ASSAY FOR THE EVALUATION OF METABOLISM DEPENDENT DRUG TOXICITY AND IDENTIFICATION OF DRUG CANDIDATES FORMING CYTOTOXIC REACTIVE METABOLITES***Albert P. Li, In Vitro ADMET Laboratories Inc., Columbia, MD, USA***P96 - CYTOTOXICITY IN PRIMARY HUMAN HEPATOCYTES EXPOSED TO VARIOUS MICROCYSTIN CONGENERS***Vicki Richardson, US EPA, Research Triangle Park, NC, USA***P97 - HIGH-THROUGHPUT LIVER-ON-A-CHIP FOR PREDICTIVE HEPATOTOXICITY SCREENING***Anthony Saleh, Mimetas Inc, Gaithersburg, MD, USA***P98 - CASE STUDIES IN QUALITY LEVELS FOR *IN VITRO* ADME ASSAYS: HEPATOCYTE STABILITY***Teresa Sierra, Cyprotex, Watertown, MA, USA***P99 - ACCELERATION OF MURINE HEPATOCYTE PROLIFERATION BY IMAZALIL THROUGH THE ACTIVATION OF NUCLEAR RECEPTOR PXR***Kouichi Yoshinari, University of Shizuoka, Shizuoka, Japan***HEPATOTOXICITY (P100)****P100 - EXPANDED PRIMARY HUMAN LIVER SINUSOIDAL ENDOTHELIAL CELLS AS A PREDICTIVE TOOL IN HEPATOTOXICITY EVALUATION***Astrid Noerenberg, upcyte technologies, Hamburg, Germany***IMMUNOTOXICOLOGY (P101)****P101 - CHARACTERISING THE IMMUNE RESPONSE TO CARBAMAZEPINE: UNDERSTANDING THE DEVELOPMENT OF IDIOSYNCRATIC DRUG REACTIONS***Alison Jee, University of Toronto, Toronto, ON, Canada****IN VITRO IN VIVO* EXTRAPOLATION (IVIVE) (P102)****P102 - *IN VITRO* TO *IN VIVO* EXTRAPOLATION OF INTRINSIC CLEARANCE FOR LOW TURNOVER COMPOUNDS USING PLATED POOLED DONOR HUMAN HEPATOCYTE CO-CULTURE SYSTEMS***Faraz Kazmi, Janssen Research & Development, Spring House, PA, USA****IN VITRO* TECHNIQUES (P103 - P116)****P103 - USING STATISTICAL ANALYSES TO DEMONSTRATE EQUIVALENCY BETWEEN AUTOMATED AND MANUAL PROCESSES TO DELIVER HIGH QUALITY *IN VITRO* ADME DATA EVEN FASTER***Jakal Amin, Charles River - Worcester, Worcester, MA, USA***P104 - CHARACTERIZATION OF CISPLATIN TOXICITY IN APPROXIMATE HUMAN PROXIMAL TUBULE CELL MONOLAYERS***Colin Brown, Newcastle University, Newcastle upon Tyne, United Kingdom***P105 - DEVELOPMENT OF A NOVEL PREDICTIVE *IN VITRO* NON HUMAN PRIMATE PROXIMAL TUBULE MODEL FOR DRUG TRANSPORTER AND NEPHROTOXICITY STUDIES***Colin Brown, Newcastle University, Newcastle upon Tyne, United Kingdom***P106 - INVESTIGATING ACETAMINOPHEN COVALENT PROTEIN BINDING TO GLUTATHIONE S-TRANSFERASES BY LC-MS/MS***Timon Geib, UQAM, Montréal, QC, Canada***P107 - COMPREHENSIVE HEPATOCELLULAR DISPOSITION PROFILING OF PARENT COMPOUND AND ITS MAJOR METABOLITES IN SANDWICH-CULTURED PXB-CELLS BY D-PREX***Katsuhiko Kanda, Hitachi High-Technologies Corporation, Hitachinaka, Ibaraki, Japan***P108 - *IN VITRO* ASSESSMENT OF THE RELATIVE TOXICITY OF A SERIES OF PYRROLIZIDINE ALKALOIDS: TAKING ACCOUNT OF METABOLIC ACTIVATION AND TOXICOKINETICS***Cindy Obringer, The Procter & Gamble Company, Mason, OH, USA*

P109 - HIGH-THROUGHPUT, PERFUSED INTESTINAL TUBULES FOR REAL-TIME ASSESSMENT OF DRUG-INDUCED BARRIER DISRUPTION*John Lowman, Mimetas Inc, Gaithersburg, MD, USA***P110 - BBB-ON-A-CHIP: A 3D *IN VITRO* MODEL OF THE HUMAN BLOOD-BRAIN BARRIER***John Lowman, Mimetas, Gaithersburg, MD, USA***P111 - INTERACTIONS OF HERBAL SLIMMING AGENTS WITH CYP SUBSTRATES: AN *IN VITRO* STUDY USING HUMAN LIVER MICROSOMES***Satheeshkumar Nanjappan, National Institute of Pharmaceutical Education and Research [NIPER-HYDERABAD], Hyderabad, India***P112 - INTESTINAL ABSORPTION AND RODENT BRAIN EXPOSURE ESTIMATED BY LOW EFFLUX CELLS***Alicia Pietrasiewicz, Biogen, Cambridge, MA, USA***P113 - HIGH-THROUGHPUT KIDNEY PROXIMAL TUBULES-ON-A-CHIP FOR PREDICTIVE RENAL TOXICITY SCREENING***Anthony Saleh, Mimetas Inc, Gaithersburg, MD, USA***P114 - HUMAN *EX VIVO* MODEL TO STUDY INTESTINAL PROCESSES AND MICROBIOME INDUCED METABOLISM***Lianne Stevens, TNO, Utrecht, Netherlands***P115 - METHOD DEVELOPMENT FOR THE SOLUBILIZATION OF BIOLOGICAL MATRICES***Guy Webber, ENVIGO, Huntingdon, United Kingdom***P116 - CO-CULTURE OF PRIMARY HEPATIC STELLATE CELLS AND HEPATOCYTES IN MODELING OF LIVER FIBROSIS IN 2D AND 3D SPHEROIDS***Rafal Witek, Thermo Fisher Scientific, Frederick, MD, USA***P117 - ABSTRACT WITHDRAWN****METABOLISM (P118 - P134)****P118 - QUANTITATIVE MASS BALANCE, TISSUE DISTRIBUTION, PHARMACOKINETICS AND BIOTRANSFORMATION PATHWAY OF PRALICIGUAT, A CLINICAL-STAGE SGC STIMULATOR, AFTER ORAL ADMINISTRATION IN RATS***Ali Banijamali, Ironwood Pharmaceuticals, Cambridge, MA, USA***P119 - LAMISIL (TERBINAFINE): DETERMINING BIOACTIVATION PATHWAYS USING COMPUTATIONAL MODELING AND EXPERIMENTAL APPROACHES***Dustyn Barnette, University of AR for Medical Sciences, Maumelle, AR, USA***P120 - METABOLISM OF PEVONEDISTAT IN PATIENTS WITH ADVANCED SOLID TUMORS AFTER INTRAVENOUS INFUSION OF [14C] PEVONEDISTAT***Hao Chen, Millennium Pharmaceuticals, Inc., a wholly owned subsidiary of Takeda Pharmaceutical Company Limited, Cambridge, MA, USA***P121 - STUDYING THE METABOLISM OF SUNSCREEN COMPOUNDS *IN VITRO* BY LC-MS/MS***Amal Guesmi, UQAM, Montreal, QC, Canada***P122 - PREDICTION OF HUMAN-SPECIFIC METABOLITES OF MIANSERIN, CYPROHEPTADINE, AND CARBAZERAN USING CHIMERIC MICE WITH HUMANIZED LIVER (PXB-MICE)***Suguru Kato, Takeda Pharmaceuticals International Co., Cambridge, MA, USA***P123 - METABOLITE PROFILING USING DRIED BLOOD SPOT***Kishore Katyayan, Eli Lilly and Company, Indianapolis, IN, USA***P124 - COPE ELIMINATION MEDIATED BY HUMAN FMO1 LEADS TO FORMATION OF REACTIVE MICHAEL ACCEPTOR INTERMEDIATE***Weidong Lai, Eisai Inc., Andover, MA, USA***P125 - BIOTRANSFORMATION OF PYRROLIZIDINE ALKALOID N-OXIDE TO HEPATOTOXIC PYRROLIZIDINE ALKALOID***Ge Lin, The Chinese University of Hong Kong, Hong Kong, Hong Kong***P126 - COMPARATIVE BIOTRANSFORMATION AND MASS-BALANCE OF [14C] BMS-986205, AN INHIBITOR OF IDO1, AFTER ORAL ADMINISTRATION TO RATS, DOGS AND HUMANS***Peggy Liu-kreyche, Bristol Myers Squibb Company, Lawrenceville, NJ, USA***P127 - CONTRIBUTION OF UGT1A1, CYP2A6, CYP2C9, AND CYP3A4 IN METABOLISM OF BELINOSTAT***Gang Luo, Covance Laboratories Inc., Madison, WI, USA***P128 - UNRAVELING THE METABOLIC FATE OF POTENTIAL THERAPEUTIC DIMER COMPOUNDS FOR PARKINSON'S DISEASE***Chukwunonso Nwabufu, University of Saskatchewan, Saskatoon, SK, Canada***P129 - SEQUENTIAL METABOLISM KINETICS OF Δ 9-TETRAHYDROCANNABINOL (THC) AND ITS PSYCHOACTIVE 11-OH-THC METABOLITE***Gabriela Patilea-Vrana, University of Washington, Seattle, WA, USA***P130 - POTENTIAL EXPOSURE TO DI-2-ETHYLHEXYL TEREPHTHALATE AND DINCH, TWO PHTHALATE REPLACEMENTS, IN AMERICAN ADULTS***Manori Silva, Centers for Disease Control and Prevention, Atlanta, GA, USA***P131 - THERAPEUTIC TARGETING OF THE PYRUVATE DEHYDROGENASE COMPLEX/ PYRUVATE DEHYDROGENASE KINASE (PDC/PDK) AXIS FOR CONGENITAL AND ACQUIRED METABOLIC DISEASES***Peter Stacpoole, University of Florida, Gainesville, FL, USA***P132 - *IN VITRO* METABOLIC AND TRANSPORTER PROFILING FOR MARIBAVIR (SHP620)***Devin Welty, Shire Pharmaceuticals, Cambridge, MA, USA***P133 - QUANTITATIVE PREDICTION OF METABOLITE EXPOSURES IN HUMANS USING CHIMERIC MICE WITH HUMANIZED-LIVER***Ryosuke Watari, Shionogi & Co., Ltd., Osaka, Japan***P134 - CHARACTERIZATION OF THE CYP AND UGT ENZYMES INVOLVED IN REACTIVE METABOLITE GENERATION FROM BROMFENAC AND BROMFENAC INDOLINONE***Aprajita Yadav, MyoKardia Inc, South San Francisco, CA, USA***METABOLITE IDENTIFICATION (P135)****P135 - A FACILE CHEMICAL DERIVATIZATION METHOD TO DISCERN THE IDENTITY OF GLUCRONIDE CONJUGATES OF CARBOXYLIC ACID DRUGS UNDER MILD CONDITIONS***Kai Wang, Janssen R&D, LLC, San Diego, CA, USA*

NON-P450 PHASE I ENZYMES (P136 - P139)**P136 - THE ROLE OF REDUCTASES IN DRUG DISCOVERY AND DEVELOPMENT**

Li Di, Pfizer Inc., Groton, CT, USA

P137 - ALDEHYDE OXIDASE ACTIVITY IN HUMAN VASCULAR TISSUE AND ITS POTENTIAL CONTRIBUTION TO EXTRA-HEPATIC METABOLISM

Kirk Kozminski, Takeda Pharmaceutical Company Ltd., San Diego, CA, USA

P138 - MUTATIONS OF FLAVIN-CONTAINING MONOOXYGENASE 3 (FMO3) GENE IN JAPANESE COHORTS

Makiko Shimizu, Showa Pharmaceutical University, Machida, Japan

P139 - ELIMINATION OF [14C]LY3023414 BY ALDEHYDE OXIDASE AND CYP ENZYMES IN HUMANS FOLLOWING ORAL ADMINISTRATION

Lian Zhou, Eli Lilly and Company, Indianapolis, IN, USA

NUCLEAR RECEPTORS (P140)**P140 - PROFILING OF FLAVORED NON-ALCOHOLIC BEVERAGES TOWARD TRANSCRIPTIONAL ACTIVITY OF PPAR GAMMA USING A NOVEL REPORTER CELL LINE PAZ-PPARG**

Peter Illes, Department of Cell Biology and Genetics, Faculty of Science Palacky University Olomouc, Olomouc, Czech Republic

PESTICIDES AND RENAL CLEARANCE (P141)**P141 - EFFECT OF RENAL TRANSPLANTATION ON ORGANOCHLORINE PESTICIDE (OCPS) LEVELS IN CHRONIC KIDNEY DISEASE PATIENTS (CKD-5D): A LONGITUDINAL STUDY**

Amit Kumar, AIIMS, New Delhi, Delhi, India

PHARMACOGENETICS (P142 - P143)**P142 - MRP4 (ABCC4) IS A DETERMINANT OF OBSERVED CAPECITABINE AND ITS METABOLITE CONCENTRATIONS DURING CANCER THERAPY**

Ahmed A. Almousa, Western University, London, ON, Canada

P143 - RPL28 PROMOTER POLYMORPHISM RS4806668 IS ASSOCIATED WITH REDUCED SURVIVAL IN FOLFIRI-TREATED METASTATIC COLORECTAL CANCER PATIENTS

Adrien Labriet, Pharmacogenomics Laboratory, CHU de Quebec Research Center and Faculty of Pharmacy, Laval University, Quebec, QC, Canada

PHARMACOKINETIC MODELING (P144 - P146)**P144 - HUMAN AMYLOID-BETA 1-40 DISPOSITION AFTER INTRAVENOUS AND INTRACEREBRAL INJECTIONS IN THE RAT**

Hao Benson Peng, Leslie Dan Faculty of Pharmacy, University of Toronto, Toronto, ON, Canada

P145 - A NON-LINEAR MIXED-EFFECTS MODEL TO DESCRIBE THE POPULATION PHARMACOKINETICS OF MYCOPHENOLIC ACID AND THE EFFECTS OF CO-VARIATES IN ADULT, DE-NOVO KIDNEY TRANSPLANT PATIENTS ON STEROID-FREE ANTI-REJECTION REGIMENS

Yan Rong, Faculty of Pharmacy and Pharmaceutical Sciences, University of Alberta, Edmonton, AB, Canada

P146 - POPULATION PHARMACOKINETICS OF IMMEDIATE-RELEASE TACROLIMUS IN STEROID-FREE ADULT RENAL TRANSPLANT RECIPIENTS

Yan Rong, Faculty of Pharmacy and Pharmaceutical Sciences, University of Alberta, Edmonton, AB, Canada

PHARMACOKINETIC PREDICTION (P147 - P149)**P147 - EFFECTS OF MYCOPHENOLIC ACID AND CLINICAL VARIABLES ON TACROLIMUS EXPOSURE IN DE NOVO, STEROID-FREE ADULT RENAL TRANSPLANT PATIENTS**

Tony KL Kiang, Faculty of Pharmacy and Pharmaceutical Sciences, University of Alberta, Edmonton, AB, Canada

P148 - APPLICATION OF DMPK TOOLBOX IN PREDICTING HUMAN PHARMACOKINETICS FOR BACK-UP RIP1 INHIBITORS: LEARNINGS FROM GSK2982772 IN CLINIC

Mukesh Mahajan, GlaxoSmithKline, Collegeville, PA, USA

P149 - THE HURDLE OF HUMAN PK PREDICTIONS FOR HEPATIC OATP SUBSTRATES: LESSONS LEARNED FROM RAT ALLOMETRY

Hong Mei, Merck & Co, Inc., Kenilworth, NJ, USA

PHARMACOKINETICS AND PHARMACODYNAMICS (P150 - P155)**P150 - LC-MS/MS RAPID IDENTIFICATION OF A NOVEL TRACER FOR A SUBTYPE SPECIFIC PHOSPHODIESTERASE (PDE) WITH NO KNOWN LIGAND**

Jie Chen, Dart Neuroscience, San Diego, CA, USA

P151 - A PHARMACOKINETIC NATURAL PRODUCT-DISEASE-DRUG INTERACTION: A DOUBLE-HIT ON HEPATIC TRANSPORTERS

John Clarke, Washington State University, Spokane, WA, USA

P152 - ABSTRACT WITHDRAWN**P153 - INTEGRATING PHARMACOKINETIC-PHARMACODYNAMIC MODELING IN PRECLINICAL ASSESSMENT OF MUTANT SELECTIVE EGFR COVALENT TYROSINE KINASE INHIBITOR EGF816**

Chun Li, Genomics Institute of the Novartis Research Foundation, San Diego, CA, USA

P154 - ABSTRACT WITHDRAWN**P155 - FACTORS THAT INFLUENCE TRANEXAMIC ACID OVERDOSE IN CARDIAC SURGICAL PATIENTS WITH CHRONIC RENAL DYSFUNCTION**

Qi (Joy) Yang, Department of Pharmaceutical Sciences, Leslie Dan Faculty of Pharmacy, University of Toronto, Toronto, ON, Canada

PHYSIOLOGICALLY-BASED PHARMACOKINETICS (PBPK) (P156 - P163)**P156 - APPLICATION OF PBPK MODELING TO EVALUATE PHARMACOKINETIC DRUG-DRUG INTERACTIONS DURING THE DEVELOPMENT OF NEW ANTIMALARIAL COMBINATION THERAPIES**

Nada Abba, Medicines for Malaria Venture, Geneva, Switzerland, Geneva, Switzerland

P157 - PREDICTIVE PERFORMANCE OF SIMCYP DEFAULT MODELS OF 8 CYTOCHROME P450 MODULATORS IN DIFFERENT CLINICAL SCENARIOS.

Caroline Samer, Hôpitaux Universitaires de Genève, Geneva, Switzerland

P158 - REDUCED PARENT-METABOLITE(S) PHYSIOLOGICALLY-BASED PHARMACOKINETIC MODEL: APPLICATION TO MYCOPHENOLIC ACID

Norikazu Matsunaga, University of Manchester, Manchester, United Kingdom

P159 - SEMI-PHYSIOLOGICALLY BASED PHARMACOKINETIC MODEL ALLOWS PREDICTION OF CNS DISPOSITION OF ONO-2333MS IN HUMANS

Norikazu Matsunaga, Ono Pharmaceutical Co., Ltd., Shimamoto-cho Mishima-gun, Japan

P160 - PHYSIOLOGICALLY BASED PHARMACOKINETIC MODEL PREDICTIONS OF IVOSIDENIB (AG-120) AS A VICTIM AND PERPETRATOR OF DRUG-DRUG INTERACTIONS

Chandra Prakash, Agios, Cambridge, MA, USA

P161 - QUALITY-BY-DESIGN (QBD) APPROACH TO ADDRESS RIGOR AND REPRODUCIBILITY IN DMET QUANTITATIVE PROTEOMICS

Bhagwat Prasad, University of Washington, Seattle, WA, USA

P162 - A NOVEL 'BOTTOM-UP' PHYSIOLOGICALLY BASED PHARMACOKINETIC (PBP) MODEL OF ITRACONAZOLE AND ITS METABOLITES: THE IMPORTANCE OF ENZYME KINETICS AND PROTEIN BINDING

Luna Prieto Garcia, AstraZeneca, Mölndal, Sweden

P163 - QUANTITATIVE PREDICTION OF DRUG INTERACTION POTENTIAL BETWEEN COBICISTAT AND RUZASVIR USING A PHYSIOLOGICAL BASED PHARMACOKINETIC MODELING APPROACH

Ying-Hong Wang, Merck & Co., Inc., West Point, PA, USA

TRANSPORTERS (P164 - P186)**P164 - THE PHENOTYPING OF SOLUTE CARRIER TRANSPORTERS IN HUMAN PRIMARY HEPATOCYTES**

Yi-an Bi, Pfizer Inc, Groton, CT, USA

P165 - EQUILBRATIVE NUCLEOSIDE TRANSPORTER 1 (ENT1) FACILITATES TRANSFER OF THE ANTIRETROVIRAL DRUG ABACAVIR ACROSS THE PLACENTA

Lukas Cerveny, Faculty of Pharmacy in Hradec Kralove, Charles University, Hradec Kralove, Czech Republic

P166 - DEVELOPMENT AND VALIDATION OF AN LC-MS/MS METHOD FOR VESICLE ASSAY USING CORNING® TRANSPORTOCYTES™ HEK293-DERIVED ABC TRANSPORTER MEMBRANE VESICLES BCRP AND MRP2

Kirsten Cooper, Corning, Bedford, MA, USA

P167 - APPARENT NONCOMPETITIVE INHIBITION OF BSEP IN PRIMARY HUMAN HEPATOCYTES ASSOCIATED WITH SEVERE DRUG-INDUCED LIVER INJURY

Kan He, Biotranex LLC, Monmouth Junction, NJ, USA

P168 - EFFECTS OF PEG200 AND PEG400 ON HUMAN RENAL UPTAKE/EFFLUX TRANSPORTERS

Robert Houle, Pharmacokinetics, Pharmacodynamics & Drug Metabolism (PPDM), Merck & Co. Inc, Rahway, NJ, USA, Rahway, NJ, USA

P169 - EXPRESSION OF CONCENTRATIVE NUCLEOSIDE TRANSPORTERS (SLC28A) IN THE HUMAN PLACENTA; EFFECTS OF GESTATION AGE AND PROTOTYPE DIFFERENTIATION-AFFECTING AGENTS

Lucie Jiraskova, Charles University, Faculty of Pharmacy, Hradec Kralove, Hradec Králové, Czech Republic

P170 - AMILORIDE AS A PROBE SUBSTRATE FOR INVESTIGATION OF ORGANIC CATION TRANSPORT SYSTEM

Chisa Kaneko, Aichi Gakuin University, Nagoya, Japan

P171 - ABC XENOBIOTIC TRANSPORTERS PLAY IMPORTANT ROLES IN SYSTEMIC EXPOSURE AND DERMAL DISTRIBUTION OF TYROSINE KINASE INHIBITOR REGORAFENIB AND ITS ACTIVE METABOLITES

Yukio Kato, Kanazawa University, Faculty of Pharmacy, Kanazawa, Japan

P172 - INVESTIGATION OF HUMAN ORGANIC ANION TRANSPORTING POLYPEPTIDE 2B1 USING FLUORESCENT ANIONS

Tatsuya KAWASAKI, Aichi Gakuin University, Nagoya, Japan

P173 - QUANTITATION OF PLASMA MEMBRANE DRUG TRANSPORTERS ENABLES BOTTOM-UP PBP MODELING OF TRANSPORTER SUBSTRATES

Ryota Kikuchi, AbbVie Inc., North Chicago, IL, USA

P174 - SIMULTANEOUS MEASUREMENTS OF N1-METHYLNICOTINAMIDE, CREATININE, ISOBUTYRYL-L-CARNITINE BY LIQUID CHROMATOGRAPH WITH HIGH RESOLUTION MASS SPECTROMETRY FOR ASSESSING THE ACTIVITIES OF MULTIPLE RENAL CATIONIC TRANSPORTERS IN FIRST-IN-HUMAN CLINICAL TRIAL

Lina Luo, Pfizer Inc, Groton, CT, USA

P175 - LST-3TM12 IS PART OF THE FXR MODULATED GENE NETWORK IN HEPATOCYTES

Vanessa Malagnino, University of Basel; Department of Pharmaceutical Sciences, Biopharmacy, Basel, Switzerland

P176 - LST-3TM12 IS A MEMBER OF THE OATP1B-FAMILY AND A FUNCTIONAL TRANSPORTER INFLUENCED BY GENETIC VARIANTS

Henriette Meyer zu Schwabedissen, University of Basel; Department of Pharmaceutical Sciences, Biopharmacy, Basel, Switzerland

P177 - UTILITY AND LIMITATIONS OF DUAL CHOLATE SHUNT ASSAY IN PRECLINICAL SPECIES

Vijay More, Celgene, Scotch Plains, NJ, USA

P178 - SUBSTRATE-DEPENDENT INTERACTIONS BETWEEN NATURAL FLAVONOIDS AND DRUG TRANSPORTER OATP2B1

Tomohiro Nabekura, Aichi Gakuin University, Nagoya, Japan

P179 - ESTABLISHED CHEMICAL KNOCKOUT CONDITION FOR P-GP MEDIATED EFFLUX AT THE BLOOD-BRAIN-BARRIER IN CYNOMOLGUS MONKEY

Masanori Nakakariya, Takeda California, San Diego, CA, USA

P180 - HEPATOBILIARY TRANSPORTER EXPRESSION AND FUNCTIONAL UPTAKE OF SUBSTRATES IN 2D SANDWICH CULTURES USING UPCYTE® HEPATOCYTES

Astrid Noerenberg, upcyte technologies, Hamburg, Germany

P181 - A DIRECT COMPARISON OF ASSAY DETECTION METHODS FOR THE ASSESSMENT OF TRANSPORTER-MEDIATED DRUG INTERACTIONS

Rachel Sayer, Covance Laboratories Limited, Harrogate, United Kingdom

P182 - CHARACTERIZATION OF GCDC TRANSPORT BY HUMAN HEPATIC UPTAKE TRANSPORTERS FOR IN VITRO TESTING PURPOSES

Beata Toth, Solvo Biotechnology, Budaors, Hungary

P183 - SIMULTANEOUS ASSESSMENT OF TRANSPORTER DRUG-DRUG INTERACTIONS USING A PROBE DRUG COCKTAIL IN CYNOMOLGUS MONKEY

Manthena Varma, Pfizer Inc., Groton, CT, USA

P184 - INHIBITION OF SOLUTE CARRIER (SLC) TRANSPORTER PROTEINS USING CORNING® TRANSPORTOCELLS™ FOR DDI ASSESSMENT

Guy Webber, ENVIGO, Huntingdon, United Kingdom

P185 - TANSINONE IIA REVERSES RIFAMPICIN-INDUCED LIVER INJURY VIA ACTIVATING NRF2-MEDIATED REGULATION OF HUMAN NTCP TRANSPORTER EXPRESSION

Yujie Yang, West China School of Pharmacy, Sichuan University, Chengdu, China

P186 - UP-REGULATION OF ATP-BINDING CASSETTE TRANSPORTERS IN THE PLACENTA DURING PRE-ECLAMPSIA AND THE POTENTIAL ROLE OF NRF2

Lu Yu, West China School of Pharmacy, Sichuan University, Chengdu, China

XENOBIOTIC METABOLISING ENZYME POLYMORPHISM (P187)

P187 - ASSOCIATION OF GLUTATHIONE S-TRANSFERASE GENES (GSTM1 AND GSTT1) WITH BLOOD LEAD LEVELS IN OCCUPATIONALLY LEAD-EXPOSED WORKERS

Himani, SGT University, Gurgaon, Gurugram, India

A1 - NOVEL INSIGHTS INTO PREDICTING HEPATIC DDI LIABILITIES WHEN TRANSPORTERS AND ENZYMES ARE INVOLVED

Gabriela Patilea-Vrana and Jashvant Unadkat
University of Washington

For dual transporter/enzyme substrate drugs, the extended clearance model (ECM) can be used to predict the rate-determining step(s) (RDS) of a drug and hence predict its drug-drug interaction (DDI) liabilities (i.e. transport, metabolism, or both). We have identified that in order to predict the RDS in the hepatic clearance of a drug, contrary to conventional wisdom, the magnitude of sinusoidal uptake clearance ($CL^{s_{in}}$) as well as the metabolic-plus-biliary clearance to sinusoidal efflux clearance ratio ($CL_{met+bile}/CL^{s_{ef}}$) needs to be considered. Through theoretical simulations, we demonstrate that in order to establish sinusoidal uptake as the RDS of a drug (RDS_{uptake}) the magnitude of $CL^{s_{in}}$ needs to be considered only if the $CL_{met+bile}/CL^{s_{ef}}$ ratio ≤ 4 . Indeed, by analyzing reports of *in vitro* quantified hepatobiliary clearance, we observed that most drugs have $CL_{met+bile}/CL^{s_{ef}}$ ratio ≤ 4 , and hence in practice, the magnitude of $CL^{s_{in}}$ is important when establishing the RDS in the hepatic clearance of a drug. In order to predict when DDI's should be expected for victim drugs that are dual enzyme/transporter substrates, we defined a new metric, the $PI_{met+bile}$, as the percent inhibition of $CL_{met+bile}$ at which a significant AUC change ($AUCR \geq 1.25$) for a drug with RDS_{uptake} will start to be observed. We applied this metric to predict *in vivo* DDI's using *in vitro* published hepatobiliary data and found good agreement for atorvastatin *in vivo* predicted DDI liabilities. DDI liability predictions depend on the magnitude of $CL^{s_{in}}$ and/or the $CL_{met+bile}/CL^{s_{ef}}$ ratio, and as such, special emphasis needs to be put on quantifying $CL^{s_{ef}}$ along with $CL^{s_{in}}$ and $CL_{met+bile}$ since the $CL_{met+bile}/CL^{s_{ef}}$ ratio is one of the anchor points when establishing the RDS. Further investigation using the RDS framework identified that mislabeling of the RDS is more sensitive to quantification errors in $CL_{met+bile}$ than $CL^{s_{in}}$. If *in vitro* studies suggest that the hepatic clearance of a victim drug is determined by both metabolism and transport (RDS_{all}) but it has been mislabeled as RDS_{uptake} , then the predicted *in vivo* DDI liability due to inhibition of both transporter and metabolic activity will be underestimated. Therefore, the most conservative approach is to assume a drug has RDS_{all} , however, such an assumption would lead to an increase in negative DDI studies, particularly when conducting metabolic/biliary efflux DDI studies if the victim drug has RDS_{uptake} . In summary, we built a theoretical RDS framework and, through theoretical and practical examples, identified important factors to consider when predicting DDI liabilities for dual transporter/enzymes substrate drugs. Supported by NIDA Grant P01DA032507.

A2 - A MOUSE MODEL FOR INVESTIGATING HUMAN BRAIN CYP2D6

Edgor Cole Toledo¹, Marlaina Stocco¹, Sharon Miksys¹, Frank Gonzales², Fariba B Wadji¹, Bin Zhao¹, and Rachel F. Tyndale¹

¹University of Toronto, ²National Institutes of Health

Background: Genetically polymorphic human CYP2D6 metabolizes drugs, neurotransmitters, and neurotoxins. In addition to genetic variation, brain CYP2D is inducible, and brain CYP2D metabolism impacts response to centrally acting substrates. Injecting propranolol, a rat and human CYP2D mechanism-based inhibitor, directly into rat cerebral ventricles (icv), selectively inhibited brain, but not hepatic, CYP2D. Brain, but not plasma, drug levels were altered and behavioural-drug responses were changed. We have established a paradigm to investigate the role of human brain CYP2D6 using transgenic-CYP2D6 mice (Tg), which express both the mouse *CYP2D* and human *CYP2D6* genes. Methods: (1) Propranolol inhibition of *in vitro* CYP2D-mediated O-demethylation of dextromethorphan, a CYP2D-selective probe drug, to dextrorphan was investigated using C57BL/6 wild-type (WT) and Tg liver microsomes. (2) Propranolol inhibition of *in vivo* brain dextromethorphan O-demethylation was investigated by giving WT and Tg mice propranolol icv pre-treatment (80 μ g) 24-hours prior to intraperitoneal injection of dextromethorphan (30 mg/kg). Dextromethorphan and dextrorphan levels were assessed *ex vivo* in brain tissue and plasma, and dextromethorphan O-demethylation was assessed *in vitro* in brain membranes and liver microsomes. Results: (1) *In vitro*, propranolol inhibited dextromethorphan O-demethylation in WT and Tg ($IC_{50,WT}=0.081 \mu$ M, $IC_{50,Tg}=0.393 \mu$ M) liver microsomes, and inhibition was further increased by pre-incubation with propranolol and NADPH ($IC_{50,WT}=0.007 \mu$ M and $IC_{50,Tg}=0.059 \mu$ M), suggesting mechanism-based inhibition *in vitro*. This propranolol inhibition was dose- and time-dependent for WT ($K_{i,WT} = 6.1$ nM and $k_{inactivation,WT} = 0.20 \text{ min}^{-1}$) and for Tg ($K_{i,Tg} = 3.9$ nM and $k_{inactivation,Tg} = 0.10 \text{ min}^{-1}$). (2) *In vivo* in Tg given propranolol icv 24-hr pre-treatment, compared to Tg given vehicle pre-treatment, the brain dextrorphan/dextromethorphan ratio was decreased by 27% ($p=0.053$) and *in vitro* brain dextromethorphan O-demethylation was decreased by 33% ($p<0.05$); neither the brain dextrorphan/dextromethorphan ratio nor *in vitro* dextromethorphan O-demethylation were altered in WT (unpaired two-tailed t-test, $p>0.1$). In addition, giving propranolol icv 24-hr pre-treatment to either WT or Tg altered neither plasma dextrorphan/dextromethorphan levels nor *in vitro* hepatic dextromethorphan O-demethylation. Conclusion: *In vitro*, propranolol is a mechanism-based inhibitor of both WT and Tg liver microsomes, but *in vivo*, icv propranolol is a mechanism-based inhibitor of only Tg brain CYP2D, and not WT brain CYP2D; this suggests that *in vivo*, propranolol inhibits human brain CYP2D6 but not mouse brain CYP2Ds. This provides a novel approach to study the potential role of human brain CYP2D6 in the metabolism of centrally-acting substrates and behavioural outcomes *in vivo*.

A3 - THE DEVELOPMENT OF A CRISPR/CAS-MEDIATED PD-1 KNOCKOUT RAT MODEL TO STUDY IDIOSYNCRATIC DRUG REACTIONS INCLUDING NEVIRAPINE-INDUCED LIVER INJURY

Tiffany Cho, Antonia Wierk, Jeffrey Henderson, and Jack Uetrecht
University of Toronto

Idiosyncratic drug reactions (IDRs) are rare but serious adverse drug reactions that are specific to an individual and can lead to patient morbidity. Animal models are important tools for mechanistic studies of IDRs, but they must display the same clinical picture as those seen in patients. We have developed the first valid idiosyncratic drug-induced liver injury (IDILI) model using PD-1 deficient mice in conjunction with anti-CTLA-4 to block immune checkpoints. We hypothesize that most IDILI is immune mediated and immune tolerance, the dominant immune response in the liver, prevents most patients from getting serious IDILI. By impairing immune tolerance, we are able to unmask the potential of this mouse model and allowing us to vigorously test hypotheses of IDILI. However, there are species differences and a spectrum of sensitivity to drugs; thus, PD-1 deficient mice are not a good model for all IDRs. For example, therapeutic concentrations of clozapine cannot be achieved in mice due to CNS intolerance. Similarly, nevirapine can induce an immune-mediated skin rash in humans and rats, but not in mice due to the absence of the required sulfotransferase for its metabolism into a reactive metabolite. Using a CRISPR-Cas9 approach, we have generated a PD-1 mutant rat analogous to the mouse model to investigate the drugs that cannot be studied in mice. We hypothesize the PD-1 mutant rats will be more sensitive to drugs, such as nevirapine, compared to wild type animals in terms of incidence and severity of the skin rash and/or liver injury. Male/female Sprague-Dawley wild type and PD-1 mutant rats were treated with 0.2% w/w concentration of nevirapine in rodent meal. None of the rats developed a skin rash; however, nevirapine treatment led to delayed onset marked increases in ALT activity. Histopathological samples of the nevirapine-treated PD-1 mutant rat liver exhibited diffuse hepatitis with marked depletion of hepatocytes and active necrosis/apoptosis with the infiltration of mononuclear leukocytes. Interestingly, immunophenotyping of lymphocytes from the liver of female PD-1 mutant rats exhibit increases in CD3+CD8+ T-cells, suggesting the liver injury is mediated by cytotoxic T-cells. The finding of what appears to be liver failure in the CRISPR-mediated PD-1 mutant rats treated with nevirapine is exciting as we have the versatility to use this newly generated model to investigate the mechanism of IDILI. Although we were able to induce liver injury including piecemeal necrosis and small increases in bilirubin with amodiaquine in our impaired tolerance mouse model, we have never been able to produce liver failure. Future directions will determine if other drugs that cause IDILI in humans also cause more severe liver injury in the PD-1 mutant rat than in the PD-1 deficient mouse model. This research was supported by grants from the Canadian Institutes of Health Research (CIHR).

A4 - INTERINDIVIDUAL VARIABILITY IN HEPATIC EXPRESSION OF HUMAN SULFOTRANSFERASE 2A1: ABSOLUTE QUANTIFICATION BY LC-MS/MS PROTEOMICS AND EFFECT OF ETHNICITY, GENOTYPE, AGE AND GENDER

Mayurbhai Kathadhbhai Ladumor¹, Deepak Kumar Bhatt², Saranjit Singh¹, and Bhagwat Prasad²

¹National Institute of Pharmaceutical Education and Research (NIPER), ²Department of Pharmaceutics, University of Washington

Purpose: Sulfotransferase 2A1 (SULT2A1) is a hepatic enzyme responsible for sulfation of several drugs and endobiotics such as 25-hydroxyvitamin D₃ [1], dehydroepiandrosterone, testosterone, dihydrotestosterone, pregnenolone and amphipathic sterols bile acids, which are the catabolic end products of cholesterol metabolism. Quantitative information, including inter-individual variability, of hepatic abundance of SULT2A1 plays an important role in *in vitro-in vivo* extrapolation (IVIVE) within a physiologically based pharmacokinetic (PBPK) model. This in turn helps to predict SULT2A1-mediated drug disposition, drug-drug interactions (DDIs), etc. Our purpose was to quantify SULT2A1 protein levels in liver tissues, and to investigate the effect of age, gender, genotype and ethnicity on the abundance of the enzyme. **Method:** The study involved 194 human liver cytosol samples [paediatric (137) and adult (57)], which were classified as follows: a) *age*- neonatal (0 to 27 days; n=4), infancy (28 days to 364 days; n=17), early childhood (1 year to <6 years; n=30), middle childhood (6 years to <12 years; n=38), adolescence (12 years to 18 years; n=48) and adulthood (>18 years; n=57); b) *gender*- male (116), female (76) and unknown (2); c) *ethnicity*- Caucasian (123), African-American (29), Hispanic (4), Native American (1), Pacific Islander (1), Asian (1), and unknown background (35), and d) *genotype*- homozygous (n=3), heterozygous (n=21) and wild type allele (n=35) of rs296365, C>G genotype. All samples were handled individually. They were sequentially denatured, reduced, alkylated, digested by trypsin, desalted, and analyzed by robust LC-MS/MS method on three different days according to a published protocol [2]. Age (fetal to adults), ethnicity and genotype-dependent protein expression data were analyzed using Kruskal Wallis test, followed by Dunn's multiple comparison test. The effect of gender-dependent protein abundance was evaluated using the Mann-Whitney rank order U test, with p-value <0.05 considered as statistically significant. **Result:** Mean abundance of SULT2A1 in human liver was 1231.4 ± 696.1 pmol/mg cytosolic protein. Using age as a categorical variable, the protein abundance in adults was found to be 2.3 fold higher than neonates (p-value ≤ 0.01). For early childhood, the protein abundance was 1.5 times higher than adolescents (p-value ≤ 0.05). No gender effect was observed on protein levels (p-value > 0.05). As compared to Caucasians (1126.4 ± 55.1 pmol/mg cytosolic protein), the protein abundance values in African Americans and Hispanics

were 1017.5 ± 687.2 and 1990 ± 708.5 pmol/mg cytosolic protein, respectively (p -value > 0.05). The homozygous and heterozygous alleles showed lesser protein expression than the wild type, however, the data were not statistically significant. Conclusion: In summary, we did a detailed LC-MS/MS based quantitative analysis of the expression levels of SULT2A1 enzyme in 194 human liver tissues. Low to moderate (within 2.5-fold) inter-individual variability of the enzyme was found in liver tissues of different age groups. Statistically significant variability was not observed in gender, genotype and ethnicity groups. Yet the data are valuable in PBPK modeling for the prediction of SULT2A1 mediated xeno- or endobiotic disposition and DDI.

References:

1. Wong T et al., *Drug Metab Dispos*, (2018), dmd.117.078428.
2. Bhatt DK et al., *Drug Metab Dispos*, 45 (9), 1044-1048, (2017).

A5 - DIFFERENT MEASURES OF VARENICLINE ADHERENCE, NICOTINE METABOLITE RATIO AND SMOKING ABSTINENCE

Annie R. Peng¹, Robert Schnoll², Caryn Lerman², and Rachel F. Tyndale¹

¹University of Toronto, ²University of Pennsylvania

Background: Medication adherence is associated with positive outcomes. In smoking cessation trials, pill counts have traditionally been used as an indirect measure of adherence; very few studies have examined the use of a biological measure. We hypothesize: (1) salivary varenicline levels will not correlate with self-reported pill count, (2) adherence based on varenicline levels, but not self-reported pill count, will be predictive of smoking abstinence, and (3) among those treated with varenicline, the association between nicotine metabolite ratio (NMR), a genetically informed biomarker of nicotine clearance, and smoking abstinence will be stronger in adherent individuals as defined by salivary varenicline levels. Methods: Baseline blood NMR, Week 1 salivary varenicline levels, 3-, 7- and 14-day self-report pill counts, and multiple measures of biochemically-verified abstinence (exhaled carbon monoxide CO, salivary cotinine COT) were assessed in the varenicline arm of a smoking cessation trial (N=376) (NCT01314001). Receiver operating characteristic curve and logistic regression analyses were conducted to examine the relationship among adherence measures and between these measures and abstinence. Results: 3-, 7-, and 14-day pill counts were highly correlated with each other, but very weakly correlated with salivary varenicline levels (Spearman's rhos ranging from .10 to .15, p 's $\leq .05$), and were not significant discriminators of adherence based on salivary varenicline levels. Salivary varenicline, but not pill counts, correctly classified Week 1 abstinence using CO and COT-verified abstinence (area under the curve [AUC] ranging from .59 to .61, p 's $\leq .008$). Salivary varenicline levels were significant predictors of abstinence at Week 1 (odds ratio [OR] ranging from 2.75 to 3.16, p 's $< .001$). In contrast, when using a traditional cut-point of 80% of pills taken in the preceding 3, 7, or 14 days (as determined by pill count) to classify adherence, there were no statistical differences in Week 1 abstinence rate between adherent and non-adherent individuals (ORs ranging from 1.40 to 2.96, p 's $\geq .05$). Salivary varenicline levels, but not pill counts, were significant predictors of abstinence 6 months following treatment. Normal metabolizers of nicotine (NMR ≥ 0.31) were significantly more likely to be abstinent at end-of-treatment (EOT) in adherent individuals determined by varenicline levels (OR 2.00, 95% CI 1.23-3.24, $p=.005$), but not by self-reported pill counts (ORs ranging from 1.27 to 1.36, $p \geq .18$). Conclusions: The concordance between pill counts and salivary varenicline levels is poor; pill counts did not predict abstinence while varenicline levels did. Amongst adherent individuals by drug levels, normal metabolizers of nicotine have higher abstinence rates than slow metabolizers. Proper assessment of medication adherence may enhance our ability to identify individuals who may experience difficulties quitting, and improve pharmacogenomics associations with outcomes.

A6 - DOES PLASMA MEMBRANE AND TOTAL TRANSPORTER ABUNDANCE DIFFER BETWEEN SUSPENDED, PLATED, SANDWICH CULTURE HEPATOCYTES AND HUMAN LIVER TISSUE?

Vineet Kumar¹, Laurent Salphati², Cornelis E. C. A. Hop², Christopher Rowbottom³, Guangqing Xiao³, Yurong Lai⁴, Anita Mathias⁴, and Xiaoyan Chu⁵, W. Griffith Humphreys⁶, Mingxiang Liao⁷, Laigao Chen⁸, Scott Heyward⁹, and Jashvant Unadkat¹⁰

¹University of Washington, ²Genentech, Inc., ³Biogen, Inc., ⁴Gilead Sciences, Inc., ⁵Merck & Co., ⁶Bristol-Myers Squibb, ⁷Takeda Pharmaceuticals International, Inc., ⁸Pfizer Inc., ⁹BioIVT, ¹⁰University of Washington

Purpose: Different types of human hepatocyte models are used for *in-vitro* to *in-vivo* extrapolation (IVIVE) of hepatobiliary drug clearance. *In-vitro* transporter-mediated hepatic uptake clearance is usually estimated using suspended (SH) or plated hepatocytes (PH), whereas sandwich cultured hepatocytes (SCH) are used to estimate biliary clearance (CL_b) of drugs. In doing so, an implicit assumption made is that total or plasma membrane transporter abundance does not differ between these models or from that in the liver tissue. Moreover, we and others have reported that total membrane abundance of transporters observed in liver tissue is reduced when hepatocytes are cultured. However, none of these studies systemically compared the total and plasma membrane abundance of transporters between all three hepatocyte models and whether this differs from that in the liver tissue from which the hepatocytes were isolated. Here we report data

on total and plasma membrane abundance of transporters in human liver tissue (HLT), SH, PH and SCH. Methods: HLT and cryopreserved human hepatocytes isolated from the respective donors (n=4) were donated by BioIVT. HLT (~100 mg) was homogenized in a bead homogenizer @ 4°C in extraction buffer II (2 mL) and the homogenate was mixed with 2 mL of 2% SDS. Cryopreserved hepatocytes were thawed and suspended in standard Hank's Balanced Salt Solution for one hour. PH and SCH were plated (0.35 million hepatocytes/well in 24-well collagen coated plate, SCH matrigel-collagen cultured) for 5 hours and 4 days respectively. Then, SH, PH and SCH were treated with extraction buffer II (ProteoExtract native membrane extraction kit, Calbiochem) and 2% SDS (1:1). In all the above homogenates, the total cell abundance of OATP1B1/2B1, OCT1, OAT2, MRP3, MRP2, P-gp and BSEP was quantified by LC-MS/MS. Plasma membrane abundance of transporters in SH, PH and SCH was quantified using our previously published quantitative cell-surface biotinylation method. The Tukey multiple comparison test was used to compare transporter abundance between SH, PH, SCH and HLT. Results and conclusion: Total abundance of OATP1B1/2B1, OCT1, and OAT2 was not significantly different between HLT, SH, PH and SCH (Fig. 1). In contrast, total abundance of the efflux transporters MRP2, MRP3, BSEP and P-gp was significantly greater (P<0.005) in SCH than in HLT, SH or PH (except BSEP). Percent abundance of P-gp and MRP3 in the plasma membrane was significantly (P<0.05) higher in SCH (57.5±10.9, 69.3±5.7) than in PH (30.9±8.1, 53.9±8.1) or SH (27.4±6.4, 53.6±4.1). For some of the remaining transporters, minor differences were observed in percent plasma membrane abundance between SH, PH and SCH. Assuming that the quantified transporters are functional, these data suggest that any of the hepatocyte models can be used to predict hepatic uptake clearance of drugs but SCH are most suitable for estimation of CL_b, though this is likely to be over-predicted. IVIVE of transporter-mediated efflux clearance using different human hepatocyte models, without accounting for quantitative transporter abundance, could be erroneous.

This work was supported in part by the Simcyp Grant & Partnership Scheme and UWRAPT funded by Genentech, Biogen, Gilead, Merck, Bristol-Meyers Squibb, Pfizer and Takeda.

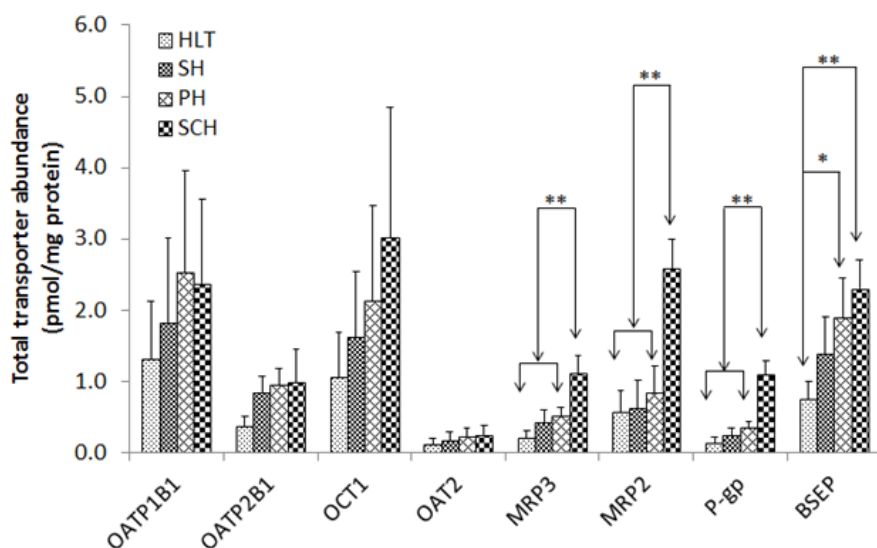


Fig. 1. Total transporter abundance in human liver tissue (HLT), suspended (SH), plated (PH) and sandwich cultured human hepatocytes (SCH) from the same donor.

**p<0.005; *p<0.01, data are shown as mean±SD, n=4

A7 - N-ACETYLATION CAPACITY OF N-ACETYLTRANSFERASE 2 IN HUMAN PERIPHERAL BLOOD MONONUCLEAR CELLS REGULATED BY NAT2 GENOTYPE AND SIRTUIN 1

Raul A. Salazar-Gonzalez¹, Eneida Turijan-Espinoza², David W Hein¹, Rosa C Milan-Segovia², and Diana P Portales-Perez²

¹University of Louisville; ²Universidad Autonoma de San Luis Potosi

N-acetyltransferase 2 (NAT2) catalyzes biotransformation of numerous arylamine and hydrazine drugs and xenobiotics. Genetic polymorphisms of NAT2 modify drug efficacy and toxicity as well as diseases related to xenobiotic exposures. *N*-acetyltransferase 2 enzymatic activity has been reported primarily in the liver and intestinal tract in humans.

Acetylation/deacetylation of cytosolic proteins is a Post Translational Modification (PTM) important in the regulatory networks of diverse cellular processes. Sirtuins (SIRT) as protein deacetylases may have a regulatory role on *N*-acetyltransferase 2 expression or *N*-acetylation capacity. The aim of the present study is to investigate the expression of NAT2 and SIRT1 in human Peripheral Blood Mononuclear Cells (PBMC). PBMCs were obtained from healthy subjects and cryoplatable human hepatocytes from a commercial vendor. NAT2 genotyping was carried out by Taqman allele-specific discrimination assay and NAT2 catalytic activity was determined by high performance liquid chromatography

(HPLC) using multiple concentrations of NAT-specific substrates isoniazid (INH) and sulfamethazine (SMZ). SIRT1 regulation of NAT2 enzymatic activity was evaluated with an SIRT1 activity enhancer (SRT1720) and silencer (anti-SIRT1 small interfering RNA). NAT2 and SIRT1 proteins were identified on PBMC with expression more prevalent on CD3+ cells, compared to other major cell subpopulations evaluated (CD19+, CD56+). NAT2 *N*-acetylation capacity V_{max} (rapid>intermediate>slow) was NAT2-genotype dependent. Individuals with rapid acetylator NAT2 genotype showed an apparent INH K_M of $14.1 \pm 2.7 \mu\text{M}$ and a V_{max} of $42.1 \pm 2.4 \text{ nM N-acetyl-INH/24h/million cells}$; individuals with intermediate acetylator NAT2 genotypes showed an apparent K_M of $11.7 \pm 3.6 \mu\text{M}$ and a V_{max} of $22.6 \pm 2.2 \text{ nM N-acetyl-INH/24h/million cells}$; and individuals with slow acetylator NAT2 genotypes showed an apparent K_M $19.7 \pm 5.2 \mu\text{M}$ and a V_{max} $19.9 \pm 1.7 \text{ nM N-acetyl-INH/24h/million cells}$. The apparent V_{max} in intermediate, and slow NAT2 genotypes was significantly lower compared to rapid acetylator NAT2 genotypes ($p < 0.001$, $p < 0.0001$ respectively). *N*-acetylation capacity of NAT2 in the presence of SIRT1 enhancer was significantly decreased compared to untreated cells ($p < 0.001$). Conversely, the SIRT1 silencing resulted in an increase of the *N*-acetylation activity of NAT2 ($p < 0.001$). These effects of SIRT1 enhancers and silencers on NAT2 activity were confirmed in cryopreserved human hepatocytes. This constitutes the first report of NAT2-expression in human PBMC regulated by both NAT2 genotype and SIRT1.

A8 - STEROIDAL ANTI-ANDROGENS INHIBIT LITHOCHOLIC ACID SULFONATION AND INCREASE LITHOCHOLIC ACID-INDUCED TOXICITY IN A HUMAN HEPATOCELLULAR CARCINOMA CELL MODEL

Siew Ying Wong, Yvonne Wan Xin Ng, and Aik Jiang Lau
National University of Singapore

Lithocholic acid (LCA), a toxic bile acid, is conjugated to glycine to form glycolithocholic acid (G-LCA) or to taurine to form tauroolithocholic acid (T-LCA). Sulfotransferase 2A1 (SULT2A1) not only plays an important role in LCA sulfonation, but it is also responsible for the metabolism of many drugs, including abiraterone, a steroidal anti-androgen drug used in prostate cancer treatment. Therefore, we determined whether steroidal anti-androgens, namely abiraterone acetate (pro-drug), abiraterone (active metabolite), and galeterone, inhibit SULT2A1-catalyzed sulfonation of LCA, G-LCA, and T-LCA, as quantified by ultra-high performance liquid chromatography-tandem mass spectrometry. Sulfonation of LCA, G-LCA, and T-LCA by human liver cytosol exhibited substrate inhibition, with apparent K_m of 0.6 ± 0.3 , 1.8 ± 0.4 , and $1.1 \pm 0.3 \mu\text{M}$, and V_{max} of 143 ± 32 , 803 ± 113 , and $324 \pm 52 \text{ pmol/min/mg protein}$, respectively. G-LCA sulfonation yielded the greatest catalytic efficiency (V_{max}/K_m), followed by T-LCA sulfonation and LCA sulfonation. Abiraterone acetate, abiraterone, and galeterone inhibited human liver cytosolic LCA, G-LCA, and T-LCA sulfonation in a similar pattern, with average IC_{50} values of 0.4 - $1.1 \mu\text{M}$. Enzyme inhibition kinetic analysis indicated that abiraterone acetate, abiraterone, and galeterone inhibited LCA sulfonation by non-competitive mode with apparent K_i of 0.6 ± 0.1 , 0.6 ± 0.1 , and $0.7 \pm 0.1 \mu\text{M}$, respectively. Comparing our experimentally-determined K_i values with the reported plasma drug concentrations (C_{max}) in humans, galeterone yielded a C_{max}/K_i ratio of 3.9, implying a high likelihood of *in vivo* inhibition of LCA sulfonation. To determine whether this inhibition of LCA sulfonation by galeterone affects LCA-induced hepatotoxicity, subsequent experiments were conducted in SULT2A1-expressing human hepatocellular carcinoma cells (HepG2). *In situ* incubation of HepG2 cells with LCA resulted in LCA sulfonation. HepG2-catalyzed LCA sulfonation followed substrate inhibition kinetics and yielded an apparent K_m of $30.7 \pm 0.7 \mu\text{M}$, V_{max} of $27.2 \pm 4.3 \text{ pmol/min}$, and catalytic efficiency (V_{max}/K_m) of $0.9 \mu\text{l/min}$. Abiraterone acetate and galeterone decreased HepG2-catalyzed LCA sulfonation in a concentration-dependent manner with an IC_{50} of 4.3 ± 0.7 (maximum inhibition of 40%) and $9.0 \pm 2.3 \mu\text{M}$ (maximum inhibition of 80%), respectively. Cell viability and cytotoxicity assays indicated that LCA ($200 \mu\text{M}$), but not LCA sulfate (10 - $200 \mu\text{M}$), depleted cellular ATP level by 54% and increased lactate dehydrogenase release by 4-fold after 24 h treatment in HepG2 cells, indicating that LCA sulfonation is a detoxification pathway. Interestingly, co-incubating LCA with varying concentrations of galeterone in HepG2 cells enhanced cellular toxicity by 3-5-fold and decreased formation of LCA sulfate in the same wells/experimental conditions, suggesting accumulation of cytotoxic LCA and enhanced toxicity as a result of SULT2A1 inhibition by galeterone. In conclusion, abiraterone acetate, abiraterone, and galeterone are potent inhibitors of LCA sulfonation and this inhibition leads to increased LCA toxicity. Our findings indicate interactions between steroidal anti-androgens and endogenous LCA, suggesting the possibility of LCA-induced hepatotoxicity in patients with high levels of LCA (e.g. cholestasis) and taking a steroidal anti-androgen.

A9 - COMPARATIVE CHANGES IN RENAL GENE EXPRESSIONS IN CHRONIC KIDNEY DISEASE AND VITAMIN D DEFICIENT MOUSE MODELS

Keumhan Noh, Qi Joy Yang, Holly P. Quach, and K. Sandy Pang
Department of Pharmaceutical Sciences, Leslie Dan Faculty of Pharmacy, University of Toronto

Patients with chronic kidney disease (CKD), characterized by reduced renal function and inflammation, also exhibit vitamin D deficiency with low levels of 1,25-dihydroxyvitamin D₃ [1,25(OH)₂D₃], the active vitamin D receptor (VDR) ligand, due to impaired renal 1 α -hydroxylase (CYP27B1) activity for 1,25(OH)₂D₃ formation. Under normal conditions, high levels of 1,25(OH)₂D₃ induce the degradation enzyme (CYP24A1) and inhibit CYP27B1 to avoid 1,25(OH)₂D₃ accumulation; under vitamin D deficiency, the low levels of 1,25(OH)₂D₃ would be accompanied by low CYP24A1 but high CYP27B1

expression levels. Although low $1,25(\text{OH})_2\text{D}_3$ levels are found in CKD, it is unclear whether vitamin D deficiency could lead to kidney damage. Our aims were to examine whether vitamin D deficiency would lead to kidney damage and whether genes were altered for vitamin D-deficient and CKD mice. We compared the changes in expression of transporters, enzymes and nuclear receptors as well as renal injury biomarkers between male C57BL/6 mice that underwent 5/6 nephrectomy to induce CKD vs. sham-operated mice at 2 weeks after surgery (purchased from Charles River, QC), and between vitamin D sufficient and deficient mice after feeding a vitamin D sufficient or deficient diet for 8 to 11 weeks. Plasma and kidney samples were harvested for measuring relative mRNA expressions of enzymes, transporters, and nuclear receptors in kidney using real-time qPCR. We observed elevated relative mRNA expression levels of renal injury markers such as Ngal (neutrophil gelatinase-associated lipocalin), Kim-1 (kidney injury molecule-1) and Col1a1 (collagen 1a1, marker of renal fibrosis), and inflammatory cytokines, including interleukin-6 (IL-6) and tumor necrosis factor alpha (TNF- α) in the CKD mice compared to age-matched sham-operated controls due to the up-regulation of transforming growth factor beta 1 (TGF- β 1) and NF- κ B, respectively, in the kidney. However, no notable change in renal injury nor the inflammation markers was observed in vitamin D deficient mice nor the vitamin sufficient controls. Moreover, patterns of up- or down-regulation were evident for VDR-targeted genes in the kidneys of both CKD and vitamin D deficiency mice, although different genes were altered. There was significant inhibition of renal Cyp24a1 but induction of Cyp27b1 mRNA expression in vitamin D-deficient mice, due to feedback control of low circulating $1,25(\text{OH})_2\text{D}_3$ levels whereas CKD mice showed increased renal Cyp24a1 but unchanged Cyp27b1 mRNA expression. Furthermore, the mRNA expressions of most of solute carrier (Slc) and solute carrier organic anion (Slco) transporters were significantly reduced (21-71%) in CKD mice compared to sham-operated controls, whereas only Oat3 mRNA expression was decreased (51%) in vitamin D deficient mice in comparison to vitamin D sufficient mice. Cyp3a11 mRNA expression was significantly increased in both CKD and vitamin D deficient mice. In conclusion, different patterns in gene and cytokine expression levels were observed in kidney between CKD and vitamin D deficient mice. There was no common mechanism that connects renal impairment to vitamin D deficiency.

A10 - AMELIORATING EFFECT OF BAICALIN IN CADMIUM INDUCED KIDNEY FIBROSIS

Manushi Siddarth, Diwesh Chawla, Alpana Raizada, Basu Dev Banerjee, and Meera Sikka
University College of Medical Sciences (University of Delhi) & GTB Hospital

Cadmium (Cd) is the ubiquitous industrial and environmental pollutant that induces a broad range of dysfunction in humans¹. The main target organ for cadmium is the kidney, due to its retention in proximal tubular cells (PTCs)². A growing volume of evidence have indicated the adverse renal effects of cadmium exposure even at low levels, causes a generalized dysfunction of the proximal tubule characterized by polyurea. Baicalin is a naturally occurring plant flavonoid found in the dry roots of the Chinese herb *Scutellaria baicalensis Georgi*. It has been reported to have a wide range of pharmacological properties³. Therefore, we carried out this study to investigate the effect of baicalin on cadmium-induced toxicity in the human renal proximal tubular epithelial cells (HK-2). HK-2 cells (CRL-2190, ATCC, USA) were treated with 2.5 μM concentration of cadmium nitrate (Sigma, USA) for 24 hrs. Reactive oxygen species (ROS) generation was determined by using fluorescent probe dihydrodichlorofluorescein diacetate ($\text{H}_2\text{DCF-DA}$). Transforming growth factor- β 1 (TGF- β 1), Smad 2, Smad 3, Smad 4, Snail and EMT markers (E-cadherin, α -SMA and fibronectin) expression were analyzed by quantitative Real Time PCR and western blotting. Cells used in the therapeutic studies were pretreated with Baicalin (5 μM) for 2hr, prior to incubation with cadmium nitrate. Cadmium nitrate significantly increased the ROS production at 2.5 μM concentration in HK-2 cells. Cadmium nitrate significantly increased TGF- β 1 expression (3.5 fold) and activated the TGF- β pathway by increasing Smad 2 (2 fold), Smad 3 (2.5 fold) and Smad 4 (2.4 fold) expression. Western blotting results revealed that cadmium nitrate significantly increased TGF- β 1 protein expression and its downstream protein molecules i.e. p-smad2/3, smad 4. Cadmium also induces protein level of mesenchymal markers i.e. α -SMA and fibronectin and decreased the protein level of epithelial marker E-cadherin. The expression of EMT-associated transcription factor snail and slug significantly induced by cadmium treatment in HK-2 cells. Pretreatment with baicalin reduced significantly the cadmium induced ROS generation approx 60% in HK-2 cells. Baicalin suppresses the cadmium-induced activation of TGF- β 1 expression and its downstream protein smad2/3 protein activation in HK-2 cells. Also, attenuates the expression of mesenchymal markers and transcription factor snail and slug in cadmium-induced HK-2 cells. Our findings concluded that cadmium-induced increased ROS generation activates the TGF- β pathway, which subsequently induce the EMT in renal tubular cells. Baicalin may protect against renal fibrosis, potentially via inhibition of TGF- β 1 production and its downstream signal transduction.

References:

1. Järup and Åkesson, Toxicol. Appl. Pharmacol. 2009, 238, 201-208.
2. Hellström et al, Am. J. Kidney Dis. 2001, 38, 1001-1008.
3. Wu et al, Ren. Fail. 2015, 37,285-291.

A11 - A PHYSIOLOGICALLY BASED PHARMACOKINETIC MODEL (PBPK) UTILIZING SPECIFIC MUSCLE TISSUE FOR INTRAMUSCULAR INJECTION OF THERAPEUTIC PROTEINSTimothy Chow¹, Matthew R. Wright², Cornelis E.C.A. Hop², and Harvey Wong¹¹University of British Columbia; ²Genentech

Therapeutic proteins continue to represent an important class of medicines for many indications. Unlike small molecule drugs, which are commonly administered orally, therapeutic proteins have not been formulated to allow oral administration due to denaturation in the stomach, proteolytic degradation within the gastrointestinal (GI) tract and minimal absorption through the GI epithelium. Several physiologically-based pharmacokinetic models (PBPK) have been developed for intravenous (IV), and subcutaneous (SC) injections but there has been a paucity of work for intramuscular (IM) injections. The objective of this study was to propose a novel PBPK model for IM administration with a specific muscle dosing site. PBPK models for all administration routes available in the literature have regarded muscle as a single organ in the body; however, anatomically the body is composed of many discrete muscle groups. Clinically, IM is administered to a specific muscle. PBPK models reported in the literature have used physiological parameters based on total muscle in the body. Our model represents the specific muscle of the IM dosing site using relevant physiological values. Systemic pharmacokinetics was modeled using compartmental modeling. A set of ordinary differential equations (ODE's) were used to mathematically describe the rate and extent of therapeutic drug pharmacokinetics. The ODE's were simulated and analyzed using SAAMII computer program (TEG, Virginia). The plasma concentration vs. time profiles of the following 7 therapeutic proteins have been reported after an IM dose in humans: alafcept, scorpion antivenom, human chorionic gonadotropin, interferon, mepolizumab, natalizumab, follicle-stimulating hormone. These represent a diverse group of seven therapeutic proteins ranging from 30 to 149 kDa from 6 different protein classes. Moreover, these clinical observations represent diversity in the muscle tissue of the IM dosing site: alafcept and scorpion antivenom were injected into the arm muscle; follicle-stimulating hormone and human chorionic gonadotropin were injected into the glute muscle; and interferon, mepolizumab, and natalizumab were injected into the thigh muscle. These therapeutic proteins served as the clinically observed values to evaluate our model. Plasma concentration-time profiles were simulated using the model under comparable conditions to where clinically observed values were obtained. We compared our model with the total muscle approach reported in the literature. Pharmacokinetic parameters C_{max} , t_{max} , and $AUC_{0-\infty}$ were calculated using non-compartmental analysis for both specific muscle and total body muscle PBPK model approaches. The prediction performance of specific compared to total body muscle was quantified using Mean Fold Error analysis. In almost all instances the prediction performance of our specific muscle IM PBPK model was comparable or better to the total muscle approach.

A12 - RELATIVE ACTIVITY FACTOR (RAF)-BASED SCALING OF UPTAKE CLEARANCE OF OATP1B SUBSTRATES FROM TRANSFECTED CELL SYSTEMS TO HUMAN HEPATOCYTES AND TO *IN VIVO*Saki Izumi¹, Yoshitane Nozaki¹, Takafumi Komori¹, Kazuya Maeda², Hiroyuki Kusuhara², and Yuichi Sugiyama³¹Eisai Co., Ltd., ²Graduate School of Pharmaceutical Sciences, University of Tokyo, ³RIKEN Innovation Center, Research Cluster for Innovation, RIKEN

Purpose: To identify drug candidates with pharmacokinetic/pharmacodynamic properties fitted in intended therapeutic areas. Prediction of human pharmacokinetic profiles is routinely performed at the preclinical stage. *In vitro-in vivo* extrapolation (IVIVE), based on the uptake clearance in human hepatocytes, has been used practically to estimate the hepatic clearance of organic anion transporting polypeptide (OATP) 1B substrates. In the present study, we focused on the relative activity factor (RAF) approach to extrapolate uptake clearance of OATP1B substrates from transporter-transfected cell systems to human hepatocytes, and also to *in vivo*.

Method: In the extrapolation of uptake clearance from transfected cells to human hepatocytes, the uptake of 14 OATP1B substrate drugs (atorvastatin, bosentan, cerivastatin, fexofenadine, fluvastatin, glibenclamide, irbesartan, nateglinide, pitavastatin, pravastatin, rosuvastatin, telmisartan, torasemide, and valsartan) into OATP1B1- and OATP1B3-transfected HEK293 cells, and 2 batches of cryopreserved human hepatocytes (suspensions) was evaluated. RAF values for OATP1B1 (RAF_{1B1}) and OATP1B3 (RAF_{1B3}) were determined by using estrone-3-sulfate and cholecystokinin-8 as respective reference substrates. RAF-based uptake clearance, extrapolated from the transfected cells, was compared with active uptake clearance observed in human hepatocytes. To directly extrapolate OATP1B1-mediated uptake activity to *in vivo*, one of the OATP1B substrates was set as a reference probe for OATP1B1; and, RAF_{1B1,vivo} was calculated by relating the uptake clearance in OATP1B1-transfected cells to the overall hepatic intrinsic clearance observed *in vivo* (CL_{int,all,vivo}). All combinations of the reference and test compounds were assessed to find an OATP1B1 reference compound that performed acceptably.

Results: All test compounds showed a temperature-dependent uptake in 2 batches of human hepatocytes. In transfected cells, OATP1B1- and OATP1B3-mediated uptakes were observed in all compounds except for telmisartan. In the extrapolation from transfected cells to human hepatocytes, RAF-based net uptake clearance, mediated by OATP1B1 and OATP1B3 were mainly accounted for by OATP1B1 (>72%), and fell within a 3-fold active uptake clearance observed in human hepatocytes in 11 out of 13 compounds (excluding telmisartan), thus indicating that the RAF approach provides a

quantitative index for OATP1B-mediated uptake clearance in human hepatocytes. Since the major contribution of OATP1B1 was suggested in the hepatic uptake of the test compounds, OATP1B1-mediated uptake clearance in transfected cells was directly related to $CL_{int,all,vivo}$ to calculate $RAF_{1B1,vivo}$ for all test substrates. When 6 compounds (irbesartan, fexofenadine, atorvastatin, bosentan, rosuvastatin, and torasemide) were used as a reference probe of OATP1B1, $CL_{int,all,vivo}$ was estimated within a 3-fold threshold for at least 8 out of 13 drugs, which was favorable compared with the predicted performance of IVIVE based on the hepatocyte uptake clearance.

Conclusions: The present study recommends the RAF approach as a first screening tool to extrapolate uptake clearance of OATP1B substrates from transfected cells to human hepatocytes, and also to *in vivo*. The RAF approach allows for the earlier estimation of hepatic clearance of OATP1B substrates, which will be helpful for optimizing the pharmacokinetic properties of OATP1B substrates at the preclinical stage of drug development.

P1 - COVALENT BINDING OF TRIMETHOPRIM: IMPLICATIONS FOR TRIMETHOPRIM-INDUCED ADVERSE REACTIONS

Yanshan Cao and Jack Uetrecht
University of Toronto

Background: Circumstantial evidence suggests that most idiosyncratic drug reactions (IDRs) are caused by a chemically reactive metabolite of the drug covalently binding to proteins. Two common targets of these reactions are the skin and the liver. The liver is the primary site of metabolism and formation of reactive metabolites; in contrast there is limited metabolism in the skin but it does have high sulfotransferase activity. Hence the mechanism of drug-induced adverse reactions may be different between the two organs. We chose to study trimethoprim (TMP), an effective antibacterial agent commonly used in combination with sulfamethoxazole. The combination is associated with high incidences of adverse reactions that are usually attributed to sulfamethoxazole; however, treatment with TMP alone is also known to cause severe skin reactions and possibly mild liver injury. TMP is known to be metabolized to a benzylic alcohol, which can potentially form a reactive sulfate. TMP is also known to form a reactive quinone methide. These potential reactive metabolites may potentially bind to proteins.

Methods: Female and male Sprague Dawley rats were treated with TMP (0.2% in rat chow) for 14 days. In addition, female Brown Norway rats were treated with 450 mg/kg/day of TMP or TMP-ketone by gavage for 3 days. Covalent binding of the drug to liver and skin proteins was studied using a Western blot with anti-TMP antibodies. In vitro experiments were performed with the S9 liver fraction and epidermal skin proteins isolated from Sprague Dawley rats. TMP, hydroxy-TMP, TMP-ketone or TMP-sulfate was incubated with liver or skin homogenate and covalent binding was studied using Western blotting.

Results: Covalent binding to hepatic proteins was observed with no significant difference between female and male Sprague Dawley rats. In the female Brown Norway rats, covalent binding in the liver was observed in the rats treated with TMP but not with TMP-ketone. That suggests that most of the binding was not due to the benzylic sulfate. Significant covalent binding of TMP to epidermal skin proteins in the treated animals was not observed. In vitro, TMP-sulfate was sufficiently reactive to covalently bind to epidermal skin proteins and liver homogenate. In vitro there was binding of hydroxy-TMP to liver proteins, presumably due to the sulfate conjugate. In summary, TMP appears to form 2 reactive metabolites: a quinone methide and a benzylic sulfate. Most of the covalent binding in the liver is due to the quinone methide, and although the sulfate is reactive, significant covalent binding was not observed in the skin. Binding in the skin may require a sulfotransferase not present in the skin of rats.

P2 - ESTABLISHMENT OF ALBUMIN-DEFICIENT NOG MICE AS A USEFUL MODEL FOR DRUG DISCOVERY RESEARCH

Hiroshi Suemizu, Yasuhiko Ando, Masafumi Yamamoto, Yoneda, Motohito Goto, Shotaro Uehara, and Riichi Takahashi
Central Institute for Experimental Animals

To overcome species differences in pharmacokinetics, we developed an experimental mouse model with a liver reconstituted with human hepatocytes (humanized-liver; Hu-liver) in thymidine kinase transgenic NOG (TK-NOG) mice. However, because of the presence of a large amount of mouse serum albumin in highly humanized liver chimeric mice, it is difficult to analyze drug-protein (human serum albumin) binding, which affects pharmacokinetics and toxicity. In the present study, we established immunodeficient NOG mice lacking the albumin gene in order to develop a humanized model of drug-protein binding. To establish an immunodeficient strain, albumin-deficient mice (B6; 129S5-*Alb^{tm1Lex}/Mmucd*) were backcrossed with NOG mice. After backcrossing up to the eighth generation, sister-brother mating took place, and albumin gene-deficient homozygotes were selected by PCR genotyping. After the third generation, 16 offspring obtained by sister-brother mating with heterozygotes, we observed the phenotype of the albumin gene-deficient mice. The results of PCR genotyping (7 of 16 mice were homozygotes) revealed that homozygous deletion for the albumin gene was not lethal. Serum albumin levels in the heterozygous and wild type mice were > 2.2 g/dL; in contrast, serum albumin levels in the homozygous mice were < 0.008 g/dL. Following this, backcrossing was performed up to the eighth generation, and the NOG-Alb KO strain was established. We confirmed that NOG-Alb KO strain was deficient in serum albumin (< 0.0006 g/dL). Currently, the NOG-Alb KO mice are being crossed with TK-NOG mice to create albumin-deficient humanized-liver chimeric mice. We hope that these chimeric mice, having a humanized drug-protein binding capability, become a useful animal model for human pharmacokinetics and toxicity studies.

P3 - IN VITRO AND IN VIVO CATABOLISM OF TAK-164, A GCC-TARGETED ANTIBODY-DRUG CONJUGATE

Jayaprakasam Bolleddula, Mohammad Shadid, Abhi Shah, Afrand Kamali, Mike Smith, Adnan Abu-Yousif, Cindy Xia, and Swapan K. Chowdhury
Takeda Pharmaceuticals International Co.

TAK-164 is an antibody-drug conjugate comprised of the full-length, human anti-guanlyl cyclase C (GCC) monoclonal antibody conjugated (via its surface lysine residue) to a cytotoxic linker payload, the indolinobenzodiazepine DNA

alkylator DGN549-L (IGN-P1), through a cleavable alanine-alanine dipeptide linker (linker/toxin technology licensed from Immunogen). TAK-164 is currently being developed for the treatment of colorectal cancers and other GI malignancies. TAK-164 was designed to deliver the payload FGN849 selectively to GCC-expressing tumor cells, resulting in tumor cell death via a DNA-damaging mechanism. To further investigate the mechanism of action of the FGN849 payload, TAK-164 catabolism and DNA binding of the payload were studied using both *in vitro* and *in vivo* models and radiolabeled TAK-164 ($[^3\text{H}]\text{TAK-164}$), with a tritium (^3H)-labeled payload. Time- and target-dependent uptake of $[^3\text{H}]\text{TAK-164}$ was observed in GCC-expressing HEK-293 cells, with approximately 12% of the total incubated radioactivity associated with DNA after 24 hours of incubation. The control incubations performed with non-targeted ADC (chKTI- $[^3\text{H}]\text{DGN549}$) exhibited <2% of the total incubated radioactivity bound to DNA. Incubation of $[^3\text{H}]\text{TAK-164}$ with the lysosomal proteolytic enzyme cathepsin B yielded the major catabolites sulfonated FGN849 (s-FGN849) and FGN849. Upon intravenous administration to tumor-bearing mice (inoculated with GCC-overexpressing cells), $[^3\text{H}]\text{TAK-164}$ exhibited a long terminal half-life of approximately 41, 51, 95, and 110 hours in the plasma, blood, liver, and tumor, respectively, with low plasma clearance (0.75 mL/hr/kg). Catabolite profiling of the extractable radioactivity in plasma and tumor samples revealed two catabolites, s-FGN849 and FGN849, as payload-related components. The radioactivity associated with DNA in both *in vitro* and *in vivo* studies is consistent with the mechanism of action of the DGN549 payload.

P4 - ABSTRACT WITHDRAWN

P5 - ESTIMATING EFFLUX TRANSPORTER-MEDIATED DISPOSITION USING TRANSPORTER GENE KNOCKOUT RATS

Taiji Miyake, Yuji Sakurai, and Masaki Ishigai
Chugai Pharmaceutical Co., Ltd.

Purpose: Transporter gene knockout rats are a practically useful tool for pharmacokinetic studies in drug discovery. P-gp and Bcrp are major efflux transporters that control absorption and bioavailability and are important when determining oral drug disposition. In our experience, the middle-sized molecules (MW >700 Da) so far launched on the market tend to be substrates for efflux transporters. The purpose of this study is to evaluate *in vivo* the impact of efflux transporters on the oral absorption process and systemic clearance using rats in which P-gp and/or Bcrp had been knocked out.

Method: We administered five substrates (asunaprevir, cyclosporin, danoprevir, simeprevir, and ledipasvir) intravenously or orally to wild-type and Mdr1a, Bcrp, and Mdr1a-Bcrp knockout rats and measured the plasma concentrations. We calculated the clearance and oral bioavailability of each substrate and compared the results between wild-type and knockout rats. Then the absorption rate–time profiles were calculated for each rat using the deconvolution method. We investigated the relationship between increased oral absorption in the knockout rats and the efflux ratio in Caco-2 cells.

Results and discussion: Systemic clearance of the substrates in the knockout rats tended to decrease slightly (<50%) compared with wild-type. When enterohepatic recirculation is taken into account, these results indicate that the efflux transporters P-gp and Bcrp do not have a big influence on clearance in rat. On the other hand, oral absorption of the substrates in the knockout rats, especially in Mdr1a knockout rats, increased greatly by between 3- and 6-fold that in wild-type. This fact suggests that rat efflux transporters, especially P-gp, greatly reduce the oral exposure of these substrates. Moreover, the absorption rate–time profile in the Mdr1a knockout rats was higher than in wild-type at all time points. These results suggest that efflux transporters are constantly active throughout the absorption time in rat. The increased oral absorption in the knockout rats does not correlate with the efflux ratios in Caco-2 cells, which implies that the cell culture model may behave differently from the *in vivo* situation. Further *in vitro-in vivo* correlation study on efflux transporter-mediated disposition is needed for human absorption prediction.

Conclusion: Transporter knockout rats are a useful *in vivo* ADME tool for estimating transporter-mediated disposition of middle-sized molecules in drug discovery.

P6 - RESISTANCE MEDIATED BY LYSOSOMAL SEQUESTRATION OF ANTICANCER AGENTS *IN VITRO*

Petr Mlejnek, Nikola Skoupa, Eliska Ruzickova, and Petr Dolezel
Palacky University Olomouc

It is believed that lysosomal sequestration of an anticancer drug results in the decreased intracellular drug accumulation while it prevents its accessibility to the drug intracellular target. This effect represents one of the possible mechanisms that contribute to the resistance to chemotherapy. Although the idea that this resistance mechanism can play a significant role in the failure of tumor treatment seems to be very attractive and reasonable, available literature dealing with this issue is rather controversial. In addition, to our knowledge, it was never directly proved in *in vitro* experiments.

Similarly to others, we observed that tyrosine kinase inhibitors (TKIs), including imatinib, nilotinib, and dasatinib, are extensively accumulated in lysosomes of cancer cells. We further found that sequestration of TKIs in lysosomes depends on their concentrations. The higher extracellular TKI concentration, the higher degree of its sequestration in lysosomes is induced. However, our data indicated that lysosomal sequestration of studied TKIs neither affected oncogenic signaling mediated by Bcr-Abl tyrosine kinase nor mediated drug resistance *in vitro*.

Acknowledgement: This work was supported by research funding from the Czech Science Foundation, project GACR 17-16614S

P7 - ABSTRACT WITHDRAWN

P8 - RAPID ADME SCREENING FOR STREAMLINED FDA SUBMISSION; A CASE STUDY ASSESSING ORAL ABSORPTION VALIDATION AND TRANSPORTER SUBSTRATE ASSESSMENT OF NEW MOLECULAR ENTITIES IN WT CACO-2 CELLS (C2BBE1)

Kevin Thomas and Shantanu Roychowdhury
Eurofins Panlabs

Profiling the absorption, distribution, metabolism, and elimination (ADME) characteristics of drug candidates is vital to lead optimization in the early stages of drug development. *In vitro* ADME screening encompasses a wide variety of assays, including: Absorption, Metabolic stability, Drug-drug interactions, Bioanalysis for early stages pharmacokinetics and Metabolite identification. The U.S. Food and Drug Administration (FDA) requires certain *in vitro* assays to be performed according to FDA guidelines in order to file a new drug application (NDA). This poster demonstrates an FDA accepted method to validate an oral absorption model and transporter substrate assessment. The model used 22 reference compounds in Caco-2 cells, a well-established cell line used for assessment of oral bio-availability as well as drug transporter substrate assessment. Caco-2 cells are derived from a human colon adenocarcinoma. They develop morphological characteristics of normal enterocytes found within the small intestine and express most of the relevant transport proteins involved in drug transport across an intestinal cell monolayer. By validating the oral absorption model, oral drug candidate submissions can obtain an FDA Waiver of Bioequivalence, allowing for quicker approvals without having to perform long, expensive *in vivo* studies. The FDA also suggests that drugs be classified as a substrate or inhibitor of specific Transport proteins including P-gp, BCRP, and MRP2. The *in vitro* model assesses apical-to-basolateral drug transport versus basolateral-to-apical drug transport, including efflux involving specific efflux transporters (Figure 2). It was employed to assess the overall oral bioavailability of a drug candidate. Apparent permeability (Papp) and fraction-absorbed (FAB) values were determined for each compound. Compounds were rank ordered by the permeability class they fell in, ranging from zero permeability to high permeability. According to the FDA, compounds with a fraction absorbed of 85% or higher are considered to be highly permeable.

P9 - DETERMINING LEVELS OF METHYLENEDIANILINE AND TOLUENEDIAMINE AS BIOMARKERS FOR ISOCYANATE EXPOSURE IN HUMAN URINE BY UPLC-MS/MS

Maggy Lépine^{1,2}, Lekha Sleno¹, Jacques Lesage¹, and Sébastien Gagné²
¹UQAM, ²IRSST

Acute and chronic effects may result from 4,4'-methylenediphenyldiisocyanate (MDI), 2,4'-toluenediisocyanate (2,4-TDI) and 2,6'-toluenediisocyanate (2,6-TDI) exposure whose primary manifestation is occupational asthma. When MDI and TDI are absorbed in the body, they get conjugated to macromolecules or acetylated before their elimination in urine. The hydrolysis of urine samples releases free amine compounds as biomarkers of exposure. 4,4'-methylenedianiline (MDA), 2,4'-toluenediamine (2,4-TDA) and 2,6'-toluenediamine (2,6-TDA) in urine are the biomarkers of MDI, 2,4-TDI and 2,6-TDI, respectively. In this study, we have developed and optimized a method by UPLC-MS/MS for the determination of MDA and TDA levels in human urine. The method was developed with the objective simple sample preparation with small sample volumes. The samples were prepared by hydrolyzing urine with sulfuric acid to produce the free amines. Neutralized samples were then subjected to a liquid-liquid extraction. The resulting extract was analyzed by UPLC-MS/MS on an Acquity Xevo-TQ (Waters) in positive electrospray ion mode with MRM detection. Chromatographic separation will be optimized to ensure retention and minimize matrix effects for the three analytes. An Acquity BEH C18 column with basic pH gradient elution showed good chromatographic separation. Indeed, the MDA and the TDA isomers (2,4-TDA and 2,6-TDA) were well separated in less than 8 minutes total run time. The hydrolysis efficiency has been evaluated using commercial MDI and TDI metabolites spiked into urine. Previous methods use long hydrolysis times beyond 16 hours. It is targeted to obtain complete hydrolysis occurred after 2 hours. Extraction has also been evaluated in order to have the best extraction efficiency. The method was developed considering the biological guidance value (BGV) of MDI at 50 nmol/L and the biological exposure indices (BEI) of TDI (2,4-TDI and 2,6-TDI) at 5µg/g creatinine. The dynamic range of the method was achieved between 5 nmol/L to 300 nmol/L. Finally, the method was tested with inter-laboratory samples coming from the G-EQUAS program.

P10 - IN VITRO-IN VIVO CORRELATION OF CLEARANCE FOR H3B-5942, A NOVEL SELECTIVE ER α COVALENT ANTAGONIST (SERCA)

Federico Colombo¹, Sherri Smith¹, Manav Korpai¹, Ming-Hung Hao², Darrel Nix¹, Morgan O'Shea¹, Sudeep Prajapati¹, John Wang², Markus Warmuth¹, Peter Smith¹, and Nathalie Rioux¹
¹H3-BIOMEDICINE, ²Eisai

Using a structure-based drug design approach we identified a novel class of ER α antagonist referred to as Selective ER α Covalent Antagonist (SERCA), which irreversibly inactivates both wild-type and mutant ER α (1). In vivo, H3B-5942, a representative SERCA, demonstrated significant single agent antitumor activity in xenograft mouse models representing ER α WT and ER α Y537S breast cancer. Targeted covalent inhibitors (TCI), such as H3B-5942, are attractive for potential enhanced biochemical efficacy, duration of action, and selectivity associated with their irreversible mechanism. From a DMPK perspective, preclinical *in vitro- in vivo* correlation (IVIVC) for the prediction of clearance (CL), and subsequently human pharmacokinetic (PK) projection, may be challenging for TCIs due to their potential for glutathione (GSH) conjugation. These occur by non-enzymatic and/or GSH-S-transferase (GST)-mediated mechanisms, in both the liver and extrahepatic tissues (2). Consequently, extrapolation from liver microsomes, S9 fractions or hepatocyte incubations are not representative of *in vivo* CL. Recent studies suggest considering blood stability when projecting *in vivo* CL of TCIs (2). In our study using high resolution LC-MS/MS technology, metabolite identification of H3B-5942 incubated with pooled rat, dog, monkey or human hepatocytes (1x10⁶ cells/mL), showed minimal formation of H3B-5942 GSH-related adducts (<1% total peak area in dog, monkey, and human, and 4.3% in rats) following a 3 hour incubation at 37°C. H3B-5942 was the major component in all species following incubation, and prominent metabolites were the result of N-dealkylation and/or oxidation. There were no human specific or disproportionate metabolites. H3B-5942 intrinsic CL values were determined to be 31, 46, 43 and 17 mL/min/10⁶ cells, in pooled rat, dog, monkey, and human hepatocytes, respectively. Moreover, H3B-5942 at 2 μ M was shown to be stable in rat whole blood, at 37°C, for up to 6 hours, suggesting minimal direct conjugation or GST-mediated metabolism. To assess IVIVC, a physiologically based PK (PBPK) modeling approach was used to simulate H3B-5942 exposures following a single 5 mg/kg intravenous (IV) bolus administration in male rats, dogs and monkeys (n=3 per species). In these PK studies, H3B-5942 CL was lower in rat (28% of hepatic blood flow), than in dog (42%) and monkey (55%). Volume of distribution varied from 1.8 (rat) to 2.6 L/kg (monkey). Based on visual inspection, adequate fit of the observed time-concentration profile of H3B-5942 was achieved by the model in all species using *in vitro* hepatocyte CL data, and resulted in the prediction of mean CL values within \pm 25% of the observed results. Thus, this study shows that good IVIVC is achievable for TCIs with minimal extrahepatic CL, and exemplifies the favorable PK profile of this series of SERCAs.

References:

1. Smith PG et al. Discovery and development of H3B-6545: A novel, oral, selective estrogen receptor covalent antagonist (SERCA) for the treatment of breast cancer. AACR Annual Meeting, Washington, DC, April 1-5, 2017 #DDT01-04
2. Leung et al. Clearance prediction of targeted covalent inhibitors by *in vitro-in vivo* extrapolation of hepatic and extrahepatic clearance mechanisms. Drug Metab Dispos 45:1-7, 2017

P11 - CAN TRANSPORTER-EXPRESSING CELLS PREDICT ROSUVASTATIN UPTAKE CLEARANCE IN SUSPENDED OR PLATED HUMAN HEPATOCYTES?

Vineet Kumar¹, Laurent Salphati², Cornelis E. C. A. Hop², Christopher Rowbottom³, Guangqing Xiao³, Yurong Lai⁴, Anita Mathias⁴, Xiaoyan Chu⁵, W. Griffith Humphreys⁶, Mingxiang Liao⁷, Laigao Chen⁸, Beáta Tóth⁹, Viktoria Juhasz⁹, Scott Heyward¹⁰, and Jashvant Unadkat¹

¹University of Washington, ² Genentech, ³Biogen, Inc., ⁴Gilead Sciences, Inc., ⁵Merck & Co., ⁶Bristol-Myers Squibb, ⁷Takeda Pharmaceuticals International, Inc., ⁸Pfizer Inc., ⁹SOLVO Biotechnology, ¹⁰BioIVT

Purpose: During drug development, suspended (SH) or plated hepatocytes (PH) are routinely used to quantify *in-vitro* transporter-mediated uptake clearance of drugs and then extrapolated to *in-vivo*. We hypothesized that uptake studies in hepatic transporter-expressing cells can be an economical and higher-throughput alternative approach to achieve the same goal. Here we present data to test this hypothesis by determining the OATP-mediated uptake clearance of rosuvastatin (RSV) into OATP-expressing cells, SH and PH and then scaling the clearance in OATP-expressing cells to that in SH or PH by the abundance of transporters in these cells (total or in the plasma membrane) determined by quantitative proteomics (LC-MS/MS). Methods: Cryopreserved human hepatocytes (n=4 donors; donated by BioIVT) were plated (0.35 million hepatocytes/well in 24-well collagen coated plates) for 5 hours or suspended before conducting the [³H]RSV uptake study. OATP1B1-expressing CHO and OATP2B1-expressing MDCKII cells (0.5 million cells/well in 24-well poly-D-lysine coated plate) were grown for 24 hours in low and high glucose Dulbecco's Modified Eagle's media respectively prior to the [³H]RSV uptake study. Then, at various time points, OATP-mediated [³H]RSV (30 nM) uptake into SH, PH, OATP1B1 or OATP2B1-expressing cells was determined in standard or sodium-free HBSS buffer (to eliminate NTCP activity) in the presence or absence of a pan-OATP inhibitor (bromosulphophthalein; 200 μ M). The total/plasma

membrane OATP abundance in these cells was determined by LC-MS/MS proteomics with/without cell-surface biotinylation (see accompanying abstract). [^3H]RSV uptake clearance in hepatocytes was predicted using transporter abundance and activity data from transporter-expressing cells. The Mann-Whitney test was used to compare the predicted and observed OATP-mediated [^3H]RSV clearance into SH or PH. Results and conclusion: [^3H]RSV uptake clearance into OATP1B1- and OATP2B1-expressing cells was 5.32 ± 0.3 and 1.22 ± 0.08 $\mu\text{L}/\text{min}/\text{pmol}$ of total transporter abundance, respectively. OATP1B1/2B1 total abundance in SH and PH was $1.83 \pm 1.18/0.83 \pm 0.24$ and $2.53 \pm 1.44/0.94 \pm 0.24$ pmol/mg protein, respectively. Percent plasma membrane abundance of the OATP1B1 in SH and PH was 73.3 and 76.2%, while that of OATP2B1 was 63.3 and 60.3% respectively. OATP-mediated and passive diffusion uptake clearance of [^3H]RSV into SH was 6.3 ± 4.9 and 0.58 ± 0.24 $\mu\text{L}/\text{min}/\text{mg}$ protein while that into PH was 8.9 ± 7.8 and 0.3 ± 0.2 $\mu\text{L}/\text{min}/\text{mg}$ protein, respectively. RSV uptake clearance into OATP-expressing cells, scaled using total cell or plasma membrane transporter abundance, successfully predicted the [^3H]RSV uptake clearance into SH or PH (Fig. 1). Of the total OATP-mediated [^3H]RSV uptake into SH and PH, >80% was mediated by OATP1B1 (based on either cell or plasma membrane abundance). OATP1B1 abundance correlated ($R^2 > 0.89$) with [^3H]RSV OATP-mediated uptake clearance into SH and PH. These data need to be refined by including the contribution of OATP1B3 and NTCP to the total hepatocyte uptake of [^3H]RSV (in progress). This successful *in-vitro* to *in-vitro* extrapolation of [^3H]RSV hepatic uptake clearance using transporter-expressing cell lines shows the promise of this approach for successful *in-vitro* to *in-vivo* extrapolation of RSV hepatic uptake clearance as previously demonstrated for the rat¹. This work was supported in part by the Simcyp Grant & Partnership Scheme and UWRAPT, funded by Genentech, Biogen, Gilead, Merck, Bristol-Meyers Squibb, Pfizer and Takeda.

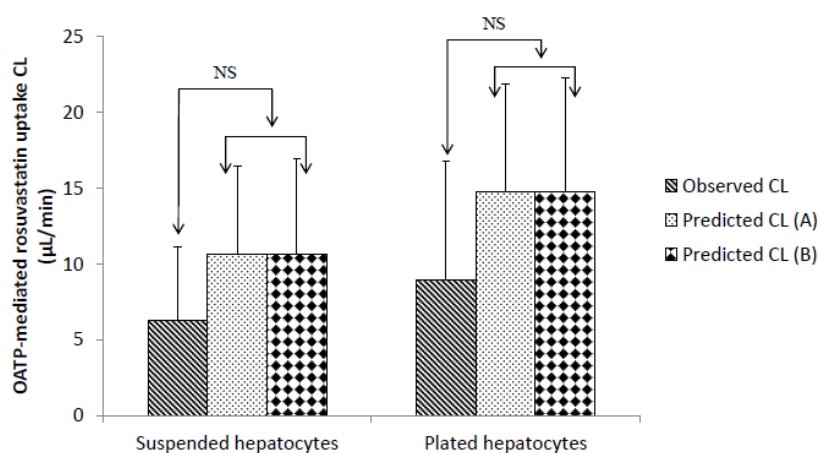


Fig. 1. Observed and predicted OATP-mediated RSV uptake clearance into SH or PH. A: based on total cell OATP1B1/2B1 abundance, B: based on only plasma membrane OATP1B1/2B1 abundance, NS: not significant, data are shown as mean \pm SD, n=4

Reference:

- Ishida K, Ullah M, Tóth B, Juhasz V and Unadkat JD; Successful Prediction of In Vivo Hepatobiliary Clearances and Hepatic Concentrations of Rosuvastatin Using Sandwich-Cultured Rat Hepatocytes, Transporter-Expressing Cell Lines, and Quantitative Proteomics. *Drug Metab Dispos.* 2018;46:66-74.

P12 - IMPACT OF HEPATIC DRUG DISTRIBUTION ON PREDICTIONS OF CLEARANCE

Jasleen K. Sodhi and Dr. Leslie Z. Benet

University of California San Francisco

Introduction: *In vitro* drug metabolism measurements frequently underpredict *in vivo* hepatic drug clearance, the degree of underprediction varies greatly by drug, and the field does not understand why. The process of *in vitro* to *in vivo* extrapolation (IVIVE) accounts for physiologic scale-up of an *in vitro* rate of drug loss (k_{inc}) by reconciling enzyme content differences between the incubation and an average human liver (i.e. scale-up of k_{inc} to k_{ss}). This straightforward approach is valid in chemistry since reactions occur in fixed-volumes, however, the field of pharmacokinetics recognizes that drug elimination rate (k) depends equally on both clearance (CL) and volume of distribution (V_d) ($CL = k \cdot V$). Although the impact of V_d on drug disposition is routinely considered in drug development, the concept has not yet been applied to IVIVE of hepatic clearance; in other words, k is scaled-up, but V is not. **Methods:** The evaluation of the impact of hepatic drug distribution on accuracy of clearance predictions involves an examination of the theoretical basis of IVIVE and an experimental component in which *in vitro* V_d of drug can vary depending on the physicochemical characteristics of the drug. **Results:** Examination of the theoretical basis for IVIVE predictions reveals that the liver was assumed to function as a homogeneous, fixed-volume system, rather than a heterogeneous organ with both hydrophilic and lipophilic regions into which drugs potentially distribute differently. A new theoretical relationship for IVIVE is derived to account for drug-specific

scale-up of volume (in addition to physiologic scale-up of k_{inc}) which includes a term R_{ss} , the ratio of the volume of distribution of drug in the whole liver at steady-state to the volume of distribution of drug in the hepatocyte water (where drug metabolizing enzymes reside). R_{ss} will vary from drug to drug, and provides a rationale for the poor and variable IVIVE predictions observed industry-wide. To investigate this concept, an *in vitro* system was designed to simulate a heterogeneous liver, allowing microsomal incubations to be performed adjacent to either a lipophilic or hydrophilic phase, with an impermeable membrane separating the two (only drug can cross). For BDDCS class 1 drugs (primarily metabolized; negligible transporter effects), k_{inc} was measured with either an adjacent lipophilic (1-octanol) or hydrophilic (buffer/microsomes) phase. Differences between lipophilic and aqueous rate constants were observed; their ratio ($k_{lipophilic} / k_{aqueous}$) ranged from 0.118 – 0.894, and the extent of difference moderately correlated with drug partitioning ($\log P$, $r^2=0.30$). However, the correlation with published IVIVE fold-difference values was not as strong ($r^2=0.15$). Conclusions: IVIVE underpredictions are due to drug-dependent distribution properties evident *in vivo* but are not considered with current *in vitro* methodologies. The *in vitro* system used in these studies does not necessarily replicate the liver, rather, allows for an *in vitro* demonstration of the impact of volume of distribution on elimination, and that lipophilic distribution of drugs must be considered to accurately predict hepatic clearance. Approaches accounting for drug distribution within the liver, such as using animal scale-up of individual drugs, are currently being evaluated by our lab.

P13 - PREDICTION OF HUMAN HEPATIC CLEARANCE FOR CYTOCHROME P450 SUBSTRATES VIA A NEW CULTURE METHOD USING THE COLLAGEN VITRIGEL MEMBRANE CHAMBER AND PXB-CELLS

Ryuji Watari and Kazutomi Kusano
Eisai Co., Ltd.

Introduction: In drug discovery, hepatocytes have been widely utilized as *in vitro* tools for predicting *in vivo* hepatic clearance (CL) and evaluating metabolic enzyme inhibition/induction of drug candidates. However, the conventional hepatocyte models do not always reproduce *in vivo* physiological functions, and cytochrome P450 (CYP) activities were decreased quite rapidly during culture. Furthermore, since the number of slowly metabolized drug candidates are increasing in drug discovery research, conventional *in vitro* assays have limitations in their ability to predict hepatic CL for these metabolically stable drugs. In order to accurately predict the hepatic CL of drug candidates, a new method of culturing hepatocytes, that activates their functional properties, including CYP activities, is in high demand. In the previous study, we established a novel long-term method for culturing hepatocytes using a collagen vitrigel membrane (CVM) chamber, which can maintain CYP activity and liver specific functions at high levels for a long period. In this study, the vitrigel culture method was applied to the predictions of hepatic CL for 23 CYP typical substrates; and, the prediction accuracy by this method was assessed by comparing CL data between predicted (obtained from *in vitro* CLint) and observed (obtained from clinical data using the dispersion model) CL values. Method: Fresh human liver chimeric cells (PXB-cells) isolated from human liver chimeric mice were used for a 2-weeks culture on CVM chambers. Subsequently, 23 CYP typical substrates were treated, and the calculated *in vitro* CL values were compared with *in vivo* hepatic CL values obtained using the dispersion model. Results / Conclusion: The vitrigel culture method using the CVM chambers and PXB-cells showed that *in vitro* CL values for about 60% (14/23) and 80% (19/23) of compounds were predicted within a 2-fold and 3-fold difference with *in vivo* CL, respectively. In addition, prediction accuracy of low CL compounds such as warfarin and tolbutamide was also high. These results suggested that the new culture method using the CVM chamber and PXB-cells is a promising *in vitro* system for predicting human hepatic CL with high accuracy for CYP substrates including very metabolically stable compounds.

P14 - CHARACTERIZATION OF HUMAN HEPATOCYTES BY QUANTITATIVE DMET PROTEOMICS ADDRESSES LOT-TO-LOT VARIABILITY: RELEVANCE IN IN-VITRO TO IN-VIVO EXTRAPOLATION OF HEPATIC DRUG CLEARANCE

Bhagwat Prasad¹, Haeyoung Zhang¹, Deepak Bhatt¹, Abdul Basit¹, and Maureen Bunger²
¹University of Washington, ²Lonza Bioscience Solutions

Background: Human hepatocytes are considered gold-standard for *in-vitro* drug metabolism and transport studies. However, inherent interindividual variability and interlaboratory methodological differences can lead to inconsistency in activity of drug metabolizing enzymes and transporters (DMET proteins), further resulting in inaccurate *in-vitro* to *in-vivo* extrapolation (IVIVE) of hepatocyte data. While hepatocyte vendors provide cytochrome P450 (CYP) activity data with each lot, activities of non-CYP enzymes and transporters are rarely provided due to less characterized functional assays. In this study, we demonstrate that quantitative proteomics for DMET proteins can be used as an alternate to DMET activity for hepatocyte characterization.

Methods: Human cryopreserved hepatocytes (n=5 donors) were subjected to membrane or cytosol isolation followed by trypsin digestion per established protocols¹. CYPs (3A4, 2E1, 1A2, 2D6, 2B6, 2C8, 2C9, 2C19, Cytochrome b5 and CYP-reductase), UGTs (1A1, 1A4, 1A6, 1A9, 2B7, 2B15 and 2B17), other non-CYPs (CES1, CES2, FMO-3, ADH1A, ADH1C and ALDH1A1) and transporters (OATP1B1, OATP1B3, OATP2B1, OCT1, P-gp, MRP2, MRP3 and BSEP) were quantified using quantitative proteomics approach. CYP and UGT activities (n=4) were measured using the following

specific probe substrates: acetaminophen (CYP1A2), bupropion (CYP2B6), desethylamodiaquine (CYP2C8), diclofenac (CYP2C9), mephenytoin (CYP2C19), dextromethorphan (CYP2D6), chlorzoxazone (CYP2E1), midazolam (CYP3A4), trifluoperazine (UGT1A4), serotonin (UGT1A6), naloxone (UGT2B7) and testosterone (UGT2B17). Metabolites were monitored using specific LC-MS/MS methods. Hepatocyte protein abundance data were compared with DMET protein abundance in a pooled (n=36) human liver tissue.

Results: Good abundance-activity correlation (r^2 values) was observed for CYP1A2 (0.99) CYP2B6 (0.74), CYP2C8 (0.46), CYP2D6 (0.91), CYP3A4 (0.44), while correlation was poor for CYP2C19, CYP2E1. UGT2B7 and UGT2B17 showed excellent correlation with activity ($r = 0.97$ and 0.70 , respectively), although no correlation was observed for trifluoperazine (UGT1A4) and serotonin (UGT1A6) possibly due to methodological reasons. Interestingly, chlorzoxazone hydroxylation correlates better with CYP b5 than CYP2E1, indicating rate determining role of CYP b5 in CYP2E1 metabolism. The average abundance of DMET proteins in human hepatocytes was within three-fold of the abundance observed in the pooled tissue samples (except for CYP2B6, UGT1A1, UGT1A6 and P-gp, where the difference was within 5-fold).

Conclusions: Quantitative proteomics can be utilized to characterize hepatocyte model for drug metabolism and transport prediction. While pooled human hepatocytes is a useful model for estimation of average drug metabolism and transport activity, individual proteomics-characterized hepatocytes can be used for prediction of interindividual variability for a specific DMET protein. Quantitative proteomics approach can also be applied to protein induction or suppression studies as well as to identify low and high expressers for evaluation of individual contribution of enzymes or transporters (f_m or f_t).

Reference:

1. Prasad et al., Clin Pharmacol Ther, 2016.

P15 - *IN VITRO* CHARACTERIZATION OF ERTUGLIFLOZIN GLUCURONIDATION

Kimberly Lapham, Ernesto Callegari, Jian Lin, Mark Niosi, Christine Orozco, Raman Sharma, and Theunis Goosen
Pfizer Worldwide Research and Development

Ertugliflozin is an oral inhibitor of sodium-dependent glucose cotransporter 2 approved for the treatment of type 2 diabetes mellitus. Ertugliflozin is primarily cleared by UDP-glucosyltransferase (UGT) mediated metabolism (86% of systemic clearance) with two major human circulating metabolites identified as 3-O- β -glucuronide (M5c) and 2-O- β -glucuronide (M5a). The aim of the *in vitro* experiments presented herein was to identify and characterize the UGT isoforms involved in ertugliflozin metabolic clearance. *In vitro* biotransformation studies of ertugliflozin were employed to characterize the kinetics and enzymes involved in catalyzing the formation of M5c and M5a. Reaction phenotyping studies were conducted with human liver microsomes (HLM) with chemical inhibitors (10 μ M digoxin, 10 μ M tranilast, or 3 μ M 16 β -phenyllongifolol) and recombinant human UGTs. The unbound substrate concentration at half-maximal velocity (K_m), maximal rate of metabolism (V_{max}), and unbound intrinsic clearance (CL_{int}) values for the formation of the primary *in vitro* glucuronide (M5c) in HLM were 10.8 μ M, 375 pmol/min/mg, and 34.7 μ l/min/mg, respectively. UGT phenotyping utilizing chemical inhibitors indicated the approximate fraction of M5c metabolism (f_m) by UGT1A9 was 0.85 and f_m for UGT2B7 was 0.14. The K_m , V_{max} , and CL_{int} for the formation of the minor *in vitro* glucuronide metabolite, M5a, were 41.7 μ M, 94.9 pmol/min/mg, and 2.28 μ l/min/mg, respectively. Conversely, phenotyping studies indicated M5a was predominately catalyzed by UGT2B7 ($f_m = 0.82$) whereas UGT1A9 was a minor enzyme responsible for M5a formation ($f_m = 0.19$). When the fractional contributions across each metabolite are combined, the primary enzyme involved in the overall UGT-mediated metabolism of ertugliflozin was UGT1A9 ($f_m \geq 0.81$) with a minor contribution of UGT2B7 ($f_m \leq 0.19$). In summary, UGT1A9 is the major enzyme involved in glucuronidation of ertugliflozin with lesser contribution from UGT2B7.

P16 - POLYMORPHISMS IN CANINE GLUTATHIONE S-TRANSFERASE (GST) GENES: PREVALENCE AND FUNCTIONAL RELEVANCE

James Sacco¹, Lauren Trepanier², Sessaly Craft Reich², Joanne Ekena², Sarah Mann¹, and Katherine Ros Luethcke²
¹Drake University, ²University of Wisconsin-Madison

Glutathione S-transferases (GSTs) conjugate reactive xenobiotics, including drug metabolites and pro-carcinogenic chemicals. Human GST genes are polymorphic, and low functioning variants in human *GSTT1*, *GSTM1*, and *GSTP1* have been associated with drug toxicities and cancer risk in humans. Although dogs are used for human preclinical drug testing, and pet dogs are treated clinically with drugs that are potential GST substrates, little is known about GSTs in dogs. The overall goals of this ongoing work are to investigate variability in canine GST genes, characterize polymorphisms with predicted functional significance, and determine their association with the risk of adverse drug reactions and environmental cancers, including lymphoma and bladder cancer, in dogs. Four major canine GST genes have been studied to date: *GSTT1*, *GSTM1*, *GSTP1*, and a novel canine GST, *GSTT5*. Three populations have been studied: healthy dogs of more than 100 breeds recruited in Wisconsin and in Iowa, and dogs for which whole genome sequencing data are available (courtesy of Dr. Elaine Ostrander, NCI). Multiple polymorphisms in *GSTT1* have been identified: one *GSTT1* 3'untranslated region (UTR) haplotype (containing *101-102 ins T) leads to a 50% reduction in

gene expression in luciferase constructs. A 6-bp coding deletion in *GSTT5* leads to virtual loss of enzyme activity in recombinant expression studies. Canine *GSTP1* has polymorphisms with predicted deleterious effects in the promoter, exon 2, exon 5 and the 3'UTR. For *GSTM1*, most of the polymorphic variability is found in the promoter, exon 8, and the 3'UTR. Ongoing work is evaluating the prevalence of these variants in bladder cancer and lymphoma in dogs, and characterizing the substrate range of these canine GSTs for therapeutic drugs and chemical carcinogens.

P17 - SCREENING FOR PHASE I AND PHASE II DRUG METABOLISM USING SUPPLEMENTED LIVER AND INTESTINAL S9 FRACTIONS: A COCKTAIL APPROACH

Kevin Thomas, Shantanu Roychowdhury, and Mitchell Martineau
Eurofins Panlabs

Metabolite Identification is a critical component of pre-clinical ADME screening of new molecular entities in early drug discovery. Identification of metabolites can further elucidate potential routes of elimination or toxic metabolites that can be early indicators of adverse events. Drug metabolism occurs in multiple phases, Phase I metabolism usually involves a functionalization of the compound (e.g. oxidation). Phase II metabolism may increase water solubility in order to promote excretion of the compound. The most prevalent Phase II conjugates exist in the form of glutathionation, glucuronidation and sulfation of the molecule. Primary hepatocytes contain all necessary enzymes and co-factors for complete metabolism of the molecule to occur., however there may be situation where molecules cannot penetrate the hepatocytes and therefore unable to elucidate Phase II drug metabolites. This poster proposes an effective way to screen for Phase I and Phase II metabolism using liver S9 supplemented with cofactors. Enzymes involved in Phase I and Phase II metabolism of a drug molecule include Cytochrome P450 enzymes, Glutathione-S-Transferases, UDP-glucuronosyltransferase and sulfotransferases and are present in S9 fractions. Supplementation of cofactors Uridine diphosphate glucuronic acid (UDPGA), reduced glutathione, 3'-phosphoadenosine-5'-phosphosulfate (PAPS) and Nicotinamide adenine dinucleotide phosphate (NADPH) are needed for initiation of the reactions in S9 fractions in order for the metabolism process to occur. Phase I and Phase II metabolism were successfully achieved upon incubation of reference compounds in S9 fractions with the "cocktail" method of metabolic identification. Reference substrates for each enzyme were assayed in a cocktail to confirm turnover of the compound as well as formation of metabolites. Each of the enzymes and subsequent metabolites were also evaluated individually, followed by a cocktail of co-factors, and results were comparable to that of human hepatocytes.

P18 - IDENTIFICATION OF DOPA-MODIFIED AMINO ACIDS USING HIGH-RESOLUTION TANDEM MASS SPECTROMETRY

Maxime Sansoucy
UQAM

Neurodegenerative disorders are mostly diagnosed based on symptomatic evidence and require post-mortem examination for confirmation. Recent progress in neurosciences has suggested a deregulated level of dopamine as a common factor. Dopamine is biosynthesized in brain from successive enzymatic modifications using tyrosine as a primary substrate. Under homeostatic conditions, tyrosine is hydroxylated to 3,4-dihydroxyphenyl-L-alanine (dopa), a precursor of dopamine. Because the electron density of dopa can spontaneously remodel to electrophilic dopaquinone, cross-linking reactions with nucleophilic amino acids are often observed. The combination of dopaquinone and cysteine to yield 5-S-cysteinyl-dopa has even been investigated in previous studies on a melanoma biomarker. Furthermore, dopa is also observed in proteins with strong underwater adhesion and load-bearing properties. Deterioration of these properties is hypothesized as being the consequence of intramolecular protein cross-linking. Although few studies have reported cross-linked proteins in bio-materials, the quantitation of these dopa-modified residues offers an alternative approach in demonstrating protein cross-linking significance. We have developed a high-resolution tandem mass spectrometry method for identifying dopa-modified amino acids. Samples were analyzed on a Shimadzu Nexera UHPLC system coupled with hybrid quadrupole time-of-flight (QqTOF) mass spectrometer. Preliminary results with standard amino acids suggested that sulfhydryl was the only group with sufficient nucleophilicity to react with dopaquinone. High-resolution extracted ion chromatogram has revealed two positional isomers of cysteinyl-dopa, with the 5-S isomer being more favored. Furthermore, tandem mass spectrometry (MS/MS) revealed diagnostic fragment ions (m/z 208, 237, 254) related to cysteinyl adducts. In contrast, reactions with amines and phenols were performed in an alkaline milieu and yet detection of these adducts were not conclusive. Micro-environments in proteins can promote nucleophilicity of amines and phenols during incubation with dopa, following complete hydrolysis under acidic conditions at high temperature. Electrophilic compounds normally target reduced cysteine. However, harsh conditions during protein hydrolysis were found to compromise adduct stability. Dopa adduction is identified by a specific mass increase ($+C_9H_{11}NO_4$, 197 Da) and by proteolytic missed cleavages. Further examination with specific and nonspecific proteases with modified model proteins are currently being finalized. Quinoid compounds are considered important electrophiles, with several examples of these reactive species formed via the metabolism of xenobiotics. Therefore, the methods developed here will be transferable to studying such modifications from catechol-containing xenobiotics as well.

P19 - METABOLISM OF 3,7-DIHYDROXYFLAVONE MEDIATED BY CYTOCHROME P450**Mirza Bojic**¹, Goran Benkovic², Zeljan Males¹, and Sinisa Tomic²¹University of Zagreb, Faculty of Pharmacy and Biochemistry, ²Croatian Agency for Medicinal Products and Medical Devices

Flavonoids are a large group of compounds, that people consume from fruits and vegetables. Biological effects of these xenobiotics have been extensively studied *in vitro*. As human body has been exposed to flavonoids through food, our organism has developed mechanism to prevent absorption or stimulate excretions e.g. transporters and metabolism. Although results of *in vitro* studies are promising due to low bioavailability these compounds do not demonstrate their pharmacological potential *in vivo*. Thus, the objective of this work was to characterize metabolism mediated by cytochromes P450 of 3,7-dihydroxyflavone, flavonoid studied for its anticancer properties. For this purpose, human liver microsomes and recombinant cytochrome P450 enzymes were used. Metabolism was monitored by liquid chromatography coupled with mass spectrometry (electron spray ionization, time of flight detection) for metabolite determination and diode array detector for quantification. Major metabolic reaction was hydroxylation generating 3,7,4'-trihydroxyflavone as a predominant product. Based on screening on human liver microsomes with specific inhibitors of cytochromes P450, major enzyme mediating metabolism of 3,7-dihydroxyflavone was shown to be CYP1A2. Catalytic efficiency of $0.012 \pm 0.005 \times 10^{-6} \text{ min}^{-1} \text{ M}^{-1}$ was determined on human liver microsomes. These data will improve understanding of pharmacokinetics of flavonoids, helping overcome low bioavailability observed *in vivo*.

P20 - MICROSOMAL CYTOCHROME P450 ENZYME ACTIVITIES IN NONALCOHOLIC STEATOHEPATITIS LIVERS**Maciej Czerwinski**¹, Brian Oberheide¹, Nicholas Hatfield¹, Bill Ewy¹, Christopher Seib¹, Eva Gatineau², Frederique Yiannikouris², Molly O'Brien¹, and Brian Ogilvie¹¹Sekisui XenoTech LLC, ²University of Kentucky, Department of Pharmacology and Nutritional Sciences

The prevalence of nonalcoholic steatohepatitis (NASH), a chronic liver disease, has increased drastically in parallel with the raise of obesity in the US. This condition affects hepatic drug metabolism and has potential to impact drug-drug interactions. Our study aimed to evaluate microsomal CYP enzyme activities, organ fibrosis and microvesicular steatosis in NASH tissues deposited in the Sekisui XenoTech Biobank, and to establish whether these tissues have application as an *in vitro* test system for the study of NASH impact on metabolism of xenobiotics. NASH tissues were identified based on the examination of hematoxylin and eosin (H&E), Masson's trichrome staining and donor history of alcohol consumption. All samples had intra-lobular inflammation, ballooning necrosis and macrovesicular fat >5%. Fibrosis stage was assigned based on Brunt *et al.* (1). The degree of microvesicular steatosis, evaluated by H&E staining, did not correlate with the body mass index (BMI) nor with progressive stages of fatty liver disease in 51 donors. However, the extent of microvesicular steatosis correlated positively with triglyceride contents ($R^2=0.66$), but not with total cholesterol levels. Microsomal protein yield was weakly negatively correlated with microvesicular fat content ($R^2=0.11$) but did not correlate with BMI. The majority of average microsomal CYP activities in NASH livers were lower than in the general population of liver donors by 6 to 65%. In contrast, the average CYP2E1 microsomal activity in NASH livers was 3.5% higher than in the general population of liver donors in the Biobank. These observations were in agreement with published clinical data. A microsomal pool of five NASH donors and tissue micro arrays containing NASH and fatty livers from donors with and without history of alcohol consumption were prepared to assist in disease evaluation. The NASH pattern of CYP enzyme activities seen in the patients and in the microsomes prepared from non-transplantable NASH livers suggest that the subcellular fraction is an appropriate test system for analysis of CYP-mediated xenobiotic metabolism associated with the disease state.

Reference:

1. Brunt, ME *et al.*, Nonalcoholic steatohepatitis: a proposal for grading and staging the histological lesions, American Journal of Gastroenterology 94, 9:2467-74, 1999

P21 - CHARACTERIZATION OF INDIVIDUAL DIFFERENCES IN CYP3A5 ACTIVITY USING A CYP3A5-SELECTIVE MARKER REACTION *IN VITRO***Klarissa Jackson**, Arsany Abouda, and Kahari Wines

Lipscomb University College of Pharmacy & Health Sciences

Cytochrome P450 (CYP) 3A5 is highly polymorphic, and the contribution of CYP3A5 to drug metabolism has been an area of intense investigation. The *CYP3A5*1* allele leads to high levels of functional protein, whereas the *CYP3A5*3* variant allele results in low to undetectable levels of CYP3A5. Until recently, *in vitro* tools to distinguish the contributions of CYP3A4 vs. CYP3A5 to drug metabolism were lacking. *N*-oxidation of T-5 (T-1032) was recently reported as a selective marker reaction to assess CYP3A5 activity *in vitro*.¹ The goal of this study was to characterize the activity of CYP3A5 in individual *CYP3A5*-genotyped human liver microsomes and assess the genotype-phenotype relationship. CYP3A and

CYP3A5-specific activity were measured in 12 individual genotyped human liver microsomal samples using midazolam and T-5 as probe substrates. Midazolam 1'-hydroxylation was used as a marker of CYP3A activity, and T-5 N-oxidation was used as a selective marker of CYP3A5 activity. Individual human liver microsomes were incubated with midazolam (2.5 microM) or T-5 (5 microM) in the presence of NADPH, and formation of 1'-hydroxymidazolam and T-5 N-oxide, respectively, was measured by liquid chromatography – tandem mass spectrometry. While midazolam 1'-hydroxylation did not significantly differ by CYP3A5 genotype among the tissues tested, T-5 N-oxide formation was significantly associated with CYP3A5 genotype. CYP3A5*1/*1 donors (expressers) formed 18-fold higher levels of T-5 N-oxide compared to CYP3A5*3/*3 donors (non-expressers). These results demonstrate that T-5 N-oxide formation is a much more selective measure of CYP3A5 activity compared to midazolam 1'-hydroxylation, and the results confirm a positive relationship between CYP3A5 genotype and CYP3A5 activity. The findings of this study will serve as the basis for future investigations to examine the impact of CYP3A5 genotype and activity on the metabolism of selected tyrosine kinase inhibitors used in cancer therapy.

Reference:

- Li, X., Jeso, V., Heyward, S., Walker, G. S., Sharma, R., Micalizio, G. C., and Cameron, M. D. (2014) Characterization of T-5 N-Oxide Formation as the First Highly Selective Measure of CYP3A5 Activity. *Drug Metab Dispos.* 42, 334-342.

P22 - PHENOBARBITAL IS AN AGONIST OF HUMAN BUT NOT MOUSE PREGNANE X RECEPTOR

Linhao Li¹, Zhihui Li¹, Bryan Mackowiak¹, Scott Heyward², and Hongbing Wang¹

¹University of Maryland, ²BioIVT

Phenobarbital (PB), a broadly used anti-seizure drug, was the first to be characterized as an inducer of hepatic cytochrome P450 (CYP) by the activation of the constitutive androstane receptor (CAR, NR1i3). While PB is recognized as a prototypical CAR activator through an well-documented indirect activation mechanism, conflicting results have been reported regarding whether PB can activate the pregnane X receptor (PXR, NR1i2), a sister receptor of CAR, across different species, and the underlying mechanisms are largely unknown. Here, we show that in the human CAR (hCAR)-knockout HepaRG cell line, both PB- and rifampicin (a selective hPXR activator)-mediated induction of CYP3A4 and CYP2B6 was intact while induction by CITCO (a selective hCAR activator) was significantly attenuated. In human primary hepatocytes and HepG2 cells, knockdown of PXR by recombinant lentivirus or co-treatment with SPA70, a potent antagonist of hPXR, inhibited CYP3A4 induction by PB and rifampicin. PB showed concentration-dependent activation of hPXR but not mouse PXR (mPXR) in HepG2 transactivation assays, while such activation was fully abolished by introducing a non-functional hPXR mutant. Mechanistically, our surface plasmon resonance binding affinity assay showed that PB directly binds to the ligand binding domain (LBD) of hPXR (KD (M) = 1.42-E05). PB also increased interactions between hPXR and the steroid receptor coactivator-1 (SRC-1) in a mammalian two-hybrid assay and increased the recruitment of hPXR to the ER6 containing region of CYP3A4 in chromatin immunoprecipitation experiments. Taken together, these results reveal that PB can directly activate hPXR but not mPXR and provides an alternative pathway for PB-mediated CYP induction.

P23 - *IN-SILICO* TOOL TO PREDICT NEW CYP3A5 SILENSOMESTM USING T-5 SUBSTRATE AND LAPATINIB AS MECHANISM-BASED INHIBITOR

Solenne Martin¹, Ashwani Sharma², Françoise Bree¹, Christophe Chesne², and Sylvain Routier³

¹Eurosafe; ²Biopredic International; ³Institut de Chimie Organique et Analytique (ICOA), Université d'Orléans

Silensomes™ are human pooled liver microsomes (HLMs) irreversibly inactivated for one specific CYP450 using mechanism based inhibitors (MBI) [1,2]. Intrinsic clearance of midazolam and testosterone measured with CYP3A4-Silensomes™ previously shown that testosterone is a specific substrate for CYP3A4, although midazolam found to be metabolized by both CYP3A4 and CYP3A5[1,2]. Due to this cross reactivity between two CYPs, there is need to address contribution of CYP3A5 in the metabolism of test compounds. Therefore, it is crucial to find specific substrate and MBI of CYP3A5 for production of Silensomes™CYP3A5. Thanks to discovery of T-5 compound and its specific oxidation reaction to N-oxide by CYP3A5 offer an opportunity to access this aim and to identify the contribution of CYP3A5 during in-vitro drug metabolism by comparison to CYP3A4 (3). In addition, discovery of Lapatinib as MBI of CYP3A5 gave clue to design Silensomes™CYP3A5 using T-5 as substrate [4]. Here, we report *in-silico* Docking approach (Geometric shape complementarity score and binding energy) to find specificity of T-5 substrate for CYP3A5 as compare to testosterone and midazolam. In addition, we evaluated the inhibition potency of inhibitors lapatinib, azamuline and ketoconazole towards CYP3A5 as inhibitor and potentially MBI. Firstly, we discovered two binding pockets: P1/P2 in the CYP3A5 (protein data bank code 5VEU) and one binding pocket in CYP3A4. Therefore, all these pockets are considered for our protein-ligand docking analysis. CYP3A5 predicted higher specificity for substrate T-5 (T-5 [score= 5718] > midazolam [score=3950]> testosterone[score=3656]) in the pocket P1. For CYP3A5 inhibitors, lapatinib (lapatinib [score=6892] > LAP-OH [score=6506] > ketoconazole [score=6004] > azamuline [score =4770]) is predicted to has higher affinity for

pocket P1. CYP3A4 also predicted specificity for substrate testosterone and T-5 (T-5 [score = 5518] > testosterone [score = 4230] > midazolam [score = 3826]) in the pocket A1. However, CYP3A4 together with CYP3A5, the T-5 will not form T-5 N-oxide as metabolite (Specific reaction catalyzed by CYP3A5). Also, lapatinib (lapatinib [score = 6286] > ketoconazole [score = 5528] > LAP-OH [score= 5302] > azamuline [score = 4774]) is found to has affinity for pocket A1 of CYP3A4; however, it forms reversible complex with CYP3A4 and its reactive metabolite forms irreversible complex with CYP3A5[4]. Therefore, our *in-silico* approach predicted that due to more specificity of T-5 for CYP3A5, T-5 could be use as substrate for CYP3A5. In addition, due to higher affinity of lapatinib for CYP3A5 predicted to be potential MBI for CYP3A5. In the poster, the detail analysis of binding energies score and interaction will be provided. Our work conclude that Silensomes CYP3A5, with CYP3A5 irreversibly inactivated by MBI lapatinib, could be produced by using T-5 as substrate to understand the metabolism of given test compound via CYP3A5.

References:

1. Parmentier et al, Xenobiotica. 2018 Jan 10:1-14.;
2. Parmentier et al, Xenobiotica. 2017 Jul;47(7):562-575.
3. Li et al, 2014, Drug Metab Dispos 42:334–342.
4. Towles et al, Drug Metab Dispos. 2016 Oct;44(10):1584-97

P24 - ARE CYP3A5 EXPRESSER SUBPOPULATIONS AT AN INCREASED RISK FOR ACETAMINOPHEN TOXICITY?

Kunihiko Mizuno and Michael Zientek
Takeda California, Inc.

Acetaminophen (APAP) is a widely used antipyretic drug, which is one of the most widely utilized, over the counter, medicines available. Acetaminophen toxicity is also one of the leading causes of acute liver failure (ALF). The key mechanism to this hepatotoxicity is cytochrome P450 catalyzed formation of the reactive metabolite, N-acetyl-p-benzoquinone imine (NAPQI), which has been shown to form protein adducts of NAPQI with protein sulfhydryl groups of cysteine triggering mitochondrial damage, oxidative stress, cjun N-terminal kinase (JNK) activation, the nuclear DNA fragmentation and cell death. Several isoforms of human P450, including 1A2, 2B6, 2C9, 2C19, 2D6, 2E1, 3A4 have been shown to catalyze this oxidative product of APAP to NAPQI. Whereas, 1A2, 2E1, 2D6 and 3A4 isoforms have been shown to be quite influential in the risk potential of acetaminophen toxicity during overdose¹.

It has been reported, individuals carrying the CYP3A5 rs776746 A allele have been overrepresented among ALF patients who had intentionally overdosed with acetaminophen compared with all other ALF patients including individuals who have the G allele, but lack active CYP3A5 enzyme because of aberrant gene splicing². This finding was not surprising in that the A allele polymorphism produces a greater quantity of CYP3A5 enzyme, and an enhanced bioactivation of acetaminophen. Hence, the aim of this work was to provide an *in vitro* kinetic understanding of those subpopulations who express CYP3A5, and how it might influence the risk of ALF in those who overdose on acetaminophen. Investigations were made into whether human CYP3A5 is involved in bioactivation of APAP, and how much compared to other isoforms of cytochrome P450. Firstly, it was confirmed that the formation of NAPQI from APAP by human recombinant CYP 3A5 enzyme does occur *in vitro*. Km and Vmax values were 438 uM and 127 pmol/min/nmol of P450, respectively. Secondly, the contribution of CYP3A5 to the formation of NAPQI was determined utilizing a representative donor of CYP3A5 extensive metabolizer (CYP3A5 EM (1*1)) and a poor metabolizer (3*3) microsomes. This kinetic data comparisons, with and without specific P450 inhibitors, provided an understanding to the involvement of CYP3A5 in NAPQI production compared to other cytochrome P450 isoforms. Our data suggests, in a limited number of CYP3A5 expressers, CYP3A5 does not contribute very much, if at all, to the production of NAPQI and therefore would not influence or enhance acetaminophen toxicity in CYP3A5 expressers.

References:

1. Laine JE, Auriola S, Pasanen M, and Juvonen RO (2009) Acetaminophen bioactivation by human cytochrome P450 enzymes and animal microsomes. Xenobiotica 39:11–21.
2. Court MH(2014) Candidate Gene Polymorphisms in Patients with Acetaminophen-Induced Acute Liver Failure. Drug Metab Dispos 42:28-32.

P25 - CYTOCHROME P450 3A ENZYME-DEPENDENT THALIDOMIDE TOXICITY AND INDUCIBILITY IN CULTURED HUMAN PLACENTAL CELLS

Norie Murayama¹, F.Peter Guengerich², and Hiroshi Yamazaki¹

¹Showa Pharmaceutical University, ²Vanderbilt University School of Medicine

Oxidative metabolism of thalidomide is important for both its teratogenicity and anticancer efficacy in primates through multiple mechanisms. Thalidomide induced limb abnormalities in whole-embryos of transchromosomal mice containing a

human cytochrome P450 (P450) 3A cluster. Although reactive metabolites are generated in the oxidation of thalidomide by human P450 enzymes in both livers and embryos, there is no information available regarding placenta in terms of metabolic activation of thalidomide. In this study, we investigated P450 3A4/5 mRNA expression and drug oxidation activities in a relevant commercially available BeWo placental cell line. Human placental BeWo cells, cultured in the recommended media, showed detectable midazolam 1'- and 4-hydroxylation and thalidomide 5-hydroxylation activities. Induction of P450 3A4/5 mRNA and oxidation activities were measured in placental BeWo cells cultured with a modified medium containing 5% charcoal-stripped fetal bovine serum to reduce any masking effects by endogenous hormones used in the recommended media. Thalidomide significantly induced P450 3A4/3A5, 2B6, and pregnane X receptor (PXR) mRNA levels 2- to 3-fold, but rifampicin only elevated P450 3A5 and PXR mRNA under the modified media conditions. Thalidomide also significantly induced midazolam 1'-hydroxylation and thalidomide 5-hydroxylation activities (3-fold) but not bupropion hydroxylation activity. These results collectively suggest activation of thalidomide to 5-hydroxythalidomide with autoinduction of P450 3A enzymes in human placentas, as well as livers, and relevance to bioactivation and toxicity.

P26 - RAPID CYP450 QUANTIFICATION BY IMMUNOAFFINITY-MASS SPECTROMETRY

Oliver Pötz¹, Helen Hammer¹, Felix Schmidt², Kathrin Klein³, Ulrich M Zanger³, and Thomas O Joos²

¹SIGNATOPE GmbH, ²NMI, ³Dr. Margarete Fischer-Bosch-Institute of Clinical Pharmacology

The quantity of CYP450s in liver impact the turnover of drugs and xenobiotics. The amount can be influenced by nuclear receptor dependent protein induction, microRNAs or of course by the genotype. To date CYP protein induction is routinely measured using mRNA as a surrogate. However, within the last decade several mass spectrometry-based approaches for the quantification of CYP450s have been established ¹⁻³. Here, the CYP expression is quantified by the analysis of CYP-isoform-specific peptides in enzymatically proteolyzed biological samples. Quantification is achieved by spiking a defined amount of corresponding ¹³C/ ¹⁵N-labeled peptide standards. However, current proteomic MS-based approaches for CYP-quantification demand for large amount of sample material since usually a laborious microsomes preparation step is required to achieve sufficient sensitivities.

Recently, we have combined immunoprecipitation of CYP-isoform specific peptides with mass spectrometry read out, which allows quantification from a minute amount of sample ^{4,5}. A multiplex assay panel can be used to determine the amount of 16 CYP proteins from 5 µg protein extract. Moreover, the antibodies applied in the immunoaffinity-enrichment step can be used for pulling down several CYP-specific peptides from different isoforms since their epitopes are motifs comprised in the peptides of interest.

We show technical validation data including accuracy, precision, linearity, short and long-term stability demonstrating robustness reproducibility of the assay panel. Using this validated method, we analyzed samples from pharmacokinetics studies in human hepatocytes cultured in in 96-well format demonstrating its suitability for routine assessment of CYP protein induction experiments required in the drug-development pipeline process. Moreover, we present the CYP expression profiles from 150 geno-typed liver biopsies.

References:

1. Jenkins, R. E.; Kitteringham, N. R.; Hunter, C. L.; Webb, S.; Hunt, T. J.; Elsby, R.; Watson, R. B.; Williams, D.; Pennington, S. R.; Park, B. K. *Proteomics* 2006, 6, 1934-1947.
2. Kawakami, H.; Ohtsuki, S.; Kamiie, J.; Suzuki, T.; Abe, T.; Terasaki, T. *J Pharm Sci* 2011, 100, 341-352.
3. Schaefer, O.; Ohtsuki, S.; Kawakami, H.; Inoue, T.; Liehner, S.; Saito, A.; Sakamoto, A.; Ishiguro, N.; Matsumaru, T.; Terasaki, T.; Ebner, T. *Drug Metab Dispos* 2012, 40, 93-103.
4. Weiss, F.; Hammer, H. S.; Klein, K.; Planatscher, H.; Zanger, U. M.; Noren, A.; Wegler, C.; Artursson, P.; Joos, T. O.; Poetz, O. *Drug Metab Dispos* 2018, 46, 387-396. (5) MacLean, C.; Weiss, F.; Poetz, O.; Ebner, T. *J Pharm Sci* 2017.

P27 - QUANTITATIVE DETERMINATION OF THE EFFECT OF DDT AND DDE TREATMENTS ON CYP1 ENZYME EXPRESSION IN MCF-7 CELLS

Brianne Raccor, Aritra Bhadra, and Shreelekha Jaligama

Campbell University College of Pharmacy and Health Sciences

Compounds that persist in the environment, such as dichlorodiphenyltrichloroethane (DDT) and dichlorodiphenyldichloroethylene (DDE), are a public health concern. DDT and DDE are endocrine disruptors that bind to the estrogen receptor (ER) and modulate gene expression. However, the activation of ER has been shown to also reduce the expression of genes under the regulation of the aryl hydrocarbon receptor (AhR).¹ An example of the genes that could be affected are the *cytochrome P450 1 enzymes (CYP1)*, specifically *CYP1A1* and *CYP1B1*, that are involved in the production of catechol estrogen metabolites in extra-hepatic tissues, such as the breast. *CYP1B1* is involved in the formation of 4-hydroxyestradiol, which can easily be oxidized to an ortho-quinone capable of adducting to DNA and initiating carcinogenesis.² The ability of DDT and DDE to modulate estrogen metabolism after ER activation has not been fully explored. Furthermore, *CYP1A1* and *CYP1B1* expression appears to be under the control of the AhR, but *CYP1B1*

may also be under the control of the ER.³ Therefore, the hypothesis of this study is that DDT or DDE will cause differential expression of the *CYP1* enzymes and will change the ratio of estrogen metabolites formed in MCF-7 cells via the activation of the ER. In order to test this hypothesis, the concentrations and incubation times used in the gene expression study were optimized. A concentration range for DDT treatment was selected based on the results of the 3-(4,5-dimethylthiazol-2-yl)-2,5-diphenyl tetrazolium (MTT) absorbance assay. The ER positive MCF-7 cells were treated with 1 nM 2,3,7,8-tetrachlorodibenzodioxin (TCDD) for 8 h, 24 h, 48 h and 72 h to determine the maximum induction of *CYP1* enzymes. TCDD is a known activator of the AhR. Maximum induction of *CYP1A1* was seen at 72 h in MCF-7 cells. MCF-7 cells were incubated with DDT at concentration range of 0.01 μ M-1 μ M, 1 nM TCDD or 1 nM estradiol for 72 h. The treatment of cells with 0.01 μ M and 1 μ M DDT significantly increased the relative expression of *CYP1B1* but decreased the relative expression of *CYP1A1*. These results suggest that activated ER plays an important role in the regulation of the *CYP1* family and could lead to the increased production of carcinogenic metabolites. These results will be further verified by quantitating the estrogen catechol metabolites formed by *CYP1A1* or *CYP1B1* after treatment with DDT or DDE using HPLC-UV and determining the amount of protein after treatment via western blot in MCF-7 cells.

References:

1. Estrogen receptor- α and aryl hydrocarbon receptor involvement in the actions of botanical estrogens in target cells. Gong P, Madak-Erdogan Z, Flaws JA, Shapiro DJ, Katzenellenbogen JA, Katzenellenbogen BS, *Molecular and Cellular Endocrinology*, 2016(437): 190.
2. Depurinating estrogen-DNA adducts, generators of cancer initiation: their minimization leads to cancer prevention. Cavalieri EL, Rogan EG, *Clinical and Translational Medicine*, 2016(5): 12.
3. Human *CYP1B1* is regulated by estradiol via estrogen receptor. Tsuchiya Y, Nakajima M, Kyo S, Kanaya T, Inoue M, Yokoi, T, *Cancer Research*, 2004(64): 119.

P28 - A NEW CYP-SILENCED CELL-BASED ASSAY FOR DIRECT MEASUREMENT OF THE CONTRIBUTION OF MAJOR CYTOCHROME P450 ENZYMES TO DRUG CLEARANCE/ METABOLISM

Ashwani Sharma, Belkacem Bouaita, Karine Rondel, Fabrice Guillet, Christophe Chesne, and Ruoya Li
Biopredic International

Background and Objectives: Drug-drug interactions (DDIs) are a serious clinical issue. The evaluation of DDIs potential is an integral part of drug development. Various *in vitro* approaches described in the FDA & EMA guidelines have been developed to identify specific enzymes involved in the metabolism of drug candidates for CYP reaction phenotyping. However, a combination of approaches is recommended by the regulatory agencies since each method has its limitations. Recently, an original strategy, called Silensomes™, to produce human liver microsomes silenced for one specific CYP450, has been developed using specific mechanism-based inhibitors (MBI) (*Y. Parmentier et al 2016, 2017*). This easy and ready-to-use *in vitro* tool, combining the advantages of existing models, allows a direct and quantitative evaluation of the human CYP contribution (fm) to drug clearance.

The aim of this proof-of-concept study was to adapt this smart MBI technology to create specific single CYP-silenced human hepatocyte model. This cell-based assay could take into account the interplay between the phase I, phase II metabolizing enzymes and phase III transporters on DDIs.

Methods and Results: Pooled primary human hepatocytes (PHH) from different donors were pre-incubated respectively with azamulin for CYP3A4 and furafyline for CYP1A2 at optimized concentration to generate targeted CYP-silenced PHH. Two batches were obtained and cryopreserved. The potent inhibition of CYP-silenced PHH batches and related PHH controls was then evaluated using CYP specific probe substrates.

The results showed that the targeted CYP activities were specifically and significantly inhibited in each specific CYP-silenced PHH batch in comparison with control-PHH. In case of the CYP3A4-Silenced PHH batch, the CYP3A4-mediated metabolism of three substrates (midazolam, nifedipine, testosterone) was also strongly inhibited, with around 80%, 83% and 93% inhibition, respectively. In case of the CYP2A1-Silenced PHH batch, around 95% of CYP1A2-mediated metabolism of phenacetin was inhibited. Additional incubations with drugs known to be metabolized by the phase I and phase II enzymes with varying Clint ratio allow to directly predict the CYP contribution to drug metabolism impacted by cellular events in comparison with Silensomes™ model.

Conclusion: This new CYP-silenced cell-based DDIs model could offer a biologically relevant substitute to predict the response of a drug on an organism predicting clinical DDIs in the early-stage drug discovery pipeline.

P29 - OXIDATIVE METABOLISM OF SYNTHETIC CANNABINOID STS-135 BY RECOMBINANT P450S AND HUMAN LIVER MICROSOMES

Azure Yarbrough, Ryoichi Fujiwara, William Fantegrossi, Paul Prather, and Anna Radomska-Pandya
University of Arkansas for Medical Sciences

Synthetic cannabinoids (SCBs), synonymous with 'K2', 'Spice' or 'synthetic marijuana', are rapidly emerging drugs of abuse that possess psychoactive properties similar to those of Δ^9 -tetrahydrocannabinol. A number of serious adverse

effects have been associated with these compounds including seizures, severe tachycardia, psychosis, and even death. Like previous "generations" of SCBs, *N*-(adamantan-1-yl)-1-(5-fluoropentyl)-1*H*-indole-3-carboxamide (STS-135) is also an indole-based drug that possesses higher affinity for the cannabinoid type 1 receptor as compared to products from previous SCBs. STS-135 undergoes Phase I and II metabolism, resulting in the formation of 29 metabolites. Among them, monohydroxy STS-135 (M25) and dihydroxy STS-135 (M21) are the major metabolites produced by human hepatocytes; however, the enzymes responsible for oxidative metabolism of this SCB have not been identified. In the present study, STS-135 was incubated with human liver microsomes (HLMs) as well as recombinant cytochrome P450s (CYPs) in the presence of a NADPH regenerating system. The enzymatic reactions were terminated and subjected to ultra-performance liquid chromatography analysis at 300 nm. M25 and M21 were also identified as the major oxidative metabolites of STS-135 in HLMs. The formation of these metabolites by HLMs was significantly reduced by the CYP3A-inhibitor ketoconazole. Among the 11 recombinant CYPs examined, CYP3A4 and CYP3A5 showed high activities for oxidation of STS-135. To investigate which CYP isoform was the most important for oxidation of STS-135 in the liver, 10 μ M STS-135 was incubated with genotyped individual HLMs for increasing time periods. The half-life for substrate disappearance ($t_{1/2}$) was 8.5 ± 0.6 min in HLMs with no CYP3A5^{*3/*3} activity, which was significantly shorter than that of HLMs with high CYP3A5^{*1/*1} activity, 21.1 ± 0.5 min. These observations indicate that CYP3A4 is the main enzyme responsible for the oxidative metabolism of STS-135 in the liver. It was further demonstrated that co-incubation with several other SCBs produced inhibitory effects on the oxidation of STS-135 by HLMs. Interestingly, CYP2J2, a CYP isoform that is highly expressed in cardiovascular tissues, showed high activity for the formation of M25 with a K_m value of 11.4 ± 2.0 μ M. Based on these studies, we hypothesize that individuals with low CYP3A4 activities could show elevated STS-135 blood concentrations, possibly leading to the development of severe toxicity. Inhibition of CYP3A4 mediated STS-135 metabolism by co-administered drugs, food, herbs, and/or SCBs could further increase concentration of STS-135 in the blood. CYP2J2 might be an important enzyme that protects individuals from STS-135 induced cardiovascular toxicity. (NIH/NIDA DA039143 to ARP and PLP).

P30 - ASSOCIATION OF HIGH BLOOD LEAD LEVELS WITH FOK1, APA1 AND BSM1 VITAMIN D RECEPTOR GENE POLYMORPHISM IN OCCUPATIONALLY EXPOSED BATTERY WORKERS

Himani¹, Sudip Kumar Datta², Raman Kumar², Jamal Akhtar³, Dilutpal Sharma³, Abbas Ali Mahdi³, and Busi Karunanand¹
¹SGT Medical College Hospital & Research Institutem ²All India Institute Of Medical Sciences, ³King George's Medical University Lucknow

Vitamin D regulates calcium and phosphate metabolism in our body mediated through a nuclear vitamin D receptor (VDR). Lead, being a divalent cation follows the pathways similar to calcium and hence affects its homeostasis.⁽¹⁾ Some VDR polymorphisms have been shown to be functional and hence may affect calcium and lead metabolism. The present study was designed to look into the association of VDR polymorphisms with blood lead levels in occupationally exposed workers. Blood levels of Vitamin D, Calcium and phosphorus were also measured. 100 occupationally lead-exposed male battery workers and 100 age matched male controls were recruited for this study with their informed consent after instructional ethical clearance. Routine biochemistry including serum calcium and phosphorous were measured using Modular P biochemistry auto-analyzer (Roche diagnostics, USA). Active Vitamin D3 was estimated by competitive ELISA (Cal biotech, El Cajon, California). Genomic DNA was extracted from EDTA blood using commercially available kits (Qiagen, Hilden, Germany). VDR gene polymorphisms (Fok1, Taq1, Apa1 and Bsm1) were studied using Polymerase Chain Reaction followed by Restriction fragment Length Polymorphism (PCR-RFLP). Blood lead levels (BLL) were determined using Inductively coupled plasma mass spectrometry (ICP-MS) from whole blood. Data was analyzed statistically using the GraphPad prism 5.0 software. Results demonstrated that there was significantly higher BLL in the occupationally lead exposed battery workers (median 28.35, range 5.5-139.7) compared to the healthy controls (median 8.85, range 0-39.6). Controls also demonstrated significantly higher serum vitamin D3 levels (53.5 ± 11.7 ng/ml) compared to the battery workers (18.9 ± 8.9 ng/ml). Apa1 and Bsm1 mutant homozygous polymorphisms were associated with higher BLL compared to wild types and heterozygous mutants. Wild type Fok1 genotypes were associated with high BLL compared to mutants. However, Taq1 polymorphisms did not reveal any such associations. Besides, these genotypes were not associated with any significant variations in vitamin D3, calcium and phosphorus levels. Wild type Fok1 genotypes (FF) and Apa1 and Bsm1 mutant homozygous (aa & bb) were associated with high BLL compared other genotypes.

Reference:

1. Agency for Toxic Substances and Disease Registry (ATSDR). Toxicological profile for lead, US Department of Health and Human Services. Atlanta GA: US Government Printing; 2005.p. 102–225.

P31 - CIRCULATING HORMONES AND NUCLEAR HORMONE RECEPTOR EXPRESSION ARE ASSOCIATED WITH TREATMENT-FREE SURVIVAL IN PATIENTS WITH CHRONIC LYMPHOCYTIC LEUKEMIA.

Eric Allain¹, Karin Venzl², Patrick Caron¹, Veronique Turcotte¹, David Simonyan³, Michaela Gruber², Trang Le², Eric Levesque¹, Chantal Geuillemette¹, and Katrina Vanura²

¹Pharmacogenomics laboratory, CHU de Quebec Research Center and Faculty of Pharmacy - Laval University, ²Division of Hematology and Hemostaseology, Department of Medicine I, Medical University of Vienna, ³Statistical and Clinical Research Platform, CHU de Quebec Research Center, Laval University

CLL is the most prevalent adult leukemia in the western world. While it is not considered a hormone-regulated cancer, sex is a known risk factor with a male/female incidence ratio of 2:1 and male patients also developing progressive disease more frequently. Despite these significant clinical observations, a detailed analysis of sex steroids, pituitary hormones, and hormone receptor expressions in CLL patients is still lacking.

This study aimed to provide a first insight into sex steroids in CLL and explore possible relationships between these hormones, their receptors, and disease progression in CLL. We hypothesized that variable hormonal exposure may have a sexually dimorphic effect on CLL progression.

We quantified 15 circulating sex steroids (androgens, estrogens and progesterone) by sensitive and specific mass spectrometry and measured two pituitary hormones (luteinizing hormone (LH) and follicle-stimulating hormone (FSH)) by immunoassay in 156 samples from mostly early-stage, treatment-free CLL patients. Nuclear receptor expression levels were measured by RT-qPCR. Data were analyzed separately by sex and univariate and multivariate analyses of treatment-free survival (TFS) were performed using Cox's proportional hazard model.

Median age of CLL patients was 59.8 and 62.9 years for men and postmenopausal women, respectively. Known CLL prognostic markers had similar frequencies between male and female cases. Median TFS was shorter for male patients than for women (80.7 vs. 135.0 months, $P=0.033$). Hormonal profiles of CLL patients differed considerably from those of healthy donors. Male CLL cases had higher levels of circulating steroids than female patients, confirming the relevance of analyzing them separately. In male CLL cases, no association was noted between steroid levels and TFS; however, higher LH levels were associated with shorter TFS in multivariate analyses with an adjusted hazard ratio (HR_{adj}) of 2.11 ($P=0.004$). In female CLL cases, high levels of potent androgen receptor (AR) ligands testosterone (T) and dihydrotestosterone (DHT) were associated with improved TFS with HR_{adj} values of 0.24 ($P=0.007$) and 0.53 ($P=0.023$), respectively. In univariate analyses, high AR expression was associated with improved outcome in female CLL cases ($HR=0.70$, $P=0.009$). Trends for improved survival with high AR expression in male patients ($HR=0.84$, $P=0.081$) and high estrogen receptor α expression ($HR=0.76$, $P=0.056$) were also noted.

This study is the first to comprehensively profile steroids and pituitary hormones in CLL patients and to establish a link between outcome of CLL patients and circulating hormones. It reveals a sex-specific hormonal imbalance associated with disease progression and suggests a possible role for nuclear steroid hormone receptor signaling in CLL cases.

This work was supported by the Canadian Institutes of Health Research to CG.

P32 - SEX DIFFERENCES IN BRAIN OXYCODONE METABOLISM AND ANALGESIA

Nicole Arguelles, Fariba Baghai Wadji, Maria Novalen, Sharon Miksys, and Rachel Tyndale
University of Toronto

Background: Sex differences are recognized in opioid analgesia, abuse, and dependence in animals and humans. The underlying mechanism is unclear but may involve differences in pharmacokinetics and/or pharmacodynamics. Numerous opioids are substrates of CYP2D, and variation in this enzyme's activity alters opioid response. We previously showed that inhibiting brain CYP2D, leaving hepatic CYP2D unchanged, in male rats increased oxycodone analgesia and oxycodone brain levels, measured by *in vivo* microdialysis, but not plasma levels; together, this suggests a role for brain CYP2D in oxycodone-induced analgesia. Our pilot data indicate that female rats have lower *ex vivo* brain CYP2D activity than males, suggesting a possible role in sex differences in opioid response. We hypothesize that females will have higher brain oxycodone levels, and thus, will experience greater analgesia in the dose-response compared to their male counterpart.

Method: Male and female rats, at different estrous cycle stages, were administered varying amounts of oxycodone orally by gavage. Oxycodone-induced analgesia was measured using tail-flick latency. Brain drug levels were measured over time through *in vivo* brain microdialysis. Data were analyzed by one-way or two-way ANOVA, with post hoc analysis for multiple comparisons.

Results: Female rats experienced greater peak analgesia and overall analgesia ($AUC_{(0-120)}$), compared to male rats at 7.5, 10, and 12.5 mg/kg oral oxycodone. Consistent with this, female rats had higher brain oxycodone levels than male rats. These differences were greatest in females in diestrus phase, both in oxycodone-induced analgesia and brain oxycodone levels. For example, at 10 mg/kg oxycodone, females in diestrus phase had a 2.0-times higher peak and 2.9-times higher $AUC_{(0-120)}$ analgesia relative to males, while females in estrus phase had a 1.2-times higher peak and 1.5-times higher $AUC_{(0-120)}$ analgesia relative to males. These were also observed at the higher and lower dose of oxycodone. We are currently characterizing the relative contribution of CYP2D to these observed sex differences.

Conclusion: These data, consistent with our pilot *ex vivo* data, suggest that females may have lower brain CYP2D activity which may vary with estrous cycle. Thus, females appear to metabolize less oxycodone in brain resulting in higher brain oxycodone levels and greater analgesia than males, which is even more pronounced during diestrus phase. This sex difference may also affect other CYP2D CNS acting substrates.

P33 - IDENTIFICATION OF METABOLOMIC BIOMARKERS FOR ENDOMETRIAL CANCER AND ITS RECURRENCE AFTER SURGERY IN POSTMENOPAUSAL WOMEN

Yannick Audet-Delage, Lyne Villeneuve, Jean Gregoire, Marie Plante, and Chantal Guillemette
CHU de Quebec Research Center - Laval University

Endometrial cancer (EC) is the most frequent gynecological cancer in developed countries. Most EC occurs after menopause and is diagnosed as endometrioid (type I) carcinomas, which exhibit a favorable prognosis. In contrast, non-endometrioid (type II) carcinomas such as serous tumors have a poor prognosis. Our goal was to investigate metabolic changes associated with EC subtypes and recurrence after surgery in postmenopausal women and identify novel blood-based biomarkers. Using mass spectrometry-based untargeted metabolomics, we examined preoperative serum metabolites among control women (n = 18) and those with non-recurrent (NR) and recurrent (R) cases of type I endometrioid (n = 24) and type II serous (n = 12) carcinomas. R and NR cases were similar with respect to pathological characteristics, body mass index and age. A total of 1592 compounds were analyzed including 14 different lipid classes. We identified putative cancer-specific and recurrence biomarkers. When we compared EC cases with controls, 137 metabolites were significantly different. Polyamine and branched-chain amino acids pathways were particularly affected in EC patients compared to controls. The combination of spermine, isovalerate, glycylvaline, and gamma-glutamyl-2-aminobutyrate resulted in an age-adjusted area under the ROC curve (AUC_{adj}) of 0.921 (95% CI = 0.843 -1.000). A total of 98 metabolites significantly distinguished type I from type II ECs. Our data identified an inflammatory mediator, bradykinin, as a putative biomarker of Type I EC, whereas modifications in pathways closely related to heme synthesis, namely the tetrahydrofolate-serine/glycine pathway, was observed for Type II EC. Compared to NR cases, type I R cases displayed lower levels of primary and secondary bile acids and elevated concentrations of inflammation-associated phosphorylated fibrinogen cleavage peptide, whereas type II R cases displayed alterations in ceramide pathways. Regardless of histotypes, the combination of 2-oleoyl-glycerol and TAG42:2-FA12:0 allowed the distinction of R cases from NR cases with an AUC_{adj} of 0.901 ($P < 0.001$); confirming the ability of these metabolites to predict recurrence. Mechanistic studies are needed to help gain insights into the underlying biological processes driving the observed changes in these metabolites. Our findings represent an important pilot study in the identification of putative serum biomarkers useful for detecting endometrial cancer and predicting recurrence following initial surgery. This work was supported by The Cancer Research Society (CRS) and Canadian Institutes of Health Research (FRN-68964).

P34 - CONTRIBUTION OF HEPATIC FMO-1 IN THE METABOLISM OF COMPOUND 1. IMPLICATION OF CLEARANCE MECHANISM AND EXTRAPOLATION OF METABOLISM DATA FROM PRECLINICAL SPECIES TO HUMANS

Steve Bowlin, Kirk Kozminski, and Amin Kamel
Takeda, San Deigo

Flavin-containing monooxygenases (FMOs) are one of the most important non-cytochrome P450s (CYPs) enzymes involved in the oxidation of nucleophilic nitrogen, sulfur, phosphorus and selenium heteroatoms of a variety of xenobiotics. Similar to CYPs, FMOs are microsomal enzymes that require O_2 and NADPH and many of the reactions catalyzed by FMOs can also be catalyzed by CYPs. However, FMOs can be differentiated from CYPs by heat inactivation and inhibition by specific competitive substrate inhibitors such as methimazole and thiourea. The complement of FMOs present in major sites of drug metabolism, such as liver, kidney, lung, and small intestine, differs qualitatively and quantitatively in human. In adult human liver, the main FMOs are FMO3 and FMO5, with FMO1 being absent. Compound 1 has a basic tertiary amine and tertiary amines are often excellent substrates for FMO and are oxygenated exclusively to the N-oxide. A notable species difference in Cl_{int} and E_h using microsomes and hepatocytes was observed with much lower Cl_{int} and E_h in human compared to all other species (mouse, rat, dog and monkey). Furthermore, *in vivo* studies in rat, dog and monkey showed high CL and results were consistent with *in vitro* findings. Therefore, *in vitro* metabolite identification studies were conducted to provide more insights on the metabolism of compound 1 and its possible contribution to the observed species difference in CL. In addition, the potential contribution of FMO in the overall metabolism of compound 1 was investigated. Structure elucidation of metabolites was carried out on an AB Sciex TripleTOF 5600 LC/MS/MS system using positive ESI mode and full scan TOF-MS with Mass Defect Filter triggered MS/MS acquisition.

Results suggested that compound 1 undergoes phase II conjugative pathways as well as phase I oxidative pathways including the formation of N-oxide. The formation of N-oxide of compound 1 was the major metabolite in rat liver microsomes (~ 55%) and only accounted for ~ 17% in human liver microsomes. The formation of compound 1 N-oxide is

mediated by rFMO1, 3, and 5 but to a larger extent by rFMO1. Contribution of hepatic FMO1 in the metabolism of compound 1 and the formation of its N-oxide metabolite may provide additional insights on clearance mechanism and help in extrapolation of metabolism data from preclinical species to humans.

P35 - CHEMICAL-INDUCED TOXICITY IS AMELIORATED BY SWIMMING EXERCISE IN CAENORHABDITIS ELEGANS

Jessica Hartman¹, Latasha Smith¹, Kacy Gordon¹, David Sherwood¹, Ricardo Laranjeiro², Monica Driscoll², and Joel Meyer¹

¹Duke University, ²Rutgers University

Exercise improves health, including reducing risk of cardiovascular disease, neurological disease, and cancer, but exercise impacts on xenobiotics (such as environmental chemicals) are less known. Further, the molecular mechanisms underlying exercise protections are poorly understood, partly due to the cost and time investment of mammalian long-term exercise intervention studies. We subjected *Caenorhabditis elegans* nematodes to a 6-day, twice daily exercise regimen, during which time the animals also experienced brief, transient food deprivation. Accordingly, we included a non-exercise group with the same transient food deprivation, and a control with *ad libitum* access to food. We hypothesized that exercised animals would be more resistant to chemical toxicity compared to non-exercised controls. We tested two well-characterized environmental chemicals that target mitochondria in their mechanism of toxicity, arsenic and rotenone. Exercise-conditioned animals (and to a lesser extent, transiently food-deprived animals) were markedly protected against lethality from acute rotenone and arsenic exposures (with 2-3 fold increased LC₅₀ values, p<0.001). We then tested measures of mitochondrial health, hypothesizing that healthier mitochondria could handle a larger chemical insult. Exercise, combined with food deprivation, protected against age-related decline in mitochondrial morphology in body-wall muscle. Transient food deprivation increased organismal basal respiration (20% increase, p<0.001); however, exercise was the sole intervention that increased spare respiratory capacity (30% increase, p<0.05) and proton leak (2-fold increase, p<0.05). Finally, we observed modestly increased lifespan in exercised animals compared to both control and transiently food-deprived nematodes (p<0.05). To clarify whether exercised animals benefited simply from a further energy expenditure compared to caloric intake, we also tested animals exercising in liquid media containing bacterial food. Those animals showed no benefits in mitochondrial respiration or lifespan; however, exercise in food also resulted in maintenance of better mitochondrial networks (p<0.01) and dramatic protection from arsenic and rotenone exposure. Thus, swimming exercise provided effective intervention in *C. elegans*, protecting from age-associated mitochondrial decline and providing remarkable resistance to chemical toxicant exposures.

P36 - ENVIRONMENTAL XENOBIOTICS SAFETY ASSESSMENT THROUGH COMPARATIVE METABOLISM STUDY IN FISH, SWINE, GOAT, CHICKEN, RAT AND HUMAN

Mingming Ma, Xiao Zhou, Vivek Badwaik, Kimberly Ralston-Hooper, Lisa Buchholz, and Tony Trullinger
Dow AgroSciences

It is essential to evaluate the safety of the environmental xenobiotics, such as agrochemical or pharmaceutical contaminants to ensure the environmental safety and human health. As the xenobiotic detoxification capability of different species directly correlates to the differential metabolism including clearance and biotransformation pathways, the interspecies comparative metabolism studies could provide valuable information to allow more accurate risk assessment and data extrapolation across species. Here we aimed to study the comparative metabolism in fish and livestock (swine, goat and chicken), which are representative species which could be potentially exposed to the environmental xenobiotics through water or diet, as well as the rat and human. Several representative ¹⁴C radiolabeled agrochemicals and non-radiolabeled pharmaceutical compounds such as verapamil and clozapine were investigated. The *in vitro* clearance and comprehensive metabolism profile were generated utilizing liver microsome or S9 fractions. The comparison across species was made to evaluate the differential metabolism behavior such as fish versus livestock and livestock versus rat/human. Furthermore, the *in vitro* results were compared with the available *in vivo* data to understand the *in vitro* to *in vivo* correlations and the relationship to the toxicity effects. The preliminary results showed interspecies variations in clearance and several test compounds exhibited species-specific metabolism at qualitative or quantitative levels. In general, slower and less extensive metabolism was observed in fish compared to the other species. The utilization of the *in vitro* hepatic incubations was further explored to predict and extrapolate the bioaccumulation potentials and toxicity effects of the xenobiotics in fish and mammals.

P37 - EFFECT OF AGE ON BRAIN EXPOSURE OF P-GP SUBSTRATES IN NEONATAL RATS

Michael Rooney, Kristopher King, Michael Calhoun, Richard Grater, Olga Golonzhka, Christopher Rowbottom, and Greg Dillon
Biogen

Design of preclinical pharmacology studies employing neonatal animals pose additional challenges such as estimating drug concentration at the site of action because a variety of factors influencing the clearance and distribution of small molecules change rapidly in developing animals¹. For instance, phosphorylation of tau is higher in the developing rat brain suggesting that juvenile rats may be a useful tool in Alzheimer's research for evaluating inhibitors of tau phosphorylation *in vivo*². Interestingly, *in vivo* studies with a small molecule inhibitor of tau phosphorylation, BG1, resulted in higher brain exposure than expected based on MDR1-MDCK substrate assays and *in vivo* brain penetration studies performed in adult rodents. These results demonstrate that developmental changes in rat metabolism, distribution, and blood brain barrier efflux pose a challenge to optimal design of PK/PD studies. To better inform the design of future *in vivo* pharmacology studies with compounds that are potent biochemical inhibitors of tau phosphorylation but are P-gP (ABCB1) substrates, brain penetration studies were performed in Sprague-Dawley rats at post-natal days 10 and 20 (P10 and P20, respectively) and adult rats. Brain and plasma were harvested at various times following IP or PO administration of BG1, the P-gP substrate, loperamide, and the BCRP (Abcg2) substrate, dantrolene. Drug concentration was determined by reverse phase HPLC-MS/MS following protein precipitation to determine total brain: plasma (Br:PI) ratios. Equilibrium dialysis experiments were performed to assess age-related changes in binding to rat plasma and brain to inform the impact of rat neonatal development on unbound Br:PI partitioning, K_p, u, u . Plasma AUC of all three compounds was highest in P10 rats compared to P20 and adult rats with exposure in P10 rats ranging from approximately 2.4- to >10-fold higher than in P-20 rats. A trend toward increased Br:PI partitioning in P10 rats was observed for the two molecules known to be P-gP substrates, BG1 and loperamide, with Br:PI ratios 2- to 3 fold higher in P10 rats than P20 rats. The impact of binding to plasma proteins and brain will also be discussed. In conclusion, plasma exposure of three small molecules was highest in P10 rats and Br:PI ratios of the P-gP substrates was also highest in P10 rats. These results suggest that unbound brain levels suitable for evaluating PK/PD relationships can be achieved with P-gP substrates lacking optimal clearance properties by using P10 rats. However, efficient design of PK/PD studies requires consideration of higher plasma exposure in neonatal rats and the impact of age-related expression of P-gP¹.

References:

1. Ghersi-Egea J-F, Saudrias B, Strazielle N. Barriers to Drug Distribution into the Perinatal and Postnatal Brain. *Pharm. Res.* (2018) 35: 84-93.
2. Yu Y, Run X, Liang Z, Li Y, Liu F, Liu Y, Iqbal K, Grundke-Iqbal I and Gong C-X. Developmental regulation of tau phosphorylation, tau kinases and tau phosphatases. *J. Neurochem.* (2009) 108: 1480-1494.

P38 - ADVERSE EFFECTS OF PSYCHIATRIC DRUGS ON BONE: DOES DRUG DISTRIBUTION TO MARROW PLAY A ROLE?

Karen Houseknecht¹, Deborah Barlow¹, Katherine Motyl², Tamara King¹

¹University of New England, ²Maine Medical Center Research Institute

Psychiatric medications, including antidepressant (AD), atypical antipsychotic (AA) and opioid (O) drugs have been reported to have negative effects on bone. Growing evidence suggests that AD and O can cause reduced bone mineral density and AA medications have been shown to increase fall and fracture rates. In 2017, the FDA added warning to the label of all AA drugs concerning increased risk of falls. The mechanism(s) underlying the negative effects of these medications on bone have not been fully elucidated. We and others have suggested that the effects of AA, AD and O on bone may be both indirect (CNS mediated) or direct. Although *in vitro* data from our lab and others indicate that these medications may directly impact osteoblast and/or osteoclast function, it is not clear to what extent these *in vitro* effects are physiologically relevant. To address this, we posed the question: Do psychiatric drugs distribute to bone marrow in clinically relevant concentrations? The bone marrow compartment is highly vascularized and innervated, so we hypothesized that drug exposure may be significant in this compartment. As there is a paucity of literature relating to drug distribution to bone and marrow, we have developed sensitive LC/MSMS analytical method to detect concentrations of AA, AD and O, relevant drug metabolites, and physiologically relevant hormones (prolactin) and neurotransmitters (dopamine, norepinephrine and their metabolites) in bone marrow collected from mice. To determine drug exposure in plasma, we dosed C57BL/6J mice with a single, clinically relevant dose of AD (fluoxetine, paroxetine; 10 mg/kg BW), AA (risperidone; 1.5 mg/kg BW or olanzapine, aripiprazole, clozapine; 10 mg/kg BW) or O (morphine; 3 mg/kg) drugs and measured exposure in plasma and marrow over 24 hr post-dose. We found that all of the psychiatric drugs tested distributed to marrow following dosing. To compare across the classes of drugs, we calculated marrow to plasma ratio (to correct for differences in dose). With the exception of risperidone (RIS), marrow:plasma values averaged less than 1.0. In the case of risperidone, marrow: plasma was significantly higher ($P < 0.001$), ranging 10-13.0, 1-3 hr post dose for the parent drug. The active metabolite, 9-OH RIS, also distributed to marrow in concentrations higher than the other drugs

tested ($P < 0.01$). As RIS has been reported to have the most significant negative impact on bone, clinically, it is tempting to speculate that this may be due, at least in part, to direct effects on bone/bone marrow. Known pharmacological targets of RIS, including dopamine, serotonin and alpha adrenergic receptors, are expressed on osteoclasts, osteoblasts and immune cells, found in the marrow compartment. Future studies will address the mechanisms underlying psychiatric drug distribution to marrow and the effects on hematopoiesis. The marrow compartment may prove to be an important target for both on and off-target effects of AA, AD and O.

P39 - DISTRIBUTION AND EXCRETION OF A NEW ORAL FORMULATION OF DOCETAXEL IN MICE

Byoung Soo Kim, Doo Hyun Yoon, Tae Hyun Choi, and Joo Hyun Kang
Korea Institute of Radiological and Medical Sciences

Docetaxel is an anticancer agent that is used widely in the treatment of breast, prostate, gastric, head and neck, and lung cancer. Intravenous administration of Taxotere® (a commercial form of docetaxel) leads to many problems such as hypersensitivity, hemolysis, cutaneous allergy, and patient refusal due to its prolonged injection. The oral absorption of Taxotere® is very low due to its hydrophobic nature. DHP23001 is an oral formulation of docetaxel that shows the improved oral bioavailability. These studies were performed to investigate the tissue distribution and excretion of radioactivity in mice following the single oral administration of [¹⁴C]DHP23001. Eight animals were euthanized and frozen at 0.25, 0.5, 1, 4, 8, 24, 48, and 96 h following an oral administration of [¹⁴C]DHP23001 to female ICR mice at a dose of 4.1 MBq/250 mg/kg. Sagittal plane sections at 6 levels were prepared using a whole body autocryotome and the distribution of radioactivity was investigated using the quantitative whole body autoradiography (QWBA) technique. The concentrations of radioactivity in tissues were expressed as ug equivalents DHP23001/g tissue. Another five mice were housed in metabolic cages following the oral administration. The urine and feces were collected at 4, 8, 24, 48, 72, and 96 h post administration. And the excretion of radioactivity in the urine and feces was determined using a liquid scintillation counter (LSC). The cumulative excretion of radioactivity in the urine and feces was measured. After the oral administration of [¹⁴C]DHP23001, relatively high levels of radioactivity were found in the gastrointestinal tract and gall bladder. And relatively low levels of radioactivity were found in liver. In other tissues, radioactivity was not different from background level. The cumulative excretion of radioactivity in the urine and feces up to 96 h was $0.51 \pm 0.25\%$ and $83.27 \pm 10.70\%$ of the dose, respectively. The total recovery of radioactivity up to 96 h was $83.92 \pm 10.61\%$ of the dose. DHP23001 mainly excreted via feces within 24 h after oral administration at a dose of 250 mg/kg in mice. It seems that the absorbed drug is eliminated mainly by biliary excretion in liver. These data would be helpful for the further development.

P40 - DISTRIBUTION AND PHARMACOKINETICS OF 3H-GEMCITABINE AFTER SINGLE AND MULTIPLE INTRAPERITONEAL TREATMENT ALONE AND IN COMBINATION WITH INTRAVENOUS DOCETAXEL IN BXP-3 TUMOR BEARING MICE

Elizabeth Spencer, Brandy Wilkinson, Sarah Wills, Phil Fernyhough, Cathleen Clutinger, Bonnie Jung, Michael J. Potchoiba, and Frederic W. Thalacker
Covance Laboratories Drug Metabolism Department

Gemcitabine is approved as a first-line therapy for the treatment of pancreatic cancer and as a second-line therapy in combination with other anti-cancer therapeutics for breast, non-small cell lung, ovarian cancer and soft tissue sarcomas. As a nucleoside analog, it is an inhibitor of DNA synthesis and must be transported into the cell for activity. Docetaxel is a second-generation taxane used as a cytotoxic chemotherapeutic agent to treat various cancers. The systemic pharmacokinetics and tissue distribution of ³H-Gemcitabine after intraperitoneal administration alone or in combination with Docetaxel administered intravenously was assessed. The use of a xenograft mouse model, with pancreatic adenocarcinoma cells, and analysis by radioanalysis and autoradiography was a novel approach providing additional information to previously published data. Athymic nude (Hsd: Athymic Nude-Foxn1^{nu}) mice were inoculated subcutaneously in the flank with 5×10^6 BxPC-3 (pancreatic adenocarcinoma) cells. Sixty-one days after inoculation, the mice were randomized into 4 groups and were administered ³H-Gemcitabine (60 mg/kg, radioactive dose of 1000 μCi/kg) by IP injection on Day 1, or on Day 11 following initial administration of Gemcitabine on Day 1. An IV injection of Docetaxel (6 mg/kg) was administered in combination with the ³H-Gemcitabine to two groups (following a single Gemcitabine dose on Day 1 and or a second Gemcitabine dose Day 11). After dose administration, mice were euthanized over 168 hours postdose; blood, serum, and selected tissues were collected and analyzed for radioactivity content and selected tissues were analyzed by microautoradiography (MARG). Tissue distribution of radioactivity was also analyzed by whole body autoradiography (QWBA). Following IP administration, ³H-Gemcitabine quickly distributed into systemic tissues; the highest concentrations were generally observed at 1 or 4 hours postdose. Exposures were highest, and in the general order of, spleen > lymph nodes > uterus > bone marrow > kidney > tumor > liver > lung and indicated a higher exposure was obtained when Gemcitabine was administered in combination with Docetaxel. Notable concentrations of radioactivity in the kidney and urinary bladder suggested renal elimination as a primary excretion pathway. Brain and spinal cord radioactivity levels were minimal, suggesting Gemcitabine and/or Gemcitabine with Docetaxel has limited blood brain barrier penetration. Radioactivity levels were detectable in blood and serum through 96 hours postdose and

exposure was again highest for groups administered Gemcitabine and Docetaxel. In conclusion, radioactivity was detected throughout the whole body following administration of ^3H -Gemcitabine, and concentrations and exposure in tissues generally increased when Docetaxel was administered in combination. While systemic exposure was observed through 96 hours postdose, radioactivity levels in tissue declined and were generally below the limit of detection by 24 hours postdose.

P41 - CELLULAR DISTRIBUTION OF BIOLOGICS: A COMPARISON OF MICROAUTORADIOGRAPHY TECHNIQUES

Stephen Harris, Claire Henson, and Andrew Whicke
Pharmaron

Purpose: Microautoradiography (MARG) is a powerful technique for determining the distribution of radiolabeled compounds at the cellular level. The technique commonly used for NCE's, proteins, peptides and oligonucleotides. Historically, the favored tissue preparation technique has involved rapid freezing of the selected tissues, followed by sectioning in a cryostat microtome, under safe-light conditions. The rationale for this approach is based on the need to retain potentially soluble material in situ. This has precluded the use of the standard histological processing techniques, which provide superior quality histology in comparison to frozen sections, and was due to the high potential for extraction of chemically based therapeutics by the organic solvents used in the processing of formalin fixed tissues for wax embedding. Formation of cross-linkages during fixation may lead to better retention of larger biologics much than for chemically extractable NCE's. The purpose of these studies was to compare the distribution of detectable radioactivity in frozen or wax embedded MARG sections, following processing using each technique

Methods: A non-specific humanized monoclonal antibody was radiolabeled with $[^3\text{H}]\text{-N-succinimidyl propionate}$ to a specific activity of approximately 500 $\mu\text{Ci}/\text{mg}$, and following radiodilution with non-labelled mAb, administered intravenously to male Sprague Dawley rats at a dose level of 5 mg/kg. At 24 hours post dose the animals were euthanized and selected tissues were removed for processing for MARG. Tissues were divided, and one half was rapidly frozen in a plastic mold surrounded by a small amount of OCT. Following freezing $5\mu\text{m}$ sections were mounted onto emulsion coated slides under safelight conditions and exposed for up to 8 weeks. The remaining tissue was fixed for 48 hours in 10% neutral buffered formalin and then processed into wax blocks, sectioned at $5\mu\text{m}$, floated onto glass slides and cleared in xylene. The resulting slides were dipped in molten emulsion under safelight conditions and exposed as per the frozen sections. Following exposure the frozen sections were formalin fixed and all slides were H and E stained using a Leica automatic stainer

Results: Examples of the resulting MARG images (kidney, liver, lung and pancreas) are presented under bright field or dark field illumination in the poster. An example of the distribution of radioactivity in the kidney using both preparative techniques is shown in Figure 1 of the abstract. Review of selected tissues indicates that radioactivity is retained in the tissue sections following processing by both the frozen sectioning technique and the standard wax embedding technique. The patterns of distribution showed a high degree of similarity in all tissues reviewed.

Conclusion: The results of these studies indicate that a high proportion of the mAb molecule was retained in situ following wax embedding and clearing, and that the patterns of distribution remained the same. The advantage of using this technique was the marked improvement in the histological quality of the sections. This aids interpretation of the intracellular distribution radioactivity under magnification. Careful consideration of the properties of smaller biological molecules such as peptides and oligonucleotides should be given before using the fixation and wax embedding technique.

P42 - ENHANCED METABOLITE IDENTIFICATION USING ORBITRAP TRIBRID MASS SPECTROMETER

Kate Comstock¹, Shuguang Ma², Seema Sharma¹, Yan Chen¹, and Caroline Ding¹

¹Thermo Fisher Scientific, ²Genentech

Introduction: High resolution mass spectrometry (HRMS) is an essential tool for metabolite identification. HRMS with sophisticated data acquisition features can provide the critical information for metabolite structure elucidation and alleviate the difficulties of matrix complexity. Here we present a study for metabolite ID using Orbitrap Tribrid MS with data acquisition features designed to significantly improve small molecule structure analysis, which include automatic background ions subtraction, inclusion/exclusion lists generation, and real-time decision-making to optimize MSn data acquisition quality and speed. The high quality information-rich MSn data generated using this improved HRMS was processed using structure analysis and data mining software "Mass Frontier" and "Compound Discoverer".

Method: Amprenavir, Bosentan, Lopinavir, and Ritonavir were selected as model compounds. The compounds, at concentration of (5 μM), were incubated with human liver microsomes (HLM) in the presence of GSH and UDPGA. Incubations without drug or without NADPH were chosen purposely to test the background subtraction feature. The LCMS analyses were performed on Vanquish Flex Binary UPLC system with DAD detector coupled to an Orbitrap Tribrid Mass Spectrometer. Mobile phases were composed of: A: H₂O/0.1% formic acid, and B: ACN/0.1% formic acid with gradient on Hypersil column (2.1X100 mm 1.9 μm). High resolution full scan and MSn data were collected in a data-dependent fashion with polarity switching. The data acquisition method was incorporated with features optimized for small molecule analysis.

Preliminary Data: These HIV drugs were selected because of their extensive metabolism. Using the Orbitrap Tribrid Mass Spectrometer's special features for small molecule data acquisition: the automatic background subtraction, inclusion/exclusion list generation, and real-time decision-making optimization of MSn spectra acquisition, the MS provides a wealth of information for metabolite identification. The automatic background subtraction feature is especially useful for identification of metabolites present in a complicated biologic matrix. The new and enhanced features that use the high quality MS/MS fragments to trigger the MSn acquisition significantly improved MSn data quality, because multi-stage MS/MS (MSn) information is essential for confident metabolite structure elucidation. For example, HRAM full scan data show that Ritonavir metabolites include four mono-oxidation products, two N-dealkylation products, and four di-oxidation products. In order to determine the structure and the sites of biotransformation of these metabolites, high quality MS/MS and higher order MS/MS spectra were obtained using the novel data collection features of Orbitrap Tribrid MS. Major and minor metabolites, both phase I and II, of these model compounds formed in the HLM microsomal incubations were quickly detected by processing the HRAM and higher level MS/MS (MSn) spectra of metabolites using Mass Frontier and Compound Discoverer. This workflow offers significant improvements in speed and confidence of routine drug metabolite identification and other small molecule structure characterization applications. Conclusion: Small molecule specific acquisition features of Orbitrap Tribrid MS improve MSn data quality and increase confidence for metabolite identification.

P43 - LIGNAN ENTEROLACTONE MODULATES CELLULAR LIPID AND CHOLESTEROL HOMEOSTASIS LINKING DIVERSE MOLECULAR MECHANISMS

Franklyn De Silva, Xiaolei Yang, Ahmed Almousa, Ahlam Hawsawai, and Jane Alcorn
University of Saskatchewan

Background: Impairment of physiological regulatory mechanisms of cholesterol and lipid homeostasis is a feature of cardiovascular disorders, various neurodegenerative disorders, diabetes, and cancer progression^{1,2}. Furthermore, dysregulated cells can exhibit elevated endoplasmic reticulum (ER) stress as an adaptive survival mechanism³. A link between flaxseed lignans (FLN) anti-cholesterolemic and anti-cancer effects might exist through the ability of FLNs to modulate both ER stress and cholesterol homeostasis as FLN are known to modulate multiple targets in dysregulated cellular signaling pathways. Identifying the molecular targets responsible for the flaxseed plant lignan metabolite (i.e. mammalian lignan) enterolactone's (ENL) ability to modulate ER stress and cholesterol homeostasis in dysregulated cell types such as cancer, will help utilize FLNs effectively in the clinical setting. Additionally, an appropriate lignan enriched product can provide a clinically relevant dose without significant toxicities⁴. Hypothesis: ENL increases ER stress and modulate cellular lipid homeostasis connecting peroxisome proliferator activated receptor (PPARY) mediated pathways in cells with dysregulated proliferation. Methods: Various key targets involved in cholesterol metabolism, ER stress, cell survival, and vesicular cholesterol trafficking were evaluated using a battery of *in vitro* assays such as qPCR, western blot, fluorescence microscopy, gene reporter assay, and substrate uptake assay using various cell lines. Results: A competitive binding assay, transactivation assay, and glucose uptake assay revealed ENL as a PPARY partial agonist. ENL modulated cholesterol and lipid metabolism targets (FASN, SREBPs, INSIG-1, LDLR, PPARY) and ER stress markers (ATF4, CHOP, GADD34 and GRP58). ENL reduced mitochondrial redox function and caused mitochondrial toxicity. ENL enhanced ability of select anticancer drugs (e.g: microtubule inhibitors) to decrease cell viability. Fluorescently labeled cholesterol treated cells along with ENL revealed altered intracellular vesicular trafficking linking the actin cytoskeleton. Conclusion: There might be a novel role among the regulation of PPARY, lipid and cholesterol metabolism, and ER stress. These findings warrant further investigations to support FLN's ability to modulate ER stress as the key mechanism involved in the disruption of dysregulated cellular proliferative signaling. ER stress and PPARY mediated signaling can influence cholesterol and lipid metabolism and therefore are relevant targets in drug discovery. Finally, lignans are safe and therefore are good candidates for adjuvant therapy that could improve patient longevity and quality of life.

References:

1. CAO, S. S.; KAUFMAN, R. J. Endoplasmic Reticulum Stress and Oxidative Stress in Cell Fate Decision and Human Disease. *Antioxidants & Redox Signaling*, 140 Huguenot Street, 3rd Floor New Rochelle, NY 10801 USA, v. 21, n. 3, p. 396-413, 04/05/accepted 2014. ISSN 1523-0864, 1557-7716.
2. CORAZZARI, M. et al. Endoplasmic Reticulum Stress, Unfolded Protein Response, and Cancer Cell Fate. *Front Oncol*, v. 7, p. 78, 2017. ISSN 2234-943X (Print), 2234-943X (Linking).
3. BASSERI, S.; AUSTIN, R. C. Endoplasmic reticulum stress and lipid metabolism: mechanisms and therapeutic potential. *Biochem Res Int*, v. 2012, p. 841362, 2012. ISSN 2090-2255 (Electronic).
4. DI, Y. et al. Influence of Flaxseed Lignan Supplementation to Older Adults on Biochemical and Functional Outcome Measures of Inflammation. *J Am Coll Nutr*, v. 36, n. 8, p. 646-653, Nov-Dec 2017. ISSN 0731-5724.

P44 - PREDICTION OF ADVERSE DRUG REACTIONS OF BIASED DATA USING BOOTSTRAP AGGREGATING AND MACHINE LEARNING TECHNIQUES

Dipayan Ghosh, Geervani Koneti, and Narayanan Ramamurthi
Tata Consultancy Services Ltd

Adverse Drug Reactions (ADRs) are unintended side effects resulting from drug or chemical exposure and they often pose major challenges such as withdrawal of drugs, increased cost of drug discovery and public healthcare etc. Of late, preclinical *in vitro* safety profiling of drug candidates is increasingly employed to predict side-effects by testing compounds with biochemical and cellular assays; however, translation to *in vivo* experimental detection remains a very challenging task both in terms of cost and efficiency. Thus, reliable *in silico* prediction of potential side-effects early offers many advantages such as reduction in the cost of drug discovery, useful insights about drug-human phenotype relationships, safe therapies to patients etc. We report herein, the application of in-house predictive toxicology platform for the prediction of five adverse events using biased data and the scope and limitations of our methodology and comparison of our results with published reports.

The biased datasets of compounds used in the present study namely arrhythmia, cardiac failure, myocardial infarction, hepatotoxicity and nephrotoxicity, were extracted from literature [1] and are used as it is for comparative purposes. We derived two types of chemical information, a) 458 molecular descriptors using in-house software and reduced them to meaningful descriptors using ANNOVA p-value test and b) 10145 fingerprints using PaDEL v2.21 software and filtered them using information gain values. The classification models were built using filtered chemical information and random forest with 5 fold cross-validation and were of poor predictive performance. With the objective of improving the performance of the models, we employed bootstrap aggregating (bagging) approach to create new training datasets (Tr_i) of equal class distribution from the four subsamples used as training data in each cross validation iteration. Each Tr_i contained all the toxic compounds and an equal number of non-toxic compounds selected at random without replacement from the original dataset. Each of the Tr_i were then trained using random forest and the models were used to classify the validation set. The final predicted class for each compound in the validation set was derived using a consensus of the prediction made by individual Tr_i sets. Based on the in-depth analyses of the performances of models derived, we infer the following: a) the performance of the models described herein is very good based on key statistical metrics such as global accuracy, balanced accuracy etc. b) the use of the bagging step has contributed to better performance than the reported model [1]. c) We have demonstrated that for building reliable models of biased data, the use of multiple chemical information types and appropriate algorithms to reduce the biased nature of the dataset are essential and we believe, our approach offers potential to be a desirable option to a researcher interested in generating the best predictive models using biased datasets.

Reference:

1. Sergey M. Ivanov, Alexey A. Lagunin, Anastasia V. Rudik, Dmitry A. Filimonov, and Vladimir V. Poroikov "ADVERPred-web service for prediction of adverse effects of drugs" Journal of Chemical Information and Modeling 2018 58 (1), 8-11.

P45 - PREDICTION OF RESPIRATORY TOXICITY USING CHEMICAL INFORMATION AND MACHINE LEARNING TECHNIQUES

Dipayan Ghosh, Geervani Koneti, and Narayanan Ramamurthi
Tata Consultancy Services Ltd

Lack of safety and efficacy are the two major reasons for the failures of drug candidates in drug discovery and development. Respiratory toxicity is one of the major reasons for the withdrawal of drug candidates and is mediated by complex mechanisms such as cytotoxic lung injury, immune-mediated, respiratory sensitization etc. Usually *in vitro* and *in vivo* methods are employed to study drug safety and efficacy issues; however, computational screening offers a number of advantages over experimental approaches such as reduction in the cost of drug discovery, useful insights about drug-human phenotype relationships, safe therapies to patients etc. The computational models based on chemical structure for safety assessment fall into three classes namely a) qualitative or classification models b) quantitative or regression models and c) read-across. Our interest in the development of a predictive toxicology platform prompted us to study the development of new approaches and algorithms to exploit different chemical information types and we describe herein our initial results in the development of reliable predictive models for respiratory toxicity.

The present study is based on a mouse intraperitoneal respiratory toxicity dataset of 2490 compounds collected from the ChemIDplus public TOXNET database by using the filters, "LUNGS, THORAX or RESPIRATION". The quality of this dataset was improved by the removal of compounds such as inorganic, metalorganic, polymers and salts to provide the final data set of 1392 compounds. It is further divided into a training set of 974 compounds and test set of 418 compounds using in-house implemented Kennard-Stone data division algorithm. The respiratory toxicity for these compounds was expressed as LD50 that is the dose required to kill half of total treated animals. We obtained three types of chemical information of these compounds, a) 458 molecular descriptors obtained from in-house software b) 10145 fingerprints

using PaDEL v2.21 and c) fragments from SARpy v1.0. We further derived meaningful chemical information out of these descriptors using ANNOVA and fingerprints using information gain values greater than 0.01. The classification models were built using the resultant 143 molecular descriptors and 323 molecular fingerprints and machine learning algorithms such as Support Vector Machine and Random Forest provided by the JAVA-ML v0.1.7 open source library and compared with models derived from SARpy v1.0. Based on the in-depth analysis of the performances of all the models reported in literature so far, we infer the following: a) most of the published reports except one are based on too small a dataset and are based on only one chemical information b) employing appropriate algorithm like Kennard-Stone for data division improves the quality of the data set and hence, the overall model performance c) use of multiple chemical information types together improves the performance of the models d) finally, the performance of our model is the best as of date, based on key performance metrics such as accuracy, sensitivity and specificity and the details of which will be discussed.

P46 - DEVELOPMENT OF A NOVEL ORALLY ACTIVE INVERSE AGONIST OF ESTROGEN-RELATED RECEPTOR GAMMA (ERR γ), KH-NDTC AS AN ENHANCER FOR SODIUM IODIDE SYMPORTER: ITS PHARMACOLOGICAL EFFECTS IN ANAPLASTIC THYROID CANCER (ATC) *IN VITRO* AND *IN VIVO*

Yong Hyun Jeon¹, Seon Hee Choi², and Sang Kyoon Kim²

¹Daegu Gyeongbuk Medical Innovation Foundation; ²Laboratory Animal Center/Daegu Gyeongbuk Medical Innovation Foundation

Hypothesis: New strategies to restore the function of sodium iodide symporter (NIS) in anaplastic thyroid cancers that are refractory to radioiodine therapy is urgently required in clinic. Herein, we report the discovery of highly selective and orally bioactive inverse agonist of estrogen-related receptor gamma (ERR γ), KH-NDTC, which restored the ability of iodide uptake in ATC tumor and rendered ATC tumor cells susceptible to radioiodine therapy.

Methods: CAL62 (anaplastic thyroid cancer cells, CAL62/effluc) expressing enhanced firefly luciferase genes were incubated with various doses of KH-NDTC for 24h, followed by iodide uptake analysis to determine NIS function with or without KClO₄ as a NIS inhibitor. Effects of KH-NDTC on ERR γ and thyroid-specific genes including NIS, TPO, TSHR, and TG were evaluated by immunoblotting assay. The cytotoxic effect of I-131 (50 μ Ci) was determined by clonogenic assay. *In vivo* PET imaging with I-124 was conducted before and at 6 day following oral administration of 200mg/kg KH-NDTC to CAL62/effluc tumor-bearing mice once daily. For *in vivo* therapy, after treatment of either vehicle or 200mg/kg KH-NDTC once a day for 6days, tumor-bearing mice received a therapeutic radioiodine (1mCi I-131) and *in vivo* bioluminescent imaging (BLI) was achieved to monitor a therapeutic outcome.

Results: KH-NDTC led to a dose-dependent increase of iodide uptake in CA62/effluc cells with its complete inhibition to basal level via co-incubation with KClO₄, which were accompanied by both the down-regulation of ERR γ protein. KH-NDTC up-regulated the expression of thyroid-specific genes in CAL62 cells with increase of fully glycosylated-membrane NIS protein level. Pre-exposure of KH-NDTC led to an enhanced susceptibility of CAL62 cells against I-131. I-124 PET/CT imaging demonstrated an enhanced iodide uptake in KH-NDTC -treated CAL62 tumor but not vehicle-treated CAL62 tumor, which is consistent with the results of bio-distribution analysis. *In vivo* BLI showed a significant inhibition of tumor growth in combination group compared with either I-131 or KH-NDTC group.

Conclusion: We successfully demonstrated that our novel and orally bioactive inverse agonist of ERR γ , KH-NDTC, confer improved susceptibility of radioiodine therapy on ATC tumor through recovery of the ability in radioiodine uptake, suggesting its potential for clinical application in the management of anaplastic thyroid cancers.

P47 - DESI-MS IMAGING TO OBSERVE THE DRUG AND DRUG-INDUCED EVENTS IN TUMOR TISSUE

Sang Kyoon Kim, Yong Hyun Jeon, Seon Hee Choi, Dongkyu Kim, Woo Suk Koh, and Kil Soo Kim

Daegu Gyeongbuk Medical Innovation Foundation

Hypothesis: Visualization techniques using mass spectrometry have been developed to identify the fate of drugs in the specific tissues *in vivo*. In many recent studies, DESI-MS imaging has shown that it can be a powerful and effective tool for monitoring the distribution of drugs and metabolites at the specific tissue sites without marking the drug. In this study, we evaluated the distribution and amount of anticancer agent (gemcitabine) and their metabolites that cause apoptosis in xenograft breast cancer tissues (MDA-MB-231) using DESI-Q-TOF. In addition, in order to determine whether apoptosis occurs at the site of actual anticancer drug, the location of the anticancer agent and the site of apoptosis were visualized by using the cell apoptosis marker, apopepII. **Method:** Tumor bearing mice were injected with gemcitabine to induce apoptosis in the tumor and an apoptosis marker, apopepII, was injected intravenously 6 hrs later. The tumor tissues were harvested 24 hrs after the injection of apopepII and directly embedded with OCT compound. Slides of frozen samples were scanned by DESI-MS. After whole tissue area scan, data was visualized based on peak detection pattern. **Result and conclusions:** As a result, the gemcitabine inducing apoptosis was observed at the edge of the cancer tissue on the slide glass using MSI, and the fluorescence labeled apopepII was also observed in the vicinity of the drug. We indirectly confirmed that our injected gemcitabine was well delivered to the tumor and that the gemcitabine in the tumor caused apoptosis. By combining the detection markers with DESI-MS in a proper manner, the merged images will be a good technique to investigate the location of the drug and drug-induced events.

References:

1. Emmanuelle Claude, Emrys A. Jones, Steven D. Pringle, DESI Mass Spectrometry Imaging (MSI), Imaging Mass Spectrometry pp 65-75, May 2017
2. Claude E, Jones EA, Pringle SD. DESI Mass Spectrometry Imaging (MSI). Methods Mol Biol_ 1618 pp65-75. 2017

P48 - ZEBRAFISH AS A SCREENING MODEL FOR TESTING THE PERMEABILITY OF BLOOD-BRAIN BARRIER TO SMALL MOLECULES

Seong Soon Kim, So Hee Im, Jung Yoon Yang, Yu-Ri Lee, Geum Ran Kim, Jin Sil Chae, Dae-Seop Shin, Jin Sook Song, Sunjoo Ahn, Hoi Lee, Jae Chun Woo, Jin Hee Ahn, Chang Soo Yun, Phiho Kim, Hyoung Rae Kim, Kyeong-Ryoon Lee, and Myung Ae Bae
Korea Research Institute of Chemical Technology

Hypothesis: The use of zebrafish (*Danio rerio*) in drug discovery and developmental research is growing rapidly because of the numerous advantages, which include the small size, rapid generation, high productivity, and transparent eggs to perform high-throughput drug screening. In addition, adult zebrafish expresses the tight junction proteins ZO-1 and claudin-5 in the endothelial vascular cells, as well as the transporter protein permeability glycoprotein (P-gp)/ATP-binding cassette transporter subfamily B (ABCB) 4/5 within the brain. The objective of this study was to evaluate the permeability of small molecules into the brain via the blood–brain barrier in zebrafish and to investigate the possibility of using this animal model as a screening tool during the early stages of drug discovery. Methods: Fifteen compounds containing BBB positive, BBB negative and unknown compounds, synthesized from Korea Research Institute of Chemical Technology (KRICT) were used to understand the permeation into the brain in zebrafish and mice. The concentrations of each compound in the blood (i.e., zebrafish), plasma (i.e., mouse), and brain homogenates were determined by a specific liquid chromatography tandem mass spectrometry (LC-MS/MS). The ratio of brain-to-plasma concentration was compared between the two animal models. Results: The partition coefficient ($K_{p,brain}$), estimated using the concentration ratio at designated times (0.167, 0.25, 0.5, or 2 h) after oral administrations (per os, p.o), ranged from 0.099 to 5.68 in zebrafish and from 0.080 to 11.8 in mice. A correlation was observed between the $K_{p,brain}$ values obtained from the zebrafish and mice, suggesting that zebrafish can be used to estimate $K_{p,brain}$ to predict drug penetration in humans. Furthermore, *in vivo* transport experiments to understand the permeability glycoprotein (P-gp) transporter-mediated behavior of loperamide (LPM) in zebrafish were performed. The zebrafish, $K_{p,brain,30min}$ of LPM was determined to be 0.099 – 0.069 after dosing with LPM alone, which increased to 0.180 – 0.115 after dosing with LPM and tariquidar (TRQ, an inhibitor of P-gp). In mouse, the $K_{p,brain,30min}$ of LPM was determined to be 0.080 – 0.004 after dosing with LPM alone and 0.237 – 0.013 after dosing with LPM and TRQ. Conclusion: These findings indicate that the zebrafish could be used as an effective screening tool during the discovery stages of new drugs to estimate their distribution in the brain.

P49 - OPTIMIZED DECISION MAKING FROM EARLY DISCOVERY TO DEVELOPMENT PHASE FOR BETTER PREDICTION OF ADME BEHAVIOR

Heasook Kim-Kang, Xiaochun/Sean Zhu, and David Heim
Q2 Solutions

Metabolic clearance is an important parameter impacting drug discovery. Metabolically stable compounds may have a better chance to achieve the desired exposure *in vivo* and are often preferred. In general, if a screened compound is shown metabolically stable *in vitro*, it may be advanced to *in vivo* evaluation. If all other characteristics (i.e., toxicity, efficacy) are favorable, ADME studies of the compound may be conducted in preclinical species using a radiolabeled drug. Occasionally inconsistent observations of a drug candidate between *discovery and development phases* are derived from but not limited to the following reasons: 1) slow turn-over drug; 2) *in-vitro* model didn't contain responsible enzymes for major metabolites detected in circulation; 3) species difference in key enzymes; 4) key circulating metabolites, not parent, formed a strong binding to plasma protein. These may lead the team to make an inappropriate decision on the next step for the test drug's development. If metabolites (formed by non-plasma enzymes) are responsible for strong binding of drug-related residues to plasma proteins, it won't be observed by *in vitro* incubation of the parent in the plasma. If metabolites are not chemically reactive, their potential for binding to hepatocyte proteins may not be observed by conventional GSH or KCN-trapping method. The strong binding to plasma proteins may not pose any toxicity issues but may have a great impact on the systemic exposure. Drugs containing sulfur within molecules via disulfide, thiazole, thiophene, thiazine, thiazolidione, or isothiazole moiety, may form thiol through metabolism, which may readily react with plasma protein (via disulfide bond). If this potential is not taken into consideration, the presence of these metabolites may go unnoticed during the early discovery stage. The case study of a test drug, encompassing results from discovery phase and unexpected results observed in the development phase, will be presented. During the discovery stage, *in-vitro* metabolism (microsome and hepatocyte suspension) and *in-vivo* metabolism in preclinical species were investigated using Synapt with Metabolyx software. QE and MicroBeta were used during the development phase. The test drug was shown to be metabolically stable in *in vitro* systems and also rats and dogs, showing parent as prominent circulating component. Thus, the drug was advanced to *in vivo* preclinical metabolism studies using ¹⁴C-test drug. *In vitro* metabolism

study using a co-culture model (Hprel) was also conducted with ^{14}C -test drug. The results showed much more complex metabolite profiles than expected as well as a poor extraction recovery of plasma residues. Incubation of plasma with TCEP released all the bound residues. The metabolites were shown to be bound to albumin based on the direct LC/MS analysis of diluted plasma. The case study results suggested that when a drug has a potential to form thiol metabolites, and show high metabolic stability during the discovery phase, additional experiments should be considered to minimize the gap between discovery and development phases. Those can be *in vitro* incubation using different hepatocyte model and incubation of *in vivo* plasma samples in TCEP to monitor the appearance/increase of any compounds after treatment.

P50 - AN INTEGRATED *IN VITRO* SCREEN USING SANDWICH-CULTURED HUMAN HEPATOCYTES FOR PREDICTION OF CHOLESTATIC HEPATOTOXICITY

Jonathan Jackson, Matthew Palmer, Caroline Moseley, Christopher Black, and Kenneth Brouwer
BioIVT

Cholestatic DILI in humans has been associated with bile salt export pump (BSEP) inhibition; however, *in vitro* BSEP IC_{50} concentrations do not correlate with *in vivo* cholestatic DILI severity. Sandwich-cultured human hepatocytes (SCHH) when treated with BSEP inhibitors respond to the resulting increased intracellular concentration (ICC) of bile acids (BA), by activation of FXR (adaptive response). This results in decreased synthesis of BA and increased expression of basolateral and canalicular efflux transporters for BA via OST alpha/beta, and BSEP which prevents cholestatic hepatotoxicity. We evaluated the time course of this adaptive response, changes in the ICC of BA, the effects of FXR antagonists, the *in vivo* relevance, and whether integration of FXR regulatory effects would improve the prediction of cholestatic DILI.

Cryopreserved, Transporter Certified™ human hepatocytes in a sandwich configuration were cultured using QualGro™ Media for 5 days. On Day 5 of culture, the time course of the adaptive response was determined by determining the effect of cyclosporine A on the biliary excretion, and ICC of endogenous bile acids (LCMS analysis), in parallel with FXR activation (gene expression - TaqMan® primer/probe sets). Mechanistic modeling was used to determine the functional effects of mRNA based changes in FXR activation. The effect on the ER stress biomarker, CHOP, following 12 hours of exposure to CsA (10 μM), Trog (100 μM), or DY268 (5 μM) under sensitization conditions (250 μM BA pool + 1 mM FFA) was also evaluated. In a separate study, 49 compounds with varying degrees of BSEP inhibition and DILI (NIH LiverTox database) were evaluated (24 hr exposure, sensitization conditions) for their potential to affect the adaptive response. Cyclosporine A decreased the biliary excretion of endogenous bile acids in a time dependent manner, with a parallel increase in the ICC of BA, followed by activation of FXR. FXR activation resulted in a 2X increase in the biliary efflux clearance, and a 6X increase in the basolateral efflux clearance (adaptive response). Co-administration of FXR antagonists reduced the FXR mediated response to 50 and 5% of control for troglitazone and DY268, respectively. Following 12 hours of exposure, CHOP mRNA content was induced ≤ 2.0 -fold above solvent control in SCHH treated with CsA (10 μM) or DY268 (5 μM) in the presence of a BA pool + FFA. CHOP mRNA content was increased to 7.1-fold above solvent control in SCHH treated with Trog (100 μM) in the presence of BA pool + FFA. Integration of the effect on the adaptive response in addition to the effect on BSEP inhibition improved the accuracy for prediction of cholestatic DILI from 22% (BSEP inhibition alone) to 93%. In addition to BSEP inhibition, integration of inhibition of basolateral efflux and/or interference with the adaptive response (FXR antagonism) allows for more accurate prediction of cholestatic DILI.

P51 - DEEP CONVOLUTION NEURAL NETWORKS ANALYSIS OF CHEMICAL IMAGES: APPLICATIONS IN DRUG DISCOVERY AND DEVELOPMENT

Geervani Koneti and Narayanan Ramamurthi
Tata Consultancy Services Ltd

Late stage failures of drug candidates can be addressed using reliable and easily applicable predictive ADMET models [Absorption, Distribution, Metabolism, and Excretion & Toxicity] as they rationalize experimental observations. Structure-activity relationships (SAR) models are one such class of predictive models that commonly use chemical information types such as fingerprints, fragments etc., derived from the whole structure of the drug candidates as model variables. However, the application of 2D and 3D images of the whole structures in SAR models generation is still in its infancy. It can be attributed to the following constraints: a) lack of efficient algorithms to analyze the chemical images b) limitations in computer time and memory and others. However, with the advances made recently in computer hardware and machine learning techniques, we believe analysis of 2D and 3D images of chemical structures becomes realistic and can be applied profitably in drug discovery and development. We report herein for the first time a) the applications of deep convolution neural networks (CNN) based 2D image analysis of drugs and drug candidates for the prediction of BBB profiles of drug candidates and b) scope and limitation of the methodology.

Reliable prediction of blood-brain barrier (BBB) permeation even before chemical synthesis still remains as one of the major challenges in drug discovery and reliable new approaches and models are in urgent need. We employed a training set of 1303 compounds with 1010 BBB (+) and 293 BBB (-) compounds and the test set of 313 compounds with 281 BBB (+) and 32 BBB (-) compounds, obtained from literature. The 2D structural color images of the compounds are procured from PubChem database with dimensions 500x500 pixels. As the ratio of similar atoms or cyclical structures varies from

one compound image to another depending on the compound size, we augmented the training dataset by performing transformations such as a) down sampling from 500x500 upto 150x150 pixels with an interval of 50, b) rotating images with interval of 30°, c) transforming all the training set images to 256x256 pixels using squash transformation. We employed two known deep CNN architectures for image analysis namely, i) AlexNet and ii) GoogLeNet (GLN) from NVIDIA Deep Learning GPU Training System (DIGITS) version 5.1. It is observed that GLN took approximately one hour to train the classifier on Intel Xeon E5-2620 v2 @2.1GHz 24 core CPU with NVIDIA Tesla K20 GPU and we validated the classifier using 313 test set compounds. Based on the in-depth analysis of the deep CNN models, we infer the following: i) the performance of GLN with Nesterov's accelerated gradient and polynomial decay learning rate is superior ii) the classification accuracy is 95% in the case of BBB (+) and BBB (-) compounds of the training set and 87.5% in the case of BBB (-) and 100% in the case of BBB (+) for positive compounds of the test set. We will discuss the scope and limitations of the current methodology and also the future directions.

P52 - GENERATION OF REPRODUCIBLE PREDICTIVE MODELS USING PARALLELIZED MODIFIED TEACHING LEARNING BASED SEARCH OPTIMIZATION METHOD AND ITS APPLICATIONS IN DRUG DISCOVERY AND DEVELOPMENT

Geervani Koneti and Narayanan Ramamurthi
Tata Consultancy Services Ltd

Quantitative structure–activity relationships (QSAR) is one of the regularly employed techniques in the pharmaceutical industry for predicting on-target and off-target activities. It helps to prioritize the compounds to be synthesized and minimize the experimental work that needs to be done. They are typically generated from a dataset of large number of compounds and structural features. Feature selection methods are employed in the selection of optimal features and the models are generated using the selected features and appropriate regression or classification techniques. They fall into three broad categories, namely, a) embedded b) filter and c) wrapper methods. Exhaustive wrapper search techniques are computationally hard and provide reproducible solutions; on the other hand, meta-heuristic wrapper methods are fast and are not reproducible. We are of the opinion that improving the reproducibility of the feature selection step of a meta-heuristic wrapper methods can result in reproducible models and if successful, offers wide range of applications within Pharmaceutical industry. We report herein a) the applications of a parallelized meta-heuristic wrapper method developed by us, henceforth, referred to as “Parallelized Modified Teaching Learning Based Search Optimization” (PMTLBSO) method for reproducible feature selection and generation of robust and reproducible EGFR kinase inhibitors models and b) the scope and limitations of PMTLBSO method and the models derived from it.

We employed epidermal growth factor receptor (EGFR) kinase dataset of 93750 compounds, downloaded from the publically available kinase knowledge base and then applied a number of filters to maintain homogeneity of data to yield 4893 compounds. EGFR kinase, a transmembrane glycoprotein, is a proven anticancer target and many EGFR inhibitors such as Gefitinib, Lapatinib etc. have been developed and approved by the FDA for the treatment of breast cancer. The pIC50 values of these compounds range from 2.18-11.6. The structural features totaling 352 are generated using our in-house tool. Stratified random sampling of the dataset in the ratio of 70:30 provided 3430 compounds as training set and 1463 compounds as test set. The feature selection was performed using PMTLBSO on graphical processing unit (GPU) and the models were generated using multiple linear regression (MLR) and random forest (RF) methods. An in-depth analyses of the results suggest that a) PMTLBSO is extremely efficient for the selection of large number of features (> 15) and the results are reproducible b) it performs well with large input data (>5000 compounds) c) the predictive power of the EGFR kinase inhibitor model is excellent based on r^2 considering the large size of the dataset d) the models provide an opportunity to interpret the model features and correlate with the dependent variable. This attribute is especially useful for medicinal chemists involved in the optimization of drug candidates based on specific features of the model and e) In conclusion, PMTLBSO has potential to be a desirous option for reproducible selection of features and models with higher prediction based on compounds and features that run into thousands in a drug discovery environment.

P53 - IN VITRO PRIMARY HUMAN HEPATOCYTE 3D SPHEROID MODEL FOR HEPATOTOXICITY STUDIES

Feng Li, Sweta Parikh, Li Cao, Kirsten Cooper, and Rongjun Zuo
Corning Incorporated-Life Sciences

Drug induced liver injury (DILI) remains a leading cause for drug development failure and costly post marketing withdrawal or black box labeling. Accumulative evidence in the literature indicates that *in vitro* 3D liver models are better at mimicking human liver and more physiologically relevant than conventional 2D culture models. Spheroids made from primary human hepatocytes (PHHs) are one of the best characterized 3D models with great potential in applications such as drug metabolism, liver toxicity as well as liver disease modeling. In this presentation, we describe a spheroid culture procedure with PHHs using Corning spheroid microplates with ultra-low attachment surface. Our results demonstrate that suitable PHH lots for 3D culture need to be pre-tested prior to their utilization for various applications. Characterization data show that major drug metabolic enzyme activity (e.g. CYP3A4) is sustained over long term spheroid culture. A comparative (2D monolayer vs. 3D liver spheroids) hepatotoxicity study was performed with 100 known DILI and control compounds. Our

results show the feasibility of conducting hepatotoxicity screening using 3D liver spheroids. Data analysis including IC₅₀, C_{max} and margin of safety (MOS) threshold demonstrated the superior performance of liver spheroids for better prediction (2-3 fold more sensitive) of liver liability than 2D PHH culture.

P54 - TRANSCRIPTOMIC BIOMARKERS TO ASSESS THE LIVER AND METABOLIC RESPONSES ASSOCIATED WITH BIOACTIVATION MECHANISMS OF DRUG INDUCED LIVER INJURY

James Monroe, Keith Tanis, Alexei Podtelezchnikov, Truyen Nguyen, Donna Lynch, Sam Machotka, Palamanda, Todd Pippert, Wendy Bailey, Stephen Pacchione, Amy Aslamkhan, Timothy Johnson, Tamara Cabalu, Pierre Daublain, Randy Miller, Kathleen Cox, Warren Glaab, Raymond Evers, Kaushik Mitra, Deborah Nicoll-Griffith, Nancy Agrawal, Frank Sistare
Merck Research Laboratories

Drug induced liver injury (DILI) is a major reason for attrition during development, denied commercialization, withdrawal from the marketplace and restricted prescribing indications of new pharmaceuticals. Metabolic bioactivation is thought to contribute to a significant number of liver associated adverse drug reactions (ADR) in humans that fail to be detected in standard preclinical animal studies. The challenge for pharmaceutical drug safety is to discriminate which drug candidates will have sufficient bioactivation potential to form sufficient chemically reactive metabolite (CRM) to pose a high risk in the clinic at projected therapeutic doses, from those that will not. We developed a rat liver transcriptional signature biomarker and a supporting *in vitro* cellular model to be used together to discern doses of drugs with bioactivation mediated hepatotoxic potential by measuring transcriptional pathways activated by electrophilic CRMs. Here we describe the establishment of this system using well benchmarked CRM forming test agents, and the subsequent evaluation of these systems using a well curated list of commercial drugs and internal Merck compounds anchored in clinical experience with respect to ADRs and hepatotoxicity. Based on 130 compounds run in short-term rodent studies and with consideration of the clinical dose administered, the approach yielded 33% sensitivity and 95% specificity for discriminating safe from hepatotoxic drugs. Additional qualification and refinement of these experimental models is ongoing with the growing confidence that they add important new information for guiding a weight-of-evidence approach that aids lead optimization and candidate selection. When used together with other strategies that can identify liver toxic liabilities resulting from other established mechanisms of DILI, overall DILI prediction sensitivity is expected to rise. Case examples are described explaining the strengths and limitations of the approach.

P55 - THE IMPACT OF PLASMA PROTEIN BINDING ON THE TISSUE DISTRIBUTION OF WARFARIN - INVESTIGATION IN NAGASE ANALBUMINEMIC RATS (NAR)

Jodie Pang, John Chen, Katherine Cunico, Jose Imperio, Jae Chang, and Justin Ly
Genentech

Background: Plasma protein binding (PPB) is central to the free drug hypothesis, which states that only the free drug is able to engage the pharmacological and toxicological targets. The opposing effects of PPB have been shown between *in vitro* target engagement and systemic exposure illustrate the futility of optimizing for PPB, however, there is only limited data showing the impact of PPB on tissue distribution. Nagase analbuminemic rat (NAR) is an albumin-deficient mutant rat strain that was first reported in 1980. It has been reported that the albumin levels in the NAR model are approximately only one tenth of what is observed in the wild-type animals.

Method: NAR and WT (wild type Sprague-Dawley) animals (N=3) received 1 mg/kg warfarin intravenously. Following 1 hr post-dose, plasma was collected along with the following tissues: white/brown adipose, brain, CSF, heart, liver, muscle, spinal cord and sciatic nerve. In addition, plasma, brain and liver were collected from NAR and WT animals that were not dosed with warfarin. In vitro binding of warfarin was measured in these matrices using equilibrium dialysis.

Results: In vitro, the free fraction (fu) of warfarin in plasma increased from 0.008 in WT animal to 0.231 in NAR model. In contrast, no significant changes in fu were observed in liver and brain homogenates. In vivo, the total plasma clearance (CL_{p,tot}) was 0.2 and 12 mL/min/kg in WT and NAR, respectively. The tissue/plasma ratio (K_p) for all tissues examined varied greatly between the WT and NAR model. Interestingly however, the total concentration across the multiple tissues was not markedly different between the two models. When considering fu, the free plasma clearance (CL_{p,u}) was comparable between the WT and NAR models with values of 25 and 52 mL/min/kg, respectively, suggesting that it is the free concentration that drives tissue distribution of warfarin.

Conclusion: These data show that while modulating fu affected the total plasma concentration, it had no impact on the free plasma concentration. This is consistent with the fact that only dose, bioavailability and/or clearance should impact systemic exposure. Consequently, the concentration of warfarin in various tissues, which is a more relevant parameter when trying to establish pharmacological and toxicological relationships, was not markedly changed. This finding suggests that higher fu does not lead to higher free exposure in target tissues, and that drug discovery efforts focused on improving PPB may not necessarily yield a more efficacious candidate.

P56 - PRECLINICAL DEVELOPMENT OF THE PI3K ALPHA SELECTIVE AND PIK3CA MUTANT SELECTIVE INHIBITOR GDC-0077 AND PREDICTION OF ITS HUMAN PHARMACOKINETICS

Jodie Pang, Matthew Baumgardner, Marie-Gabrielle Braun, Jonathan Cheong, Kyle Edgar, Lori Friedman, Emily Hanan, Allan Jaochico, Shuguang Ma, Emile Plise, Stephen Schmidt, Ning Liu, Kyung Song, Steve Staben, and Laurent Salphati
Genentech

Purpose: The phosphatidylinositol 3-kinase (PI3K) pathway is a major determinant of cell cycling and proliferation and its deregulation is associated with the development of many cancers. Among the Class I PI3Ks (p110a, p110b, p110 δ and p110 γ), p110a has been identified as the most critical in carcinomas. In recent years, this pathway has emerged as a major target for the investigation of anticancer drugs. GDC-0077 is a potent and selective inhibitor of Class I PI3K α isoform ($K_i = 0.038 \pm 0.003$ nM), with over 300-fold selectivity over the other Class I PI3K isoforms such as beta, delta, and gamma and more than 2000-fold selective over PI3K class II and III family members. GDC-0077 is also more active in PIK3CA-mutant cell lines relative to wild-type PI3K- α cells. This improved selectivity profile is expected to maximize efficacy while minimizing off-target activity compared to pan-PI3K inhibitors and other less selective inhibitors. Our objective was to evaluate the preclinical disposition of GDC-0077 and to predict human PK parameters and profiles.

Methods: The pharmacokinetic properties of GDC-0077 were assessed in pre-clinical species following intravenous and oral administrations. The permeability, plasma protein binding and metabolism were also examined *in vitro*. Radio labeled study was conducted in rats to understand the routes of elimination. PBPK modeling was performed using GastroPlus.

Results: GDC-0077 had moderate blood clearance (CL_b) of 37.3 mL/min/kg in mice, relative to liver blood flow, and high plasma clearance (CL_p) of 86.2 in rats, and low CL_p of 10.2 and 6.32 mL/min/kg in monkeys and dogs, respectively. Renal CL in rats, dogs, and monkeys ranged from 18 to 30% of total CL. The terminal half-life (t_{1/2}) ranged from 0.73 hr in mice to 4.75 hr in dogs. The steady state volume of distribution (V_{ss}) varied from approximately 1.9-fold of total body water volume in mice to 5.6-fold total body water volume in rats. Bioavailability ranged from 58% to 100%. *In vitro*, GDC-0077 displayed low plasma protein binding across species (26.6%-74.8%), and the apparent permeability determined in MDCK cells was moderate ($P_{app}=1.9 \times 10^{-6}$ cm/s). Human PK parameters were predicted using different approaches, such as IVIVC, allometric scaling and PBPK modeling. Predicted human CL ranged from 1.4 to 4 mL/min/kg, and V_{ss} was 2.5 L/kg using simple allometry.

Conclusion: Favorable human predictions from preclinical data enabled the advancement of GDC-0077 into clinical trials. PBPK predictions with GastroPlus will also be compared to clinical data.

P57 - EFFECTS OF THYROPARATHYROIDECTOMY ON CLINICAL PATHOLOGY AND BONE DENSITY IN THE RAT

Dominic Poulin, Rana Samadfam, and Jennifer Thomas
Charles River

Parathyroid hormone is critical in the maintenance of calcium homeostasis, and in the formation and maintenance of bones. A thyroparathyroidectomy (TPTx) model can potentially be used to evaluate the efficacy of new drugs for hypoparathyroidism and hypocalcaemia. However, the model has not been well characterized and subsequently has limited translation to the clinic. The objective of the present work was to investigate the effect of TPTx on serum and urine biochemistry, bone density and bone turnover markers over a period of 5 weeks following TPTx surgery.

Female Sprague-Dawley rats (N=10) had surgery (SHAM or TPTx) performed at Charles River Laboratories in Raleigh, NC. Thyroxine pellets were implanted subcutaneously to compensate for the removal of the thyroid gland and to ensure that any observed effects were related to PTH. Animals were fed PMI Nutrition Diet 5CR4. Blood samples were collected at various intervals for calcium and phosphorus analysis, and urine samples were collected on Days 1, 14 and 27 for the analysis of calcium, phosphorus and creatinine levels. At termination, a blood sample was collected for a full biochemistry panel. Femurs were collected for pQCT analysis with one section obtained from the right distal femur metaphysis and analysed for total, trabecular and cortical/subcortical area, bone mineral content and bone mineral density. A second section of the right femur diaphysis was collected and analyzed for bone geometry parameters.

Significant decreases (2.2 to 4.8 mg/dL) in calcium levels were observed in the TPTx animals when compared to the SHAM controls and levels were generally unchanged over the 28 days of the study. Significant differences in serum phosphorus were also observed in the TPTx animals, with levels being higher (2.0 to 6.1 mg/dL) than SHAM controls. In urine samples, calcium (corrected for creatinine) and phosphorus (total and corrected for creatinine) were generally decreased in TPTx animals. At study termination, changes in biochemistry included decreased triglycerides, marginal decreases in ALP (surrogate bone formation marker) and increased creatinine and urea nitrogen. Changes in the bone parameters evaluated included statistically significant increases in bone mineral content (BMC) in the metaphysis (total, trabecular and cortical/subcortical sites), while bone mineral density (BMD) was statistically increased in the trabecular site only. Other parameters evaluated were also slightly increased, but were statistically significant. The increased bone density is likely due to low bone turnover in the model; however, these changes are not consistent with the loss of bone reported in the clinic. The changes in creatinine and urea nitrogen suggest impaired kidney function and are consistent with clinical findings in patients with hypoparathyroidism.

As expected, TPTx surgery followed by thyroxine supplementation had an effect on lowering serum calcium levels. The

effect on kidney function was also consistent with reported findings in patients with hypoparathyroidism. However, the increases in bone density are in contrast with reported bone loss associated with clinical hypocalcaemia and hypoparathyroidism. Ongoing bone turnover evaluations will further assist in the characterization of this model.

P58 - APPLICATION OF NON-STANDARD APPROACHES TO INVESTIGATIONS OF HUMAN MASS BALANCE AND METABOLITE CHARACTERISATION

Iain Shaw, Walker Helen, and Peter Scholes
Quotient Sciences

Conventional human mass balance (ADME) studies are well understood study designs which help drug companies generate data to support drug development and registration typically requiring a radioactive dose of 100 μ Ci and the utilisation of liquid scintillation counting (LSC) and mass spectrometry (LC-MSMS). This poster will describe various non-standard approaches to the conduct of human ADME studies conducted at Quotient Sciences that were driven by the particular characteristics of the drugs being tested. 1. Studies with long half-life molecules will be described where it was not practical to have the volunteers resident for a sufficient time to achieve a >90% recovery. In these studies we will demonstrate how a fixed residency period with planned return visits of 24 hours duration will be adequate to satisfactorily describe the mass balance recovery of the radioactive dose. 2. Examples of studies with potent drugs and cytotoxic molecules will be shared where the mass of drug dose was such that conventional LC-MSMS could not be used to completely describe the metabolite characterisation period of the study and instead this aspect of the study was completed using accelerator mass spectrometry. 3. This poster will provide case study examples of conventional ADME studies augmented by the integration of an IVMT period which will highlight the value of such studies to enable the understanding of factors that influence bioavailability, such as dissolution, solubility, absorption, gut metabolism and first pass hepatic extraction and thus aid development of effective formulation strategies. 4. The impact on study design and conduct of the need to consider particular populations of study participants will be described with specific reference to the complexities encountered when recruiting subjects of known and precise genotype requirements. The variety in the approaches described, that can be taken to obtain human ADME data, demonstrate the advances in technology available to the DMPK scientist to investigate and understand the disposition of drugs in development.

P59 - DEVELOPMENT OF A DISCOVERY CYP INHIBITION SCREEN FOR EARLY IDENTIFICATION OF DDI LIABILITIES

Teresa Sierra, Christopher Strock, Joanne Wyglinski, and Jenifer Bradley
Cyprotex

The cytochrome P450 (CYP450) monooxygenase system is essential in first pass metabolism of drugs. The CYP450 reversible inhibition assay can be used as a preliminary screen of candidate drugs to determine drug-drug interactions which may adversely affect plasma *in vivo* levels or result in adverse drug reactions. This *in vitro* ADME technique is highly correlative to *in vivo* outcomes and can be done well in advance of IND submission to aid in designing clinical DDI studies.

We describe herein a time, cost-effective and validated one-point automated approach to cytochrome P450 reversible inhibition which increases the throughput of candidate drugs. Probe substrates used were tacrine, tolbutamide, mephenytoin, dextromethorphan and midazolam for CYP1A2, CYP2C9, CYP2C19, CYP2D6 and CYP3A4, respectively. Compounds were run at a single concentration in 384-well plates in singlicate. Vehicle and control inhibitors were run across the plate to ensure reproducibility. Quenched reactions for each of the isoforms were combined as a cassette and run on LC-MS. All compounds were corrected to percent of vehicle and candidate drugs were flagged as inhibitory when displaying greater than 50 % inhibition.

This one-point automated approach to CYP450 reversible inhibition proved successful in screening candidate compounds for CYP inhibition liabilities early in the discovery process and allows for SAR and selection of compounds with lower DDI potential.

P60 - DEVELOPMENT OF A QUANTITATIVE BIOANALYTICAL METHOD FOR THE ASSESSMENT OF BENSERAZIDE IN PRE-CLINICAL SAMPLES

Amy Q. Wang¹, Kylie M. Konrath¹, Emma Hughes², Marc D. Singleton³, Sharie Haugabook¹, Susan Perrine-Faller⁴, and Xin Xu¹

¹National Center for Advancing Translational Sciences, National Institutes of Health, ²Department of Bioengineering and Therapeutic Sciences, University of California San Francisco, ³Department of Biophysics, University of California Berkeley, ⁴School of Medicine, Boston University

Benserazide is a peripherally-acting DOPA decarboxylase inhibitor. It has been used to inhibit amino acid decarboxylase to enhance plasma and brain levels of levodopa for the treatment of Parkinson's disease and restless legs syndrome in

European Union and other countries; but has not been approved in the United States. Recently, the compound has been identified as a potent inducer of fetal globin expression and is considered as a drug candidate for the treatment of β -hemoglobinopathies. The objective of this study is to develop an accurate, sensitive and selective UPLC–MS/MS method, evaluate the benserazide stability in blood and plasma, establish the PK sample collection procedures to maintain compound *ex vivo* stability, and assess pharmacokinetics of the compound in lab animals. The quantitative bioanalysis of benserazide in biological matrices faces a number of challenges, including instability at pH 7.4, hydrophilicity, low molecular weight, and endogenous interference. With these challenges in mind, a novel method for the quantification of benserazide in plasma samples has been developed using HILIC UPLC-MS/MS. The developed method has a linear calibration range of 1.0 ng/mL to 1000 ng/mL using 30 μ L plasma and protein precipitation sample preparation. The optimized HILIC UPLC-MS/MS method provided good chromatographic retention for benserazide, separated analyte from the endogenous interference, and reduced the sample preparation and analysis time.

P61 - OPTIMIZATION OF STEPPED COLLISION ENERGIES OF HCD IN ORBITRAP MASS SPECTROMETRY FOR METABOLITE STRUCTURE ELUCIDATION

Jianwei Zhao, Qing Ye, and Peter Wang

WuXiApptec XenoBiotic Laboratories

Stepped higher-energy collisional dissociation (HCD) technique has been employed to enhance the fragmentation efficiency of peptides in protein identification^{1,2}, and to provide more specific structural information of small molecules less than 600 Da³. Thermo's Q Exactive Plus, a hybrid quadrupole-orbitrap mass spectrometer, allows collection of fragmentation ions using stepped collision energy scans, in which same precursor is injected into the HCD cell several times at different collision energies (CE). This research describes a generic QE Plus method workflow utilizing MS method with fifteen parallel-reaction monitoring (PRM) scan events, in which collision energies varied from 10 to 150%, to optimize the CE energy parameters for different parent compound and its metabolites. Target compound (or mixture of several target compounds) can be analyzed using this method by direct MS acquisition, along with fifteen times of HPLC loop injections for 30 seconds each. All MS/MS (MS^2) spectra at different CEs were acquired into one data file in about 10 minutes, which was then used to select the best combination of CEs for targeted compound(s). Two commercially available chemicals and their metabolites (midazolam and metabolite 1'-hydroxymidazolam, and diclofenac and metabolite 4'-hydroxydiclofenac) were analyzed using this method on QE Plus. Fragment ions at high mass for midazolam and 1'-hydroxymidazolam were observed starting at CE= 40, while more low mass fragment ions were observed starting at CE=90. For diclofenac and 4'-hydroxydiclofenac, more informative fragment ions were observed when stepped CE was set at 10 for high mass, and 110 for low mass. There was no big difference of MS^2 pattern when CE was between 30 and 100 for diclofenac and its metabolite. Based on these results, the combination of three stepped normalized collision energies of 50, 70, and 90 (average 70) were applied to obtain the MS/MS fragment ions of 1'-hydroxymidazolam, and CE=10, 70, and 130 (average 70) were used for 4'-hydroxydiclofenac. A comprehensive MS^2 spectrum was generated, utilizing three different CEs at the same time, and complexing three spectra into one spectrum. In conclusion, optimization of the CEs using the generic streamlined method facilitated to find the sweet combination of three stepped collision energies for parent compound and its putative metabolites. The complexed HCD MS^2 spectrum with three optimized CEs, provided more fragmentation information comparing to that with a single CE or three randomly selected CEs, when used for the elucidation of chemical structure, and determination of metabolism site.

References:

1. Olsen, J.V., Macek, B., Lange, O., Makarov, A, Horning, S. & Mann, M., "Higher-energy C-trap dissociation for peptide modification analysis", *Nature Methods*, 4(9):709–712, 2007.
2. Diedrich, J.K., Antonio F. M. Pinto, A.F. & Yates, J.R. 3rd, "Energy dependence of HCD on peptide fragmentation: Stepped collisional energy finds the sweet spot", *J. Am. Soc. Mass Spectr.*, 24(11),1690-1699, 2013
3. Bushee, J.L. & Argikar, U. A., "An experimental approach to enhance precursor ion fragmentation for metabolite identification studies: application of dual collision cells in an orbital trap", *Rapid Commun. Mass Spectrom.*, 25, 1356–1362, 2011

P62 - PRECLINIAL BIOPHARMACEUTICS AND PHARMACOKINETIC CHARACTERIZATION OF AN HIV-1 REPLICATION INHIBITOR DB213

Zhong Zuo¹, Qianwen Wang¹, Chun-Ho Wong², Yue Hu², Kin Ming Kwan², and Edwin H.Y. Chan^{2,3}

¹School of Pharmacy, The Chinese University of Hong Kong, ²School of Life Sciences, The Chinese University of Hong Kong, ³Gerald Choa Neuroscience Centre, The Chinese University of Hong Kong

DB213 is an HIV-1 replication inhibitor targeting HIV-associated neurocognitive disorders. Our previous work demonstrated that intranasally delivered DB213 could achieve 290-fold higher brain to plasma ratio in comparison to those delivered intravenously [1]. In order to further understand its biopharmaceutics and pharmacokinetic characteristics, the current study is proposed to investigate the absorption, distribution and metabolism mechanisms of DB213.

In vitro Calu-3 cell monolayer transport of DB213 was carried out to evaluate its nasal epithelium permeability. Potential transporter mediated transport of DB213 was evaluated on cell models (MDCK II-WT, MDCK II-MRP2, MDCK II-MRP3, MDCK II-MDR1, HEK 293-MOCK, HEK 293-OAT3) and brain slices [2] prepared freshly from drug-naïve Sprague Dawley (SD) rat brain in presence and absence of the corresponding inhibitors (MK571 as MRP2 and MRP3 inhibitors, Verapamil as MDR1 inhibitor, Probenecid as OAT3 inhibitor, Quinine as OCT inhibitor, and 2-Amino-2-norbornanecarboxylic acid as amino acid transporter inhibitor). The liver and brain metabolism of DB213 were investigated via incubation with freshly prepared pooled SD rat liver and brain microsomes.

It was found that DB213 demonstrated limited permeability on Calu-3 cell monolayer model with $P_{app(a \rightarrow b)}$ of 1.40 ± 0.21 , 1.87 ± 0.29 and $1.98 \pm 0.40 \times 10^{-6}$ cm/s at loading concentrations of 10, 100 and 300 mM, respectively. DB213 could be substrates of efflux transporters MRP2 and MRP3 as indicated by the significant difference on DB213 cell uptake in MDCK II-MRP2/MRP3 (versus that MDCK WT cell lines) and in presence of MK571. Moreover, the results from brain slices model suggested DB213 as a substrate of amino acid influx transporter. In addition to limited Phase I metabolism of DB213 in liver and brain (intrinsic clearance of 26.64 and 4.28 mL/min/mg, respectively), its phase II glucuronidation and sulfation metabolism was found minimal with only 97% and 86% % remained after 1 h of incubation in rat liver microsome, respectively.

In summary, limited nasal epithelium permeability and MRP2/MRP3 mediated efflux transport of DB213 could be overcome by its potential influx transport via amino acid transporter and minimal liver and brain metabolism, which further contribute to its brain uptake.

Financial support from Lui Che Woo Institute of Innovative Medicine BRAIN Initiative (Project Number 8303404) and Gerald Choa Neuroscience Centre (Project Number 7105306), the Chinese University of Hong Kong.

References:

1. Wang Q, Zhang Y, Wong C H, et al. Demonstration of Direct Nose-to-Brain Transport of Unbound HIV-1 Replication Inhibitor DB213 Via Intranasal Administration by Pharmacokinetic Modeling[J]. *The AAPS journal*, 2018, 20(1): 23.
2. Loryan I, Fridén M, Hammarlund-Udenaes M. The Brain Slice Method for Studying Drug Distribution in the CNS[J]. *Fluids and Barriers of the CNS*, 2013, 10(1): 6.

P63 - LACK OF PHARMACOKINETIC INTERACTION BETWEEN SINGLE ORAL DOSES OF LETERMIVIR (MK-8228) AND FLUCONAZOLE IN HEALTHY SUBJECTS

Adedayo Adedoyin¹, Sabrina Fox-Bosetti¹, Craig Fancourt¹, Fang Liu¹, Karsten Menzel¹, Tian Zhao¹, Patrice Auger², Angela Mirzac², Charles Tomek², Deborah Panebianco¹, Sreeraj Macha¹, Jacqueline McCrea¹, and Marian Iwamoto¹
¹Merck & Co., Inc., ²Celerion

Background: Letermovir (Prevymis™), a cytomegalovirus (CMV) terminase inhibitor, is indicated for prophylaxis of CMV infection and disease in adult CMV seropositive recipients of an allogeneic hematopoietic stem cell transplant (HSCT). Many transplant patients, in addition to anti-rejection therapy, also receive anti-infection therapy, such as fluconazole, an antifungal. Letermovir is primarily cleared by fecal elimination of intact drug. Oxidative metabolism is considered a minor elimination pathway. Letermovir is a substrate of organic anion-transporting polypeptide 1B1/3 (OATP1B1/3) transporters. Letermovir is a net moderate inhibitor of CYP3A, an inducer of CYP2C9/19, and an inhibitor of OATP1B1/3 transporters. Fluconazole is primarily eliminated by urinary excretion. It is a moderate inhibitor of CYP3A4 and potent inhibitor of CYP2C9 and CYP2C19. Based on the profiles of letermovir and fluconazole, a significant pharmacokinetic drug interaction is not anticipated. However, because of frequent co-administration, a drug interaction trial was conducted to evaluate the potential pharmacokinetic interaction between letermovir and fluconazole, to rule out any significant interaction. **Methods:** An open-label, 3-period, fixed-sequence study was performed in 14 healthy adult female subjects, aged 19 - 55 years. In Period 1, a single oral dose of 400 mg fluconazole was administered. In Period 2, a single oral dose of 480 mg letermovir was administered. In Period 3, the same single oral doses of fluconazole and letermovir were co-administered. There was a washout period of 14 days between doses in Period 1 and Period 2, and at least 7 days between Period 2 and Period 3. Pharmacokinetic samples were collected over 72 h to 168 h post dose. Pharmacokinetics and safety were evaluated. **Results:** The pharmacokinetics of fluconazole and letermovir were unchanged by co-administration. Fluconazole AUC_{0-∞} Geometric Mean Ratios (GMRs) (90% CI) (fluconazole+letermovir/fluconazole alone) was 1.03 (0.99, 1.08). Similar results were observed for C_{max} and C_{24h}; GMRs were 0.95 (0.92, 0.99) and 1.04 (1.00, 1.08), respectively. Letermovir AUC_{0-∞} GMR (90% CI) (fluconazole+letermovir/letermovir alone) was 1.11 (1.01, 1.23). Letermovir C_{max} and C_{24h} increased by 6% and 28%, respectively, with the co-administration; GMR for C_{max} was 1.06 (0.93, 1.21) and for C_{24h}, 1.28 (1.15, 1.43). Co-administration of a single oral dose of fluconazole with a single oral dose of letermovir was generally well tolerated in healthy female subjects. Observed Treatment Emergent Adverse Events (TEAEs) were generally mild and resolved by the end of the study. **Conclusions:** No clinically significant differences were observed in the exposures of fluconazole or letermovir after co-administration. Both fluconazole and letermovir were generally well tolerated upon co-administration.

P64 - EFFECTS OF ESSENTIAL OILS OF CULINARY HERBS AND SPICES ON THE CYP3A4 EXPRESSION IN PRIMARY HUMAN HEPATOCYTES AND CELL LINES**Iveta Bartonkova** and Zdenek Dvorak

Palacky University Olomouc, Faculty of Science, Department of Cell Biology and Genetics

Essential oils (EOs) of culinary herbs and spices are a common part of our daily diet. They are multicomponent mixtures of compounds with already demonstrated biological activities which represent a potential source of food-drug interactions and endocrine disruption. In the current work, we have investigated the influence of 31 EOs of commonly used culinary herbs and spices on the transcriptional activity of pregnane X receptor (PXR) and the expression of PXR target gene CYP3A4 in human cell lines and primary human hepatocytes. In the reporter gene assay, all 31 tested EOs induced PXR transcriptional activity but with different potency and efficacy. On the other hand, no decline of luciferase activity was observed after the combined treatment with any of EOs and model PXR ligand rifampicin. The expression of CYP3A4 mRNA was examined in intestinal LS180 cell line, PXR knock-out and wild-type HepaRG cell line and three different cultures of primary human hepatocytes. All of the EOs induced the expression of CYP3A4 mRNA in LS180 cell line with a different relative efficacy, reaching 8% to 70% of induction attained by rifampicin. Most significant induction of CYP3A4 mRNA in primary human hepatocytes, was achieved by EOs of nutmeg, marjoram and black pepper. No changes in CYP3A4 mRNA expression were observed in PXR knock-out HepaRG cell line, while in the wild-type HepaRG cells some induction of CYP3A4 mRNA was detected. Taken together, we show that EOs of culinary herbs and spices exhibit an agonist activity towards human PXR and induce CYP3A4 mRNA in various human cells.

Our laboratory is supported by the grant from Czech Science Foundation GACR 17-02718S. We declare no conflict of interest.

P65 - EVALUATION OF THE TIME-COURSE OF CYP INDUCTION AND IMPACT ON DRUG INTERACTION RISK ASSESSMENT FROM THE IQ INDUCTION WORKING GROUP**Niresh Hariparsad**¹, Heidi Einolf², David Buckley³, Shannon Dallas⁴, Josh Dekeyser⁵, Theunis Goosen⁶, Barry Jones⁷, Jane Kenny⁸, Mike Mohutsky⁹, Kelly Nulick⁶, Jairam Palamanda¹⁰, Diane Ramsden¹¹, Amy Siu¹², Donald Tweedie¹⁰, Simon Wong⁸, Phillip Yates⁶, and George Zhang¹³¹Vertex Pharmaceuticals, ²Novartis, ³Roivant Pharmaceuticals, ⁴Johnson and Johnson, ⁵Amgen, ⁶Pfizer Inc.,⁷AstraZeneca, ⁸Genentech, ⁹Eli Lilly, ¹⁰Merck, ¹¹Boehringer Ingelheim, ¹²Eisai, ¹³Corning

Current regulatory guidance recommends investigation of a drug candidate's potential to induce cytochrome P450 (CYP) enzymes in human hepatocytes by incubations of up to 72 hours. It was the goal of the International Consortium for Innovation and Quality in Pharmaceutical Development (IQ) Induction Working Group (IWG) to compare the *in vitro* induction response at 48 vs. 72 hours, as the former is more commonly used in industry. Particularly of value for cytotoxic compounds, shorter incubation times were also evaluated to determine if the sensitivity of the *in vitro* induction and a consistent drug-drug interaction (DDI) assessment could be maintained. Seven member companies from the IWG participated in this study by incubating hepatocytes from one human donor per company with known moderate and strong inducers. Data were generated from a time-course of induction for CYP1A2, CYP2B6, and CYP3A4 mRNA and enzyme activity (incubation times of 6, 12, 24, 48, or 72 hours). When possible, the induction parameters, EC₅₀ and E_{max}, were estimated for each time point. While variability in induction parameters was observed across donors, trends could be discerned between time-points which were consistent amongst donors when visualized on a log₂ scale. For CYP mRNA induction parameters, measurements at the 72 hour time point were not significantly different, on average, from the 48 hour time point estimates. As expected, the CYP activity E_{max} estimate had a statistically significant higher average value at 72 hours compared with 48 hours, whereas, on average, the EC₅₀ estimates were comparable. The induction potency (E_{max}/EC₅₀), which is used in several algorithms to assess clinical risk, will be evaluated across the time-points to determine consistency in the assessment of drug interaction risk. Although identical quantitative estimates of clinical drug interaction magnitude may not be possible at all incubation time points, shorter incubation times will be assessed for their utility to identify *in vitro* inducers.

P66 - THE ROLE OF NUCLEOSIDE TRANSPORTERS IN ENTECAVIR TRANSPORT ACROSS PLACENTA**Sara Karbanova**, Lukas Cerveny, and Frantisek Staud

Charles University, Faculty of Pharmacy

Entecavir is a widely used hydrophilic nucleosid-derived antiviral drug exhibiting high efficacy against hepatitis B virus (HBV). As there is lack of safety data and information about mechanism involved in entecavir placental transfer, its use during pregnancy is limited. Entecavir is suggested substrate of nucleoside transporters (NTs) that are categorized in two subfamilies – equilibrative nucleoside transporters (ENTs) and concentrative Na⁺ dependent nucleoside transporters (CNTs)². In the present study, we aimed to evaluate role of NTs entecavir placental uptake and transfer into fetal circulation. For this purpose, we employed an *in vitro* uptake experiment in BeWo cells at 37°C and 4°C¹, an *ex vivo* model of uptake in fresh villous fragments from human placenta, and an *in situ* dually perfused rat term placenta model

(open-circuit and recirculation), analyzing materno-fetal (M-F) and feto-maternal (F-M) transplacental clearances of entecavir on the organ level. Using BeWo cell line model we observed significant decrease of [³H]-entecavir intracellular concentration in presence of 100 μM NBMPR, 5 mM uridine, or 1 mM adenosine. In fresh villous fragments preserving functional architecture of the placental barrier we showed time dependent [³H]-entecavir accumulation that was significantly reduced by 100 μM NBMPR that inhibits ENT1 and ENT2. Importantly, 100 μM NBMPR decreased [³H]-entecavir total clearance in both directions M-F and F-M directions. In M-F direction the significance appeared also in presence of 0.1 μM NBMPR, inhibiting only ENT1 and similarly in presence 5 mM uridine that reduces function of all nucleoside transporters. In this experimental approach [³H]-entecavir M-F and F-M clearances showed low level of its transplacental permeation, with negligible placental accumulation after the perfusion (≤1% of the [³H]-entecavir dose). As we observed 2-fold higher transport in F-M direction, we also carry out dual perfusion study at concentration equilibrium, revealing no active transport. Lack of interactions between highly expressed placental active efflux transporters, P-glycoprotein, Breast Cancer Resistance Protein and Multidrug Resistance-Associated Protein 2 was further confirmed using bi-directional transport across MDCKII cells.

In conclusion, our data suggest involvement of ENTs and CNTs in placental uptake and transfer of entecavir. Further studies have to be performed to specify the subtypes of ENTs or CNTs involved in entecavir placental pharmacokinetics and propensity of entecavir to drug-drug interactions on these carriers.

The study was supported by GAUK 812216/C/2016, GAČR 17-16169S and SVV/ 2017/260-414.

References

1. T. YAMAMOTO, K. KUNIKI, Y. TAKEKUMA, T. HIRANO, K. ISEKI, AND M. SUGAWARA, "Ribavirin uptake by cultured human choriocarcinoma (BeWo) cells and *Xenopus laevis* oocytes expressing recombinant plasma membrane human nucleoside transporters.," *Eur. J. Pharmacol.*, vol. 557, no. 1, pp. 1–8, Feb. 2007.
2. Z. MA, X. YANG, T. JIANG, M. BAI, C. ZHENG, D. SUNG, H. JIANG, "Multiple SLC and ABC transporters contribute to the placental transfer of entecavir.," *Drug metab. Dispos.*, Jan. 2017.

P67 - REACTIVE METABOLITE FORMATION BY IRREVERSIBLE AND QUASI-IRREVERSIBLE CYTOCHROME P450 INHIBITORS

Jennifer Thomas¹, Jelle Reinen², Martijn Smit², and Mira Wenker²

¹Charles River Laboratories, ²Charles River Laboratories Den Bosch B.V.

Drug metabolism mediated by Cytochrome P450 enzymes (CYPs) is responsible for the majority of the metabolism of known drugs in humans and inhibition of CYP enzymes is a well-recognized cause of drug-drug interactions (DDIs). CYP inhibition may result from direct inhibition by the drug itself or metabolism-dependent inhibition (MDI) by drug metabolite(s). MDI can be reversible (a metabolite is a more potent inhibitor than the parent drug) or mechanism-based (MBI). When a reactive metabolite binds covalently to the heme or apoprotein, MBI is irreversible; when a reactive metabolite forms a stable metabolic intermediate complex (MIC) through a coordinate bond with the ferrous heme iron, MBI is quasi-irreversible. Irreversible MBI can lead to hapten formation which can subsequently trigger an autoimmune response leading to hepatotoxicity. For accurate assessment of the risk of MBI, it is therefore very important to determine which type of MBI is involved. As a result, various experimental methodologies have been developed to study the exact type of MDI. In the current study, it was investigated if differences exist between irreversible and quasi-irreversible MDIs with respect to formation and GSH trapping of reactive metabolites. For a selection of irreversible (mifepristone and paroxetine) and quasi-irreversible (troleandomycine and verapamil) MBIs formation of MICs and reactive metabolites was investigated. A ferricyanide-based reversibility assay in combination with a spectrophotometric MIC assay was performed to determine if either irreversible or quasi-irreversible MBI occurred. Subsequently, experiments were performed to study the possible formation of CYP-mediated GSH-adducts in HLM incubations in the presence and absence of NADPH and GSH. The current study gives an overview of methodologies that can be used to study MBI and therefore is of added value for risk evaluation of CYP-mediated DDIs.

P68 - ATP-BINDING CASSETTE TRANSPORTERS AND CYP450 ISOFORMS ARE POSSIBLE SITES OF RIBOCICLIB DRUG INTERACTIONS

Ales Sorf, Jakub Hofman, Radim Kucera, Lukas Cervený, Frantisek Staud, and Martina Ceckova
Charles University, Faculty of Pharmacy in Hradec Kralove

Ribociclib is a novel CDK 4 and 6 selective inhibitor that recently gained approval for advanced breast cancer treatment and is currently evaluated in clinical trials dealing with various tumors. It is well recognized that ATP-binding cassette (ABC) transporters as well as CYP450 isoenzymes may become a site of severe drug interactions and above all also mechanism of multidrug resistance (MDR) development. With respect to rapid progress of ribociclib in the clinical field, we aimed to identify its interactions with ABC transporters and also CYP450 isoenzymes. Using established transport assay across MDCKII-ABCB1 monolayer, we showed accelerated, ABCB1 inhibitor LY335979-sensitive, basolateral-to-apical transport of ribociclib, revealing thereby this CDKI as ABCB1 substrate. The antiproliferative studies supported this finding

by demonstrating significantly higher IC₅₀ value in ABCB1-, but not ABCG2- or ABCC1-expressing MDCKII cells, when compared to the parental MDCKII cell line. Furthermore, we revealed significant inhibitory effect of ribociclib on both ABCB1 and ABCG2 transporters as well as on the activity of CYP1A2, CYP3A4, CYP3A5 and CYP2C9 isoforms in human CYP450 expressing insect microsomes. The ABCB1 and ABCG2 inhibition was further able to reverse daunorubicin and mitoxantrone resistance in MDCKII cell lines and in human breast carcinoma cell line MCF-7. Clear synergistic antiproliferative effect was found for these drug combinations, while no changes in the expression of ABCB1 or ABCG2 were observed. To conclude, ribociclib showed broad potential for pharmacokinetic drug-drug interactions being a substrate to ABCB1 and inhibitor to ABCB1, ABCG2 and several CYP450 isoenzymes. The drug also demonstrated ability to reverse drug resistance to conventional cytotoxic agents MDCKII and breast cancer cells, which should be taken into account and may be beneficially exploited when administering ribociclib in clinical therapeutic regimens. This study was supported by the Czech Science Foundation (Grant No. 16-26849S) and Grant Agency of Charles University (SVV 2018/260 414).

P69 - METHYLINDOLES AND METHOXYINDOLES ARE AGONISTS AND ANTAGONISTS OF HUMAN ARLY HYDROCARBON RECEPTOR AHR

Zdenek Dvorak¹, Martina Stepankova¹, Iveta Bartonkova¹, Eva Jiskrova¹, Radim Vrzal¹, Sridhar Mani², and Sandhya Kortagere³

¹Department of Cell Biology and Genetics, Faculty of Science, Palacky University, ²Department of Genetics and Department of Medicine, Albert Einstein College of Medicine, ³Department of Microbiology & Immunology, Drexel University College of Medicine

Aryl hydrocarbon receptor (AhR) is a ligand-activated transcriptional factor that regulates xenobiotic metabolizing enzymes, but also plays a role in many physiological and pathophysiological processes. AhR is activated by a number of exogenous and endogenous compounds. Here we report novel methyl-indoles as endobiotic and xenobiotic ligands of human AhR. We investigated the effects of 22 methyl- and methoxy-substituted indoles on the transcriptional activity of AhR. By the means of reporter gene assays, we determined full agonist, partial agonist or antagonist activities of tested indoles, displaying substantially variable EC₅₀, IC₅₀ and relative efficacies. The most effective agonists of AhR were 4-Me-indole, 6-Me-indole and 7-MeO-indole. The most effective antagonists of AhR included 3-Me-indole, 2,3-diMe-indole and 2,3,7-triMe-indole. RT-PCR analyses of CYP1A1 mRNA in LS180 cells were consistent with the data from reporter gene assays. For lead compounds, 4-Me-indole and 7-MeO-indole, fluorescent immunohistochemistry demonstrated nuclear translocation of AhR, and chromatin immunoprecipitation assays revealed enriched binding of AhR to CYP1A1 promoter, respectively. Molecular modeling and docking studies showed that indole agonists and antagonists share the same binding pocket but have unique binding modes that code for their affinity. Altogether our data show a dependence on subtle and specific chemical indole structures as AhR modulators and furthermore underscore the importance of complete evaluation of indole compounds as nuclear receptor ligands.

Acknowledgements: Financial support from Czech Science Foundation (grant No. P303/12/G163) is acknowledged.

P70 - GENOTYPE-SENSITIVE REVERSIBLE AND TIME-DEPENDENT CYP2D6 INHIBITION IN HUMAN LIVER MICROSOMES

Flavia Storelli, Jules Desmeules, and Youssef Daali
Geneva University Hospitals

Cytochrome P450 (CYP) 2D6 metabolizes a wide range of xenobiotics and is characterized by a huge inter-individual variability. Recent in-vivo studies in humans highlighted differential magnitude of CYP inhibition as a function of genotype. In a recent clinical study, we showed that *CYP2D6* genotype had an impact on the rate of phenoconversion and the magnitude of drug-drug interactions in genetically-predicted extensive metabolizers (EMs) (1). The aim of this study was to investigate *in vitro* the effect of *CYP2D6* genotype on the inhibition of dextromethorphan O-demethylation by duloxetine and paroxetine in genetically-characterized human liver microsomes (HLM) in order to build a PBPK model able to predict DDIs as a function of genotype. The study focused on genotypes defined by the combination of two fully-functional alleles (activity score 2, AS 2), of one fully-functional combined with one reduced allele (activity score 1.5, AS 1.5) and of one fully-functional combined with one non-functional allele (activity score 1, AS 1), which all predict CYP2D6 EM phenotype. The kinetics of dextromethorphan O-demethylation was characterized in 16 batches of HLMs from different donors (6 AS 1, 4 AS 1.5 and 6 AS 2) by incubating dextromethorphan (0.5- 100 µM) in a reaction mixture containing a total microsomal protein amount of 0.5 mg/ml. The metabolite dextrophan was then quantified by LC-MS/MS. Then the reversible and irreversible inhibition parameters of duloxetine (0.5-150 µM) and paroxetine (0.1-10 µM), respectively were determined using appropriate standard protocols. All kinetic and inhibitory parameters were calculated by nonlinear regression using GraphPad Prism version 7 (La Jolla, CA, USA). Kinetic experiments showed that maximal reaction velocity was affected by *CYP2D6* genotype, with a reduction of 33% of V_{max} in AS 1 HLMs compared to AS 2 (p<0.05). However, no difference in inhibition parameters K_i, K_i and K_{inact} was observed neither with the competitive inhibitor duloxetine nor with the time-dependent inhibitor paroxetine. Therefore, we concluded that genotype-sensitive DDI magnitude observed in our previous

clinical study is likely to be due to differential abundance of functional enzymes at the microsomal level rather than to a difference in inhibition potencies across genotypes, which motivates for further quantitative proteomic investigations.

P71 - ASSESSMENT OF INTERACTION WITH NUCLEOSIDAL TRANSPORTERS BETWEEN ENASIDENIB AND AZACITIDINE

Usha Yerramilli, Matthew Hoffmann, Sekhar Surapaneni, and Zeen Tong

Celgene

Azacitidine is an analog of the pyrimidine nucleoside cytidine and a DNA methyltransferase inhibitor, and is used for the treatment of acute myeloid leukemia (AML). Enasidenib is a specific inhibitor of isocitrate dehydrogenase 2 (IDH2) mutant protein, and has been approved by FDA for the treatment of relapsed or refractory AML adult patients with an IDH2 mutation. A synergistic pharmacodynamic activity between azacitidine and enasidenib could occur through a combined impact on DNA methylation. A clinical study of enasidenib in combination with azacitidine is currently ongoing in AML patients. Studies have shown that uptake of azacitidine is mediated by human nucleoside transporters (hNTs) including concentrative nucleoside transporters (hCNTs) hCNT1, hCNT2 and hCNT3, as well as human equilibrative nucleoside transporters (hENTs) hENT1, hENT2, hENT3 and hENT4. The present study investigated the effect of enasidenib on hNT activities in hNT-expressing oocytes and uptake of azacitidine in AML and normal cell lines. Experiments with oocytes expressing hNTs showed that enasidenib inhibits hENT1, hENT2, hENT3 and hENT4 but did not show significant inhibition of hCNTs. The IC_{50} values were 7, 63, 27 and 76 μ M for hENT1, hENT2, hENT3 and hENT4, respectively. The effect of enasidenib on uptake of azacitidine in AML and normal B-lymphoblast peripheral blood (PBC) cell lines was studied in buffer containing sodium ions (active hCNTs and hENTs), sodium free buffer (only hENTs active) and in human plasma. Azacitidine uptake was at least 3-fold higher in AML cell lines than PBC. Enasidenib inhibited uptake of azacitidine in a concentration-dependent manner in sodium and sodium free buffer with IC_{50} values of 0.27 μ M, 1.7 μ M, and 1.0 μ M in sodium buffer in OCI-AML2, TF-1 and PBC cell lines, respectively. However, the IC_{50} values for enasidenib inhibition of azacitidine uptake into cell lines in human plasma was approximately 100-fold higher (27 μ M in OCI-AML2, 162 μ M in TF-1, and 129 μ M in PBC), likely due to high human plasma protein binding of enasidenib (98.5% bound). Results from this study indicate that enasidenib inhibits hENTs and azacitidine uptake *in vitro*. However, these interactions may not be clinically significant since plasma C_{max} (27 μ M) of enasidenib at the therapeutic dose of 100 mg is comparable to or lower than the IC_{50} values obtained *in vitro* using human plasma.

P72 - QUALIFICATION AND APPLICATION OF AN *IN VITRO* LIVER MODEL EARLY IN PHARMACEUTICAL DEVELOPMENT TO HELP DERISK DRUG-INDUCED LIVER INJURY (DILI)

Kaushik Mitra, Wen Kang, Keith Tanis, Stephen Pacchione, Ming Su, Zhibin Wang, Kimberly Bleicher, Thomas Griffiths, George Laws, Matthew Kuhls, Alexei Podtelezchnikov, James Monroe, Timothy Johnson, Donald Marsh, Ian Knemeyer, Qing Chen, Jose Lebron, and Frank Sistare
Merck

Drug-induced liver injury (DILI) remains a major safety concern for pharmaceutical development despite significant efforts across academia and industry to improve liver safety assessment early in development. Over the past few years, Merck investigators have deployed a set of liver transcriptional biomarkers *in vivo* and *in vitro* to inform on the potential of drug candidates to generate high liver burden of chemically reactive metabolites (CRM) and to help predict risk for clinical hepatotoxicity. Here we describe the 9-day *in vitro* assay using micro-patterned human and rat hepatocyte co-culture systems (HepatoPac) as a compound-, animal- and time-sparing approach to de-risk compound series shown to have high CRM burden *in vivo*. We established a transcriptional biomarker signature *in vitro*, and qualified the use of the signature in the HepatoPac model using 90+ commercial drugs and internal Merck compounds, including liver safe and unsafe analogs to demonstrate high structural specificity. The assay showed a high concordance (80%) with results obtained *in vivo*. Taking into the consideration calculated human liver inlet clinical exposures, the *in vitro* rat model provides ~80% sensitivity and ~90% specificity for distinguishing liver safe drugs from hepatotoxic ones. While overall performance between the human and rat models was similar, appreciable differences were observed for several compounds, suggesting species differences in drug metabolic pathways, turnover rates, and/or xenobiotic responses that could drive discrepant biomarker responses. In conclusion, we show that the HepatoPac micro-patterned co-culture liver model is a resource sparing approach to improve DILI risk assessment from CRM early in preclinical development.

P73 - A NOVEL STRATEGY FOR CYP3A4 INDUCTION SCREENING IN DRUG DISCOVERY: USE OF HEPARG CELLS AND SIMPLIFIED RELATIVE INDUCTION SCORE METHOD

Yusuke Aratsu, Kenji Morita, Mai Shimizu, Toshio Taniguchi, Yukihiko Nomura, and Motohiro Kogayu
JAPAN TOBACCO INC

The evaluation of inductive effects of new drug entities on Cytochrome P450 (CYP) 3A4 is essential in the early drug discovery stage in order to reduce the risk of Drug-Drug-Interaction (DDI). In this study we tried to develop an easy/simple approach for CYP3A4 induction screening. We selected HepaRG, which is known as a human hepatocyte-like cell line with minor lot-to-lot variations, and we investigated if the conventional workflow of HepaRG for CYP induction assessment can be simplified by adding some modifications such as reduction of the number of medium changes. As a result, an easy method for CYP3A4 induction assessment using HepaRG was developed. For DDI risk prediction, a simple method based on the Relative Induction Score (RIS) Method (hereafter referred to as the simplified RIS (smRIS) method) was developed. The smRIS method was established based on the assumption that the $[I]$ (the unbound maximum plasma concentration of drug) in the equation for RIS ($RIS = [I] \times E_{max} / ([I] + EC_{50})$) is much lower than the EC_{50} value, in short, $[I] \ll EC_{50}$ and C means the drug concentration at that point. Therefore, smRIS can be expressed as follows: $smRIS = [I] \times E_{max} / EC_{50}$. Through the investigation using several typical CYP3A4 inducers, it was suggested that the smRIS method is reliable since the smRIS values were comparable to the values obtained by the conventional RIS method. In this way, the laborious experiments for obtaining EC_{50} and E_{max} can be skipped in DDI prediction by the smRIS method. Therefore smRIS method is useful to estimate DDI risk in the screening stage. Furthermore, since the DDI risk can be assessed at lower drug concentrations, the smRIS method is expected to be applicable to highly cytotoxic compounds. In conclusion, we have developed a novel screening approach for the assessment of CYP3A4 induction utilizing HepaRG and the smRIS method.

P74 - QUANTITATIVE PREDICTION OF CYP3A4 INDUCTION USING SIMPLE RELATIVE FACTOR APPROACH

Shino Kuramoto, Motohiro Kato, Hidetoshi Shindoh, and Masaki Ishigai
Chugai Pharmaceutical Co. Ltd.

Purpose: It is important to predict CYP3A enzyme induction in the drug-discovery process to avoid drug-drug interaction in human. Previously, we reported that we could provide a robust and relevant threshold for CYP3A4 induction risk in the clinical setting using relative factor (RF) approach that satisfies FDA and EMA guidelines¹⁾. The RF approach is a simple prediction method and the RF value is designated as the ratio of the induction detection limit concentration (IDLC) for a standard inducer, such as rifampicin (RIF) or phenobarbital (PB), to that for a test compound (RF_{RIF} is $IDLC_{RIF}/IDLC_{cpd}$; RF_{PB} is $IDLC_{PB}/IDLC_{cpd}$). In this study, we tried to predict CYP3A4 induction using RF approach and to evaluate the predictability of *in vivo* DDI ratio quantitatively.

Method: *In vitro* induction assays were performed for 8 typical CYP3A4 inducers and standard inducers RIF and PB using cryopreserved human hepatocytes (3 donors). We conducted the following analysis with each donor to normalize the induction response of different donors. First, $IDLC_{cpd}$ value was estimated from the *in vitro* induction curves and then RF_{RIF} value was calculated for 8 typical inducers and PB using RIF as reference standard. Next, we calculated *in vivo* DDI ratio of CYP3A4 (the ratio of CL_{int} with or without treatment of an inducer) and the converted *in vivo* unbound steady state plasma concentration ($C_{ss,u}$) of RIF ($RF_{RIF} \times C_{ss,u}$) in clinical data from literature. *In vivo* E_{max} and EC_{50} of RIF were evaluated from the data of RIF and PB. Finally, *in vivo* DDI ratio were predicted for 8 typical inducers from $RF_{RIF} \times C_{ss,u}$ and E_{max} model.

Result: *In vivo* E_{max} and EC_{50} values for RIF in each donor were calculated to be 5.07 to 5.51-fold and 19.1 to 37.8 nM, respectively, using *in vivo* DDI ratio and $RF_{RIF} \times C_{ss,u}$ of RIF and PB. *In vivo* DDI ratio for 8 inducers could be predicted in each donor using these E_{max} and EC_{50} and good predictability was observed for these 8 inducers. For one example, the observed DDI ratio (DDI_{obs}) of Carbamazepine (CRB) at 600 mg was 2.44 and predicted DDI ratio (DDI_{pred}) from E_{max} model was 1.72 to 3.40. DDI_{obs}/DDI_{pred} ratio of CRB was within 2-fold.

Conclusion: *In vivo* induction ratio of CYP3A4 were predicted from simple RF approach. RF approach is useful method which can assess not only qualitative but also quantitative CYP3A4 induction risk in clinical settings.

Reference:

1. Kuramoto S, Simple evaluation method for CYP3A4 induction from human hepatocytes; The relative factor approach with an induction detection limit concentration based on the E_{max} model, Drug Metab Dispos, 45: 1139-1145, 2017

P75 - CRYOPRESERVED HUMAN INTESTINAL MUCOSA: A NOVEL *IN VITRO* 3-D ORGAN CULTURE FOR THE EVALUATION OF P450 INDUCTION IN HUMAN INTESTINES**Albert P. Li**

In Vitro ADMET Laboratories Inc.

Human small intestine is known to contribute significantly to the first pass metabolism of orally administered drugs, especially drugs that are substrates of CYP3A, the major intestinal P450 isoform. As of now, enteric P450 induction has been reported in preclinical laboratory animals and in humans *in vivo*. Unlikely hepatic P450 induction that can be readily studied in primary cultured cryopreserved human hepatocytes, at present, there are very limited *in vitro* experimental approaches for the evaluation of enteric P450 induction. We report here the first successful demonstration of CYP3A4 induction in a cryopreserved human enteric experimental model: cryopreserved human intestinal mucosa (CHIM). We recently reported on successful isolation and cryopreservation of purified human enterocytes from the small intestine (Ho et al., *Drug Metabolism and Disposition* (2017) 45:686-91). The cryopreserved enterocytes represent a useful system for the evaluation of short-term (hours) metabolism studies, cannot be cultured for the evaluation of P450 induction. Most recently, we developed another novel intestinal system, cryopreserved human intestinal mucosa (CHIM). CHIM is an organoid system retaining the three-dimensional structure of the intestinal mucosa. Upon thawing, CHIM were found to retain viability and robust drug metabolizing enzyme activities. We subsequently developed a relatively long-term (24 hours) culture system for CHIM and initiated studies to investigate the application of this organ culture system towards the evaluation of intestinal P450 induction. We report here results of P450 induction studies with two known inducers of intestinal CYP3A4: vitamin D3 and rifampin. For the study, CHIM were isolated and cryopreserved from the duodenum (lot number HE3061) of a 58-year-old Hispanic male. After thawing and recovery, CHIM were plated into 24-well plates and treated with various concentrations of vitamin D3 (0.14 to 100 nM) and rifampin (0.02 to 20 mM). Gene expression for CYP3A4 and the two vitamin D-responsive genes (CYP24A and TRPV6). Results with vitamin D3 showed that CHIM could reproduce the known intestinal effects of vitamin D, with dose-dependent induction of all three genes. Maximal vitamin D-induced gene expression values were observed at the highest concentration evaluated of 100 nM: 12,400% for CYP24A, 602% for TRPV6, and 315% for CYP3A4. Rifampin also showed dose-dependent induction of CYP3A4 with maximal induction of 392% observed at 10 mM and a slightly reduced induction of 341% at 20 mM. Rifampin was found not to be an inducer of CYP24A nor TRPV6 at the concentrations evaluated. Similar results were obtained in multiple repeat experiments. Results with vitamin D3 and rifampin suggest that CHIM represent a convenient and physiologically relevant experimental system for the evaluation of CYP3A4 induction for the evaluation of drug-drug interaction via CYP3A4 induction. The extensive response of CHIM to vitamin D3-specific pathways suggest that this experimental system may also be used to further our understanding of vitamin D pathways, for the evaluation of the relative potencies of vitamin D analogs, and to be used as a pharmacological and toxicological system for the discovery of new therapies for intestinal diseases.

P76 - CHARACTERIZATION OF CYP2C INDUCTION IN CRYOPRESERVED HUMAN HEPATOCYTES AND ITS APPLICATION IN THE PREDICTION OF THE CLINICAL CONSEQUENCES OF THE INDUCTION**Mika Nagai¹**, Takuomi Hosaka², Masahiro Satsukawa¹, and Kouichi Yoshinari²¹Kaken Pharmaceutical Co., LTD., ²School of Pharmaceutical Sciences, University of Shizuoka

The induction of cytochrome P450s (P450s) is one of the important mechanisms causing drug-drug interactions (DDIs), which can affect the pharmacokinetic, pharmacologic and toxicological effects of concomitantly administered drugs. *In vitro* induction assays using human hepatocytes are one of the standard methods to evaluate the DDI risk via induction. The regulatory agencies in the United States, European Union and Japan have recently recommend that the inducing potential for CYP1A2, CYP2B6, and CYP3A4/5 should be evaluated at first, followed by CYP2C induction if necessary, in cases in which the test compound induces CYP3A4/5. Meanwhile, several clinical DDIs of warfarin caused by CYP2C9 induction are reported with aprepitant, carbamazepine, and rifampin. In the present study, we have investigated the relationships between CYP2C induction and those of CYP3A4 and/or CYP2B6 with several types of P450 inducers to assess the contribution of pregnane X receptor (PXR) and constitutive androstane receptor (CAR) to the CYP2C inductions. Furthermore, an *in vitro-in vivo* extrapolation method, which could enable us to estimate the clinical consequences caused by the induction, has been established as to CYP2C9 induction. Cryopreserved human hepatocytes were treated with various compounds at multiple concentrations and P450 mRNA levels were determined. Since the fold-induction values of CYP2C8 and CYP2C9 showed good correlation with those of CYP3A4 and CYP2B6, the fold-induction values of CYP2C8 and CYP2C9 were well expressed as the functions of those of CYP3A4 and CYP2B6 using the multiple regression models established but the contribution ratios of CYP3A4 and CYP2B6 inductions were different between CYP2C8 and CYP2C9. The applicability of the regression models for CYP2C8 and CYP2C9 induction were verified using the published data. Although variability in the magnitude of P450 inductions was observed among the different lots of hepatocytes used, most of the fold-induction values of CYP2C8 and CYP2C9 were well predicted using the multiple regression models. Since CYP3A4 and CYP2B6 inductions are mediated mainly by PXR and CAR, our present results suggest that CYP2C8 and CYP2C9 induction are regulated by not only PXR but also CAR with different

contributions. Finally, to predict the clinical consequences caused by CYP2C9 induction, simple correlation analyses were performed and positive correlations were observed with the apparent E_{max} values in hepatocytes and $I_{max,u}$ or $I_{in,max,u}$ values obtained from the literature. Thus, the clinical risk of CYP2C9 induction might be estimated using *in vitro* fold-induction values and unbound plasma or hepatic-inlet concentration of inducers. Taken together, the present results will advance our understanding of CYP2C induction in human hepatocytes and its clinical relevance.

P77 - REVISITING EVALUATION OF CYP2C9 AND CYP2C19 INDUCTION *IN VITRO*: POTENTIAL FOR ROBUST INDUCTION RESPONSES WITH \geq 4-DAY HEPATOCYTE EXPOSURE TIMES

David Stresser, Paul Lesniak, Kelly Desino, and Jun Sun
AbbVie

Regulatory agencies (e.g. FDA, EMA) recommend evaluation of CYP1A2, 2B6 and 3A4 induction *in vitro*. These enzymes are sensitive markers of compound interaction with PXR/CAR (CYP3A4, CYP2B6) and AhR (CYP1A2). FDA guidance also states that the sponsor should evaluate CYP2C8, 2C9 and 2C19 if a compound exhibits CYP3A4 induction *in vitro* or *in vivo*, since these enzymes share a regulatory mechanism similar to CYP3A4. However, the dynamic range for CYP2C enzyme induction in plated human hepatocytes assay has long been considered inadequate, often necessitating evaluation of CYP2C enzyme induction *in vivo*. In the current investigation, we describe significant increases in CYP2C induction assay dynamic ranges when rifampicin, phenytoin and phenobarbital treatment periods were extended beyond the typical 2-3 day period. The rifampin treatment period of 4 or 6 days increased the assay window for all three inducible CYP2C enzyme mRNA and catalytic activity to \geq 6-fold above vehicle control, a value suggested as a minimum to ascertain that a $<$ 2-fold induction response from a test compound would be considered as a negative finding. These data suggest that treatment of hepatocytes two or more times longer than the historical convention may provide opportunity for robust evaluation of CYP2C enzyme induction *in vitro*. Induction occurs when an increase in the ratio of the CYP synthesis rate to the degradation rate. With extended treatment times, the primary mechanism of increased fold induction of CYP2C enzymes appears to be attributable primarily to a decrease in loss in CYP2C mRNA in test compound treated cells compared to vehicle control treated cells.

All authors are employees of AbbVie. The design, study conduct, and financial support for this research was provided by AbbVie. AbbVie participated in the interpretation of data, review, and approval of the publication.

P78 - RECOMMENDATIONS FOR *IN VITRO* CYP3A4 MRNA DATA ANALYSIS FOR DRUG-DRUG INTERACTION RISK ASSESSMENT FROM THE IQ INDUCTION WORKING GROUP

Donald Tweedie¹, Jane R Kenny², Diane Ramsden³, David Buckley⁴, Shannon Dallas⁵, Conrad Fung⁶, Michael Mohutsky⁷, Heidi J Einolf⁸, Liangfu Chen⁹, Josh Dekeyser¹⁰, Maria Fitzgerald¹¹, Theunis Goosen¹², and Y. Amy Siu¹³, Robert Walsky¹⁴, George Zhang¹⁵, Nireesh Hariparsad⁶
¹Merck, ²Genentech, ³Alnylam, ⁴Roivant, ⁵Janssen R&D, ⁶Vertex, ⁷Eli Lilly and Company, ⁸Novartis, ⁹GSK, ¹⁰Amgen, ¹¹Genzyme, ¹²Pfizer Inc., ¹³Eisai, ¹⁴emdserono, ¹⁵Corning

The Induction Working Group (IWG) of the International Consortium of Innovation and Quality in Pharmaceutical Development (IQ) recently published a white paper¹ addressing several recommendations from regulatory agencies on induction aspects of DDI guidances. The IWG has also conducted a data-driven evaluation of *in vitro* and clinical induction data with a focus on data interpretation. While there are some differences in the recommendations between regulatory agencies (EMA, FDA, PMDA), all agree that *in vitro* induction studies should measure changes in mRNA, include at minimum three human hepatocyte donors, and investigate concentrations spanning what is clinically relevant. There is also agreement that a positive *in vitro* signal is an increase in mRNA of 2-fold, with stipulation of concentration dependence from EMA and PMDA. An *in vitro* change in mRNA of $<$ 100% ($<$ 2-fold) is considered negative only if it is also $<$ 20% of the positive control response (EMA and PMDA). Due to the abundance of CYP3A4 mRNA data, this was the focus of the IWG in considering response thresholds, variability, application of controls and translation to clinical risk assessment. Aspects of *in vitro* induction of CYP1A2 and CYP2B6 will be addressed in a future publication. The goal of the CYP3A4 mRNA evaluation was to assess the appropriateness of a 2-fold threshold for positive induction, the necessity of a negative control, the value of normalizing the data to a percent of positive response and the application of the various simplistic models that regulatory agencies recommend for conducting clinical induction risk assessment. Through these endeavors the IWG amassed a very large dataset of *in vitro* and clinical induction data. Induction parameters (EC50, Emax and F2) were compiled for prototypical CYP3A4 inducers from multiple human hepatocyte donors, which allowed for a thorough investigation into intra-donor and inter-lab variability. Additionally, both *in vitro* induction data and clinical study data were collected for 51 compounds, of which 16 were proprietary (IQ companies). While both *in vitro* and clinical data exhibited a large extent of variability, *in vitro* data provided a reasonable assessment of clinical induction potential, allowing DDI risk evaluation. Applying this comprehensive analysis of a large dataset, the IWG is providing several recommendations, specifically on the minimal number of donors, threshold for an acceptable positive response, whether a negative control is necessary and the value of representing data expressed as a percentage of a positive control.

Reference:

1. Hariparsad, N. et al. (2016) Considerations from the IQ Induction Working Group in Response to Drug-Drug Interaction Guidances from Regulatory Agencies: Focus on Down-regulation, CYP2C Induction and CYP2B6 Positive Control. *Drug Metabolism and Disposition* 45, 1049-1059

P79 - EXPRESSION AND INDUCTION ABILITY OF CYTOCHROME P450 IN HUMAN HEPATOCYTES ISOLATED FROM CHIMERIC MICE WITH HUMANIZED LIVERS

Shotaro Uehara¹, Yuichiro Higuchi¹, Nao Yoneda¹, Hiroshi Yamazaki², ¹Hiroshi Suemizu

¹Central Institute for Experimental Animals, ²Showa Pharmaceutical University

The evaluation of cytochrome P450 (P450) induction using human hepatocytes is important for predicting drug-drug interactions. However, it is difficult to perform reproducible studies using the same origin because of the limited number of hepatocytes available from a single donor. We isolated hepatocytes from chimeric mice with a humanized liver (reconstituted with human hepatocytes). This study aimed to assess the expression and induction ability of P450 in these human hepatocytes isolated from chimeric mice. The purity and viability of the prepared hepatocytes (Hu-liver cells) were analyzed using flow cytometry. Up to 97% of the Hu-liver cells stained positive for human leukocyte antigen (HLA), and the mean viability exceeded 85% (n = 10). Monolayer cultured Hu-liver cells displayed a cobblestone cell morphology and were bi-nucleated. These characteristics are usually observed in cultures of cryopreserved human hepatocytes. The mRNA expression levels of 16 P450 forms belonging to P450 subfamilies 1 to 4 in Hu-liver cells were correlated well with the expression levels in human donor hepatocytes. The variations in individual P450 mRNA levels between Hu-liver cells and donor human hepatocytes were within 5- fold for 13 P450 forms. Similar to findings in donor human hepatocytes, CYP1A2 and CYP3A4 mRNA in Hu-liver cells were induced (>2.0- fold) by omeprazole/ β -naphthoflavone and rifampicin/phenobarbital, while CYP2B6, CYP2C8, CYP2C9, and CYP2C19 mRNA were induced (>2.0- fold) by those inducers in only few Hu-liver cell lots. Furthermore, we investigated the induction ability of enzymatic activity in Hu-liver cells using testosterone as a CYP3A probe. The production of 6 β -hydroxytestosterone was significantly increased by treatment with the CYP3A inducer rifampicin in Hu-liver cells. These results indicated that Hu-liver cells have characteristics similar to those of human hepatocytes in terms of mRNA expression levels and the induction abilities of P450 forms. Thus, Hu-liver cells can potentially be used for *in vitro* induction assays of human hepatic P450.

P80 - EVALUATION OF A PRE-CONSTRUCTED RELATIVE INDUCTION SCORE (RIS) CURVE FOR PREDICTION OF CYP3A4 INDUCTION RESPONSE *IN VIVO*

George Zhang¹, Thuy Ho¹, Robert. J Clark¹, Sarah Trisdale¹, Kanika Choughule¹, Lisa Fox¹, and Diane Ramsden²

¹Corning Life Sciences, ²Alnylam Pharmaceuticals Inc.

Both the FDA (2017) and EMA (2013) advocate the use of correlation methods such as relative induction score (RIS) to assess the clinical induction potential of an investigational drug towards drug metabolizing enzymes in humans. In this approach, *in vitro* induction parameters are generated for a set of clinical inducers and non-inducers, a RIS score is calculated and plotted against observed clinical AUC decreases to develop a correlation curve. The clinical CYP3A4 induction potential for investigational drugs is then predicted by inputting the RIS score calculated from the same lot of hepatocytes into the pre-constructed RIS correlation curve. The induction parameters used in the RIS calibration approach are typically generated using mRNA as an input parameter. Based on the experience in this lab, there is often a large degree of inter-day variability observed in mRNA levels within a hepatocyte lot. We therefore sought to explore the impact of this variability on clinical drug-drug interaction (DDI) prediction using the correlation method by characterizing the inter-day variability of induction parameters EC₅₀, E_{max}, and RIS for rifampicin (RIF) and pleconaril (PLE), strong and weak clinical CYP3A4 inducers, respectively. The prediction performance for additional CYP3A4 clinical inducers, with a focus on mild and moderate inducers, was examined using mRNA and enzyme activity data in a pre-qualified lot of hepatocytes. Hepatocytes were treated with 8 concentrations of avasimibe (AVA), felbamate (FEL), flucloxacillin (FLU), lersivirine (LER), nafcillin (NAF), oxcarbazepine (OXC), rufinamide (RUF), RIF and PLE for two days. After treatment, CYP3A4 induction was measured by mRNA and enzyme activity. The inter-day variability of induction parameters obtained from CYP3A4 mRNA was analyzed from 8 data sets. The variability for EC₅₀, E_{max} and RIS was similar across the data sets with %CV ranging from 27 to 54% for both RIF and PLE. Consistent with our previous report, the EC₅₀ values generated from CYP3A4 mRNA and activity were overall comparable (within 2-fold) except for OXC. The AUC decrease of victim drugs by FLU, LER, NAF, OXC, RIF and PLE, was reasonably predicted from both RIS curves (mRNA or activity). Importantly no false-negatives were observed despite either under- or over-prediction of % AUC decrease for AVA, FEL and RUF. These data demonstrate that pre-constructed RIS curves from both mRNA and enzyme activity data can be used in predicting clinical inducers of CYP3A4, despite high inter-day variability of mRNA induction parameters. Integrating results of mRNA and enzyme activity may provide more confidence in data interpretation as compared to analysis using either endpoint alone.

P81 - INHIBITION OF LITHOCHOLIC ACID 3-OXIDATION BY SELECTIVE ESTROGEN RECEPTOR MODULATORS

Sumit Bansal, Josephine Si Min Teo, and Aik Jiang Lau
National University of Singapore

Lithocholic acid (LCA) is the most toxic bile acid amongst bile acids, and it has been shown to induce cholestasis, hepatotoxicity, and carcinogenesis. Previously, LCA was reported to be metabolized to a major oxidative metabolite, 3-ketocholanoic acid (3-KCA), by human cytochrome P450 3A4 (CYP3A4). Tamoxifen and raloxifene, which are selective estrogen receptor modulators (SERMs), act as reversible inhibitors or mechanism-based inactivators of CYP3A4-catalyzed testosterone 6 β -hydroxylation. Therefore, we compared the effect of various structural classes of SERMs, namely triphenylethylene derivatives (clomifene, tamoxifen, toremifene, ospemifene, droloxifene), benzothiophene derivatives (raloxifene, arzoxifene), naphthalene derivatives (lasofoxifene, nafoxidine), indole derivative (bazedoxifene), and benzopyran derivative (acolibifene), on LCA 3-oxidation, which was quantified by ultra-high performance liquid chromatography-tandem mass spectrometry. LCA 3-oxidation catalyzed by human liver microsomes, CYP3A4, and CYP3A5 followed Michaelis-Menten kinetics. The apparent K_m values were 21.6 ± 2.7 , 28.3 ± 2.3 , and 32.5 ± 2.6 μM , whereas the V_{max} values were 367.5 ± 40.7 pmol/min/mg protein, 8.9 ± 0.5 pmol/min/pmol P450, and 11.5 ± 0.7 pmol/min/pmol P450 for LCA 3-oxidation catalyzed by human liver microsomes, CYP3A4, and CYP3A5, respectively. Interestingly, human liver cytosol also catalyzed the oxidation of LCA to 3-KCA, and this occurred without the addition of exogenous NADPH to the enzymatic incubation. The apparent K_m and V_{max} values were 0.5 ± 0.1 μM and 71.4 ± 2.6 pmol/min/mg protein, respectively, and the reaction followed Michaelis-Menten kinetics. The catalytic efficiency (V_{max}/K_m) was 9 times greater for LCA 3-oxidation catalyzed by human liver cytosol than human liver microsomes. Among the 11 SERMs investigated, only bazedoxifene and ospemifene, at 10 μM , inhibited human liver microsomal LCA 3-oxidation, whereas each of the SERMs inhibited testosterone 6 β -hydroxylation (a CYP3A-catalyzed reaction; positive control), with the most effective inhibitors, raloxifene, arzoxifene, and bazedoxifene, inhibiting testosterone 6 β -hydroxylation by almost 90%. In contrast to the findings in human liver microsomes, each of the SERMs investigated in the present study inhibited LCA 3-oxidation catalyzed by recombinant CYP3A4, whereas toremifene, ospemifene, raloxifene, arzoxifene, and bazedoxifene inhibited LCA 3-oxidation catalyzed by recombinant CYP3A5. Preincubation of a SERM with human liver microsomes for 30 or 60 min did not influence LCA 3-oxidation, but clomifene, toremifene, ospemifene, raloxifene, arzoxifene, bazedoxifene, and acolbifene enhanced the decrease in testosterone 6 β -hydroxylation. Only droloxifene and acolbifene inhibited human liver cytosol-catalyzed LCA 3-oxidation. In conclusion, substrate-dependent differences exist for the inhibition and inactivation of CYP3A by SERMs. Raloxifene (benzothiophene derivative), arzoxifene (benzothiophene derivative), and bazedoxifene (indole derivative) were most effective in inhibiting CYP3A4- and CYP3A5-catalyzed LCA 3-oxidation, but only bazedoxifene inhibited LCA 3-oxidation catalyzed by human liver microsomes and droloxifene and acolbifene weakly inhibited human liver cytosolic LCA 3-oxidation. Overall, our findings suggest potential impact of SERMs on LCA detoxification.

P82 - DEVELOPMENT OF UGT1A7 AND UGT1A8 INHIBITION ASSAYS USING RECOMBINANT ENZYMES AS A TEST SYSTEM

Ritu Singh, Lisa Jacob, Timothy Creegan, and George Zhang
Corning Gentest Contract Research Services

It is well established that the liver has the greatest abundance of UDP-glucuronosyltransferase (UGT) enzymes, while the kidney and gastro-intestinal tract are considered important extra-hepatic sites for drug metabolism. Although hepatic UGT enzymes play a key role in the metabolism of drugs, the significance of intestinal UGTs in pharmacokinetics and drug-drug interactions has recently gained prominence¹. UGT1A7, UGT1A8 and UGT1A10 enzymes are expressed mainly in the small intestine and colon and are absent in the liver. Orally administered drugs that are extensively metabolized by intestinal UGT enzymes exhibit poor bioavailability. Drugs that inhibit these isoforms may greatly alter the bioavailability of orally co-administered drugs that are substrates of intestinal UGTs. Guidelines provided by the European Medicines Agency (EMA) on the investigation of drug interactions recommend studying inhibition of UGTs if direct glucuronidation is one of the major elimination pathways of an investigational drug². Methods to determine inhibition of hepatic UGT enzymes are well established; however there is a need to develop methods to assess inhibition potential of intestinal enzymes. The purpose of this study was to develop an assay to assess inhibition of UGT1A7 and UGT1A8 isoforms using recombinant enzymes. Propofol served as the probe substrate for both enzymes. Linear metabolic conditions and kinetic parameters were determined in recombinant UGT1A7 and UGT1A8 enzymes. Sigmoidal enzyme kinetics was observed for propofol glucuronidation by recombinant UGT1A7 and UGT1A8 enzymes, with S_{50} values of 42 μM and 81 μM , respectively. Inhibition of propofol glucuronidation was achieved using magnolol (UGT1A7) and troglitazone (UGT1A8) with IC_{50} values of 0.93 and 0.82 μM , respectively. This newly developed *in vitro* method for UGT1A7 and UGT1A8 enzymes can be utilized to assess the inhibition potential of new chemical entities.

References:

1. Oda S, Fujiwara R, Kutsuno Y, Fukami T, Itoh T, Yokoi T, and Nakajima M (2015) Targeted screen for human UDP-glucuronyltransferases inhibitors and the evaluation of potential drug-drug interactions with Zafirlukast. *Drug Metab Dispos* 43:812-818.
2. European Medicines Agency, 'Guideline on the Investigation of Drug Interactions'. January, 2013.

P83 - INHIBITION OF UGT ENZYMES USING RECOMBINANT UGT ENZYMES FOR DDI ASSESSMENT**Guy Webber**

ENVIGO

Drug-drug interactions (DDI) mediated by glucuronide metabolites produced via uridine di-phospho - glucuronosyltransferase (UGT) enzymes are of increasing focus. To complement our current DDI assessment program we have undertaken a validation of UGT-inhibition assays for the six major UGT isoforms using in the first instance recombinant rUGT enzymes and a universal UGT inhibitor, nicardipine (subsequent work will include human liver microsomes). The assays included using low levels of protein (0.01 – 0.25 mg/mL/5-125 pmol UGT equivalents) and including a membrane activation phase using alamethacin (15 mg/mL). Results obtained: rUGT1A1-mediated glucuronidation of estradiol vs nicardipine as inhibitor IC₅₀ = 1.7 μM, rUGT1A3-mediated glucuronidation of chenodeoxycholic acid vs nicardipine as inhibitor IC₅₀ = 27 μM, rUGT1A4-mediated glucuronidation of trifluoroperazine vs nicardipine as inhibitor IC₅₀ = 32 μM, rUGT1A6-mediated glucuronidation of propofol vs nicardipine as inhibitor IC₅₀ = 87 μM, rUGT1A9-mediated glucuronidation of propofol vs nicardipine as inhibitor IC₅₀ = 13 μM and rUGT2B7-mediated glucuronidation of naloxone vs nicardipine as inhibitor IC₅₀ = 52 μM.

P84 - CHARACTERIZATION OF ANTIHYPERTENSIVE DRUGS AS POTENT INHIBITORS OF CYP2J2**Satoshi Yamaori**¹, Noriaki Ikemura¹, Chinatsu Kobayashi², Shinobu Kamijo², and Shigeru Ohmori¹¹Shinshu University Hospital, ²Shinshu University

Cytochrome P450 2J2 (CYP2J2) is shown to be highly expressed in various cancer cells and tumors. CYP2J2 converts arachidonic acid to epoxyeicosatrienoic acids (EETs), which play pivotal roles in tumor growth and metastasis. It has been previously reported that overexpression of CYP2J2 in carcinoma cell lines and murine xenograft tumor model accelerates cell proliferation. Conversely, a reduced production of EETs via suppression of CYP2J2 expression and chemical inhibition of CYP2J2 activity in cancer cells has been shown to lead to antitumorogenesis. Furthermore, it has been recently reported that CYP2J2 metabolizes several tyrosine kinase inhibitors (TKIs). These findings suggest that the chemical inhibition of intratumoral CYP2J2 activity may be a novel strategy for the treatment of cancer. The TKIs targeting vascular endothelial growth factor receptor commonly cause hypertension, one of the major side effects. In this case, the administration of antihypertensive drugs is recommended. If there are potent inhibitors of CYP2J2 among the concomitantly administered antihypertensive drugs, it is possible that these drugs may contribute not only to a reduction in the side effect but also to potentiation of antitumor effect of TKIs and suppression of EET-induced tumor cell proliferation. However, the study on CYP2J2 inhibition by antihypertensive drugs has not been investigated in detail. In this study, inhibitory effects of antihypertensive drugs (dihydropyridine calcium channel blockers, angiotensin II receptor blockers, and angiotensin-converting enzyme inhibitors) on CYP2J2 activity were examined with recombinant CYP2J2. The luciferin-2J2/4F12 O-dealkylase activity was measured by using a luminometer. Amlodipine, azelnidipine, barnidipine, benidipine, cilnidipine, efonidipine, felodipine, manidipine, nicardipine, nifedipine, nilvadipine, nisoldipine, nitrendipine, telmisartan, delapril, and quinapril inhibited CYP2J2 activity in a concentration-dependent manner (IC₅₀ = 0.103 – 9.14 μM). In particular, azelnidipine and manidipine potently inhibited the activity with the IC₅₀ values of 0.110 and 0.103 μM, respectively. The effect of preincubation on CYP2J2 inhibition was next examined to determine whether these antihypertensive drugs inhibit CYP2J2 activity in a metabolism-dependent manner. A 20-min preincubation of azelnidipine and felodipine in the presence of NADPH potentiated CYP2J2 inhibition. In addition, azelnidipine inactivated CYP2J2 activity with a k_{inact}/K_i value of 351 l/mmol/min. These results indicated that azelnidipine and manidipine are characterized to be a potent mechanism-based inhibitor and potent direct inhibitor of CYP2J2, respectively.

P85 - CRYOPRESERVED HUMAN INTESTINAL MUCOSA AS A 3-DIMENSIONAL ORGANOID CULTURE FOR THE EVALUATION OF INTESTINAL DRUG METABOLISM, DRUG-DRUG INTERACTIONS, ENTEROTOXICITY, AND ENTEROPHARMACOLOGY**Albert P. Li**, David Ho, Carol Loretz, Qian Yang, Walter Mitchell, Kirsten Amaral, and Novera Alam
In Vitro ADMET Laboratories Inc.

The human small intestine is known to contribute significantly to the first pass metabolism of orally administered drugs, especially drugs that are substrates of CYP3A, the major intestinal P450 isoform. Furthermore, enteric drug-drug interactions such as grapefruit juice inhibition of enteric drug metabolism is known to have clinically significant effects

independent of hepatic drug metabolism. We recently reported on successful isolation and cryopreservation of purified human enterocytes from the small intestine (Ho et al., Drug Metabolism and Disposition, 45(6), 686-691.). We report here a 3-d organoid system, namely, cryopreserved human intestinal mucosa (CHIM) for the evaluation of enteric drug metabolism drug-drug interaction, drug toxicity, and pharmacology. Intestinal mucosa were isolated from human small intestines supplied to us by the International Institute for the Advancement of Medicine (Edison, NJ). The isolated mucosa were washed and gently homogenized to viable multiple cellular fragments retaining the original cell-cell interactions as demonstrated by phase contrast microscopy. The isolated mucosa were cryopreserved in a programmable liquid nitrogen cell freezer and stored in liquid nitrogen. After thawing and recovery, CHIM were found to retain cell viability as demonstrated by robust drug metabolizing enzyme activities, cellular ATP contents, and responsiveness to vitamin D3 induction of gene expression. Drug metabolizing activities (substrates) observed include CYP1A1 (7-ethoxyresorufin), CYP1A2 (phenacetin), CYP2B6 (bupropion), CYP2C8 (paclitaxel), CYP2C9 (diclofenac), CYP2C19 (s-mephenytoin), CYP2D6 (dextromethorphan), CYP2E1 (chlorzoxazone), CYP3A4 (midazolam; testosterone); UGT and ST (hydroxycoumarin), FMO (benzylamine), MAO (kynuramine), NAT1 (4-aminobenzoic acid), NAT-2 (sulfamethazine), CYP2J2 (astemizole), and CES2 (irinotecan). The presence of these drug metabolizing enzyme pathways suggests that CHIM can be used for the assessment of bioavailability and metabolic fate of intestinal metabolism of orally administered drugs. Using CHIM, dose-dependent decreases in cell viability quantified by cellular ATP contents was observed for naproxen and acetaminophen, with a higher enterotoxicity observed for naproxen as observed in humans *in vivo*. The results therefore suggest that CHIM may be a useful tool for the screening of enterotoxicity of drug candidates intended to be administered orally. Another exciting finding is the dose-dependent and potent induction of CYP24A by vitamin D3 after a 24-hr treatment, suggesting that CHIM can be used for the evaluation of enteric P450 induction and vitamin D pharmacology. Our results suggest that CHIM represent an useful *in vitro* experimental system for the evaluation of enteric metabolism, drug-drug interactions, enterotoxicity, and enteropharmacology.

P86 - INFLUENCE OF DICHLOROACETATE TREATMENT ON THE CONTRIBUTIONS OF RODENT BRAIN, HEART, LIVER AND KIDNEY IN THE ACTIVITY OF GSTZ1

Edwin Squirewell, Marci Smeltz, Laura Faux, Peter Stacpoole, and Margaret James
University of Florida

Dichloroacetate (DCA) is an investigational drug utilized in the treatment of cancer, arterial pulmonary hypertension, and genetic mitochondrial diseases. DCA is converted to glyoxylate in reactions catalyzed by glutathione transferase zeta 1 (GSTZ1), a critical enzyme in tyrosine catabolism responsible for the *trans*-isomerization of maleylacetoacetate (MAA) and maleylacetone (MA). DCA is a mechanism-based inactivator of GSTZ1 and consequently inhibits its metabolism under chronic administration. Moreover, the tissue accumulation of DCA, MAA, and MA due to inactivation of GSTZ1 may be a mechanism responsible for the development of peripheral neuropathy in patients treated with DCA. Although liver is the main site of GSTZ1 expression and activity, extrahepatic tissues also express GSTZ1, and after a single dose of DCA to female rats, GSTZ1 expression and activity were reduced in liver to a greater extent than in kidney, brain and heart. The role of extrahepatic tissues in metabolism of DCA, MAA and MA following repeated doses of DCA that mimic therapy has not been studied. This study was designed to test the hypothesis that extrahepatic tissues contribute to the GSTZ1-catalyzed metabolism of DCA after multiple doses of DCA. Adult female Sprague Dawley rats, 8 per group, were treated with sodium DCA (100 mg/kg) or sodium acetate, 100 mg/kg, by oral gavage daily for 8 consecutive days. On the 9th day the tissues were removed and used to prepare cytosolic and mitochondrial subcellular fractions. The activity of GSTZ1 for DCA was examined under conditions of linear product formation; GSTZ1 expression was assessed via Western blot using a polyclonal antibody to rat GSTZ1. In comparison to the acetate-treated control animals, the recovery of total cytosolic GSTZ1 activity in the liver, kidney, heart, and brain of DCA-treated animals was 1.1%, 0.6%, 0.7%, and 1.4%, respectively. In controls, liver cytosol demonstrated the highest specific activity with DCA of 2.89 ± 0.54 nmol glyoxylate formed/min/mg protein (mean \pm S.D., n=8), followed by kidney, 0.34 ± 0.10 . Activity in heart and brain cytosol was much lower, 0.074 ± 0.027 and 0.032 ± 0.015 respectively. Considering the higher protein yield and larger size of liver compared with the extrahepatic tissues, this study demonstrated that most DCA metabolism is expected to occur in the liver, even after repeated treatment with DCA.

Supported in part by the US Public Health Service GM 099871

P87 - TISSUE-SPECIFIC MECHANISMS OF IRINOTECAN METABOLISM

Marc Vrana and Bhagwat Prasad
University of Washington

Background: Irinotecan is a widely used chemotherapeutic prodrug for treatment of colorectal or non-small cell lung cancers. It is hydrolyzed to the active metabolite, SN-38, via carboxylesterase 1 or 2 (CES1 or CES2). Current physiologically-based pharmacokinetic (PBPK) models include liver and intestine as locations of irinotecan metabolism. However, CES1 and CES2 are differentially expressed in many body tissues not represented in these models. Further, arylacetamide deacetylase (AADAC), has been shown to have overlapping substrate specificity with CES1 and CES2

introducing the potential that it may contribute to SN-38 formation. Therefore, our hypothesis is that extensive expression of CESs and AADAC in multiple body tissues poses local tissue toxicity risk. To address this, the aims of this research were:

< >To quantify CES1, CES2, and AADAC expression in isolated liver tissue subcellular fractions, as well as pooled S9 fractions from liver, kidney, intestine, and lung by LC-MS/MS. To determine organ-specific formation of SN-38 to evaluate potential for localized toxicity. To elucidate if AADAC contributes to SN-38 formation. Methodology: In-house isolated hepatic subcellular fractions and pooled S9 fractions from liver, kidney, intestine and lung (XenoTech, LLC, Kansas City) were quantified for CES1, CES2, and AADAC using validated surrogate peptide methods in order to evaluate the contribution of each enzyme to the formation of SN-38. Because CES2 is established to efficiently metabolize irinotecan, intestinal fractions prepared with phenylmethylsulfonyl fluoride (PNSF), a strong CES inhibitor, were used to determine the role of AADAC in SN-38 formation.

Results: CES1, CES2, AADAC expression (relative to liver) in intestine, kidney and lungs were 0.03, 0.02, 0.02 vs. 6.54, 2.03, 0.0 vs. 1.98, 0.75, 0.55, respectively. In liver subcellular fractions, at physiologic levels (20 μ M), SN-38 formation was correlated well with CES1 ($r^2 = 0.89$) and CES2 ($r^2 = 0.90$) expression levels. However, CES1 and CES2 expression levels were also highly correlated with each other in liver. In extra-hepatic tissues, kidney produced the highest amount of metabolite per mg of protein, while the PNSF-treated intestinal tissue generated the lowest (Fig. 1). Lung tissue generated significant amounts of SN-38 which, when combined with low CES expression, could indicate the role of another esterase. AADAC was found to not correlate with SN-38 formation irrespective of subcellular fraction or organ.

Conclusions: While CES1 is significantly more highly expressed in the liver when compared to CES2, expression levels of these two enzymes strongly correlate. While SN-38 formation correlates with CES expression, determining specific contribution of each to the *in vivo* pharmacokinetics of SN-38 requires further study. In kidney, CES1 was not expressed and CES2 was the primary enzyme for SN-38 formation. Lung tissue had low CES1 and CES2 expression, but similar SN-38 formation to kidney indicates the potential role of another esterase. Intestine had substantial SN-38 formation despite PNSF presence, perhaps caused by residual CES2 activity or another esterase. Together, these experiments show that i) the potential for extra-hepatic activation of irinotecan which could pose localized toxicity risk and ii) AADAC does not have significant role in SN-38 formation.

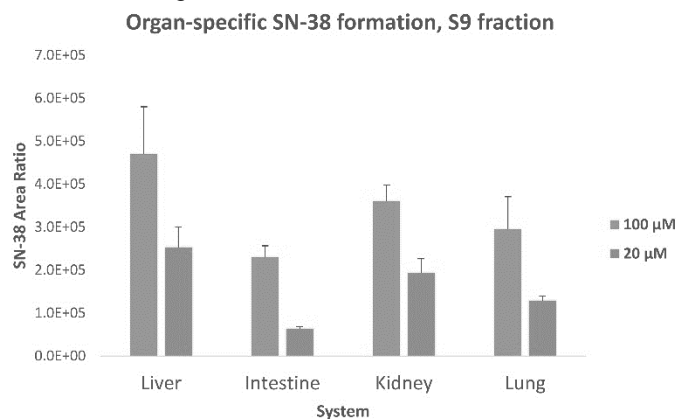


Figure 1: SN-38 formation

P88 - PEGYLATED CRUSHED GOLD SHELL-RADIOLABELED CORE NANOBALLS FOR IN VIVO TUMOR IMAGING WITH DUAL POSITRON EMISSION TOMOGRAPHY AND CERENKOV LUMINESCENT IMAGING

Yong Hyun Jeon¹, Seon Hee Choi^{1,2}, and Sang Kyoon Kim^{1,2}

¹Daegu-Gyeongbuk Medical Innovation Foundation, ²Laboratory Animal Center

Hypothesis: Radioactive isotope-labeled gold nanomaterials have potential biomedical applications. Here, we report the synthesis and characterization of PEGylated crushed gold shell-radioactive iodide-124-labeled gold core nanoballs (PEG-124I-Au@AuCBs) for *in vivo* tumor imaging applications through combined positron emission tomography and Cerenkov luminescent imaging (PET/CLI).

Methods: PEGylated crushed gold shell-radioactive iodide-124-labeled gold core nanoballs (PEG-124I-Au@AuCBs) was synthesized using a tannic acid coated AuNPs. The radiostability of PEG-124I-Au@AuCBs was confirmed in various pH solutions and serum. The toxicity of prepared particles was determined in CHO and DC2.4 cells. For *in vivo* imaging of tumor, 4T1 tumor bearing mice received the particles, followed by PET/CLI imaging and biodistribution analysis at designated times.

Results: PEG-124I-Au@AuCBs showed high stability and sensitivity in various pH solutions, serum, and *in vivo* conditions and were not toxic to immune cells and normal cells. Combined PET/CLI clearly revealed tumor lesions at 1 h after injection of particles, and both signals remained visible in tumor lesions at 24 h, consistent with the biodistribution results.

Conclusion: Taken together, these data provided strong evidence for application of PEG-124I-Au@AuCBs as promising imaging agents in nuclear medicine imaging of various biological systems, particularly in cancer diagnosis.

P89 - UNDERSTANDING THE TRANSLATIONAL CAPABILITY OF *IN VITRO* ACTIVE HEPATIC OATP UPTAKE DATA USING PBPK MODELING

Christine Bowman¹, Eugene Chen², Liuxi Chen², Jia Ren², Shu Zhang², Buyun Chen², Xiaorong Liang², Matthew Wright², Yuan Chen², and Jialin Mao²

¹University of California, San Francisco, ²Genentech

The use of physiologically based pharmacokinetic (PBPK) modeling has provided advantages in predicting human PK for drugs that are substrates of uptake transporters¹. However, when generating transporter data for *in vitro* to *in vivo* extrapolation (IVIVE) in PBPK modeling, there are still questions in the field related to the most relevant *in vitro* system to use, the type of data to generate (CL_{int} vs. J_{max}/K_m), and the difference in transporter expression levels between various *in vitro* systems and the physiological situation. The objective of this study was to evaluate the uptake of four known OATP substrates (pravastatin, rosuvastatin, pitavastatin, repaglinide) using Corning TransportoCells™ (human OATP1B1*1a, OATP1B3, and control cells) and understand the translational capability of the data using PBPK modeling. Given the possibility of albumin-facilitated uptake, the uptake of the four OATP substrates in the HEK293 cells in both buffer and human plasma incubations was tested. The morphology and viability of the cells in plasma were examined and while visually the cells appeared to clump in the plasma incubations, the viability in both incubations was high and comparable (>80%). The concentration-dependent uptake of the four substrates in buffer incubations aligned well with previous studies in the literature. In plasma incubations, the compounds with lower protein binding, pravastatin (f_{up}=0.49) and rosuvastatin (f_{up}=0.11), had comparable K_{m,u} and CL_{int,u} values to that obtained from the buffer incubations, whereas the compounds with higher protein binding, repaglinide (f_{up}=0.023) and pitavastatin (f_{up}=0.0045), had higher affinity (decreased K_{m,u}) as well as higher CL_{int,u} in the plasma. The amount of active uptake vs. passive diffusion occurring in the two incubations was also examined, and the percentage of active uptake (compared to total uptake) increased in the plasma incubations for the highly bound compounds. To scale up the *in vitro* data for PBPK modeling, OATP1B1 and 1B3 abundance in each cell line was quantitated by LC-MS/MS. A modified PBPK model of pravastatin was developed in Simcyp®, a population-based ADME simulator². The *in vitro* data (both from buffer and plasma) were incorporated into the model and able to predict the shape of the concentration-time curve of pravastatin given both IV and orally reasonably well. The PBPK modeling work for the remaining compounds is currently on-going, which will provide a systematic understanding of how the *in vitro* active uptake data can be quantitatively translated using the PBPK approach.

References:

1. Watanabe, T., Kushihara, H., Maeda, K., Shitara, Y., & Sugiyama, Y. Physiologically Based Pharmacokinetic Modeling to Predict Transporter-Mediated Clearance and Distribution of Pravastatin in Humans. *J Pharmacol Exp Ther* 328, 652-662 (2009).
2. Mao, J.; Doshi, U.; Wright, M.; Hop, C.; Li, A. P.; Chen, Y., Prediction of the Pharmacokinetics of Pravastatin as an OATP Substrate using Plateable Human Hepatocytes with Human Plasma Data and PBPK Modeling. *CPT Pharmacometrics Syst Pharmacol* (2018).

P90 - AN EFFICIENT HIGH THROUGHPUT 96-WELL PLATED HUMAN HEPATOCYTES ASSAY FOR DRUG UPTAKE AND UPTAKE TRANSPORTER INHIBITION

Albert P. Li, Kirsten Amaral, David Ho, and Novera Alam
In Vitro ADMET Laboratories Inc.

Identification of a new chemical entity as either an uptake transporter substrate or a transporter inhibitor is now a routine activity in drug development with implications in hepatic clearance and drug-drug interaction potential. Intact hepatocytes with complete hepatic uptake transporters and drug metabolizing enzyme pathways represent the most appropriate *in vitro* experimental system for the evaluation of hepatic uptake transporter activities. In the past, the oil-spin method is employed with which hepatocytes are incubated in suspension with the test chemicals followed by a time-consuming and lengthy assay procedures including centrifugation of the cells in a centrifuge tube containing silicon oil and recovery of the hepatocyte pellet. We report here a novel procedure for the evaluation of drug uptake using plated human hepatocytes. The procedures can be used in multi-well plates, include 96-well plate for higher throughput applications. The procedures for the evaluation of transporter-dependent uptake are as follows, with all operations performed at 37 deg. C (e.g. using a waterbath): 1. Plating of 50K human hepatocytes into each well of a 96-well plate in 50 mL of uptake medium (In Vitro ADMET Laboratories). 2. Prepare 2X dosing solutions containing uptake substrate with or without 20 mM rifampin. 3. Addition of 50 mL of the dosing solution to Row A (12 wells per row, thereby allowing 4 treatment conditions with 3 wells per condition) at time 0 followed by addition to each of Rows B – H at designated time intervals and termination of the entire plate at one single time interval by washing 3 times with a cold (4 deg. C) buffer to remove extracellular chemicals (IHRM, In Vitro ADMET Laboratories) and addition of 100 mL acetonitrile containing internal standard (e.g. terfenadine)

followed by LC/MS-MS quantification of the intended uptake transporter substrate. The staggered addition of dosing solutions and terminations at a single timepoint allows the evaluation of 4 dosing solution configurations at 8 timepoints. In general, a time 0 control plus 7 additional timepoints are used in our laboratory. Using this higher throughput assay, concentration and time-dependent of pravastatin were observed as well as concentration-dependent inhibition of pravastatin uptake by rifampin. Using cryopreserved human hepatocytes from multiple donors, the expected individual variations in pravastatin uptake was observed, reflecting individual differences in uptake transporter activities. This procedure is now routinely used with pravastatin in the presence and absence of rifampin for the qualification of plateable cryopreserved human hepatocytes with robust uptake transport activities as well as an assay for the evaluation of uptake transporter inhibitory potential of new chemical entities, using rifampin as the positive control, to aid drug optimization to allow the selection of new chemical entities with acceptable transporter inhibition liability for further development.

P91 - EX VIVO WHOLE LIVER PERFUSION MODEL FOR PREDICTION OF DRUG-DRUG INTERACTIONS AND BILIARY EXCRETION OF ROSUVASTATIN

Evita van de Steeg¹, Arianne van Koppen¹, Angelique E.A.M. Speulman¹, Arjan van der Plaats², Emma Offringa², Lianne J. Stevens¹, Irene H.G. Nooijen¹, Steven L.A. Erpelinck¹, and Wouter H.J. Vaes¹

¹TNO, ²OrganAssist

Current models to predict biliary excretion often fail due to species differences (rodent/dog) or due to differences in transporter expression in *in vitro* assays (e.g. sandwich cultured hepatocytes). An increasing number of compounds is subjective to enterohepatic circulation (EHC), resulting in difficulties in good prediction of plasma profiles after oral and iv administration. Moreover, in case a compound is subjective to EHC, it is more prone to cause drug-drug interaction (DDI) and/or drug induced liver injury. In order to study the feasibility to set-up a preclinical model to investigate hepatic clearance, biliary excretion and the effect of drug-drug interaction on these processes, we have applied whole porcine liver on a pressure-controlled perfusion machine (Liver Assist).

Prior to isolation of the liver from the anaesthetized pigs, the blood was heparinized, portal vein and hepatic artery were cannulated and directly after cutting the hepatic inferior vena cava the liver was flushed with warm Ringers buffer. Bile duct was cannulated directly after positioning of the liver on the Liver Assist device, on which it underwent normothermic perfusion at 37°C. Gas delivery consisted of 95% oxygen and 5% carbon dioxide. Rosuvastatin was used a model compound to study hepatic clearance and biliary excretion in the absence and presence of rifampicin. A bolus injection of 3 mg of rosuvastatin was applied to the portal vein and blood samples were taken at 15, 30, 45 and 60 minutes after dosing. Subsequently, 75 minutes after the first rosuvastatin dose, a second bolus injection of 3 mg rosuvastatin was applied together with a 300 mg rifampicin bolus injection and continuous infusion of 300 mg rifampicin/h. Blood samples were taken at 15, 30, 45 and 60 minutes after the second dosing of rosuvastatin and rifampicin. Bile was collected over 15 minute fractions during the experiment.

Results demonstrate clearance of rosuvastatin within 60 minutes from the circulation by hepatic excretion and excretion into the bile (80-90% of dose was excreted into the bile as parent drug and 10% as active metabolite N-desmethyl rosuvastatin). Upon inhibition of hepatic uptake and (thereby) biliary excretion of rosuvastatin by co-administration of rifampicin, plasma levels were 600-fold increased and biliary excretion 4- to 5-fold reduced. Results obtained with *ex vivo* porcine perfused liver were comparable to pharmacokinetics and biliary excretion of rosuvastatin in pigs *in vivo*.

We have demonstrated the application of *ex vivo* perfused porcine liver as a valuable tool to predict hepatic clearance and biliary excretion of rosuvastatin. We will further evaluate the model using porcine liver for prediction of plasma exposure and DDI, making use of slaughterhouse piglet livers in order to reduce animal experiments. Moreover, in the future we will investigate the influence of disease processes, such as NASH/cirrhosis, on hepatic disposition and biliary excretion of drugs by applying diseased human livers.

P92 - THE COMBINED APPLICATION OF LONG TERM HEPATIC CO-CULTURE AND RNA INTERFERENCE FOR REACTION PHENOTYPING: LESSONS LEARNED

Anthony Borel¹, Uma Fogueri², Jayakumar Surendradoss³, Richard Moulton¹, Keith Goldstein¹, David Bedwell¹, and Michael Mohutsky¹

¹Eil Lilly and Company; ²University of Colorado, ³The Centre for Drug Research and Development, Vancouver

The co-culture of hepatocytes and non-parenchymal cells provides a hepatic model that is well suited to long-term culture. Coupled to hepatic co-culture, the complementary application of short-interfering RNA (siRNA) for gene silencing provides an ideal opportunity for reaction phenotyping, especially in challenging cases involving low clearance compounds and/or compounds metabolized by less understood enzymes. CYP3A4, UGT2B7, AO1 and CES1 were investigated as representative drug metabolizing enzymes to assess the suitability of this application for inclusion in our ADME toolbox. Methods: Experimental conditions involved treatment of primary human hepatocyte co-cultures with 2 mM Accell SmartPool siRNA for CYP3A4, UGT2B7, AO1, CES1 or non-targeting control (NTC) compared with a vehicle (untreated) control (UC). Hepatic co-cultures were treated with siRNA for 120 h, with medium and siRNA replacement at 48 and 96 hours. After 120 hours treatment, hepatocytes were directed to either (1) RNA isolation followed by RT-qPCR to measure

gene expression, or (2) substrate selective enzyme reactions for CYP3A4 (midazolam), UGT2B7 (azidothymidine), AO1 (zoniporide) or CES1 (oseltamivir). Results: (1) Transcripts for the targeted genes CYP3A4, UGT2B7, AO1 and CES1 were knocked down, as expected, by >10-fold. Interestingly, non-specific knockdown was also evident. For example, NTC knocked down genes for CYP2E1 and CYP3A4 by 7-fold and 2-fold, respectively and siRNA for AO1 knocked down CYP3A4 by 10-fold in comparison to UC. (2) Treatments with siRNAs for CYP3A4, UGT2B7, AO1 and CES1 led to 30%, 50%, 85% and 40% decreases in respective enzyme activity compared with NTC. As observed for gene expression, non-specific effects on enzyme activity with siRNA were also evident, for example, NTC mediated a 30% reduction in CYP3A4 activity and a 40% increase in AO1 activity compared to UC. Conclusion: The combined application of RNA interference in hepatocyte co-culture elicited moderate knockdown of activity with well-known probe enzymes accompanied by non-specific effects on gene expression. Taken together, further characterization of this approach is necessary and application to reaction phenotyping of novel drug candidates is premature at this time.

P93 - HEPATIC 3D SPHEROIDS: AN *IN VITRO* TOOL FOR STUDYING HEPATIC FUNCTION AND DRUG TOXICITY

Sujoy Lahiri, Michael Connolly, Mark Kennedy, Debra L. Johnson, Deborah K. Tieberg, Rafal Witek, and Bina Khaniya
Thermo Fisher Scientific

Primary Human Hepatocytes (PHH) are the gold standard *in vitro* models for studying hepatic biology, liver function, and drug-induced hepatotoxicity. The conventional way of culturing PHH in 2-dimensional (2D) monolayers has major pitfalls, including the rapid de-differentiation and loss of hepatic-specific functions in a week. Therefore, there is a need for more robust *in vitro* models that reflects *in vivo* liver biology more accurately and maintains the liver functions for a longer time. 3-dimensional (3D) hepatic *in vitro* models are gaining a lot of attention for their ability to recapitulate the hepatic function and greater longevity.

Recently our group has developed an easy-to-assemble, user-friendly *in vitro* PHH 3D-spheroid model. Our initial work shows that hepatic spheroids can consistently and reproducibly assemble using super low attachment 96-well U-bottom microplates and standard centrifugation method in 3-5 days following seeding. We have shown that seeding 1,500 PHH/well resulted in spheroid formation with homogenous morphology and consistent size (~200 µm diameter). The resulting hepatic spheroids lived at least 28 days in culture and remain phenotypically stable. To assess whether hepatocyte-specific functions were maintained in PHH spheroids during prolonged culture, albumin secretion, CYP3A4 activity, and levels of ATP synthesized were analyzed. These parameters were found to remain stable during this extended culture period. Also, gene expression profiles at 5, 7, 14 and 21 days of culture showed relatively higher expression of hepatocyte-specific genes compared to Day 5 of the 2D-culture.

These results indicate that the PHH 3D-spheroid system constitutes a promising *in vitro* tool to evaluate hepatic function. As part of our future work, we are investigating the possibility of introducing nonparenchymal liver cells like Kupffer and Stellate cells to the spheroid system to assess the feasibility of creating various liver disease models.

P94 - EFFECTIVE INHIBITION OF CYP3A4-DEPENDENT DRUG OXIDATION BY ANTI-CYP3A4 ANTIBODIES IN METMAX CRYOPRESERVED HUMAN HEPATOCYTES

Albert P. Li¹, Carol Loretz¹, Jerome Lasker², and David Ho¹

¹In Vitro ADMET Laboratories Inc., ²P450-GP Inc.

Identification of the P450 isoforms underlying metabolism of an investigational drug, or reaction phenotyping, is critical to the development of new therapeutics, with applications in structural modification to optimize drug properties including the improvement of metabolic stability, estimation of drug-drug interaction potential, and estimation of species and interindividual differences in metabolism. P450 chemical inhibitors are widely applied for reaction phenotyping studies but the results are sometimes equivocal due to the non-specific effects of these compounds. On the other hand, inhibitory P450 antibodies offer high specificity and irreversibility, and may represent a superior approach for identifying specific P450 enzyme involvement in drug metabolism. While P450 antibodies can be readily employed with cell-free metabolic systems such as human liver microsomes, these immunoreagents are known to have limited utility with human hepatocytes, the "gold standard" of *in vitro* metabolism model systems, due to their inability to cross the plasma membrane. We recently developed a novel hepatocyte system, namely MetMax™ cryopreserved human hepatocytes (MMHH), in which the cells have been permeabilized and cryopreserved. MMHH were found to possess drug-metabolizing enzyme activities similar to that of conventional cryopreserved human hepatocytes (Li, AP., et al. (2018) Drug Metabolism and Disposition DMD117.). We hypothesized that inhibitory P450 antibodies are effective in MMHH as the permeabilized cell membrane may allow the antibodies to enter and interact with intracellular P450 enzymes. To test this hypothesis, cryopreserved MMHH (pool of 10 donors) were incubated with various amounts of anti-CYP3A4 antibodies, followed by quantification of CYP3A4 catalytic activity. Dose-dependent inhibition of CYP3A4 activity was observed, with approximately 90% inhibition observed at an anti-CYP3A4 IgG/hepatocyte ratio of 1 mg antibodies/10⁶ hepatocytes. Control (pre-immune) antibodies had no effect on substrate metabolism. Our results show that inhibitory antibodies coupled with MMHH represents a novel and powerful approach for evaluating involvement of specific P450 isoforms in the metabolism of therapeutics in hepatocytes. Results on the specificity of other inhibitory P450 antibodies

with MMHH will be presented based upon LC/MS-MS quantification of metabolite formation from P450 isoform-selective substrates. Using inhibitory antibodies with permeabilized human hepatocytes may represent the most accurate model for phenotyping due to the specificity and irreversibility of the inhibitory antibodies, and the presence of complete drug metabolism pathways in human hepatocytes.

P95 - METMAX HUMAN HEPATOCYTE/HEK293 CYTOTOXICITY ASSAY FOR THE EVALUATION OF METABOLISM DEPENDENT DRUG TOXICITY AND IDENTIFICATION OF DRUG CANDIDATES FORMING CYTOTOXIC REACTIVE METABOLITES

Albert P. Li, Carol Loretz, and David Ho
In Vitro ADMET Laboratories Inc.

We report here a novel experimental system, the MetMax™ Human Hepatocyte/HEK293 Cytotoxicity Assay (MMHH/HEK Assay) for the identification of drugs with metabolism-dependent toxicity, and the MMHH/HEK293 GSH Rescue Cytotoxicity Assay for the identification of drugs forming cytotoxic reactive metabolites. A drug with toxicity elicited by cytotoxic metabolites may have two complications in safety evaluation: 1. Inaccuracy of extrapolation of preclinical animal results to humans due to species differences in metabolism; and 2. Potential idiosyncratic drug toxicity in limited human populations due to individual environmental and genetic differences in drug metabolism. In these assays, drug toxicity is determined in HEK293 cells in the presence of MMHH as an exogenous activating system for prototoxicants – toxicants with toxicity enhanced by metabolism, HEK293 is a drug metabolism incompetent cell line routinely used for *in vitro* cytotoxicity assays. MMHH are permeabilized, cofactor-supplemented cryopreserved human hepatocytes that represent an effective and convenient hepatocyte system for the evaluation of drug metabolism (Li, AP., et al.(2018) *Drug Metabolism and Disposition* DMD117.; patent pending). The key advantages of MMHH over conventional cryopreserved human hepatocytes are that the MMHH cells can be stored at -80°C, can be used directly after thawing without the need for centrifugation and microscopic examination, and cofactor components, including GSH concentration, can be readily controlled by exogenous addition. Most importantly for the assay, metabolism activity of MMHH is not affected by cytotoxicity as in conventional hepatocytes and that the permeabilized membranes of the MMHH allow hepatic metabolites to readily diffuse from the hepatocytes to interact with the target cells. In the proof-of-concept study, HEK cells were seeded in a 96-well plate. After overnight culturing, the cells were treated with solvent control and 7 concentrations of four model chemicals known to have metabolism-dependent cytotoxicity: acetaminophen, cyclophosphamide, ifosfamide and 2-naphthylamine, in the presence and absence of MMHH. Heat-inactivated MMHH were used as a negative control. All four chemicals were shown to have cytotoxicity towards HEK293 cells significantly enhanced by the presence of MMHH, and with metabolic activation abolished by heat-inactivation. Our results suggest that MMHH represent a promising experimental system to provide exogenous hepatic metabolism to *in vitro* toxicity assays that do not possess metabolic capacity. Based on this assay, we developed a novel approach to demonstrate the formation of cytotoxic reactive metabolites: the MMHH/HEK293 GSH Rescue Assay. The principle of this assay is that demonstration of GSH attenuation of cytotoxicity would indicate the presence of cytotoxic reactive metabolites. We observed that the addition of 20 mM GSH effectively decreased the cytotoxicity of acetaminophen and cyclophosphamide towards HEK293 cells in the presence but not in the absence of MMHH, suggesting that MMHH metabolized the drugs to cytotoxic reactive metabolites, and that the cytotoxic reactive metabolite would form GSH-conjugates, leading to a decrease in cytotoxicity. We have therefore successfully demonstrated that the MMHH/HEK293 Cytotoxicity Assay can be used for the identification of drugs with metabolism-dependent toxicity, and the MMHH/HEK293 GSH Rescue Cytotoxicity Assay can be used to further identify drugs forming cytotoxic reactive metabolites.

P96 - CYTOTOXICITY IN PRIMARY HUMAN HEPATOCYTES EXPOSED TO VARIOUS MICROCYSTIN CONGENERS

Vicki Richardson¹, Joseph Strasser², and Elizabeth Hilborn¹

¹US EPA, ²Oak Ridge Associated Universities;

Microcystins (MCs) are monocyclic heptapeptide algal toxins produced by cyanobacterial species. MCs are among the most common cyanotoxin found in the environment and are found in many surface waters worldwide. MCs pose a risk to humans and animals due to their presence in drinking and recreational waters. Over 100 MC congeners have been identified with variable amino acid compositions. The amino acid composition determines physical/chemical properties including hydrophilicity and is also thought to determine the chemicals' kinetics that will in part determine the toxicity of each congener. Microcystin-LR (MCLR), the most commonly studied congener, is considered highly toxic and induces hepatic apoptosis and an accumulation of reactive oxygen species (ROS) when administered to laboratory animals. In contrast to MCLR, toxicity data for other MCs are limited. In this study, the effects of the more hydrophobic (MCLF, -LW, -LA) and the more hydrophilic (MCLR, -WR, -YR) congeners on cell viability and ROS production were determined using primary human hepatocytes (HH). HH were plated in 96-well microtiter plates at a density of 50,000 cells/well. 24 hours after plating, the HH were exposed to MCLR, -LW, -LA, -LF, -WR, or -YR at 10 different concentrations (0 to 20 µM) for 24 hours. After 24 hours, the HH were assayed for viability (CellTiter Glo 2.0; Promega Corp.). The EC₅₀ was then determined for each congener. Based on the EC₅₀, the rank order of cytotoxicity to HH was MCLW>LA>LF>LR>WR>YR.

To analyze ROS production in response to MC exposure, HH were plated as previously described. 24 hours after plating, HH were exposed to MCLR, -LW, -LA, -LF, -WR, or -YR at respective EC₅₀ concentrations (as determined in viability studies) for 6 hours. After the exposure period, the HH were assayed for ROS (ROS-Glo H₂O₂; Promega Corp.). MCLW, one of the most hydrophobic congeners, was the only congener that displayed a statistically significant increase in ROS in HH. These results indicate that the more hydrophobic congeners caused a greater decrease in cell viability in HH, compared to the more hydrophilic congeners. These results also suggest that the cytotoxic effects of each congener do not necessarily involve ROS, but can involve other mechanisms of cytotoxicity. When coupled with kinetic information on uptake and distribution, our results can be important in understanding and predicting toxic effects produced by these congeners *in vivo*.

This abstract of a proposed presentation does not necessarily reflect the policies of the US EPA.

P97 - HIGH-THROUGHPUT LIVER-ON-A-CHIP FOR PREDICTIVE HEPATOTOXICITY SCREENING

Anthony Saleh¹, Richard DeBiasio², Karlijn Wilschut³, Lawrence Verneti², D. Lansing Taylor², Paul Vulto³, Albert Gough², and Anup Sharma²

¹Mimetas Inc, ²University of Pittsburgh Drug Discovery Institute, ³Mimetas BV

Accurate prediction of hepatotoxicity is a crucial need in the pharmaceutical industry, as roughly two-thirds of drug development failures are attributed to hepatotoxicity. Animal hepatotoxicity testing is expensive, low-throughput, and overall has unreliable concordance with human hepatotoxicity, while standard *in vitro* systems have, at best, marginally improved productivity. The purpose of this study was to optimize a 3D *in vitro* model of the human liver, and concordantly predictive hepatotoxicity assays, by adapting the sequentially layered, self-assembly liver model (SQL-SAL) developed by the University of Pittsburgh Drug Discovery Institute into MIMETAS' high-throughput microfluidic system. The resulting platform contains 96 x 3D microfluidic co-culture mimics of the liver sinusoid, including human primary or iPS hepatocytes and stellate cells incorporated in an ECM protein gel, fed by microfluidic nutrient perfusion from an adjacent endothelial and Kupffer cell-lined blood vessel mimic. Cell viability of the co-culture remained stable (80-90%) through 10 days in culture. We report long-term maintenance of metabolic activity, including CYP3A4 (1-10 days) and albumin production (1-10 days). Per million cells, this model produced greater than 800 ng albumin/day. Using multi-parameter high-content imaging, we have optimized toxicity assays with fluorescent readouts to measure viability, mitochondrial function, and steatosis following the administration of known hepatotoxicants, including acetaminophen (APAP) and troglitazone. The cell viability assay revealed a more physiologically-relevant sensitivity to APAP in this liver-on-a-chip system, as 300 µM APAP (human C_{max}: 130 µM) reduced the viability of the culture by 90 percent and ≥10 mM was required to obtain a comparable response in the 2D culture of hepatocytes. Exposure to troglitazone triggered a concentration-dependent accumulation of lipids in the cultures, indicating the potential for characterizing toxic compound effects on lipid metabolism (steatosis). These studies display the feasibility of using our 3D human model as a high-throughput screening platform for the assessment of pharmaceutical and chemical hepatotoxicity.

P98 - CASE STUDIES IN QUALITY LEVELS FOR *IN VITRO* ADME ASSAYS: HEPATOCYTE STABILITY

Teresa Sierra, Christopher Strock, and Adam Brockman
Cyprotex US, LLC

Hepatocyte stability is an important component of the ADME suite typically used to accurately define intrinsic clearance values. This parameter is used to predict systemic exposure, assess potential for drug-drug-interactions, to support medicinal chemists in drug design, and to rank potential drug candidates during discovery lead optimization. High throughput and other screening-quality ADME assays are fit-for-purpose to rank large numbers of compounds, however, the DMPK community has long been concerned that lower-quality data could be inappropriately used for late stage development purposes. Later stage candidates require greater accuracy and precision for use in first-in-human-enabling work to predict human exposure and assess drug-drug-interaction liabilities. We present a case study in which the results of a compound run in singlicate in a HT-ADME assay appeared to have low clearance in multiple species. The compound appeared to show an increase in abundance at the first timepoint after T0 suggesting solubility issues. The use of a high throughput approach in this case prevented the observation of compound precipitation in samples with singlicate analysis contributed to a deceptive clearance result by random chance. In response to these observations the compound was run in triplicate after using heat (40 °C) and sonication in the incubation buffer to maximize solubility prior to adding hepatocytes. With the increased solubility, the compound demonstrated a much higher clearance than was previously assessed through the screening quality, HT-ADME assay and evidence of solubility issues were no longer evident. This case study helps to demonstrate the importance of a higher quality level for proper evaluation of ADME characteristics for a development candidate.

P99 - ACCELERATION OF MURINE HEPATOCYTE PROLIFERATION BY IMAZALIL THROUGH THE ACTIVATION OF NUCLEAR RECEPTOR PXR

Kouichi Yoshinari, Shohei Yoshimaru, Ryota Shizu, Satoshi Tsuruta, Yuto Amaike, Makoto Kano, Takuomi Hosaka, and Takamitsu Sasaki
University of Shizuoka

The nuclear receptor PXR is highly expressed in the liver and intestines and plays key roles in the xenobiotic-induced expression of drug-metabolizing enzymes and transporters. PXR activation is also associated with diverse liver functions including glucose and energy metabolism. The receptor is activated by structurally diverse variety of chemical compounds including drugs, food components, pesticides, industrial chemicals and so on. Recently, we have reported in mice that PXR activation accelerates hepatocyte proliferation mediated by CAR and PPAR α activators as well as carbon tetrachloride-induced liver injury although PXR activation itself does not induce hepatocyte proliferation [1,2]. These results suggest that the exposure to PXR activators increases the sensitivity to liver tumor promoters and risk of liver tumor formation, at least in rodents. Food additives are taken in combination with other chemical compounds in daily life. But their safety is evaluated in animal study as a single compound and information on the combination effects is very limited. In this study, we have thus investigated the influences of food additives and related compounds on mouse PXR (mPXR) to understand their potential adverse effects associated with chemical carcinogenesis. We first performed reporter gene assays in mPXR-expressing HepG2 cells to investigate mPXR-activating ability of 25 food additives and related compounds *in vitro* and found that imazalil (also known as enilconazole) activated mPXR as strong as pregnenolone 16 α -carbonitrile, a potent mPXR activator. Next, mice were treated intraperitoneally with imazalil to investigate whether imazalil could also activate mPXR *in vivo*. As a result, imazalil treatment increased hepatic mRNA levels of *Cyp3a11*, a well-known mPXR target gene. Finally, to investigate whether imazalil exposure could stimulate CAR-mediated hepatocyte proliferation, mice were treated with imazalil in combination with or without TCPOBOP, a potent CAR ligand, and hepatocyte proliferation was assessed by immunostaining of liver sections for Ki-67 and measuring hepatic mRNA levels of *Mcm2*, both of which are known as makers of proliferating cells. Although imazalil treatment alone did not increase the number of Ki-67-positive nuclei and *Mcm2* mRNA levels in the liver, it augmented the TCPOBOP-mediated increase in those levels. In contrast, imazalil treatment did not increase the TCPOBOP-induced increase in the hepatic mRNA levels of *Cyp2b10*, a CAR target gene. These results suggest that imazalil, which is widely used as a food additive or postharvest fungicide, activates mPXR to accelerate hepatocytes proliferation induced by CAR in mice, corroborating a unique role of PXR in the regulation of cell proliferation.

P100 - EXPANDED PRIMARY HUMAN LIVER SINUSOIDAL ENDOTHELIAL CELLS AS A PREDICTIVE TOOL IN HEPATOTOXICITY EVALUATION

Astrid Noerenberg¹, Dana Brauer², Maren Klett², Andreas Schober², and Timo Johannssen¹
¹upcyte technologies, ²Technical University Ilmenau

Liver sinusoidal endothelial cells (LSECs) are highly specialized endothelial cells forming the highly permeable hepatic sinusoidal wall. They are responsible for endocytosis of macromolecules, liver regeneration as well as immune tolerance. On the other hand, in pathological conditions, LSECs play a key role in drug-induced liver injury. Despite their significant contribution to liver homeostasis, LSECs are often ignored in hepatotoxicity studies due to the insufficient cell numbers after isolation and limited proliferation capacity. However, it is hypothesized that the incorporation of LSECs into hepatotoxicity assays could boost the predictability of such assays [1]. Therefore, we applied our previously described upcyte® technology for the expansion of primary LSECs by lentiviral transduction of proliferation inducing genes [2]. With this technology, proliferating primary LSECs from three different donors were generated in large numbers which could perform in culture up to 25 additional population doublings compared to their naïve primary counterparts. The obtained so called upcyte® LSECs expressed typical endothelial cell markers (CD31, von Willebrand factor) as well as LSEC-specific receptors (mannose receptor, LYVE-1 and L-SIGN). Additionally, they showed uptake of several macromolecule ligands (e.g. serum albumin, aggregated IgG). To investigate whether the incorporation of LSECs into drug-induced liver toxicity studies results in better predictability, we first challenged LSECs 2D monolayers with acetaminophen (APAP) and compared the toxicity to expanded hepatocytes. Interestingly, we observed that LSECs showed an increased sensitivity towards APAP when compared to upcyte® hepatocytes. Furthermore, we found that a co-culture with hepatocytes in 3D scaffolds was the most sensitive model to detect acetaminophen-induced toxicity, indicating that these cells are a promising tool to complement hepatotoxicity evaluation in the future. Taken together, our data suggest that upcyte® LSECs combine many characteristics of primary LSECs with the advantage of an extended lifespan, facilitating their use in hepatotoxicity assays under reproducible and standardized conditions.

References:

1. DeLeve, L.D. Liver sinusoidal endothelial cells and liver regeneration. *J Clin Invest*, 1861-1866, 123(5), 2013
2. Levy, G. et al. Long-term culture and expansion of primary human hepatocytes. *Nature Biotechnology*, 1264-1271, 33(12), 2015.

P101 - CHARACTERISING THE IMMUNE RESPONSE TO CARBAMAZEPINE: UNDERSTANDING THE DEVELOPMENT OF IDIOSYNCRATIC DRUG REACTIONS

Alison Jee and Jack Uetrecht
University of Toronto

Idiosyncratic drug reactions (IDRs) can be serious, life-threatening reactions. Most IDRs have been shown to be immune-mediated, but it is unknown how drugs induce such an immune response. It has long been observed that the most severe form of an IDR (e.g. Steven-Johnsons syndrome/toxic epidermal necrolysis or liver failure) occurs with a very low incidence, while a similar but milder form of the IDR occurs in response to the same drug in a larger proportion of patients (e.g. maculopapular skin rash, mild liver injury). Medications that cause IDRs may elicit an even milder, subclinical immune response that spontaneously resolves in an even larger proportion of patients. For example, clozapine causes an immune response in most patients evidenced by fever and an increase in IL-6 and TNF- α , but this has never been studied for most drugs. Unfortunately, obtaining patients for study of clozapine has proved to be very challenging. We will therefore study carbamazepine, a widely used antiepileptic that causes a range of serious IDRs involving the skin, liver, and blood. Our hypothesis is that drugs that elicit IDRs cause a subclinical immune response in most patients that resolves through immune tolerance. An animal model will be used to study the immune response under controlled conditions and in multiple organs. Samples from the liver, lymph nodes, and blood from C57BL/6J mice administered carbamazepine will be analysed by histology, for infiltrating immune cells, and qPCR, for changes in expression of inflammatory and anti-inflammatory markers. These results will then need to be validated in human patients. Thus far, we have developed a dosing protocol that produces a therapeutic blood level in mice and causes a significant increase in alanine aminotransferase (ALT) in PD-1 knockout mice, a model utilising immune checkpoint inhibition for idiosyncratic drug-induced liver injury.¹ This is consistent with the hypothesis that this liver injury is immune-mediated. Further studies will be performed to characterise the cells populations that are involved in this liver injury. Ultimately, we aim to find a biomarker to predict the ability of a drug to cause IDRs, which would save patients' lives and reduce risk in the drug development process.

References:

1. Metushi, I. G., Hayes, M. A. & Uetrecht, J. Treatment of PD-1 $-/-$ mice with amodiaquine and anti-CTLA4 leads to liver injury similar to idiosyncratic liver injury in patients. *Hepatology* **61**, 1332–1342 (2015).

P102 - *IN VITRO* TO *IN VIVO* EXTRAPOLATION OF INTRINSIC CLEARANCE FOR LOW TURNOVER COMPOUNDS USING PLATED POOLED DONOR HUMAN HEPATOCYTE CO-CULTURE SYSTEMS

Faraz Kazmi, Carlo Sensenhauser, and Shannon Dallas
Janssen Research & Development

Determination of *in vitro* hepatic intrinsic clearance (CL_{int}) is an important parameter used to estimate *in vivo* metabolic clearance through *in vitro* to *in vivo* extrapolation (IVIVE). Typically, *in vitro* CL_{int} values are generated in conventional systems such as pooled human liver microsomes and pooled suspended primary human hepatocytes. However, these *in vitro* test systems lose metabolic capability over time and have short incubation windows (< 2 hours for microsomes and < 4 hours for hepatocytes), suitable only for moderate to high turnover compounds where half-life can be reliably estimated. In the case of low or slowly turned over compounds, these conventional *in vitro* systems fail to provide sufficient compound turnover to enable reliable CL_{int} estimation. To circumvent this issue, new test systems have been developed using plated primary human hepatocytes co-cultured with non-parenchymal stromal cells that maintain metabolic capability for up to seven days without media change. In the present study we initially evaluated the *in vitro* CL_{int} of six low turnover compounds (disopyramide, timolol, theophylline, prednisolone, tolbutamide and warfarin) in two commercially available pooled (n = 5) plated primary human hepatocyte co-culture systems head-to-head, namely micropatterned human hepatocyte co-culture (HepatoPac; Ascendence Biotechnology, Medford, MA) and mixed human hepatocyte co-culture (H μ rel Corporation; North Brunswick, NJ). Pooled human hepatocyte co-culture plates were obtained from each respective vendor and incubated in vendor provided maintenance media for at least 48 hours prior to test compound incubation (1 μ M) for 0, 8, 16, 24, 32, 48, 72, and 96 hours in vendor provided incubation media. Reactions were terminated in duplicate at each time point, followed by LC-MS/MS analysis of residual parent compound. IVIVE of CL_{int} was performed with the well-stirred model and scaled *in vitro* CL_{int} values were compared to reported *in vivo* clearance values for each compound. Of the compounds tested, disopyramide (CYP3A4 metabolic pathway) CL_{int} was ~10-fold overpredicted in HepatoPac, whereas there was a ~10-fold underprediction with H μ rel plates. Timolol (CYP2D6) *in vitro* CL_{int} was within 2-fold of the *in vivo* value in HepatoPac, whereas a ~10-fold underprediction was observed in the H μ rel system. For theophylline (CYP1A2), neither test system was able to turnover the compound significantly. Prednisolone (CYP3A4) CL_{int} was ~7-fold overpredicted in HepatoPac, and ~3-fold underpredicted in the H μ rel model. Tolbutamide (CYP2C9/3A4) CL_{int} was ~10-fold overpredicted in HepatoPac, and within 2-fold in the H μ rel model. Lastly, warfarin (CYP2C9/3A4) was ~40-fold overpredicted in HepatoPac and within 2-fold in the H μ rel system. These findings

demonstrate that both human hepatocyte co-culture models, due to their extended metabolic incubation windows, allow for the determination of CL_{int} for low turnover compounds with reasonable *in vivo* predictions.

P103 - USING STATISTICAL ANALYSES TO DEMONSTRATE EQUIVALENCY BETWEEN AUTOMATED AND MANUAL PROCESSES TO DELIVER HIGH QUALITY *IN VITRO* ADME DATA EVEN FASTER

Jakal Amin, Francoise Powell, David Plourde, Allison Lewia, Patty Walton, Gaurang Patel, Susan Dearborn, and Adrian Sheldon
Charles River Laboratories

The role of lab automation to enable drug discovery and compound screening related to *in vitro* ADME assays has been well established over the past 10-20 years. As bio-pharmaceutical companies continue to evolve from performing ADME assays in-house to outsourcing, it has become necessary for the contract research organizations (CROs) to adopt this paradigm shift and invest in automation technologies to enable and support large scale ADME analysis. Based on client expectations, our objective was to provide high quality data within 5 days for up to 500 compounds per week for three primary screening assays: Metabolic Stability, Plasma Protein Binding using RED, and Permeability (Caco-2 and MDCK-MDR1). To enable this, dual liquid-handlers (Hamilton Vantage®) were established to perform multiple biological experiments with minimal human intervention. The implementation of the high-throughput work-flow involved deployment of key features such as cherry-picking and dilution of stock solutions (10 mM compound in DMSO) from multiple barcoded source plates to intermediate plates prior to the commencement of biological experiments. For the LC-MS/MS analysis, Apricot Designs Dual Arm (ADDA) was selected as the primary autosampler coupled with Sciex 5500 LC-MS/MS systems. ADDA provided flexible high-throughput bioanalysis capability in 384-well plate format to perform both trap/elute methods (~10 seconds/cycle) along with gradient methods when required. Multiple validation experiments were performed to demonstrate an agnostic statistical equivalency of T/E vs. gradient-based analyses for diverse new chemical entities (NCEs) and marketed compounds. Comparison of data between different platforms were based on the confidence and tolerance, concordance correlation and Minimum Significant Ratio. The purpose of the presentation will be to provide the strategies taken to deploy the HT approach, validation performed and the knowledge gained.

P104 - CHARACTERIZATION OF CISPLATIN TOXICITY IN APROXIMATE HUMAN PROXIMAL TUBULE CELL MONOLAYERS

Colin Brown¹, Git Chung², Mike Nicholds², and Lyle Armstrong²
¹Newcastle University, ²Newcells Biotechnology

Around 50 % of preclinical *in vivo* toxicity screens fail to predict subsequent human toxicity, leading to significant attrition of drug molecules during drug development. Renal toxicity accounts for about 20 % of the unexpected toxicity at first in man. Understanding nephrotoxicity has been hampered by the lack of a good renal model. Here we demonstrate the utility of aProximate™ human proximal tubule cell (hPTC) monolayers as an *in vitro* tool to investigate nephrotoxicity by demonstrating the effects of the well characterised nephrotoxin cisplatin upon the release of the clinically relevant biomarkers NGAL, KIM-1 and clusterin by the cells in response to cisplatin challenge. Freshly isolated hPTCs were seeded onto Transwell filters and grown to confluency before challenged with 10µM cisplatin for 72 hours. Biomarker generation was assessed using a custom NGAL/Kim-1/clusterin Multi-Array Technology plate (Meso Scale Developments), monolayer integrity was assessed by measurement of transepithelial electrical resistance (TEER) and cell viability was assessed using a RealTime-Glo™ MT Cell Viability Assay (Promega) viability and a LDH assay to measure LDH release. Changes in gene expression after challenge with cisplatin were measured using a 80-gene PCR Array from SABiosciences. Treatment of the hPTCs with the cisplatin (10µM) resulted in a significant ($P < 0.001$) increase in the levels of KIM-1 (2.5 ± 0.1 fold), NGAL (3.1 ± 0.2 fold), and clusterin (2.4 ± 0.2 fold). In the presence of cisplatin cell viability fell to $53.4 \pm 2.6\%$ of control ($P < 0.001$) and LDH release increased significantly to $56.2 \pm 3.4\%$ of total cellular LDH content. Cisplatin challenge generated a significant decrease in TEER from $87.8 \pm 3.6 \Omega \cdot \text{cm}^2$ to $16.7 \pm 1.3 \Omega \cdot \text{cm}^2$ ($P < 0.001$). At the gene level, cisplatin challenge resulted in significant increases in genes associated with apoptosis at the qPCR level. These included the death receptors; Fas (3.9 fold) CD70 (11 fold) and TNFR (3.8 fold), intrinsic pathway mediators BAX (3.9 fold) and BAK1 (4.1 fold) together with AIF (1.9 fold) and DIABLO (2.35 fold) and ER stress pathway markers resulting in significant increases in downstream caspase production leading to apoptosis. Importantly cisplatin also stimulated mRNA levels of the anti-apoptotic proteins; caspase 14 (21.8 fold) and BCL2A1 (11.1 fold). In summary, aProximate™ human proximal tubule cell monolayers retain a remarkable degree of differentiation, express clinically relevant biomarkers of nephrotoxicity and signalling pathways that translate to an appropriate response to cisplatin challenge. aProximate™ human proximal tubule cell monolayers show excellent potential as an *in vitro* predictive human toxicology screening platform during the drug development process.

P105 - DEVELOPMENT OF A NOVEL PREDICTIVE *IN VITRO* NON HUMAN PRIMATE PROXIMAL TUBULE MODEL FOR DRUG TRANSPORTER AND NEPHROTOXICITY STUDIES**Colin Brown**

Newcastle University

Nephrotoxicity is a major reason for drugs failing during clinical development. Currently there is no *in vitro* platform that enables cross-species comparisons of drug transport or nephrotoxicity. Our innovative solution to this is to develop of an assay platform measuring both drug transport and a range of biomarkers associated with drug induced kidney injury using primary renal proximal tubule cells (PTCs) derived from key animal species. To generate an Non human Primate (NHP) PTC platform, PTCs were isolated from kidney cortex using a collagenase digest and Percoll density gradient protocol. NHP PTCs were seeded onto Transwell filters and grown to confluency in a chemically defined media for 7 days. Gene expression was measured by qPCR. Digoxin flux was measured using [³H] digoxin. Biomarkers were assessed using an NHP-specific clusterin ELISA assay. Monolayer integrity was measured as transepithelial electrical resistance (TEER) and cell viability using MTS. NHP PTCs grown on permeable filter supports formed confluent monolayers with a TEER value of 90.9±5.6 Ω.cm² (n=4) at day 7 in culture versus 114.2± 4.7 Ω.cm² and 98.6±6.1 Ω.cm² for primary human and rat PTC monolayers. At the qPCR level, NHP PTCs expressed message for a range of key drug transporters including MDR1, MRP4, BCRP, OCT2, OATP4C1 and lower levels OAT1. Functionally, we could demonstrate a net digoxin secretion across NHP monolayers: At 10µM digoxin, the apical to basolateral flux (J_{ab}) was 3.3±0.2 pmol/cm²/h significantly smaller than the basolateral to apical flux (J_{ba}) of 15.8 ±0.2 pmol/cm²/h. Net secretion of digoxin was significantly inhibited by addition of triiodothyronine (10µM) or estrone-3-sulfate (10µM) to the basolateral membrane, or GF120918 to the apical membrane. Results consistent with OATPC41-mediated uptake of digoxin and apical efflux of digoxin mediated by MDR1. To test the utility of NHP PTC monolayers as a predictive models of nephrotoxicity, cells were challenged with a range of well characterised nephrotoxins and the impact upon the biomarker clusterin, TEER and cell viability was assessed. In response to cisplatin challenge (10µM) for 72 hours, clusterin release in to the apical media was substantially increased (2.8 +0.2 fold, P<0.01, n=4) compared to control, clusterin release into the basolateral media was unchanged by cisplatin challenge. Cisplatin challenge was also accompanied by both a significant decrease in cell viability to 34.4±4.4% and of TEER value to 16.3±3.1 % of control values respectively. In addition to cisplatin induced toxicity, a significant increase in clusterin release was found in response to challenge with either 10µM cyclosporin (1.5 fold), 10µM methotrexate (2.2 fold), 200µg/ml polymyxin B (4.5 fold) or 200µg/ml gentamicin (1.4 fold). Interestingly, both cyclosporin and gentamicin had no effect upon either TEER or cell viability. Methotrexate and polymyxin B challenge resulted in a significant fall in both TEER and cell viability. Taken together these results report for the first time the successful production of a primary NHP PTC monolayer which, similar to our human and rat aProximate™ PTC models may prove useful as a predictive *in vitro* PTC model of drug transport and drug toxicity.

P106 - INVESTIGATING ACETAMINOPHEN COVALENT PROTEIN BINDING TO GLUTATHIONE S-TRANSFERASES BY LC-MS/MS**Timon Geib**¹, Andrew Fairman², Derek Wilson², and Lekha Sleno¹¹UQAM, ²York University

Hypothesis: Acetaminophen (APAP)-induced hepatotoxicity is linked to covalent protein binding to cysteine residues, induced by metabolic activation to *N*-acetyl *p*-benzoquinone imine (NAPQI). At therapeutic doses, NAPQI formation is considered harmless due to rapid conjugation with glutathione via glutathione S-transferases (GSTs). However, at higher doses or under conditions where hepatic glutathione is depleted, APAP acts as a potent hepatotoxin, and can cause severe liver insult and even death. In this work, we developed and applied a novel method to investigate the formation of NAPQI-adducts to different GST isoforms. Methods: Our method uses bioactivation of APAP with CYP3A4, while adding purified GSTs to the incubation. Cytosolic human GST alpha 1, mu 1 and 2, and pi 1 were expressed and purified prior to protein binding experiments. Further sample preparation employed proteolytic digestion, solid-phase extraction and high-pH reversed-phase fractionation on a C18 column, coupled to liquid chromatography-tandem mass spectrometry (LC-MS/MS). LC-MS/MS was performed using a quadrupole-time-of-flight platform (QqTOF), as well as a quadrupole-linear ion trap (QqLIT). Supporting Data and Results: Method optimization was carefully performed to yield high sequence coverage. Optimal conditions for CYP3A4 incubation with GST, APAP and NADPH were determined, followed by dithiothreitol reduction, iodoacetamide alkylation, and either tryptic or peptic digestion. LC-MS/MS files of data-dependent acquisition experiments (QqTOF) were searched against the UniProtKB/Swiss-Prot protein database. The search algorithm was altered to find potential NAPQI-cysteine adducts. Additionally, multiple reaction monitoring (MRM) experiments (QqLIT) were used for high-sensitivity identification by comparison to custom-designed standards. Standards were based on a positional isomer to the NAPQI-modified protein, yielding a surrogate peptide after proteolysis. Two sites on GST mu 2 were found to be modified by NAPQI *in vitro*, using MRM screening. One of these sites was confirmed with a MS/MS spectral confidence >99% within 10 ppm mass accuracy, combined with the presence of NAPQI-cysteine related diagnostic product ions. No sites were modified on the other screened GSTs based on high-resolution data. MRM results were currently still being compiled for these other GSTs. Conclusions: This high-sensitivity screening of APAP-

related protein binding can provide fast LC-MS/MS analyses of complex samples, including NAPQI exposed liver microsomes and S9 fractions.

P107 - COMPREHENSIVE HEPATOCELLULAR DISPOSITION PROFILING OF PARENT COMPOUND AND ITS MAJOR METABOLITES IN SANDWICH-CULTURED PXB-CELLS BY D-PREX

Katsuhiro Kanda

Hitachi High-Technologies Corporation

Purpose: This study aimed to examine the total disposition profiling of parent and its major metabolites by a single systematic procedure called D-PREX (Disposition Profile Exploration)¹, using sandwich-cultured PXB-cells (SCPC). In this D-PREX system, drug uptake and metabolism is performed under the intact SCPC, followed by simultaneous evaluation of biliary and basolateral efflux by measuring supernatants, then cell lysis to understand the intracellular residues. **Methods:** SCPC were exposed to the standard Hanks' balanced salt solution (Std HBSS) including 10 μ M parent compound at 37?? for over time (10-120 min), which were terminated by rinsing with ice-cold Std HBSS. Subsequently, the cells were incubated 10 min with Std HBSS at 37?? for stabilization of the following efflux evaluation (conditioning efflux step). Then the cells were separated into three groups: intact and disrupted bile canalicular structures with and without Ca²⁺ ion conditions at 37??, and that of intact with Ca²⁺ at 4??, respectively. Each supernatant was collected after 10 min incubation, followed by the cell lysate samplings. The amount of compounds in the collected samples were quantitated by LC-MS/MS analyses, which were used to calculate the respective disposition endpoints. Gene expression levels of conjugation enzymes and efflux transporters in SCPC were evaluated by Real-time RT-PCR on Day 1 and 8. **Results & Discussion:** The majority of the related enzymes and transporters were upregulated in SCPC compared to the freshly isolated hepatocytes. In terms of acetaminophen (APAP), the metabolism seemed to follow the uptake of APAP, which saturated after 60 min incubation. The proportion of the major metabolites of glucuronide (APAP-Gluc) and sulfate (APAP-Sulf) corresponded to the known human metabolism properties². In addition, these compounds mostly transported to basolateral efflux than biliary excretion, which represented the tendency of urinary elimination. Further, in terms of basolateral efflux, APAP showed relatively higher passive diffusion portion than that of transporter-mediated, whereas APAP-Gluc and -Sulf represented opposite trend, suggested the hydrophilic property of the conjugates mediated by the transporters. **Conclusion:** D-PREX can be used for the simultaneous evaluation of total disposition profiles not only the parent compounds but also their metabolites, resulted from the complex interplay of the hepatic metabolism and transport. Further evaluations using probes regarding active-metabolites and human-specific metabolites are under examination.

References:

1. Takahashi R, Ichikawa H, and Kanda K (2016) Novel multiple assessment of hepatocellular drug disposition in a single packaged procedure. *Drug Metab Pharmacokinet* 31(2): 167-171.
2. Bertolini A, Ferrari A, Ottani A, Guerzoni S, Tacchi R, and Leone S (2006) Paracetamol: New vistas of an old drug. *CNS Drug Reviews* 12(3-4): 250-275.

P108 - IN VITRO ASSESSMENT OF THE RELATIVE TOXICITY OF A SERIES OF PYRROLIZIDINE ALKALOIDS: TAKING ACCOUNT OF METABOLIC ACTIVATION AND TOXICOKINETICS

Cindy Obringer, Cathy Lester, John Troutman, Mike Karb, Catherine Mahony, Beatrice Nyagode, Amy Roe, Peter Stoffolano, and Ken Wehmeyer

The Procter & Gamble Company

1,2-unsaturated pyrrolizidine alkaloids (PAs) are hepatotoxic compounds produced in some flowering weeds that can contaminate crops used for food or herbal medicines. The liver is the primary organ of toxicity making PAs a concern for safety assessment. PAs display a strong structure toxicity relationship with relative potencies spanning two orders of magnitude across structural classes. Current regulatory approaches to risk assessment take a precautionary approach and assume all PAs display the same toxicity as the most potent PA lasiocarpine. Here we outline an *in vitro* metabolism approach to support the assessment of the relative potencies of a structurally diverse group of PAs. Metabolic activation is catalyzed by P450 isozymes and results in the formation of a pyrrolizine reactive intermediate known to bind proteins, glutathione and DNA. Because all hepatotoxic PAs exhibit the same mode of action, *in vitro* measurement of metabolic clearance and DNA adduct formation may be used to determine and rank relative PA potency. Here we present data for substrate depletion of lasiocarpine and heliotrine and their N-oxides. Effects of oxygen tension on oxidative and reductive metabolism by pooled male Sprague-Dawley rat liver microsomes is considered. Intrinsic clearance values are calculated using the $t_{1/2}$ method providing information on intracellular biotransformation kinetics. Under ambient oxygen levels, the intrinsic clearance for 1 mM lasiocarpine and 1 μ M heliotrine is 355 and 33.4 μ L/min/mg protein, respectively, while no substrate loss was detected for their corresponding N-oxides. Under hypoxic conditions (2% O₂), intrinsic clearance values for lasiocarpine and lasiocarpine N-oxide are 170 μ L/min/mg protein and 11 μ L/min/mg protein, respectively. DNA adduct formation has been associated with the incidence of tumor formation *in vivo* and is often studied *in vitro* in liver microsomal preparations in the presence of calf thymus DNA. We demonstrate enhanced sensitivity and simplification of

this measurement by replacing calf thymus DNA with deoxyguanosine and deoxyadenosine in the microsomal incubation. The application of the tools presented here are being used to inform a strategy to assess the relative potencies of PAs and their N-oxides *in vitro*.

P109 - HIGH-THROUGHPUT, PERFUSED INTESTINAL TUBULES FOR REAL-TIME ASSESSMENT OF DRUG-INDUCED BARRIER DISRUPTION

John Lowman¹, Remko van Vught², Sebastiaan Trietsch², Elena Naumovska², Dorota Kurek², Karlijn Wilschut², Henriette Lanz², Arnaud Nicolas², Stefan Kustermann³, Adrian Roth³, Paul Vulto², Annie Moisan³

¹Mimetas Inc, ²Mimetas BV, ³Roche Innovation Center Basel

In vitro models that better reflect *in vivo* epithelial barrier (patho-)physiology are urgently required to better predict adverse drug effects ahead of clinical trials. Here, we describe extracellular matrix-supported intestinal tubules, continuously-perfused in a high-throughput microfluidic system (Mimetas' OrganoPlate®). These tubules exhibit key tissue polarization markers (ErB1, ErB2, Ezrin, ZO-1), relevant transporters (Glut-2, MRP2), and crypt-like morphology. Leak-tight polarization of these gut-on-a-chip barrier tubules was achieved after just 4 days in culture, and high-content characterization of the tubules was possible due to the absence of a filter membrane in the microfluidics.

Functional drug-induced toxicity was assessed by apical exposure of model compounds to these *in vitro* intestinal barriers. Within each OrganoPlate®, forty leak-tight intestinal tubules were cultured in parallel, and their response to pharmacological stimuli was recorded over 125 hours of exposure. Overall, a study comprising 357 gut-on-a-chip tubes is performed, of which 93% are leak tight before exposure. EC50-time curves could be extracted that provide insight in both concentration and exposure time response.

Full compatibility with standard equipment and user-friendly operation make this Organ-on-a-Chip platform readily applicable in routine laboratories.

P110 - BBB-ON-A-CHIP: A 3D *IN VITRO* MODEL OF THE HUMAN BLOOD-BRAIN BARRIER

John Lowman¹, Nienke Wevers², Xandor Spijkers², Karlijn Wilschut², Remko van Vught², Sebastiaan Trietsch², and Paul Vulto²

¹Mimetas Inc, ²Mimetas BV

The BBB ensures a homeostatic environment for the brain and is made up of specialized endothelial cells and supporting astrocytes and pericytes. The BBB protects the brain from harmful substances. It also prevents large lipophilic compounds, including most therapeutic drugs, from entering the brain. This makes it difficult to treat brain diseases. While recent developments in microfluidic engineering have resulted in promising *in vitro* models of the BBB, the throughput and ease of use of these systems is low. This makes these models not suited for regular academic research and drug development. Here we present a novel BBB model using the 3-lane OrganoPlate®. This platform is based on a 384-well microtiter plate and allows for parallel culture of 40 perfused miniaturized tissues, making it fully compatible with standard lab procedures and equipment.

The BBB-on-a-chip model comprises a perfused 3D microvessel of human brain microvascular endothelial cells. Perfusion through the lumen of the vessel is induced without pumps and can be controlled to model mechanical cues. In addition, the microvessel is supported by human astrocytes and pericytes that interact and support the endothelial vessel. The phenotype of the BBB-on-a-chip was characterized using immunofluorescent staining and showed presence of junctional markers VE-cadherin, PECAM-1, Claudin-5, and ZO-1. In addition, we have confirmed barrier function and adopted transporter assays to show functionality of two major BBB transporters, Pgp and GLUT1.

In conclusion, we present a novel human BBB model in an easy to use microfluidic platform. This model can be used for fundamental BBB research, drug development or studying neurological disorders.

P111 - INTERACTIONS OF HERBAL SLIMMING AGENTS WITH CYP SUBSTRATES: AN *IN VITRO* STUDY USING HUMAN LIVER MICROSOMES

Satheeshkumar Nanjappan¹, Lavanya Bolla², Pratima Srivastava³

¹National Institute of Pharmaceutical Education and Research [NIPER-HYDERABAD], ²Drug Metabolism and Interaction Research Lab, Department of Pharmaceutical Analysis, National Institute of Pharmaceutical Edu, ³Drug Metabolism and Pharmacokinetic department, Biology Division, GVK Biosciences Private Limited

With increasing intake of traditional medicines, herbal slimming agents are commonly consumed by obese patients. Obesity is a complex disease which facilitates other metabolic disorders requiring the concomitant use of drugs such as lipase inhibitors, antihyperglycemic drugs, HMG-CoA reductase inhibitors and hypocholesterolemic agents along with herbal slimming agents, posing high potential to cytochrome P450 (CYP) isoenzymes mediated herb-drug interactions (HDIs). In the present study, *in vitro* effects of herbal slimming agents like *Garcinia cambogia* extract, Green coffee bean extract, Acai berry extract and Raspberry ketone extract and phytomolecules of *Garcinia cambogia* (Garcinol and HCA)

on the activities of eight CYP isozymes (CYP1A2, CYP2B6, CYP2C8, CYP2C9, CYP2C19, CYP2D6, CYP2E1 and CYP3A4) were studied to predict potential interactions. Herbal slimming agents were incubated with human liver microsomes and cocktail of eight CYP probe substrates (Tacrine (CYP1A2), Bupropion (CYP2B6), Diclofenac (CYP2C9), S-mephenytoin (CYP2C19), Dextromethorphan (CYP2D6), Chlorzoxazone (CYP2E1), Paclitaxel (CYP2C8) and midazolam (CYP3A4) under optimized incubation conditions and the samples were analysed using LC-MS/MS. The respective metabolites (i.e., 1-hydroxy tacrine/ 4-hydroxy Diclofenac/ 4-hydroxy mephenytoin/ Dextrophan/ 6-hydroxychlorzoxazone/ Hydroxy bupropion/ 6-hydroxy paclitaxel/ 1-hydroxy midazolam) were quantified. Garcinol, an active ingredient of *Garcinia cambogia* showed strong inhibition towards CYP enzymes with IC_{50} values of CYP1A2 (7.6 μ M), CYP2C9 (8.0 μ M), CYP2B6 (2.1 μ M), CYP2D6 (9.5 μ M) and CYP3A4 (5.1 μ M) and moderate inhibition towards CYP2C19 (16.4 μ M) and 2E1 (19.0 μ M). K_i values were calculated; 3.3 μ M, 3.5 μ M, 0.9 μ M, 4.2 μ M, 3.4 μ M, 1.9 μ M and 0.037 μ M for CYP1A2, CYP2C9, CYP2B6, CYP2D6, CYP3A4, CYP2C19 and 2E1 respectively. Green coffee bean extract showed inhibition towards CYP2B6 (70.3 μ M) and CYP2C9 (84.7 μ M) with K_i values of 31.2 μ M and 37.6 μ M respectively. These results indicate that herb-drug interactions may occur by Garcinol and Green coffee bean extracts which have the potential to inhibit CYP enzymes, thereby altering the metabolism of other drugs.

P112 - INTESTINAL ABSORPTION AND RODENT BRAIN EXPOSURE ESTIMATED BY LOW EFFLUX CELLS

Alicia Pietrasiewicz, Christopher Rowbottom, Sudarshan Kapadnis, and Elvana Veizaj

Biogen

Intrinsic permeability of small molecules has been assessed in-vitro with many tools such as polarized cell monolayers and non cell-based assays (physicochemical properties, PAMPA, etc). Recently the selection and development of a low efflux (LE) cell line has allowed for a high throughput mechanism to quantify para and transcellular permeability. The Madin-Darby canine kidney (MDCK) cell line is commonly used for single-transfection of MDR1 or BCRP. Due to the involvement of these transporters in restricting therapeutic small molecule Blood Brain Barrier (BBB) penetration, methodologies have been implemented to scale screening assays to 96-well transwell footprints. Using the existing HT plate formats and liquid handler methods for MDCK-MDR1 and -BCRP, from 40 clones, a single clone of MDCK cells (ATCC) was isolated by the dilution method^{1,2} which showed low functional active efflux by P-gp or BCRP via 20 probe substrates. Utilizing this MDCK-Low Efflux (LE) assay and 14 commercially available compounds, the intrinsic permeability ($P_{app\ a-b}$) was then calibrated to published human intestinal absorption. Based upon these compounds, an internal cutoff value was established, $P_{app\ a-b} > 5 \times 10^{-6}$ cm/s suggests >80% intestinal absorption is likely (previous studies correlate rat to human intestinal absorption very well, data not shown). We questioned if the ability of a compound to passively diffuse through the intestinal wall would quantifiably compare to the BBB, and if the same cutoff value can be used for BBB penetration, as measured by $K_{p,uu}$ (4 hour constant IV infusion). We selected over 40 commercial and internal Biogen compounds with various levels of intrinsic permeability and low active efflux for in-vitro and in-vivo assessment. Through this exercise we determined that a permeability cut-off value of $P_{app\ a-b} > 10 \times 10^{-6}$ cm/s in the MDCK-LE cell line is required for sufficient brain penetration of many early stage CNS programs (rat $K_{p,uu} > 0.35$).

References:

1. C Boiselle, D Bednarzyk, FASEB, 1 April 2015
2. Li Di, J Pharm Sci, 2011

P113 - HIGH-THROUGHPUT KIDNEY PROXIMAL TUBULES-ON-A-CHIP FOR PREDICTIVE RENAL TOXICITY SCREENING

Anthony Saleh¹, Marianne Vormann², Linda Gijzen², Remko van Vught², Sebastiaan Trietsch², Jos Joore², Paul Vulto², and Henriette Lanz²

¹Mimetas Inc, ²Mimetas BV

Drug toxicity remains a major issue in drug discovery and stresses the need for better predictive models. Here, we describe the development of a perfused renal proximal tubule cell (RPTC) model in Mimetas' OrganoPlates® to predict kidney toxicity. The OrganoPlate® is a microfluidic platform, which enables high-throughput culture of boundary tissues in miniaturized organ models. In OrganoPlates®, extracellular matrix (ECM) gels can be freely patterned in microchambers through the use of PhaseGuide technology. PhaseGuides (capillary pressure barriers) define channels within microchambers that can be used for ECM deposition or medium perfusion. The microfluidic channel dimensions not only allow solid tissue and barrier formation, but also perfused tubular epithelial vessel structures can be grown. The goal of developing a perfused RPTC model is to reconstruct viable and leak-tight boundaries for performing cytotoxicity, as well as transport and efficacy studies.

Human RPTC (SA7K clone, Sigma) were grown against an ECM in a 3channel OrganoPlate®, yielding access to both the apical and basal side. Confocal imaging revealed that the cells formed a tubular structure. Staining showed tight junction formations (ZO-1), cilia pointing into the lumen (acetylated tubulin) and correct polarization with microvilli on the apical side of the tubule (ezrin). Tightness of the boundary over several days was shown by diffusion of a dextran dye added to

the lumen of the tubule. Addition of toxic compounds resulted in disruption of the barrier which could be monitored in time. The time point of loss of integrity corresponds with the concentration and the toxic effect of the compound. Furthermore, fluorescent transport assays showed functional transport activity of in- and efflux transporters. Recently, even transporter-mediated drug interactions were demonstrated in this microfluidic *in vitro* system.

The 3D proximal tubules cultured in the OrganoPlate® are suitable for high-throughput toxicity screening, trans-epithelial transport studies, and complex co-culture models to recreate an *in vivo*-like microenvironment.

P114 - HUMAN EX VIVO MODEL TO STUDY INTESTINAL PROCESSES AND MICROBIOME INDUCED METABOLISM

Lianne Stevens¹, Irene Nooijen¹, Steven Erpelinck¹, Ronald Scott Obach², Gregory Walker², Frank Schuren¹, Angelique Speulman¹, Mariska Grollers¹, Wouter Vaes¹, Evita van de Steeg¹

¹TNO, ²Pfizer Inc.

A majority of the screening and predictive models do not reflect properly the physiological situation of the human intestinal tract resulting in low translational value to the clinical situation. Currently used models are not well suited to investigate the different processes that determine the oral bioavailability, such as intestinal metabolism or regional differences in absorption, or processes involved in general gut health aspects. Additionally, the presence of the microbiota is lacking in current predictive models despite having an important role in the metabolism of xenobiotics. Recent studies have interestingly linked the human gut microbiome to the efficacy and toxicity of prescribed drugs. It has been demonstrated that gut microbiota can directly metabolize xenobiotics into active, inactive or toxic metabolites, thereby influencing pharmacokinetics, efficacy and toxicity profiles of drugs. In order to be able to study these processes, highly realistic models resembling the human *in vivo* situation are needed, for instance *ex vivo* models.

TNO has developed two *ex vivo* predictive models, the InTESTine-on-a-chip model in which chronic drug exposure effects can be studied using a microfluidic device, and the I-screen platform which is a screening multi-well platform simulating the human colonic microbiota conditions to study microbiota induced metabolic transformation of drugs using pooled human colonic microbiota under fully anaerobic conditions.

Twelve drugs were tested in I-screen, among which five were demonstrated to generate metabolites (sulindac, sulfapyrazone, nizatidine, sulfasalazine, and risperidone), one (metronidazole) was observed to decline in incubations however metabolites were not detectable, and the other six were not shown to generate metabolites (omeprazole, simvastatin, levodopa, acetaminophen, zonisamide, and dapsone). Besides microbiome-induced metabolism, the effect of intestinal wall metabolism on absorption was shown in the InTESTine on-a-chip set-up applying human intestinal tissue and testosterone as a CYP3A4 substrate. We provide evidence that transport and metabolic functionality of the tissue was maintained during 24 hours. Within this timeframe the innate immune response was stimulated using known inflammatory stimuli flagellin, LPS and/or TNF by showing increased pro-inflammatory cytokine secretion (i.e. IL-8, IL-6, TNF- α).

Currently, we are investigating host-microbe interactions by co-culturing (supernatant of anaerobic) microbiota and human intestinal tissue, determining the inflammatory responses in the presence of various microbiota and effect on barrier integrity and intestinal absorption.

In conclusion, we here present two *ex vivo* models representing the microbiome and intestinal epithelium, which can be combined in order to create a physiological representation of human intestinal processes including intestinal permeability as well as (anaerobic) host-microbe-immune responses.

P115 - METHOD DEVELOPMENT FOR THE SOLUBILIZATION OF BIOLOGICAL MATRICES

Guy Webber and Sara Penketh

ENVIGO

Animal metabolism studies form a key part of the safety testing of pharmaceuticals and crop protection chemicals. They provide important supporting data for toxicity studies and whilst most commonly performed in the rat, studies in dogs, primates, livestock (hens and goats) and fish are also conducted. To allow absorption, distribution, metabolism and excretion to be followed the studies are conducted using a radiotracer incorporated into the test material. The most common radiotracers used are carbon-14 or tritium (hydrogen-3).

Measurement of the radiotracer within the biological matrices is performed using liquid scintillation counting (LSC). The use of automatic sample oxidisers for the processing of solid samples is a tried and tested process, widely accepted as a reliable way of determining radioactivity concentrations within a sample. However it is an expensive and time-consuming method for preparation prior to LSC. The work described focused on establishing solubilization processing methods to prepare samples for LSC, using reagents which are far cheaper and needing less man-hours compared to sample oxidation.

Experiments were conducted with rat feces and human whole blood samples containing carbon-14 or tritium radiolabel. To establish the solubilisation methods, samples were mixed with varying volumes of two different solubilizers (Goldisol or Soluene-350) in combination with two different types of scintillation fluid (UltimaGold or ProSafe). The results were compared with data obtained from sample oxidation and LSC using established protocols.

Replicate portions of feces homogenates were mixed with 1 or 2 mL of solubilizer. The mixtures were incubated at 55°C for at least 12 hours and scintillation fluid added prior to LSC. Counting parameters (eg SQPE and chemiluminescence) were within the instrument calibration range in all cases. For the optimized method, disintegrations per minute per gram (dpm/g) values were in the range 101.4 – 105.0% for [14C] and 103.1 – 104.0% for [3H] of expected values. For whole blood, replicate portions were solubilized using broadly the same approach as feces. In addition, trials were needed to establish the method for bleaching the samples due to the highly coloured content prior to LSC. The optimized method utilized 0.02M EDTA and hydrogen peroxide and gave dpm/g values compared to oxidation in the range 106.0 – 110.2% for [14C]. Results for [3H] samples were in the range 89.3 – 95.2% indicating the method required further optimization. Reproducibility of each solubilization method was confirmed with a variance of $\leq 3.8\%$. Future work will be conducted to establish solubilisation methods for other matrices. This will include chicken, goat, human and dog excreta; rat, goat and fish tissue samples.

P116 - CO-CULTURE OF PRIMARY HEPATIC STELLATE CELLS AND HEPATOCYTES IN MODELING OF LIVER FIBROSIS IN 2D AND 3D SPHEROIDS

Rafal Witek, Deborah Tieberg, Sujoy Lahiri, Bina Khaniya, Mark Kennedy, Michael Connolly, and Debra Johnson
Thermo Fisher Scientific

Human hepatic stellate cells (HSC) are the major contributor to collagen deposition following liver damage. During injury, hepatic stellate cells activate to a phenotype characterized by increased proliferation, motility, contractility, and synthesis of extracellular matrix components that results in progressive liver fibrosis. To understand the activation process of q-HSC and to facilitate cell-cell interactions and predict their effect on hepatocyte function, we have developed co-culture 2D and 3D spheroid systems to model the progression and reversion of liver fibrosis *in vitro*. Following isolation of q-HSC from human cadaveric tissue, their quiescence was indicated by the presence of vitamin A, the presence of GFAP and absence of α -SMA. As expected, after plating and culturing for 10 days on rigid plastic, q-HSC activated to the myofibroblastic (MF) phenotype, which is shown by increased α -SMA expression. Activated HSCs were also positive for Vimentin and CD271 indicating their mesenchymal origin. In order to determine the role of various factors on the activation, q-HSC were maintained in culture until viable culture was established after which they were cryopreserved at passage 5 and used for all subsequent experiments. Using 2D and 3D co-culture systems, TGF- β , PDGF, and *Methotrexate* were used to induce MF-HSC to produce ECM and to stimulate cytokine, chemokine, and growth factor production as observed in the physiological *in-vivo* setting during fibrogenic liver injury. This response was monitored by Luminex multiplex panels and qRT-PCR that were used to evaluate protein release and gene expression. When co-cultured with hepatocytes, either in 2D plated plates or 3D spheroid cultures, HSCs stabilized cultures of primary human hepatocytes and elicited responses observed during liver fibrosis that included significantly upregulated collagen deposition and α -SMA expression. In conclusion, we have generated primary human quiescent and activated hepatic stellate cells with high purity and function. Those cells can be co-cultured in 2D plated system and 3D spheroid system to model the liver fibrogenic response. Our data indicates involvement of HSC produced growth factors, cytokines and chemokines in function of hepatocytes with implications in modeling fibrosis for drug metabolism and toxicity testing.

P117 - ABSTRACT WITHDRAWN

P118 - QUANTITATIVE MASS BALANCE, TISSUE DISTRIBUTION, PHARMACOKINETICS AND BIOTRANSFORMATION PATHWAY OF PRALICIGUAT, A CLINICAL-STAGE SGC STIMULATOR, AFTER ORAL ADMINISTRATION IN RATS

Ali Banijamali, Andrew Carvalho, James Wakefield, Peter Germano, Maria Ribadeneira, Timothy Barden, Daniel Zimmer, Jaime Masferrer, Albert Profy, Mark Currie, Todd Milne, and Peter Germano
Ironwood Pharmaceuticals

Praliciguat (IW-1973) is a selective soluble guanylate cyclase (sGC) stimulator in Phase 2 clinical development for the treatment of diabetic nephropathy and heart failure with preserved ejection fraction. The pharmacokinetics (PK), metabolism, excretion, mass balance, and tissue distribution of [¹⁴C]praliciguat were evaluated following oral administration of a 3-mg/kg dose in a mass-balance study conducted in Sprague-Dawley rats and in a quantitative whole-body autoradiography (QWBA) study conducted in male Long-Evans rats. Plasma T_{max} was 1 h and the $t_{1/2}$ of total plasma radioactivity was 23.7 h. Unchanged praliciguat accounted for 87.4% of the total radioactivity in plasma through 48 h (AUC_{0-48h}). A minor circulating metabolite, (*N*-dealkylated-praliciguat) accounted for 7.6% of AUC_{0-48h} . High tissue-to-plasma AUC_{all} ratios were observed for liver, kidney, lung, heart, brown and white adipose and lower ratios were observed in bone and pigmented eye lens. Most of the [¹⁴C]praliciguat-derived radioactivity was excreted within 48 hours after oral administration. Mean cumulative recovery of the administered radioactivity in urine and feces over 168 h was 3.7 and 95.7%, respectively. No quantifiable unchanged praliciguat was recovered in urine or bile from cannulated rats; however, based on the total radioactivity in these fluids, a minimum of approximately 82% of the orally administered dose was absorbed. [¹⁴C]Praliciguat was extensively metabolized in rats via hydroxylation, *N*-dealkylation, glucuronidation, sulfation,

and glutathione conjugation. The most abundant metabolites recovered in bile were praliguat-glucuronide and hydroxy-praliguat-glucuronide. These results indicate that praliguat had rapid absorption, high bioavailability, a $t_{1/2}$ consistent with once-daily dosing in human, and elimination primarily via hepatic metabolism. High tissue-to-plasma ratios support investigation of praliguat for diseases associated with tissue inflammation and fibrosis.

P119 - LAMISIL (TERBINAFINE): DETERMINING BIOACTIVATION PATHWAYS USING COMPUTATIONAL MODELING AND EXPERIMENTAL APPROACHES

Dustyn Barnette¹, Mary Davis¹, Lena Dang², S. Joshua Swamidass², and Grover Miller¹

¹University of AR for Medical Sciences, ²Washington University - St. Louis

Lamisil (terbinafine) may cause idiosyncratic liver toxicity through a proposed toxicological mechanism involving the reactive metabolite 6,6-dimethyl-2-hepten-4-ynal (TBF-A). TBF-A toxicological relevance remains unclear due to a lack of identification of pathways leading to and competing with TBF-A formation. We resolved this knowledge gap by combining computational and experimental modeling of *in vitro* hepatic N-dealkylation of terbinafine. Our deep learning model predicted a high probability for N-demethylation to yield desmethyl-terbinafine followed by N-dealkylation to TBF-A and marginal contributions from other possible pathways. Moreover, we carried out steady-state kinetic experiments with pooled human liver microsomes that relied on development of labeling methods to expand metabolite characterization. Those efforts revealed high levels of TBF-A formation and first order decay during metabolic reactions; actual TBF-A levels would then reflect the balance between those processes as well as reflect the impact of stabilizing adduction with glutathione and other biological molecules. Modeling predictions and experimental studies agreed on the significance of N-demethylation and insignificance of N-dealkylation in terbinafine metabolism, yet differed on importance of direct TBF-A formation. Under steady-state conditions, that pathway was the most important source of the reactive metabolite. Nevertheless, therapeutic dosing leads to accumulation of desmethyl-terbinafine due to poor clearance so that likely sources for TBF-A would draw from metabolism of the major metabolite and parent drug based on our modeling and experimental studies. Through this combination of novel modeling and experimental approaches, we are the first to identify pathways leading to generation of TBF-A for assessing its role in idiosyncratic adverse drug interactions.

P120 - METABOLISM OF PEVONEDISTAT IN PATIENTS WITH ADVANCED SOLID TUMORS AFTER INTRAVENOUS INFUSION OF [¹⁴C] PEVONEDISTAT

Hao Chen, Xiaofei Zhou, Farhad Sedarati, Lawrence H. Cohen, Sandeepraj Pusalkar, Karthik Venkatakrishnan, Swapan Chowdhury, and Jayaprakasam Bolleddula

Millennium Pharmaceuticals, Inc., a wholly owned subsidiary of Takeda Pharmaceutical Company Limited

Pevonedistat (MLN4924; TAK-924) is a first-in-class inhibitor of the NEDD8-activating enzyme (NAE) currently in clinical development across multiple cancers, including low-blast AML and higher risk MDS. A clinical study (NCT03057366) was conducted to determine mass balance, metabolism, and excretion of [¹⁴C]pevonedistat in seven patients with advanced solid tumors after a 1-hour IV infusion of [¹⁴C]pevonedistat at 25 mg/m² (60~80 mCi radioactive dose). A total of greater than 95% of the administered radioactivity was recovered, with ~42% and ~54% eliminated in urine and feces, respectively. The metabolite profiles of [¹⁴C]pevonedistat in plasma were established using HPLC fractionation and accelerator mass spectrometer (AMS) and those in excreta (urine and feces) by HPLC coupled to traditional radiometric analysis. The metabolite identification and structure elucidation was performed using LC-HRMS analysis. Pevonedistat undergoes extensive biotransformation in humans after a single IV dose of [¹⁴C]pevonedistat. Unchanged parent drug accounted for approximately 49% of total circulating radioactivity. The major metabolites were M1 and M2 (>10% of total radioactivity) in plasma and accounted for approximately 15% and 22% of the total radioactivity, respectively. M1 resulted from hydroxylation and M2 from hydroxylation followed by further oxidation to a ketone. M3 (hydroxylation) and M10b (hydroxylation and glucuronidation) represented approximately 5% and 7% of the total circulating plasma radioactivity, respectively. In urine, unchanged pevonedistat accounted for approximately 4% of the dose. Metabolite M1 is the major metabolite in urine and accounted for approximately 20% of the total administered dose. Metabolites M2 and M3 represented approximately 8% and 4% of the administered dose, respectively. In feces, M2 was the most abundant drug-related component and represented approximately 18% of the administered dose. Unchanged pevonedistat accounted for 17% of the dose in feces. Metabolites M1 and M3 accounted for approximately 7% and 11% of the administered dose, respectively. Overall, pevonedistat was primarily eliminated via oxidation to M1, M2, and M3 which accounted for 27%, 26%, and 15% of the administered dose, respectively.

Reaction phenotyping studies suggest contributions of CYP3A4/5 as well as extrahepatic CYPs 1A1 and 2J2 for clearance of pevonedistat, which may potentially explain the observed lack of clinically relevant impact of strong CYP3A inhibition on the pharmacokinetics of pevonedistat after intravenous administration in a clinical drug-drug interaction study with itraconazole¹.

Reference:

1. Faessel HM, Harvey RD, Lockhart AC, Bauer TM, Wang L, Sedarati F, Santillana S, Nemunaitis JJ. Drug-drug interaction study between the investigational NAE inhibitor pevonedistat (TAK-924/MLN4924) and fluconazole or itraconazole in patients with advanced solid tumors. ASCPT Annual Meeting, March 91-12, 2016, San Deigo, CA.

P121 - STUDYING THE METABOLISM OF SUNSCREEN COMPOUNDS *IN VITRO* BY LC-MS/MS

Amal Guesmi, Meriem Benmaouche, Leanne Ohlund, and Lekha Sleno

UQAM

The exposure to UV radiation can induce adverse effects on human health, such as photo-aging, immunosuppression and cancers. Sunscreens are used as UV protection agents. However, some UV filters can also act as endocrine disruptors and carcinogens. The metabolism of active ingredients contained in sunscreens was studied using human and rat liver microsomes with liquid chromatography coupled to high-resolution tandem mass spectrometry. A focus of this study was to determine if these compounds can form reactive metabolites with potential toxic effects.

Six sunscreen compounds, including avobenzone, oxybenzone, homosalate, octisalate, octinoxate and octocrylene, were incubated with human and rat liver microsomes, NADPH and GSH. Controls were prepared without cofactors. Metabolite analysis was performed on a Shimadzu Nexera HPLC coupled with a Sciex 5600 TripleTOF system, in positive and negative electrospray mode. LC separation used a biphenyl reversed-phase column and gradient elution with water and ACN (both with 0.1% formic acid). Data were examined using Metabolite Pilot, and Masterview softwares (Sciex) to find metabolites and adducts formed in these incubations.

We have detected GSH adducts in four of the tested compounds in both human and rat. We also detected hydrolysis products under incubation conditions for compounds containing ester groups. Avobenzone forms an isomer from the transition between keto to enol forms of the molecule, which causes interpretation of the metabolism results to be more complicated. High resolution MS/MS data was used for structural elucidation of metabolites.

P122 - PREDICTION OF HUMAN-SPECIFIC METABOLITES OF MIANSERIN, CYPROHEPTADINE, AND CARBAZERAN USING CHIMERIC MICE WITH HUMANIZED LIVER (PXB-MICE)

Suguru Kato¹, Abhi Shah¹, Jessica Wisniewski¹, Yoshinari Miyata², Swapan Chowdhury¹, and Jayaprakasam Bolleddula¹

¹Takeda Pharmaceuticals International Co, ²PhoenixBio USA Corporation

The translation of preclinical metabolism results to humans is often challenging because of differential expression of metabolic enzymes between humans and preclinical species. Sometimes, metabolites may be human specific or formed in less abundance in preclinical species; hence, an understanding of human metabolism is very important in discovery and early stages of drug development. Recently there has been significant interest in developing alternative tools to assess human metabolism at preclinical stages of drug development. One such model is composed of chimeric mice with a humanized liver (PXB-mice), generated by grafting cDNA-urokinase-type plasminogen activator (cDNA-uPA)/severe combined immunodeficient (SCID) mice with human hepatocytes; the PXB-mice then become highly repopulated by human hepatocytes (>70%). PXB-mice have been utilized in various Drug Metabolism and Pharmacokinetics (DMPK) applications, including prediction of human metabolites, determining drug induction and inhibition properties, human pharmacokinetic (PK) prediction, etc. In the present study, three compounds, mianserin, cyproheptadine, and carbazeran, were used to predict human-specific and disproportionate metabolites using PXB-mice (SCID mice were used as controls). Mianserin and cyproheptadine are known to generate human-specific metabolites by UGT1A4 and carbazeran has been reported to generate disproportionate human metabolites through aldehyde oxidase (AO) catalyses. After a single oral administration of [³H]mianserin, [³H]carbazeran, and cyproheptadine to PXB-mice and SCID mice, blood (processed into plasma), urine, bile, and feces were collected. The samples were processed and analyzed by liquid chromatography-mass spectrometry (LC/MS) and/or via a radiometric detector to establish the metabolite profiles. Quaternary ammonium glucuronide was a major metabolite in PXB-mice but not in SCID mice dosed with cyproheptadine. Similarly, direct glucuronide isomer (quaternary) metabolites were observed in PXB-mice but were absent in SCID mice dosed with mianserin. Interestingly, a direct glucuronide of carbazeran was observed as a major metabolite along with AO-mediated oxidative metabolites disproportionately in PXB-mice as compared to SCID mice. Although a direct glucuronide metabolite was not reported in the corresponding human mass balance study, a recent study conducted using a micropatterned co-culture hepatocyte system showed that a direct glucuronide metabolite was formed disproportionately in humans. In summary, the results from the present study demonstrated that the PXB-Mouse model predicted human-specific metabolites for mianserin and cyproheptadine and disproportionate metabolites for carbazeran. Hence, PXB-mice can be used as a potential tool for the prediction of human-specific and disproportionate metabolites.

P123 - METABOLITE PROFILING USING DRIED BLOOD SPOT**Kishore Katyayan** and Yu-Hua Hui

Eli Lilly and Company

In present study, we investigated use of DBS for metabolite profiling of six compounds following oral and intravenous dosing to male Sprague Dawley rats. Six compounds selected were genistein, carbamazepine, losartan, sunitinib, sildenafil, and zonisamide that are metabolized by a variety of enzymes including cytochrome P450s, uridine 5'-diphosphoglucuronosyltransferase, aldehyde oxidase and combination of thereof. Rats were dosed orally and intravenously, plasma and DBS were collected at various time points, and PK and metabolite profile were determined. Method development including extraction using different reagents and recovery in DBS was optimized using the parent compound and at least one metabolite of each of these six compounds by spiking standard solutions in to blood and then spotting onto DBS cards and comparing with rat plasma and neat standards. Similar evaluation was also done in human DBS. In general, recovery and lower limit of quantification (LLOQ) in human DBS was similar to human plasma and was also similar to in rat DBS and plasma. Rat DBS metabolite profile of six compounds were similar to plasma metabolite profile, however phase II metabolites (and unstable compounds) appeared to be harder to extract than phase I metabolites. PK parameters of the parent were determined by DBS sample analysis and compared with the literature values. In summary, the study showed that the DBS could be very useful not only for bioanalytical assays but also for metabolite profiling.

P124 - COPE ELIMINATION MEDIATED BY HUMAN FMO1 LEADS TO FORMATION OF REACTIVE MICHAEL ACCEPTOR INTERMEDIATE**Weidong Lai**¹, Amy Siu¹, Robert Yu¹, and George Moniz²¹Eisai Inc., ²Biogen Inc.

E7016 was an inhibitor of poly (ADP-ribose) polymerase and investigated for anticancer therapy. The study revealed the role of flavin-containing monooxygenase (FMO) 1 in the metabolism E7016 that involved with a unique two-step oxidation process: dehydrogenation of the 4-hydroxypiperidine to a 4-piperidone followed by FMO1-mediated Cope elimination to a reactive Michael Acceptor intermediate which could be trapped by either water or glutathione (GSH) resulting in ring-opening adduct with protonated molecular ion (MH⁺) of *m/z* 382 or 671, respectively. This metabolic pathway was demonstrated in both human kidney S9 fractions and recombinant FMO1 fortified with kidney cytosol. In these systems, the reaction circle was found to be NAD(P)⁺-dependent and could be inhibited by 4-methylpyrazole, methimazole, or a heat treatment. The two steps of oxidation were apparently self-sustained by regeneration of cofactors for each other. Further proving the proposed mechanism, the 4-piperidone intermediate (ER-879819) could be directly bioactivated by either human kidney microsomes or recombinant FMO1 in an NAD(P)H-dependent manner, leading to the same ring-opening adduct with either water or GSH. Structures of these adducts were elucidated based on tandem mass spectrometry (MS/MS) and nuclear magnetic resonance (NMR), and confirmed the proposed bioactivation mechanism. This is a novel and unique case of generating a reactive Michael Acceptor via FMO-mediated Cope elimination reaction.

P125 - BIOTRANSFORMATION OF PYRROLIZIDINE ALKALOID N-OXIDE TO HEPATOTOXIC PYRROLIZIDINE ALKALOID**Ge Lin** and Mengbi Yang

The Chinese University of Hong Kong

Pyrrrolizidine alkaloids (PAs) are one of the most significant groups of phytotoxins present in over 6000 plants in the world. PA-induced hepatotoxicity is known for a long time and has been extensively studied. Numerous liver injury cases have been reported associated with the intake of PA-containing plants and PA-contaminated foodstuffs. PAs elicit hepatotoxicity via metabolic activation mediated by cytochrome P450 monooxygenases (CYPs) to form reactive metabolites, which interact with proteins to generate metabolite-derived protein adducts (pyrrole-protein adducts) leading to toxicity. Hepatotoxic PAs and their corresponding PA *N*-oxides co-exist with variable compositions in plants. However, the toxicity of PA *N*-oxide is rarely investigated. Recently, we reported PA *N*-oxide-induced hepatotoxicity in humans and rodents, but the toxic potency of PA *N*-oxides was significantly lower than the corresponding PAs. We also suggested that metabolic conversion of PA *N*-oxides to the toxic PAs might be associated with PA *N*-oxide intoxication. However, the details of metabolism-mediated PA *N*-oxide-induced hepatotoxicity is largely unknown. The present study, using male SD rat model, investigated biotransformation of representative PA *N*-oxides to the corresponding PAs in both gastrointestinal tract and liver and pharmacokinetics of PAs and PA *N*-oxides by UHPLC-MS analysis of all biological samples. The results demonstrated that biotransformation of PA *N*-oxides to PAs was mediated primarily by intestinal microbiota and also by hepatic CYPs. Subsequently, the formed PAs were metabolically activated predominantly by hepatic CYPs to form reactive metabolites exerting toxicity. Pharmacokinetic profiles of PA and PA *N*-oxide were significantly different. PAs demonstrated very short T_{max} and high C_{max}, whereas PA *N*-oxides had delayed T_{max} and lower C_{max}. In PA *N*-oxide-treated groups, the corresponding PAs were determined as the major metabolites and their pharmacokinetic profiles followed the same trend as PA *N*-oxides. For instance, comparing retrorsine *N*-oxide with retrorsine, significantly lower C_{max} of the

formed PAs were determined in PA *N*-oxide-dosed rats than that of PA-dosed rats 347.1 ± 66.5 vs 2658.3 ± 740.9 ng/mL, $p < 0.001$), indicating significantly lower exposure to toxic PAs after the intake of PA *N*-oxide. Further, the formation of hepatic pyrrole-protein adducts was also significantly lower in *N*-oxide-dosed group than that in PA-dosed group (1.61 ± 0.15 vs 3.26 ± 0.13 nmol/g, $p < 0.001$). Our findings delineated, for the first time, that the metabolism-mediated PA *N*-oxide intoxication involved the biotransformation of PA *N*-oxides to their corresponding PAs primarily in the intestine followed by metabolic activation of the resultant PAs in the liver to generate reactive metabolites which interact with cellular proteins leading to hepatotoxicity. However, the significantly lower exposure to toxic PA and the resultant less formation of pyrrole-protein adducts after PA *N*-oxide dosing were proven as the principal reason for the remarkably lower hepatotoxic potency of PA *N*-oxide.

The present studies were supported by Research Grant Council of Hong Kong (GRF Grant, Project No.: 14111816) and CUHK (Direct Grants: 4054302)

P126 - COMPARATIVE BIOTRANSFORMATION AND MASS-BALANCE OF [¹⁴C] BMS-986205, AN INHIBITOR OF IDO1, AFTER ORAL ADMINISTRATION TO RATS, DOGS AND HUMANS

Peggy Liu-kreyche, Li Ma, Wenying Li, Ramaswamy Iyer, and William Humphreys

Bristol-Myers Squibb

BMS-986205 is an orally available, active, potent and selective small molecule inhibitor of IDO1 enzyme and is currently in phase III evaluation for multiple malignancies. A series of studies were conducted to determine the routes of excretion and biotransformation of [¹⁴C]BMS-986205 following oral administration to intact and bile-duct cannulated (BDC) rats, dogs, and humans. Urine, bile, feces, and plasma samples were collected at various time intervals and measured for radioactivity by liquid scintillation counting. Metabolites of [¹⁴C]BMS-986205 were profiled with HPLC-MS and HPLC-radioactivity detection. BMS-986205-derived radioactivity was eliminated mainly via fecal excretion in rats, dogs and humans. Percent radioactivity dose recovered in feces ranged from 70.0% in rats and 19.7% in dogs. Percent radioactivity dose recovered in urine ranged from 27.1% in rats and 35.7% in dogs. In human, in the bile collection group ($n=3$), 9.5% of radioactive dose was recovered in bile during the 6 h collection period; 17.3% and 66.4% of the dose was recovered in the urine and feces, respectively. For the non-bile collection group ($n=6$), 14.4% and 79.4% of the dose was recovered in the urine and feces, respectively. The extent of *in vivo* metabolism was similar in animals compared to humans. The parent compound comprised of <5 % of the excreted dose (urine + feces), indicating that BMS-986205 was highly metabolized in all species. The pathways for metabolism of BMS-986205 were hydrolysis (esterase-mediated: CES1, CES2, ~7% of dose) and oxidation (mediated by CYP3A4 and CYP1A1/A2, about 80% of dose) followed by formation of glucuronide, sulfate and GSH conjugates. All metabolites found in humans were found in at least one of the animal species.

P127 - CONTRIBUTION OF UGT1A1, CYP2A6, CYP2C9, AND CYP3A4 IN METABOLISM OF BELINOSTAT

Gang Luo¹, Michael Schicker¹, Deborah Lee¹, Sara Leitz¹, Donald McKenzie¹, Daniel Albaugh¹, and Guru Reddy²

¹Covance Laboratories Inc., ²Spectrum Pharmaceuticals, Inc.

Belinostat, a potent inhibitor of class I and class II histone deacetylase enzymes, has been approved for the treatment of patients with relapsed or refractory peripheral T-cell lymphoma. Previous work demonstrated that UGT1A1-mediated glucuronidation was a significant metabolic pathway of belinostat. A separate report suggests that belinostat was metabolized by recombinant human CYP enzymes. In the present study, contribution of UGT1A1, CYP2A6, CYP2C9, and CYP3A4 in metabolism of ¹⁴C-belinostat was assessed using *in vitro* test systems. ¹⁴C-Belinostat was extensively metabolized by human liver microsomes (HLM) in the presence of both uridine 5'-diphosphoglucuronic acid (UGPDA) and dihydronicotinamide-adenine dinucleotide phosphate (NADPH). Identified metabolites include belinostat glucuronide (major), belinostat amide (minor), and belinostat acid (minor). For example, belinostat glucuronide, belinostat amide, and belinostat acid accounted for 54.6 to 55.1, 2.68 to 2.71, and 1.45 to 1.78% of the total radioactivity, respectively, after ¹⁴C-belinostat (10 and 100 μ M) was incubated with human hepatic microsomes (1 mg/mL) for 60 minutes. K_m and V_{max} of glucuronidation were determined to be 72.8 μ M and 2160 pmol/min/mg, respectively. The projected hepatic clearances obtained from time-dependent total metabolism of belinostat (9.67 to 10.8 mL/min/kg) and from K_m/V_{max} (12.9 mL/min/kg) of belinostat glucuronidation were equivalent to human *in vivo* clearance (estimated as 12.6 to 14.7 mL/min/kg). Rates of belinostat glucuronidation by HLM prepared from six individual UGT1A1 genotyped donors were significant different between allelic variants of *1*1 and *28*28) and highly correlated with that of estradiol glucuronidation ($r^2 = 0.9613$). Belinostat amide and acid generated in HLM from all six donors were minor, and more importantly, their amounts were almost identical among the different UGT1A1 genotyped donors. Therefore, it was concluded that UGT1A1 plays a predominant role whereas CYP enzymes play little or no role in metabolism of belinostat.

P128 - UNRAVELING THE METABOLIC FATE OF POTENTIAL THERAPEUTIC DIMER COMPOUNDS FOR PARKINSON'S DISEASE

Chukwunonso Nwabuo and Edward Krol
University of Saskatchewan

Disease-modifying treatments and improved diagnostic tools are a major focus of research in Parkinson's disease (PD). Alpha-synuclein (AS) has been identified as a putative target for drug discovery and diagnosis in PD(1). Recently, we reported that two dimer compounds comprising of a caffeine scaffold attached to nicotine (C₈-6-N), and 1-aminoindan (C₈-6-I) were the most promising candidates in preventing AS-induced cell death in a yeast model of PD(2). Although Caffeine linked to Caffeine (C₈-6-C₈) did not show therapeutic potentials, its sufficient binding to AS makes it a suitable candidate for the development of imaging probes for diagnosis of PD. Given the therapeutic and diagnostic potentials of these novel compounds, it is of great importance to understand their metabolic profile. We are investigating the *in vitro* metabolic profile of these compounds in human liver microsomes (HLM), rat liver microsomes (RLM), and mouse liver microsomes (MLM), and will use the information obtained from this study to guide our design and development of Fluorine-18(¹⁸F) labeled dimer compounds towards their use in treatment or diagnosis of PD. In addition, comparison of the metabolic profile of C₈-6-N, C₈-6-I, and C₈-6-C₈ in RLM and MLM with those of HLM will help to identify the most relevant model for future toxicological studies. We performed *in-vitro* incubations of C₈-6-N, C₈-6-I, and C₈-6-C₈ using HLM, MLM, and RLM at 37°C for 60 minutes. Chlorzoxazone conversion to 6-hydroxychlorzoxazone was used as a positive control for HLM, MLM, and RLM viability, negative controls included incubations in the absence of NADPH or with heat-inactivated microsomes. The metabolites were identified and confirmed with accurate mass measurement and tandem mass spectrometry using a quadrupole/time of flight mass spectrometer (QToF). Two metabolites were identified for both C₈-6-I and C₈-6-N, whereas no metabolite was observed for C₈-6-C₈. The metabolites identified for C₈-6-I were generated from de-alkylation (M1) and hydroxylation (M2) while for C₈-6-N, the metabolites corresponded to de-alkylation (M3) and hydroxylation (M4). Although C₈-6-N and C₈-6-I are metabolized in HLM, MLM, and RLM, C₈-6-N undergoes extensive metabolism as it was depleted within the 60 minutes incubation period. Furthermore, the metabolism of C₈-6-N and C₈-6-I is dependent on NADPH and active liver microsomes. The same metabolic profile was observed for C₈-6-N and C₈-6-I in HLM, MLM, and RLM. Consequently, mouse and rat may be useful models for future toxicological studies of C₈-6-I and C₈-6-N. The tandem mass spectrometric information obtained from this study may be useful for future pharmacokinetic studies of C₈-6-N, C₈-6-I, and C₈-6-C₈.

References

1. Kakish J, Lee D, Lee JS. Drugs That Bind to alpha-Synuclein: Neuroprotective or Neurotoxic? ACS Chem Neurosci. 2015;6(12):1930-40.
2. Kakish J, Allen KJ, Harkness TA, Krol ES, Lee JS. Novel Dimer Compounds That Bind alpha-Synuclein Can Rescue Cell Growth in a Yeast Model Overexpressing alpha-Synuclein. A Possible Prevention Strategy for Parkinson's Disease. ACS Chem Neurosci. 2016;7(12):1671-80.

P129 - SEQUENTIAL METABOLISM KINETICS OF Δ⁹-TETRAHYDROCANNABINOL (THC) AND ITS PSYCHOACTIVE 11-OH-THC METABOLITE

Gabriela Patilea-Vrana and Jashvant Unadkat
University Washington

Aims: Use of marijuana during pregnancy has been associated with negative fetal outcomes. These risks may be perpetrated by fetal exposure to the most abundant and psychoactive component in marijuana, Δ⁹-tetrahydrocannabinol (THC) and its psychoactive metabolite 11-hydroxy-Δ⁹-THC (11-OH-THC). Since fetal cannabinoid exposure, and therefore fetal risk, will be driven by maternal concentrations, it is necessary to predict maternal cannabinoid disposition. Here, we report hepatic metabolism kinetic parameters (V_{max} and K_m) necessary to predict maternal-fetal cannabinoid exposure through our published maternal-fetal physiologically-based pharmacokinetic (PBPK) model. **Methods:** Substrate depletion studies of THC (0.01 – 14 μM) and 11-OH-THC (0.01 – 60 μM), were conducted using pooled (n=50) human liver microsomes (HLMs) in the presence of co-factors NADPH (CYP enzymes) and UDPGA (UGT enzymes). Substrate depletion and metabolite formation was monitored via LC-MS/MS. Final parameters (V_{max} and K_m) were estimated using a population PK approach, where datasets from 3-4 independent experiments were simultaneously analyzed using a comprehensive sequential metabolism model (Figure 1) built in Phoenix (Certara). The final model was selected based on the following criteria: -2LL, AIC, BIC, visual predictive check, and diagnostic goodness-of-fit plots. The tube adsorption method was used to quantify microsomal binding ($f_{u,mic}$) of THC/11-OH-THC (n=4). **Results:** Table 1 shows the final population estimates and $f_{u,mic}$ values. 11-OH-THC formation accounts for 71% of THC depletion. Formation of COOH-THC via CYPs accounts for 4.3% of 11-OH-THC depletion. UGT and CYP enzymes account for 72% and 28% depletion of 11-OH-THC, respectively. **Conclusions:** Kinetic results (CL_{int}) are similar to the fractional contribution (fm) values we previously estimated for THC/11-OH-THC. In those depletion studies, at clinically relevant plasma concentrations of THC/11-OH-THC in the presence of selective inhibitors, we found that CYP2C9 primarily depletes THC (fm = 0.97) and

forms 11-OH-THC ($f_m = 0.90$), CYP3A4 primarily depletes 11-OH-THC ($f_m = 0.75$) and UGT and CYP enzymes contribute to 60% and 40% of total 11-OH-THC depletion, respectively. The reported fraction unbound of THC in plasma is comparable to the $f_{u,mic}$ values reported here. Considering the different THC plasma concentrations achieved via inhalation (0.09 – 0.73 μM) versus oral administration (0.001 – 0.045 μM), 11-OH-THC formation will be saturated in the former but not the latter. Interestingly, COOH-THC was not the main metabolite of 11-OH-THC, even though it is the most abundant circulating plasma metabolite. The mechanistic data presented here, along with cannabinoid fractional enzyme contribution, will be incorporated into our maternal-fetal PBPK model to predict cannabinoid maternal and fetal exposure throughout pregnancy.

Supported by NCATS TL1 TR000422 and NIDA P01DA032507.

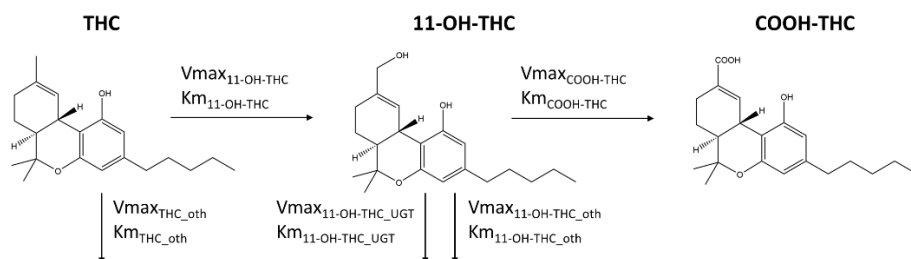


Figure 1. Sequential metabolism model for THC/11-OH-THC

	Estimate (CV%)	CL _{int} (ml/min/mg)	f _{u,mic} (mean±SD)	CL _{int,u} (ml/min/mg)
V _{max} _{11-OH-THC} (nmol/min/mg)	0.699 (7.2%)	6.79	THC 0.04 ± 0.02	168
K _m _{11-OH-THC} (μM)	0.103 (12%)			
V _{max} _{THC_oth} (nmol/min/mg)	3.86 (23%)	2.83	11-OH-THC 0.06 ± 0.03	70.8
K _m _{THC_oth} (μM)	1.36 (45%)			
V _{max} _{COOH-THC} (nmol/min/mg)	0.005 (7.2%)	0.009	11-OH-THC 0.06 ± 0.03	0.156
K _m _{COOH-THC} (μM)	0.577 (20%)			
V _{max} _{11-OH-THC_oth} (nmol/min/mg)	2.07 (34%)	0.211	11-OH-THC 0.06 ± 0.03	3.46
K _m _{11-OH-THC_oth} (μM)	9.78 (41%)			
V _{max} _{11-OH-THC_UGT} (nmol/min/mg)	0.412 (16%)	0.506	11-OH-THC 0.06 ± 0.03	8.30
K _m _{11-OH-THC_UGT} (μM)	0.814 (22%)			

P130 - POTENTIAL EXPOSURE TO DI-2-ETHYLHEXYL TEREPHTHALATE AND DINCH, TWO PHTHALATE REPLACEMENTS, IN AMERICAN ADULTS

Manori Silva, James Preau, Ella Samandar, Lily Jia, Antonia Calafat, and Xiaoyun Ye
Centers for Disease Control and Prevention

Because of concerns and uncertainty over potential adverse health effects, the Consumer Products Safety Improvement Act of 2008 banned the use of six phthalates, including di-isononyl phthalate (DINP) and di-2-ethylhexyl phthalate (DEHP), in children's toys in the United States. As a result, industries substituted phthalates for other alternative chemicals in their products, including children's products. We quantified the urinary concentrations of oxidative metabolites of two of these phthalate alternatives, namely 1,2-cyclohexane dicarboxylic acid, diisononyl ester (DINCH), a complex mixture of nine-carbon branched-chain isomers used as a replacement plasticizer for DINP, and di-2-ethylhexyl terephthalate (DEHTP), a structural isomer of DEHP by online solid phase extraction-high performance liquid chromatography-tandem mass spectrometry. We examined the concentrations of these metabolites in urine collected anonymously between 2000 and 2017 from convenience samples of U.S. adults. The detection frequency of the concentrations of DINCH biomarkers, cyclohexane-1,2-dicarboxylic acid-monocarboxy isooctyl ester (MCOCH), and cyclohexane-1,2-dicarboxylic acid-mono(hydroxy-isononyl) ester (MHNCH), in urine collected in 2007 (N=23), 2009 (N=118), 2011 (N=94), 2012 (N=121) and 2017 (N=100) progressively increased over time. DINCH metabolites were not detected in samples collected in 2000 (N=114) and 2001 (N=57). Similarly, in urine collected in 2000 (N=44), 2009 (N=61), 2011 (N=50), 2013 (N=60), 2016 (N=149) and 2017 (N=100), we observed progressively increasing concentrations and detection frequencies of two DEHTP biomarkers, mono-2-ethyl-5-carboxypentyl terephthalate (MECPTP) and mono-2-ethyl-5-hydroxyhexyl terephthalate (MEHHTP). For comparison, we also quantified the analogous DEHP metabolites mono-2-ethyl-5-hydroxyhexyl phthalate (MEHHP) and mono-2-ethyl-5-carboxypentyl phthalate

(MECPP). We observed a downward trend in urinary concentrations of MEHHP and MECPP from 2000 to 2017. These preliminary data suggest that exposure to DINCH and DEHP might be increasing in the United States whereas exposure to DEHP is decreasing.

P131 - THERAPEUTIC TARGETING OF THE PYRUVATE DEHYDROGENASE COMPLEX/ PYRUVATE DEHYDROGENASE KINASE (PDC/PDK) AXIS FOR CONGENITAL AND ACQUIRED METABOLIC DISEASES

Peter Stacpoole and Aaron Aponick
University of Florida

The mitochondrial PDC irreversibly decarboxylates pyruvate to form acetyl coenzyme A, thereby linking glycolysis to the tricarboxylic acid cycle and defining a critical step in cellular bioenergetics. PDC activity may be compromised by both loss-of-function mutations in any component of the complex (congenital PDC deficiency) or by up-regulation of any of four PDK isoforms that inhibit PDC by phosphorylation. This latter mechanism has been associated with an ever-expanding list of congenital or acquired disorders of metabolic integration. These include genetic diseases (e.g., Friedrick's ataxia, amyotrophic lateral sclerosis) not caused by PDC mutations and diverse inflammatory and proliferative conditions (e.g., pulmonary or cardiovascular diseases, insulin resistance syndromes and cancer) in which one or more PDKs is over-expressed.

Heightened appreciation of the integral role of the PDC/PDK axis in human disease has led to the development of a new generation of small molecule PDK inhibitors both by academia and by industry. Although many structurally unique compounds have been prepared, a sizeable percentage of these new molecules is based structurally on dichloroacetate (DCA), the prototypic PDK inhibitor and one of only two such compounds currently being investigated clinically. Here we summarize the developmental status of PDK inhibitor molecules and, using DCA as an example, indicate the potential breath of how these compounds could find therapeutic relevance in many inborn and acquired human disorders.

P132 - *IN VITRO* METABOLIC AND TRANSPORTER PROFILING FOR MARIBAVIR (SHP620)

Devin Welty, Kefeng Sun, Haojing Rong, and Ivy Song
Shire Pharmaceuticals

Introduction: Maribavir (SHP620), a benzimidazole riboside, is a potent and orally bioavailable antiviral drug with a novel mechanism of action against cytomegalovirus (CMV). Ongoing clinical trials are evaluating the efficacy and safety of maribavir for treatment of CMV infections in solid organ transplant and stem cell transplant recipients. A complete understanding of the metabolism and disposition pathways of maribavir is necessary in planning clinical pharmacology studies, as well as informing potential drug-drug interactions with co-medications in clinical trials. Methods: Cytochrome P450 (CYP) phenotyping: Maribavir was incubated with human liver microsomes (HLM) and recombinant CYP enzymes without or with CYP inhibitors. Intrinsic clearance (CL_{int}) values were calculated when possible. Uridine diphosphate glucuronosyltransferase (UGT) phenotyping: Maribavir was incubated with UDPGA-fortified HLM without or with inhibitors for UGT subtypes. Loss of parent and formation of maribavir glucuronides were determined and these results were then confirmed with recombinant UGTs for CL_{int} calculation. UGT inhibition: UDPGA-fortified HLM was incubated with probe substrates of UGT subtypes without or with maribavir. IC₅₀ was calculated by plotting % enzyme activity against maribavir concentrations. Transporter uptake phenotyping: Human embryonic kidney (HEK) 293 cells transfected with each uptake transporter or control vector were incubated with different concentrations of maribavir for short durations. Cellular uptake parameters (K_m and maximal net influx rate, NIR_{max}) were calculated by plotting maribavir NIR against concentrations. Transporter inhibition: Uptake of transporter-specific probe substrates was studied without and with maribavir in transporter or vector control HEK293 cells. IC₅₀ was calculated by plotting % transporter activity against maribavir concentration. Results: Oxidative metabolism of maribavir is principally catalyzed by CYP3A4 (70% – 85%) and CYP1A2 (15% – 30%). UGT1A1, UGT1A3, UGT2B7 and possibly UGT1A9 were involved in the glucuronidation of maribavir; however, CL_{int} was too low to be quantified. Maribavir is a weak inhibitor for UGT1A1 (IC₅₀ 32 μM) and UGT1A3, UGT1A9 and UGT2B7 (IC₅₀'s >100 μM); maribavir does not inhibit UGT1A4 or UGT1A6 at up to 500 μM. Maribavir is not a substrate of OATP1B1 or OATP1B3 at up to 500 μM, but is an *in vitro* substrate of OCT1 and BCRP. Maribavir is not an *in vitro* inhibitor of OCT2, OAT1 or MATE2K. Maribavir is a weak inhibitor of OATP1B1, OATP1B3, OCT1, OAT3, MATE1 (IC₅₀'s 33 – 340 μM) and BCRP (IC₅₀ 7 μM). These IC₅₀ values were much lower than unbound plasma concentrations observed for the maribavir doses administered in clinical trials (400 – 1200 mg twice daily). Conclusions: These results suggest that maribavir exposure may be affected when co-administered with a CYP3A inhibitor or inducer. Maribavir exposure is unlikely affected by co-administration with inhibitors of UGTs or certain transporters. Maribavir is not expected to affect exposures of UGT substrates or certain transporter substrates when co-administered.

P133 - QUANTITATIVE PREDICTION OF METABOLITE EXPOSURES IN HUMANS USING CHIMERIC MICE WITH HUMANIZED-LIVER

Ryosuke Watari, Kazutaka Sekiguchi, Aiko Nagano, Akihiro Matsuda, Shuichi Ohnishi, and Hiroshi Hasegawa
Shionogi & Co., Ltd

Purpose: According to the FDA guidance for Safety Testing of Drug Metabolites¹⁾, human metabolites that can raise a safety concern are those formed at greater than 10% of total drug-related exposure. Therefore, it is important to estimate the plasma exposure of metabolites in humans to select the drug candidate without potential toxicities including the metabolites. Despite the widespread availability of qualitative prediction methods for human metabolites (human hepatocytes or chimeric mice with humanized-liver etc.), there are few reports to quantitatively predict the plasma exposure of metabolites in humans. S-2367, a potent and selective neuropeptide Y Y5 receptor antagonist, was mainly metabolized to hydroxylated form (S-2367-OH) in human hepatocytes, while hydrolyzed form (sulfamine carboxylic acid, SACA) and glucuronide after hydroxylation (S-2367-OH-Glu) was detected as a major metabolite in mice and human plasma, respectively. In this study, S-2367 was used as a model compound, which has a species difference in the metabolic pathway between mice and humans, and it was verified whether the plasma exposure ratios of S-2367 metabolites to the total S-2367-related exposure in human could be predicted using chimeric mice with humanized-liver. Methods: S-2367 was orally administered to chimeric mice with humanized-liver generated from TK-NOG mice (chimeric mice) and the plasma concentrations of S-2367 and its major metabolites in human plasma were measured by LC-MS/MS to calculate the plasma exposure ratio of individual metabolite to the total exposure of the S-2367 and its major metabolites in human plasma (AUC ratio, assumed as the total S-2367-related exposure). The predictability was assessed by comparing the AUC ratios in chimeric mice with those in human. In addition, mass balance study was conducted to evaluate the metabolites in urine and feces after oral administration of [¹⁴C]-S-2367 to chimeric mice. Results and Discussion: The plasma concentration of S-2367-OH-Glu was increased and of SACA was decreased with elevating the replacement ratio of human liver in chimeric mice. The AUC ratios of S-2367-OH-Glu and SACA in chimeric mice with higher replacement ratio were within 3-fold range of those in humans. Since the AUC ratio of S-2367-OH-Glu in chimeric mice was lower than that in humans, mass balance study in the chimeric mice was conducted to reveal the difference of AUC ratio between chimeric mice and humans. Carboxylated form (S-2367-COOH), which is a metabolite of S-2367-OH and a major metabolite in mice feces, was detected in the feces of chimeric mice, indicating that the difference of AUC ratio between chimeric mice and human would be due to the residual mouse metabolic activity. Conclusion: Plasma exposure ratios of individual S-2367 metabolite to the total S-2367-related exposure could be quantitatively predicted using chimeric mice with humanized-liver. Chimeric mice with humanized-liver would be a useful tool to predict the plasma exposure ratios of metabolites in humans.

Reference:

1. U.S. Food and Drug Administration, Safety Testing of Drug Metabolites Guidance for Industry, 2016

P134 - CHARACTERIZATION OF THE CYP AND UGT ENZYMES INVOLVED IN REACTIVE METABOLITE GENERATION FROM BROMFENAC AND BROMFENAC INDOLINONE

Aprajita Yadav, Timothy Carlson, and James P Driscoll
MyoKardia Inc

Nonsteroidal anti-inflammatory drugs (NSAID) have been used to safely and effectively treat pain and inflammation for many years. Some NSAIDs have been shown to cause liver damage and have been withdrawn from the market in the United States. Bromfenac is an example of an NSAID that was approved and subsequently withdrawn from the market due to acute cases of hepatotoxicity and incidences of liver failure and death. Evidence suggests a role for biotransformation in the hepatotoxic effects of bromfenac. In a mass balance study with healthy volunteers, bromfenac indolinone (BI) was found to be the major metabolite in human urine. (1) In recent *in vitro* studies, it was revealed that bromfenac requires UDPGA and alamethicin supplemented liver microsomes to form BI. (2) Bromfenac and BI were shown to form thioether adducts through a bioactivation pathway in liver microsomes and hepatocytes. The objective of the current work is to characterize the enzymatic pathways involved in the metabolism of bromfenac and BI. Upon incubation with human liver microsomes supplemented with NADPH, BI was observed to have a significantly shorter half-life than bromfenac, suggesting higher rates of metabolism of BI than for bromfenac. Cytochrome P450 (CYP) and UDP-glucuronosyltransferase (UGT) reaction phenotyping experiments were performed on bromfenac and BI to determine the specific CYP and UGT enzymes responsible for metabolism. Using recombinant UGT enzymes and recombinant CYP enzymes, it was determined that UGT2B7 converts bromfenac to BI, and that CYP2C9 catalyzes the conversion of bromfenac to hydroxybromfenac. Further studies were done with BI and recombinant enzymes, and it was observed that multiple CYP enzymes metabolize BI, including CYP1A2, CYP2C9, CYP2C19, CYP2D6 and 3A4. Since bromfenac and BI were shown to be metabolized to reactive metabolites, we then investigated whether these molecules were time dependent inhibitors (TDI) of CYP enzymes. The CYP TDI studies were conducted with bromfenac and BI in human liver microsomes with the goal of determining if a reactive species formed by a CYP enzyme could subsequently inhibit the

enzyme. It was found that BI is a time dependent inhibitor of CYP 3A4, and that the inhibition was both time and NADPH-dependent. The results of these metabolism studies with bromfenac and bromfenac indolinone add to our understanding of the relationship between biotransformation, reactive intermediate generation, and provide a potential link to hepatotoxicity for this compound.

References:

1. Osman, M., Chandrasekaran, A., Chan, K., Scatina, J., Ermer, J., Cevallos, W., Sisenwine, S. F., (1998) Metabolic disposition of ^{14}C -bromfenac in healthy male volunteers. *Journal of clinical pharmacology* 38 744-752
2. Driscoll, J. P., Yadav, A. S., Shah, N. R. (2018) The Role of Glucuronidation and P450 Oxidation in the Bioactivation of Bromfenac. *Chem. Res. Toxicol.* DOI: 10.1021/acs.chemrestox.7b00293

P135 - A FACILE CHEMICAL DERIVATIZATION METHOD TO DISCERN THE IDENTITY OF GLUCRONIDE CONJUGATES OF CARBOXYLIC ACID DRUGS UNDER MILD CONDITIONS

Kai Wang, Jiejun Wu, Tatiana Koudriakova, and Kevin Coe
Janssen R&D, LLC

A major route of metabolism for carboxylic acid drugs is through acyl glucuronidation mediated by UDP-glucuronosyltransferases (UGTs). Due to the facile loss of the glucuronide conjugate during tandem MS analysis, confirming the identity of an acyl glucuronide can be challenging when carboxylic acid drugs (or their metabolites) contain other polar functional groups (e.g. OH, NH₂) also susceptible to UGT-mediated conjugation. One solution is to employ derivatization agents to elucidate the site of conjugation. Such derivatizations are highly desirable if they are fast and selective, conducted under mild conditions, and can readily be detected by analytical instrumentation, such as liquid chromatography–mass spectrometry (LC-MS). In our study, we investigated a series of hydrazino and amino derivatization agents that selectively react with free carboxylic acid functional groups to unambiguously identify the acyl glucuronide and phenolic glucuronide of salicylic acid by LC-MS at biologically relevant concentrations. Most significantly, the chemical derivatization could be conducted in aqueous solutions at room temperature for 30 min. No strong acids, bases, or other highly reactive species were generated during the derivatization process, and samples required minimal processing before subjected to LC-MS analysis. In conclusion, through use of this facile and efficient chemical derivatization method, the metabolite identity can be discerned for carboxylic acid drugs that bear additional polar functional groups and could be of value when characterizing carboxylic acid drug metabolism.

P136 - THE ROLE OF REDUCTASES IN DRUG DISCOVERY AND DEVELOPMENT

Li Di
Pfizer Inc.

Reductases are important enzymes for drug metabolism of ketones and aldehydes, which tend to be intrinsically reactive. Significant functional redundancy has been found for reductases, presumably due to the critical nature in eliminating the reactive compounds. Limited ADME knowledge is available for these enzymes and literature information is often quite controversial. This presentation will discuss the important properties of carbonyl reductase 1 (CBR1) and 11b-hydroxysteroid dehydrogenase 1 (11b-HSD1) for drug metabolism and disposition. To understanding the tissue distribution and individual variability of the enzymes, we developed the novel proteomic approaches to quantify the protein levels of the enzymes in human tissues using LC-MS/MS. The results showed that CBR1 is most abundant in the intestine followed by the liver and the kidney, and 11b-HSD1 is mostly expressed in the human liver and not detectable in the intestine and the kidney. Inter-individual variability is moderate with approximately 3- and 4-fold differences for 11b-HSD1 and CBR1, respectively. Relative activity and relative expression factors were determined for scaling of clearance. Selective inhibitors and substrates were evaluated to enable reaction phenotyping and IVIVE. PF-915275 has been identified as a selective inhibitor and cortisone to cortisol formation as the selective substrate reaction for 11b-HSD1. Doxorubicin to doxorubicinol reaction is partially selective for CBR1, but also involves 11b-HSD1 and AKRs. Hydroxyl-PP-Me inhibits CBR1, but not 11b-HSD1. However, it is not selective against the CYP enzymes. Further research is needed to identify selective substrate and inhibitor for CBR1. During this study, we also discovered for the 1st time that 11b-HSD1 is involved in doxorubicin (one of the most effective anti-cancer drug) metabolism accounting for approximately 30% of doxorubicinol formation in human hepatocytes. Developing dual inhibitors of CBR1 and 11b-HSD1 are likely to be more effective in reducing cardio-toxic doxorubicinol formation and to improve therapeutic index.

P137 - ALDEHYDE OXIDASE ACTIVITY IN HUMAN VASCULAR TISSUE AND ITS POTENTIAL CONTRIBUTION TO EXTRA-HEPATIC METABOLISMKirk Kozminski¹, Scott Heyward², Michael Zientek¹¹Takeda Pharmaceutical Company Ltd., ²BioreclamationIVT

Aldehyde oxidase (AO) is a molybdenum-containing, soluble enzyme with cytosolic localization. This enzyme has the capacity to catalyze the oxidation of nitrogen-containing heterocycles and aldehydes, and it can also reduce N-O and N-S bonds. These structural features are found in many new chemical entities, often as part of strategies to avoid P450 oxidation and/or improve physicochemical properties. Predicting human pharmacokinetics for AO substrates has been problematic though and has led to multiple clinical failures. Animal species commonly used to predict human PK may have variable AO levels or no expression, and *in vitro* data using human liver S9 or cytosol generally underestimates *in vivo* clearance, especially for moderate to high AO CL_{int} compounds. The underestimation of *in vitro* data for predicting *in vivo* clearance for AO substrates could be in part due to AO being expressed in tissues beyond the liver. Activity therein may contribute to extrahepatic drug clearance. Several studies have shown extrahepatic AO expression, but activities are generally poorly understood.

In this current study, human vascular tissue derived S9 fractions were tested for the presence of AO activity with an aim of connecting vessel clearance rate to the known under prediction of AO systemic clearance. S9 fractions were prepared from the interior linings of iliac arteries collected during liver harvesting (n=3 donors). The vessel S9 fractions (1 mg/mL protein) were incubated with various concentrations (1-30 µM) of AO substrates carbazeran or zoniporide, and aliquots were removed and quenched at time points out to 90 minutes. Metabolite formation (4-oxo-carbazeran or 2-oxo-zoniporide) was monitored and quantified against authentic standards using an AB Sciex triple 4500 triple quadrupole mass spectrometer. For carbazeran, a parallel study was conducted with known AO inhibitor hydralazine (100 µM). All aforementioned studies were also conducted in matching donor liver S9 fractions to compare activities.

For the carbazeran incubations, results show clear formation of 4-oxo-carbazeran in each donor tissue, and the formation can be blocked completely by co-incubating with hydralazine. Using authentic metabolite standards, a K_m (average = 4.4 µM) and V_{max} (average = 1.8 pmol/min/mg) can be quantified. The K_m value is consistent with previously published work. Likewise, for zoniporide, there is quantifiable formation of 2-oxo-zoniporide, but only with incubations at higher substrate concentrations (10-30 µM). This is not surprising based on expected turnover rate. This study demonstrates that there is quantifiable AO activity in human vascular tissue. Activity is low and is likely of little consequence based on preliminary scaling exercises. However, there may be additive impact if activity exists in other tissue compartments, and the current study only investigated limited sections (iliac artery) of the human vascular system.

P138 - MUTATIONS OF FLAVIN-CONTAINING MONOOXYGENASE 3 (FMO3) GENE IN JAPANESE COHORTSMakiko Shimizu¹, Komei Nakakuki¹, Hiromi Yoda¹, Masahiro Hiratsuka², Hiroshi Yamazaki¹¹Showa Pharmaceutical University, ²Tohoku University

The flavin-containing mono-oxygenase (FMO) is an NADPH-dependent enzyme that catalyzes the oxygenation of a wide variety of *N*- and *S*-containing medicines and xenobiotic substances, including trimethylamine. Genetic polymorphisms of *FMO3* contribute to an inherited disorder trimethylaminuria. The trimethylaminuria is caused by excessive malodorous trimethylamine excreted via urine and body secretion. We found some novel mutations of *FMO3* gene in self-reported trimethylaminuria volunteers phenotyped for *FMO3* by urine tests in Japanese. The aim of the present study was to investigate the novel mutations of *FMO3* in a Japanese big genome database and to investigate the function of novel *FMO3* variant proteins. In the database, the known twelve single nucleotide substitutions p.(Trp41Ter), p.(Asn114Ser), p.(Glu158Lys), p.(Asp198Glu), p.(Arg205Cys), p.(Val257Met), p.(Met260Val), p.(Glu308Gly), p.(Ile486Met), p.(Thr488Ala), p.(Arg492Gln), and p.(Arg500Ter) were found. Furthermore, novel three mutations were identified. The novel variant *FMO3* p.Ala311Pro protein recombinantly expressed in *Escherichia coli* membranes exhibited decreased activities toward benzydamine or trimethylamine *N*-oxygenations compared with those of wild-type *FMO3*. The allele frequencies of these novel variants were low (~1%). The present results collectively suggest that new *FMO3* variants found in Japanese genome database may cause abnormal trimethylamine *N*-oxygenation.

P139 - ELIMINATION OF [14C]LY3023414 BY ALDEHYDE OXIDASE AND CYP ENZYMES IN HUMANS FOLLOWING ORAL ADMINISTRATIONLian Zhou, Darlene Satonin, Jill Chappell, Ping Yi, Richard Moulton, Sophie Callies, and Kenneth Cassidy
Eli Lilly and Company

The class I phosphatidylinositol-3-kinase-protein kinase B-mammalian target of rapamycin (PI3K/AKT/mTOR) pathway regulates the cell cycle and is altered in cancer cell growth and survival.¹ LY3023414 is an orally available, potent, selective small molecule dual kinase inhibitor of this pathway¹ investigated as a potential treatment for patients with prostate cancer. The pharmacokinetics and disposition of [14C]-LY3023414 were investigated in healthy subjects (N=5) following oral administration of a single dose of unlabeled and radiolabeled LY3023414 corresponding to a total

LY3023414 dose of 150 mg with approximately 100 mCi of radioactivity. Plasma samples were analyzed for LY3023414 using a validated liquid chromatography with tandem mass spectrometry method. Whole blood, plasma, urine, and fecal concentrations of radioactivity were determined using liquid scintillation counting techniques. Pharmacokinetic parameter estimates for whole blood and plasma total radioactivity, and plasma LY3023414 were calculated by standard noncompartmental methods. The enzymes responsible for the LY3023414 metabolism were determined using recombinant cytochrome P450 (CYP) enzymes, human liver microsomes and cytosol in the presence and absence of a probe inhibitor. The enzyme kinetic parameter values were determined by detection of metabolite formation in human liver microsomes and cytosol. LY3023414 was rapidly absorbed; the median time to maximum observed concentration postdose was 0.5 hours and the mean half-life was 2.59 hours. The overall recovery of radioactivity over 120 hours was 96.1%, corresponding to 71.5% and 24.6 % of the dose excreted in feces and in urine, respectively, indicating that LY3023414 is eliminated completely from the body following an oral dose. LY3023414 was cleared primarily by metabolism with only 5% of the dose being excreted as parent drug. The major metabolic clearance pathways involved were aromatic hydroxylation of the quinoline moiety (M2), *N*-demethylation (M5), and quinoline oxidation with *N*-demethylation (M12) (Figure 1). LY3023414 exposure accounted for approximately 46% of total plasma radioactivity based on area under the concentration versus time curve from zero to infinity, indicating significant amounts of metabolites circulating. Parent LY3023414 and metabolites, M2, M5, and M12, accounted for 62%, 23%, 3%, and 9% of the circulating radioactivity, respectively, in plasma over 12 hours postdose. In vitro studies using human liver microsomes and cytosol confirmed M2 and M5 were formed through aldehyde oxidase (AO)- and CYP-mediated pathways, respectively. An $f_{m,AO}$ of 0.46 and an $f_{m,CYP}$ of 0.54 were calculated from kinetic parameters determined for the formation of M2 and M5. M12 was formed from M2 and M5 through CYP- and AO-mediated pathways, respectively. The drug-related adverse events with single-dose LY3023414 included dysgeusia, oral paraesthesia, dizziness, nausea, and diarrhea; all were mild in severity and resolved without treatment. In conclusion, LY3023414 was absorbed rapidly and eliminated completely after oral dosing, with metabolism as the predominant route of elimination in humans. Both AO and CYP enzymes were responsible for the metabolic clearance of LY3023414 with the non-CYP enzymes mediating approximately half of the clearance of the drug.

Reference:

1. Smith MC, et al. Characterization of LY3023414, a Novel PI3K/mTOR dual inhibitor eliciting transient target modulation to impede tumor growth. *Mol Cancer Ther* 2016;15(10):2344-56.

P140 - PROFILING OF FLAVORED NON-ALCOHOLIC BEVERAGES TOWARD TRANSCRIPTIONAL ACTIVITY OF PPAR GAMMA USING A NOVEL REPORTER CELL LINE PAZ-PPARG

Peter Illés and Zdenek Dvorak

Department of Cell Biology and Genetics, Faculty of Science Palacky University Olomouc

A variety of xenobiotic, but also naturally occurring compounds that can possibly interfere with regulatory pathways of nuclear receptors, are taken up in the diet on daily basis. We developed a novel human reporter cell line for assessment of PPARgamma transcriptional activity – PAZ-PPARG that can be utilized as a tool in various food safety and environmental applications. Reporter cell line was used for screening of 27 flavored non-alcoholic beverages for their potentially disrupting effects on transcriptional activity of PPARgamma. Stably transfected cell line was prepared by transfecting the human bladder carcinoma cell line T24/83 with reporter plasmid pNL2.1[Nluc/Hygro] containing three copies of PPARgamma response element, coupled with minimal promoter. In the cells treated with PPARgamma ligand 15d-PGJ2 and prostaglandin PGD2, luciferase activity ranged from 60-fold to 120-fold. Combined treatments of the cells with model ligands and selective antagonist of PPARgamma T0070907 resulted in significant decrease of luciferase activity, indicating the specific response of PAZ-PPARG to 15d-PGJ2 and PGD2. In addition, specificity of the PAZ-PPARG cell line was confirmed using model ligands of selected nuclear and steroid receptors. After the treatment of the cells with ligands for TR, VDR, RXR, RAR, GR, MR, ER, PR, AR and PPARalpha, any significant induction of luciferase activity was not observed. Time-course experiments revealed that the luciferase activity induced by 15d-PGJ2 and PGD2 is measurable as soon as after the 12-h application of ligands. The PAZ-PPARG cell line was also tested for survivability after the cryopreservation and the long-time cultivation. The inducibility of luciferase activity remained unaffected after the freeze-thaw cycle and even after 25 passages of the cell culture. Finally, there were no significant differences in morphology of the PAZ-PPARG cells compared to the parental T24/83 cells. The PAZ-PPARG cell line was used for testing of 9 extracts of ready-to-drink teas and 18 extracts of flavored mineral waters. Based on the measurements of luciferase activity, none of the 27 examined samples induced transcriptional activity of PPARgamma in the PAZ-PPARG cell line. Interestingly, we identified two ready-to-drink teas and five flavored mineral waters that substantially decreased luciferase activity in the PAZ-PPARG cells treated with extracts of beverages in combination with 15d-PGJ2. Luciferase activity ranged from 49% to 72% of activity induced by natural ligand, and one sample of mineral water completely abolished luciferase activity. These findings indicate that some of the commonly marketed flavored non-alcoholic beverages are capable to inhibit transcriptional activity of PPARgamma and thus possibly affect the regulation of gene

expression mediated by PPARgamma.

This research was supported by the grant from Czech Science Foundation GACR 16-07544S.

P141 - EFFECT OF RENAL TRANSPLANTATION ON ORGANOCHLORINE PESTICIDE (OCPs) LEVELS IN CHRONIC KIDNEY DISEASE PATIENTS (CKD-5D): A LONGITUDINAL STUDY

Amit Kumar, Himani, Himani Thakkar, Archna Singh, Sandeep Mahajan, and Sudip Datta

AllMS, New Delhi

Patients with CKD have been reported to have high levels of OCPs due to decreased renal excretion. This study was designed to evaluate the effect of renal transplantation on the blood OCP levels following post-transplant improvement of estimated glomerular filtration rate (eGFR) in CKD stage-5D patients. 51 adult CKD stage-5D patients planned for renal transplantation were recruited for this study after informed consent and institutional ethical clearance. Blood samples were drawn twice; first, one day before renal transplantation and second, after confirmation of graft stabilization (eGFR >40 ml/min/1.73 m² by MDRD formula) approx. 6 months after transplantation (n=43). 8 patients were lost during follow-up. Blood OCPs levels were analyzed by gas chromatography with electron capture detector (GC-ECD) after solid phase extraction and clean-up as per USEPA 3620B method. Amongst the twenty pesticides that were screened for using the OCP standard mix (Supelco, Bellefonte, PA, USA) α -BHC, methoxychlor and Aldrin were detected in more than 90% samples. DDT, DDE, Heptachlor and Endrin Ketone were detected in less than 10% of samples. Endosulfan sulphate was not extracted and detectable by our methods. Amongst the pre-transplant samples α -BHC (Median 146.7ppb, range – ND to 621.04ppb) showed the highest levels. Other compounds showing significant levels were β -BHC, Heptachlor and γ -Chlordane. When we compared the pre-transplantation and post-transplantation samples, we found that no OCPs showed significant difference in levels. Surprisingly, β -BHC was found raised significantly among the post-transplant samples compared to pre-renal transplantation (90.2 ppb vs. 49 ppb respectively; p value < 0.001). Median values for α -BHC, δ -BHC, γ -chlordane showed a decreasing trend. Summarily, most OCPs did not show significant reduction after renal transplant within the time frame of the follow-up. This necessitates studies with longer follow-up period. However, ongoing exposure of the patients during the follow-up period should also be ruled out.

P142 - MRP4 (ABCC4) IS A DETERMINANT OF OBSERVED CAPECITABINE AND ITS METABOLITE CONCENTRATIONS DURING CANCER THERAPY

Ahmed A. Almousa

Western University

Capecitabine is a fluoropyrimidine carbamate oral precursor of 5-fluorouracil (5-FU) and its active metabolite 5'-deoxy-5-fluorouridine (5'-DFUR). Capecitabine is widely prescribed for the treatment of colorectal, gastric and breast cancers. Currently, dihydropyrimidine dehydrogenase (DPYD) genotyping is considered a corner stone in dose stratification for capecitabine or 5-FU. However, a large proportion of adverse effects during capecitabine or 5-FU therapy, can not be accounted for by known DPYD genetic variations. Recently a study has identified single nucleotide polymorphism (SNP) in the 3'-UTR (rs3752106) of ATP-Binding Cassette-4 subfamily C (ABCC4/MRP4)(1), thought to be a microRNA (miRNA) binding site, resulting in altered MRP4 expression and efficacy to capecitabine or 5-FU during therapy. However, the role of this *MRP4* SNP to attained pharmacokinetic profile of capecitabine or 5-FU has not been defined. Therefore, the objective of this study is to assess the impact of *MRP4* rs3752106 on the pharmacokinetic profiles of capecitabine and its metabolites among patients on capecitabine therapy. 26 cancer patients receiving capecitabine (1250 mg/m²) were enrolled for a detailed pharmacokinetic study. Plasma sampling was performed at pre-dose, 0.25, 0.5, 1, 1.5, 2, 3, 4, 6, 8 hours, and concentrations of capecitabine, 5-FU, FUPA, FBAL, 5'-DFUR and 5'-DFCR were measured using liquid-liquid extraction and HPLC-HESI/MSMS. Taqman real-time PCR assay (Thermo Fisher Scientific) was used to genotype rs3742106. Pharmacokinetic analysis was carried using PK solver 2.0 and GraphPad Prism 6.0 was used for statistical analysis. The average capecitabine dose was 2854 mg/day. *MRP4* rs3742106 genotype in our cohort showed A/A (n= 7), A/C (n=15) and C/C (n=4). Exposure assessed through AUC_{0-8hr} was significantly different (p < 0.05) for 5-FU and 5'-DFUR (A/C and C/C) when compared to A/A genotype. 5'-DFUR AUC_{0-8hr} (mean \pm S.D) was 9.10 \pm 2.96, 5.67 \pm 1.83 and 4.77 \pm 1.39 ng*hr/mL for genotypes A/A, A/C and C/C respectively. In conclusion, *MRP4* rs3742106 SNP alters exposure to 5-FU and 5'-DFUR during capecitabine therapy. Our findings suggest genetic variation in efflux transporters such as MRP4 are clinically relevant determinants of fluoropyrimidine therapy. Accordingly, it will be important to integrate genetic variation in drug transporters as well as enzymes such as DPYD, for personalizing capecitabine and 5-FU dosing for cancer chemotherapy.

Reference:

1. Q. Chen *et al.*, A polymorphism in ABCC4 is related to efficacy of 5-FU/capecitabine-based chemotherapy in colorectal cancer patients. *Sci Rep* 7, 7059 (2017).

P143 - RPL28 PROMOTER POLYMORPHISM RS4806668 IS ASSOCIATED WITH REDUCED SURVIVAL IN FOLFIRI-TREATED METASTATIC COLORECTAL CANCER PATIENTS.

Adrien Labriet¹, Eric Levesque¹, Erika Cecchin², Elena De Mattia², Derek Jonker³, Felix Couture¹, David Simonyan⁴, Angela Buonadonna⁵, Mario D'Andrea⁶, Lyne Villeneuve¹, Giuseppe Toffoli², Chantal Guillemette¹

¹Pharmacogenomics Laboratory, CHU de Quebec Research Center and Faculty of Pharmacy, Laval University, ²Clinical and Experimental Pharmacology, Centro di Riferimento Oncologico - National Cancer Institute, ³Division of Medical Oncology, Department of Medicine, Ottawa Hospital, University of Ottawa, ⁴Clinical and Evaluative Research Platform, CHU de Quebec Research Center, ⁵Medical Oncology Unit, Centro di Riferimento Oncologico - National Cancer Institute, ⁶Medical Oncology Unit, San Filippo Neri Hospital

Fluorouracil (5-FU), folinic acid, and irinotecan (FOLFIRI) is an effective regimen for treatment of metastatic colorectal cancer (mCRC). The aim of the study was to investigate the potential of single nucleotide polymorphisms (SNPs) of *RPL28* as predictor of survival after FOLFIRI treatment in mCRC patients. This is based on the observation that *in vitro* silencing of *RPL28* gene, encoding a ribosomal protein that is a component of the ribosomal 60S subunit, enhances sensitivity to 5-FU and irinotecan in human colorectal carcinoma HCT 116 cells.¹ A recent report also showed that, in patients with myelodysplasia and other related neoplasms, those with a lower level of *RPL28* have prolonged overall survival (OS) after treatment with azacitidine.² The mechanism underlying these effects remains unknown but variable expression of this gene in colorectal cancers compared to adjacent normal tissues has been observed.³ We used a haplotype-tagging SNPs (htSNPs) approach to maximize coverage of the genetic variability of *RPL28*. Our study included a discovery cohort of 167 patients recruited in Eastern Canada as well as an independent replication set composed of 250 mCRC cases from Northeast Italy, all treated with FOLFIRI. DNA genotyping was performed using time-of-flight mass spectrometry iPLEX Sequenom Technology. Associations between htSNPs and clinical outcomes were tested using Cox proportional hazards model adjusted for covariates. *RPL28* rs4806668G>T was associated with a shorter progression-free survival (PFS) in the Canadian (HR 3.23, $P = 0.013$), Italian (HR 3.28, $P = 0.021$) and combined (HR 3.36, $P < 0.001$) cohorts. This marker was also associated with a reduced OS in the Canadian (HR 3.09, $P = 0.032$), Italian (HR 3.05, $P = 0.030$) and combined (HR 3.07, $P = 0.002$) cohorts. *RPL28* rs4806668 variation is located in the promoter region and is in strong linkage disequilibrium with six other SNPs upstream of the gene, potentially affecting gene expression. In support, the rs4806668T allele was associated with increased *RPL28* expression in colon tissues of healthy individuals of the GTEx cohort, compared to rs4806668G carriers. These results suggest that *RPL28* rs4806668G>T might be a predictive marker of survival after FOLFIRI treatment. Functional investigations are required to elucidate the underlying molecular mechanism by which the ribosomal *RPL28* protein may influence cancer cell response to FOLFIRI treatment. This work is supported by the Canadian Institutes of Health Research.

References:

1. Allen et al. Mol Cancer Ther. 2012 Jan;11(1):119-31
2. Belickova et al. Int J Hematol. 2016;104:566-573
3. Kasai et al. J Histochem Cytochem. 2003 May;51(5):567-74

P144 - HUMAN AMYLOID-BETA 1-40 DISPOSITION AFTER INTRAVENOUS AND INTRACEREBRAL INJECTIONS IN THE RAT

Hao Benson Peng¹, Keumhan Noh¹, Rui Sophie Pan², Victor Saldiva², Sylvia Serson², Anja Toscan², Ines deLannoy², and K. Sandy Pang¹

¹Leslie Dan Faculty of Pharmacy, University of Toronto; ²InterVivo Solutions Inc.

Amyloid- β (A β) 1-40 and 1-42 are monomeric peptides formed from the sequential cleavage of Amyloid Precursor Protein (APP) via β - and γ -secretases that could aggregate and lead to the formation of toxic oligomers and extracellular plaques in Alzheimer's disease (AD), a pathological hallmark and basis of the amyloid cascade hypothesis. In addition to the amyloid hypothesis, the amyloid clearance hypothesis further postulates that it is the reduction in clearance of A β and not hastened synthesis that contributes to its accumulation, aggregation, and plaque formation. The aim of this study was to determine the disposition of hA β ₁₋₄₀ in male Sprague-Dawley rats (200-300 g) after hA β ₁₋₄₀ intravenous (IV, 200 μ L) injection into the jugular vein or intracerebroventricular (ICV, 10 μ L) injection into right ventricle of the brain with stereotaxic instrument and guide cannula administration. hA β ₁₋₄₀ peptide powder, dissolved then vacuum dried, was reconstituted in NaOH:PBS:ddH₂O (10:45:45, v/v/v) and diluted with PBS to make the doses (20 μ g). hA β ₁₋₄₀ in plasma and CSF was assayed utilizing a commercially available ELISA kit with and without solid-phase extraction (SPE) or by LCMS. The decay profile was best fit by 2-compartment model with first-order elimination (ADAPT5[®]). Parameter estimates for hA β ₁₋₄₀ were similar: $t_{1/2\beta}$ were 23.8 \pm 2.5, 21.6 \pm 4.5, and 14.9 \pm 3.9 min, V_{ss} were 234.6 \pm 95.8, 329.4 \pm 64.7, and 128.3 \pm 29.6 mL/kg, and CL_{sys} were 14.5 \pm 6.2, 20.7 \pm 5.1, and 9.9 \pm 4.1 mL/min/kg for the ELISA (n= 8), ELISA-SPE (n= 5) and LCMS/MS (n= 8) assays, respectively, for IV dosing; CSF was detectable after IV administration and the plasma:CSF concentration ratio was 0.2 \pm 0.3 (n= 3). For ICV injection (n= 3), $t_{1/2\beta}$ in plasma was 26.2 \pm 11.5 min and CSF was 25.8 \pm 8.2 min, V_{CSF} was 1.7 \pm 0.4 mL/kg, CL_{CSF} was 0.2 \pm 0.04 mL/min/kg, and the CSF:plasma concentration

ratio was 1495 ± 1021 . From both IV and ICV injections, the data showed that hA β ₁₋₄₀ was able to transverse (efflux) across the blood-brain barrier (BBB) into the systemic circulation and from plasma to cross the BBB back into the brain or CSF.

P145 - A NON-LINEAR MIXED-EFFECTS MODEL TO DESCRIBE THE POPULATION PHARMACOKINETICS OF MYCOPHENOLIC ACID AND THE EFFECTS OF CO-VARIATES IN ADULT, DE-NOVO KIDNEY TRANSPLANT PATIENTS ON STEROID-FREE ANTI-REJECTION REGIMENS

Yan Rong and Tony KL Kiang

Faculty of Pharmacy and Pharmaceutical Sciences, University of Alberta

Introduction: Mycophenolic acid (MPA) is frequently used as a part of a combinatorial anti-rejection regimen (with a calcineurin inhibitor such as tacrolimus [FK], with or without corticosteroids) for preventing graft rejection in adult kidney transplant recipients. In subjects with reduced immunologic risk, there is an increasing trend for using steroid-free regimens to minimize adverse effects and pill burden. Many population pharmacokinetic (PK) models of MPA have been published in the literature characterizing population estimates and sources of variability in various solid-organ transplant recipients (1). However, to our knowledge, no population PK model is available for adult kidney transplant recipients on *steroid-free* regimens. As such, we aimed to construct a non-linear mixed-effects model to describe the population PK of MPA (co-administered with FK) and effects of co-variates in this specific population. We hypothesized that the population PK estimates in adult steroid-free subjects are different from steroid-based patients. **Methods:** The following patient parameters were collected: gender, age, weight, height, albumin, serum creatinine (SrCr), estimated-glomerular filtration rate (eGFR), MPA/FK doses, and MPA/FK concentrations. FK area-under the concentration-time curve (AUC, a marker of exposure) was calculated using trapezoidal rule in a subset of subjects undergoing intense sampling (N=28, set 1) or using limited-sampling strategies in another subset with sparse sampling (N=18, set 2). Non-linear mixed-effects PK modeling was performed with Monolix (Lixoft, version 2018R1) using stochastic approximation of the standard expectation maximization algorithm. **Results:** A total of 334 MPA concentrations from 46 subjects were available for the development of the population PK model. Patient characteristics were: gender(N=26 females), age(50 ± 13 years, mean \pm SD), weight(71.9 ± 18.5 kg), height(166.8 ± 9.8 cm), albumin(40.6 ± 4.5 g/L), SrCr(106.5 ± 25.6 μ mol/L), eGFR(57.8 ± 14.0 mL/min/1.73m²), MPA dose(0.8 ± 0.3 g/dosing interval), FK dose(3.5 ± 2.0 mg/dosing interval), FK trough concentration(7.7 ± 2.8 μ g/L), and FK exposure(133.6 ± 38.2 μ g \cdot h/L). The pharmacokinetics of MPA can be best described by a two-compartmental, first-order absorption, and linear elimination structural model. The final population PK parameter values (population mean estimate \pm standard error) were as follow: absorption rate constant (ka)(1.17 ± 0.264 h⁻¹), oral clearance (CL/F)(3.5 ± 1.92 L/h), inter-compartmental clearance (Q)(31.5 ± 3.1 L/h), central compartment volume of distribution (V₁/F)(19.8 ± 6.25 L), and peripheral compartment volume of distribution (V₂/F)(302 ± 74.4 L). Compared to published population mean estimates in subjects on *steroid-based* anti-rejection regimens, ka (vs. reference population value ranges in steroid-based patients: 2-4 h⁻¹) and CL/F (vs. 13-31 L/h in steroid-based patients) were generally lower in our subjects on *steroid-free* regimens. Estimates of between-subject variability for ka, CL/F, Q, V₁/F, and V₂/F were 54%, 115%, 35%, 99% and 53%, respectively. "Weight" was found to be a significant covariate for CL/F and Q, whereas "eGFR" and "gender" were identified as significant covariates for ka and Q. The final structural model was validated using goodness-of-fit plots and visual predictive checks. **Conclusion:** We have constructed a novel model describing the population PK of MPA in steroid-free adult kidney transplant patients. Our findings indicate differences in the population PK of MPA in this specific population.

Reference:

1. Kiang TKL, Ensom MHH. Population Pharmacokinetics of Mycophenolic Acid: An Update. Clin Pharmacokinet 2017, Aug 31 [epub ahead of print]. doi: 10.1007/s40262-017-0593-6

P146 - POPULATION PHARMACOKINETICS OF IMMEDIATE-RELEASE TACROLIMUS IN STEROID-FREE ADULT RENAL TRANSPLANT RECIPIENTS

Yan Rong¹, Patrick Mayo¹, Mary HH Ensom², and Tony KL Kiang¹

¹Faculty of Pharmacy and Pharmaceutical Sciences, University of Alberta, ²University of British Columbia

Introduction: In adult kidney transplant recipients with low immunologic risk, tacrolimus (FK) is frequently used in combination with mycophenolic acid (MPA) in a *steroid-free* anti-rejection regimen for the prevention of organ rejection. Various population pharmacokinetic (PK) models for FK are available in the literature describing population mean estimates and sources of variability in various solid-organ transplant patients. However, to our knowledge, a population PK model is still lacking for FK in adult kidney transplant recipients on *steroid-free* regimens. As such, we aimed to develop and validate a non-linear mixed-effects model to describe the population PK of FK (co-administered with MPA) and effects of co-variates in this patient population. We hypothesized that the mean population estimates and variabilities in adult *steroid-free* subjects are different than steroid-based patients. **Methods:** The collected patient parameters were: gender, age, weight, height, albumin, serum creatinine (SrCr), estimated-glomerular filtration rate (eGFR), FK or MPA

doses, and FK or MPA concentrations. MPA area-under the concentration-time curves (AUC, a marker of exposure) were calculated using linear trapezoidal rule in those subjects undergoing intense sampling (N=28) or with a validated limited-sampling strategy in subjects with sparse sampling (N=21). Non-linear mixed effects modeling using stochastic approximation of the expectation maximization algorithm was conducted in Monolix (Lixoft, version 2018R1). Co-variables were deemed significant only if all of the following conditions were satisfied: 1) Pearson's correlation test for random effects vs. covariates had a p value <0.005 (corrected based on Bonferroni adjustment), 2) the coefficient of correlation was >0.5 , 3) the distribution of the affected population parameter was apparently dependent on the co-variate, and 4) the overall objective function value for the model was reduced with the addition of the co-variate. Results: A total of 320 FK concentrations from 49 subjects were utilized for population PK model development. Patient demographic and clinical biochemistries were: gender (N=27 females), age(50 ± 12 y, mean \pm SD), weight(72 ± 18 kg), height(167 ± 10 cm), albumin(40 ± 5 g/L), SrCr(108 ± 26 μ mol/L), eGFR(58 ± 15 mL/min/ 1.73m^2), FK dose(6.7 ± 4.1 mg/d), MPA dose(1617 ± 500 mg/d), and MPA exposure(37 ± 14 mg/h/L). The population PK of FK is best illustrated by two-compartment, first-order absorption with lag time, and linear elimination structural model (with constant error model). The final population PK parameter values (mean estimate \pm standard error) were: absorption lag time (Tlag)(0.317 ± 0.044 h), absorption rate constant (ka)(3.13 ± 0.8 h $^{-1}$), apparent oral clearance (CL/F)(12.5 ± 2.01 L/h), apparent inter-compartmental clearance (Q/F)(4.02 ± 4.77 L/h), apparent central compartment volume of distribution (V₁/F)(111 ± 7.57 L), and apparent peripheral compartment volume of distribution (V₂/F) (257 ± 53.6 L). These population mean estimates are generally comparable (i.e. within the ranges) to those published in subjects on steroid-based regimens. No co-variables satisfied our *a priori* defined modeling conditions. The estimates for between-subject variability for Tlag, ka, CL/F, Q/F, V₁/F, and V₂/F were 138%, 93%, 63%, 13%, 26%, and 40% respectively. The final model was validated using goodness-of-fit plots and visual predictive checks. Conclusion: We have developed/validated a novel model describing FK's population PK in *steroid-free* adult kidney transplant recipients. Further modeling activities are ongoing to establish complex absorption, clearance, and Bayesian forecasting models.

P147 - EFFECTS OF MYCOPHENOLIC ACID AND CLINICAL VARIABLES ON TACROLIMUS EXPOSURE IN DE NOVO, STEROID-FREE ADULT RENAL TRANSPLANT PATIENTS

Tony KL Kiang¹, Mary HH Ensom², and Yan Rong¹

¹Faculty of Pharmacy and Pharmaceutical Sciences, University of Alberta, ²Faculty of Pharmaceutical Sciences, University of British Columbia

Introduction: Tacrolimus (FK) is frequently administered with mycophenolic acid (MPA) and/or corticosteroids for immunosuppression in renal transplant recipients. MPA has been shown to decrease FK intrinsic clearance, by inhibiting cytochrome P450 3A4, under specific *in vitro* experimental conditions. However, conflicting clinical drug-drug interaction data from MPA co-administration on FK exposure have been reported. Due to facts that i) there is an increasing trend in the administration of steroid-free anti-rejection regimens, ii) steroids are known to affect FK clearance, and iii) the majority of FK pharmacokinetic studies have been conducted in the presence of steroids, we proceeded to fill the important literature gap by hypothesizing that select clinical variables (e.g. MPA exposure) can be used to predict FK exposure in adult kidney transplant patients on steroid-free regimens. Methods: An open-label, prospective cohort study involving patients (N=49) on steroid-free FK and MPA pharmacotherapy was conducted. Following patient consent, the following clinical data were collected: sex, age, weight, height, serum creatinine (SrCr), estimated-glomerular filtration rate (eGFR), albumin, MPA dose, and FK/MPA concentrations. FK and MPA exposures were represented by area-under the concentration-time curve (AUC) values, which were calculated using trapezoidal rule (subjects undergoing intense sampling (N=28, set 1)) or limited-sampling strategies (subjects with sparse sampling (N=21, set 2)). Single and multiple regression (forward and backward stepwise) modelling were carried out with SigmaStat on log-transformed data. Differences between groups were determined by one-way ANOVA (with post-hoc analyses if appropriate) and results deemed significant if $p<0.05$. Results: The following data were obtained in the combined dataset: sex (N=27 females), age (50 ± 13 years, mean \pm SD), weight (71.8 ± 18.2 kg), height (166.9 ± 9.7 cm), SrCr (1.2 ± 0.3 mg/dL), eGFR (57.7 ± 14.5 mL/min/ 1.73m^2), albumin (4.0 ± 0.5 g/dL), weight-normalized MPA dose (22.8 ± 7.9 mg/kg/day), dose-normalized FK trough concentration (1.46 ± 0.72 μ g/L/mg), dose-normalized FK exposure (25.0 ± 14.4 μ g·h/L/mg), and dose-normalized MPA exposure (25.3 ± 11.0 mg·h/L/g). Initial control analysis revealed significant direct correlations between trough FK concentrations and dose-normalized FK AUCs ($R^2 = 0.8$); therefore, only dose-normalized FK AUC (the better marker) was utilized as the dependent variable. Linear regression analyses of clinical variables (using various combinations of set 1 and 2 data) indicated that "SrCr" ($R=-0.56$), "eGFR" ($R=0.58$), "weight-normalized MPA dose" ($R=0.31$), and "age" ($R=0.36$) were significantly associated with FK exposure. Stepwise multiple regression models using a variety of combinations of significant variables (including MPA exposure) also confirmed that only "eGFR" and "age" ($R^2=0.47$) were significant predictors of FK exposure. Moreover, when patients were sub-categorized based on MPA exposure (i.e. AUC < 20 , $20 - 30$, or > 30 mg·h/L/g), no statistical significant differences in FK exposure were evident between these groups. Conclusions: Our novel findings indicate that FK exposure may be associated with select clinical variables (i.e. eGFR and age), but a clinically significant drug-drug interaction between MPA and FK was not identified in this specific population. Further analyses using non-linear mixed-effects modeling are on-going.

P148 - APPLICATION OF DMPK TOOLBOX IN PREDICTING HUMAN PHARMACOKINETICS FOR BACK-UP RIP1 INHIBITORS: LEARNINGS FROM GSK2982772 IN CLINIC

Mukesh Mahajan, Phil Harris, David Zhang, Lauren Richards-Peterson, Steven Thomas, Debbie Tompson, Jill Marinis, Scott Berger, Robert Marquis, John Bertin, and Michael Reilly
GlaxoSmithKline

The first RIPK1 inhibitor GSK2982772 to enter the clinic is currently in Phase 2a trials targeting inflammatory diseases such as psoriasis, rheumatoid arthritis and Ulcerative Colitis. GSK2982772 demonstrated a shorter half-life in the Phase 1 (FTIH) studies than predicted from *in vitro* data and *in vivo* rat and monkey studies. The observed major route of metabolism in FTIH was via *N*-glucuronidation on triazole moiety, the predominant metabolite in blood (~70% of drug related material (DRM)) and urine (~85% of DRM). Two potential back-up molecules to GSK2982772 (GSK'A and GSK'B) have a similar triazole moiety. Mechanistic investigations were initiated to better understand the role of glucuronidation pathway in metabolic disposition of these compounds. In glucuronidation studies using human liver microsomes fortified with UDPGA with assessment via mass spectral response, concentration and time dependent formation of glucuronide metabolites were observed for both GSK'A and GSK'B. However, both back-up molecules demonstrated a significantly lower propensity for glucuronidation pathway compared to GSK2982772. Following generation of authentic glucuronide standards for the lead and back-up compounds from human urine and chemical synthesis, respectively, glucuronidation kinetic investigation further demonstrated ~4-fold lower rate of glucuronide formation for GSK'B (CL_{int} = 3.3 μL/min/mg) compared to GSK2982772 (CL_{int} = 12 μL/min/mg). While difficult to scale to the predicted clinical clearance in the absence of robust scaling factors for glucuronidation pathway, glucuronidation mediated clearance was predicted to be favorable for the back-up compounds compared to lead compound. To identify more relevant preclinical species for RIPK1 inhibitors in prediction of human pharmacokinetic parameters, GSK'A and GSK'B were further evaluated in dog (all studies were conducted in accordance with the GSK Policy on the Care, Welfare and Treatment of Laboratory Animals and were reviewed the Institutional Animal Care and Use Committee either at GSK or by the ethical review process at the institution where the work was performed). Pharmacokinetic parameters from three species (rat, monkey and dog) were then utilized in prediction of human pharmacokinetics for the back-up compounds. The data presented in the poster will highlight the rational application of DMPK resources in understanding the fate of back-up compounds in light of clinical findings.

P149 - THE HURDLE OF HUMAN PK PREDICTIONS FOR HEPATIC OATP SUBSTRATES: LESSONS LEARNED FROM RAT ALLOMETRY

Hong Mei, Raymond Evers, and Randall Miller
Merck & Co, Inc.

For hepatic OATP substrates, clearance (CL) is often thought to be the most challenging pharmacokinetic parameter for human predictions. When liver uptake is the rate-determining step in hepatic clearance, CL in humans can be predicted using *in vitro* hepatocyte uptake CL together with an *in vivo* rat scaling factor. However, without knowing the rate-determining step in CL at the early stages of drug discovery, rat allometry is often employed as a default method. This investigation explored the predictive performance of rat allometry on CL, volume of distribution at steady state (V_{dss}) and mean residence time (MRT) for 17 hepatic OATP substrates. Surprisingly, CL was much better predicted than V_{dss} and MRT. We examined the impact of entero-hepatic circulation (EHC) on CL, V_{dss} and MRT using rosuvastatin with and without bile cannulation in rats, and illustrated that the impact of EHC on V_{dss} and MRT is much higher than on CL. Thus, we propose that the hurdle for human PK predictions is biliary excretion-associated EHC. The impact of EHC on V_{dss} and MRT is species dependent, dose-dependent, and associated with high inter- and intra- individual variability. Thus, for hepatic OATP substrates, prediction of V_{dss} and MRT in humans is much more challenging than prediction of CL.

P150 - LC-MS/MS RAPID IDENTIFICATION OF A NOVEL TRACER FOR A SUBTYPE SPECIFIC PHOSPHODIESTERASE (PDE) WITH NO KNOWN LIGAND

Jie Chen, Trevor Scott, Guibao Gu, Lindsay Crickard, Doug Zook, Jenny Chen, Michael Chung, Vinny Santora, Yu-wen Li, Jef Vivian, Anne Danks, Kathe Stauber, and Ali Tabatabaei
Dart Neuroscience

Target specific radiolabeled tracers are frequently employed to quantify the receptor occupancy of NCEs intended for central nervous system (CNS) indications. They may be subsequently developed into a positron emission tomography (PET) ligands for use in clinical trials. The traditional approach to tracer development entails by *in vivo* characterization of radiolabeled tracer candidates until one with appropriate ligand binding properties is identified. This approach is not only expensive, time consuming and resource intensive, but is also associated with high attrition rate. Due to these challenges, many CNS targets may not have a target specific radiolabeled tracer available for occupancy studies. We used a triple quad, positive ionization mode LC-MS/MS assay to screen the brain distribution of cold tracer candidates after iv. micro-dosing. The LLOQ of this assay was as low as 10 pg/mL. This assay result in the rapid identification of a novel tracer. This

molecule, compound-30, showed reasonable specificity (striatum/thalamus ratio of 2.2) and uptake (0.2% injected dose/g tissue) in the *in vivo* rat studies with cold compound. Subsequently, its target affinity (K_D) and target density (B_{max}) were determined to be 0.8 nM and 58 fmol/mg of protein, respectively, using tritium labelled compound-30 on rat brain homogenate. The tritium labelled compound-30 showed saturated binding in the *in vitro* rat brain homogenate. The specific binding was blocked by another, structurally distinct, target specific inhibitor. In summary, the implementation of LC-MS/MS assay in the early ligand screening greatly increased the success rate of the tracer discovery, was both time and cost effective and was environmentally friendly by avoiding the radiolabeling of many candidates. It is the first time a tracer was reported in the literature for this target. Compound-30 may eventually show appropriate properties to be further developed into a PET ligand.

P151 - A PHARMACOKINETIC NATURAL PRODUCT-DISEASE-DRUG INTERACTION: A DOUBLE-HIT ON HEPATIC TRANSPORTERS

John Clarke, Tarana Arman, Mary Paine, and Michelle Gastecki
Washington State University

Background: Nonalcoholic fatty liver disease (NAFLD) is the most common liver disease in the United States. The botanical natural product silymarin is used to self-treat NAFLD and other liver diseases. Silymarin contains flavonolignans that inhibit the hepatic uptake transporters, organic anion transporting polypeptides (OATPs), and biliary efflux transporter, breast cancer resistance protein (BCRP), at low micromolar concentrations (IC_{50} , 1-3 μ M). Patients with NAFLD exhibit lower hepatic OATP1B3 and higher BCRP expression compared to healthy subjects. In addition, plasma exposure to silymarin (aggregate flavonolignans) was 3.3-fold higher in NAFLD patients compared to healthy subjects. Because NAFLD patients often take multiple medications, these patients may be at increased risk for adverse silymarin-drug interactions. The purpose of this study was to determine whether the combination of silymarin and nonalcoholic steatohepatitis (NASH), an advanced stage of NAFLD, alters the disposition of the cholesterol lowering drug and model OATP substrate pitavastatin by a greater extent than each 'hit' alone. Methods: Male Sprague Dawley rats (n=4-5) were fed a control or methionine and choline deficient diet (NASH model) for 8 weeks. Silymarin (10 mg/kg) or vehicle was administered intravenously, followed by pitavastatin (0.5 mg/kg). Plasma and bile were collected from 0-120 minutes. The pharmacokinetics of flavonolignans (silybin A, silybin B, isosilybin A, isosilybin B, silychristin, silydianin) and pitavastatin were determined using noncompartmental methods. Results: Mean plasma concentration of silybin A at 2 minutes was 1.7 and 2.7 μ M in healthy and NASH rats, respectively, which were within C_{max} values (0.9-4.2 μ M) observed in NAFLD and hepatitis C patients administered silymarin orally (560-700 mg). Compared to healthy rats, mean total flavonolignan area under the plasma concentration-time curve ($AUC_{0-120min}$) increased 1.7-fold, and terminal half-lives of silybin B and isosilybin A increased ~1.8-fold in NASH rats, consistent with observations in NAFLD patients. Silymarin increased pitavastatin plasma $AUC_{0-120min}$ in both healthy and NASH rats by ~2-fold. NASH alone increased pitavastatin plasma concentrations from 2-40 minutes, but $AUC_{0-120min}$ was unchanged. The combination of silymarin and NASH increased pitavastatin $AUC_{0-120min}$ 2.9-fold compared to healthy vehicle-treated rats, suggesting that NASH and silymarin combined have a synergistic effect on hepatic Oatp function. NASH-associated increase in hepatic Bcrp increased the total amount of pitavastatin excreted into the bile ~2.7-fold compared to healthy rats, whereas silymarin decreased pitavastatin biliary clearance ~3-fold in both healthy and NASH rats. Conclusion: This demonstration of a double-hit of disease and natural product on hepatic transporters may represent a novel mechanism underlying pharmacokinetic drug interactions.

P152 - ABSTRACT WITHDRAWN

P153 - INTEGRATING PHARMACOKINETIC-PHARMACODYNAMIC MODELING IN PRECLINICAL ASSESSMENT OF MUTANT SELECTIVE EGFR COVALENT TYROSINE KINASE INHIBITOR EGF816

Chun Li, Yong Jia, Gerald Lelais, Jie Li, Michael Shapiro, Todd Groessl, Mei-Ting Vaillancourt, Celin Tompkins, Tove Tuntland, John Isbell, Steve Bender, and Xiaoming Cui
Novartis Institute for Biomedical Research

EGF816 (nazartinib) is a third generation, irreversible mutant selective EGFR tyrosine kinase inhibitor (TKI) which is currently in clinical development for the treatment of non-small cell lung cancer harboring EGFR mutations, including T790M.

In preclinical studies following 14 days of once daily oral administration, EGF816 demonstrated dose dependent anti-tumor efficacy and regression in human NSCLC H1975 (EGFR L858R/T790M) xenograft models in both nude mice and nude rats. EGF816 was very well tolerated in both xenograft models at fully efficacious doses without noticeable toxicity. Plasma exposures of EGF816 in both mouse and rat H1975 xenograft studies increased approximately dose proportionally. A semi-mechanistic tumor kinetic PK/PD model was developed, and it described the tumor growth kinetics and inhibition by EGF816 very well. This modeling approach allowed the identification of both drug specific potency and system related parameters. The tumor static concentration (TSC), which represents the steady-state EGF816 plasma concentration whereby tumor growth and death rates are instantaneously equal and tumor volume remains unchanged,

can be derived from the model. Consistent results were obtained from modeling both mouse and rat H1975 xenografts, with TSC of 150 to 200 ng/mL. The human equivalent TSC (100 ng/mL) was derived by correcting for species difference in plasma protein binding.

The time course of target inhibition was determined in a single oral dose PK/PD study of EGF816 at 3, 10 and 30 mg/kg to H1975 tumor bearing nude mice. Dose dependent inactivation of the target enzyme, as measured by tumor pEGFR levels, was demonstrated. At the 30 mg/kg dose, tumor pEGFR levels were inhibited for >80% in the 24 hour period. An indirect turn-over PK/PD model incorporating irreversible inactivation was used to model the time course of pEGFR inhibition. The kinetics of pEGFR inhibition is determined by the kinetics of enzyme synthesis, degradation and inactivation by EGF816. The turn-over rate of pEGFR is relatively fast with an estimated turn-over half-life of 15~16 h in mouse H1975 xenograft, supporting the use of daily dosing in the clinic. Comparing the *in vivo* IC₅₀ derived from the PK/PD model for pEGFR inhibition with the TSC derived from tumor kinetic modeling, near complete inhibition of pEGFR is required to achieve good anti-tumor efficacy.

PK/PD modeling from preclinical studies and the derived tumor static concentration (TSC) are very informative and provided a rational estimate of therapeutically active *in vivo* drug concentration that needs to be targeted in the clinic.

P154 - ABSTRACT WITHDRAWN

P155 - FACTORS THAT INFLUENCE TRANEXAMIC ACID OVERDOSE IN CARDIAC SURGICAL PATIENTS WITH CHRONIC RENAL DYSFUNCTION

Qi (Joy) Yang¹, Angela Jerath², Marcin Wąsowicz², and K. Sandy Pang¹

¹Department of Pharmaceutical Sciences, Leslie Dan Faculty of Pharmacy, University of Toronto, ²Toronto General Hospital University Health Network; Faculty of Medicine, University of Toronto

Purpose: Tranexamic acid (TXA), an anti-fibrinolytic commonly used to minimize bleeding during cardiac surgery, is cleared by renal filtration only. Since 50% of cardiac surgical patients also have chronic kidney disease (CKD), a higher risk of TXA toxicity or seizures due to reduction of glomerular filtration rate (GFR) may occur in these patients. Our recent publication¹ indeed found a strong correlation between TXA clearance and eGFR. The observation led to the recommendation of dose adjustment of the BART regimen (Blood Conservation Using Anti-fibrinolytics Trial that comprises of a loading dose and maintenance infusion). We suggested reduction of the maintenance infusion rate according to the eGFR, but there was no need to alter the loading dose¹ to maintain TXA concentrations at the effective concentration of ~100 mg/L, the threshold concentration for maximal anti-fibrinolysis. The aim of this study was to revisit other factors such as the total dose of TXA infused and the duration of infusion in addition to the maintenance infusion rate, which may be associated with elevated TXA exposure and therefore toxicity. Methods: We revisited our TXA pharmacokinetic study in forty-eight cardiac surgical patients with stages 1 (mild) to 5 (severe) CKD¹. Among the patients, half (stages 1-5) underwent low-risk surgeries and received a 50 mg/kg intravenous dose. The other half (stages 1-5) underwent high-risk and extensive surgeries and received the BART regimen: a loading dose 30 mg/kg infused over 15 min followed by the maintenance infusion of 16 mg/kg/h, and 2 mg/kg was present in the cardiopulmonary bypass device during the bypass stage. Here, seizure was observed among 4 patients in stages 3 and 5 CKD. We revisited both data sets and examined the total TXA dose and infusion duration for each stage of the CKD patients. We further defined TXA over-exposure as the area under curve (AUC) in excess of 100 mg/L (AUC_{>100mg/L}). Results: The total TXA dose (normalized by body weight) was similar among all patients with different stages of CKD. For patients who underwent high-risk cardiac surgeries, the AUC_{>100mg/L} was consistently elevated to almost 1600 mg/L*h with the BART dose, increasing with the severity of CKD. The four patients who suffered from postoperative seizure displayed AUC_{>100mg/L} above 400 mg/L*h. By contrast, no seizure occurred in low-risk cardiac patients and their AUC_{>100mg/L} was below 250 mg/L*h, even for dialysis (stage 5) patients. A significant correlation was found between the infusion time and AUC_{>100mg/L} ($P = 0.005$), suggesting higher AUC_{>100mg/L} with increased infusion time. Due to CKD and reduced GFR function, the infusion time, in addition to the maintenance infusion rate, should be reduced to prevent postoperative seizures in CKD patients. Discussion: Other than the maintenance infusion rate, the TXA infusion time may be another significant factor contributing to TXA overdose and post-operative seizures. Notably, other institutions shorten the maintenance infusion time and stop infusion when a total dose of 50 mg/kg is reached.

Reference:

1. Jerath A et al. (2018) Tranexamic Acid Dosing for Cardiac Surgical Patients With Chronic Renal Dysfunction: A New Dosing Regimen. *Anesth Analg* [Epub ahead of print]

P156 - APPLICATION OF PBPK MODELING TO EVALUATE PHARMACOKINETIC DRUG-DRUG INTERACTIONS DURING THE DEVELOPMENT OF NEW ANTIMALARIAL COMBINATION THERAPIES

Nada Abia¹, Lisa Almond², Maurice Dickins², Nathalie Gobeau¹, Susan A. Charman³, Karen Rowland-Yeo², Myriam El Gaaloul¹, Zoe Barter², Joerg Moehrle¹, David Wesche^{4,5} and Jeremy Burrows¹

¹Medicines for Malaria Venture, ²Simcyp Limited (a Certara Company), ³Monash University, ⁴Bill & Melinda Gates Foundation, ⁵Great Lakes Drug Development (a Certara Company)

In 2016, an estimated 216 million cases of malaria occurred worldwide, with an estimated 445 000 deaths. The current WHO recommendation for the treatment of uncomplicated falciparum malaria is artemisinin-based combination therapies (ACTs)¹. However, due to the emerging resistance to artemisinin derivatives, research is now focusing on the development of new fixed-dose combinations of 2 or more antimalarial drugs to decrease the risk of resistance and increase the chances of cure². As such, understanding potential pharmacokinetic drug-drug interactions (PK-DDIs) among partner drugs is critical for the strategy to optimize the clinical development and dose selection of combinations of antimalarial drugs. Moreover, malaria is often complicated by comorbidities such as infection with human immunodeficiency virus (HIV). Therefore, PK-DDIs with comedications should also be evaluated.

The objectives of this work are to apply PBPK modeling and simulations to predict PK-DDIs and optimize the development of new combinations of antimalarial compounds. As part of an effort to establish a PBPK model library for antimalarial drugs, we generated the following *in vitro* and physicochemical data at the Centre for Drug Candidate Optimisation, Monash University, Australia: Log D 7.4, pKa, apparent permeability and efflux ratio in Caco-2 cells, plasma protein binding, blood to plasma ratio, fraction unbound in microsomes, intrinsic clearance in human liver microsomes, aqueous solubility at pH 7.4, solubility in FaSSiF, FeSSiF and FaSSGF, direct and time-dependent CYP inhibition and CYP reaction phenotyping. UGT reaction phenotyping and inhibition data were generated at external laboratories. These data were used as initial input parameters for building PBPK models for compounds DSM265 (and its metabolite DSM450), MMV390048 and artefenomel, using Simcyp software (a Certara Company, Sheffield, UK). The model development followed the following workflow: an initial model was built using *in vitro* DMPK and physicochemical data, it was then evaluated and refined using clinical pharmacokinetic and drug-drug interaction data, when available, and finally verified using an independent clinical data set. PK-DDI potential of different combinations of development compounds DSM265, MMV390048 and artefenomel, together or with strong CYP inhibitors, was evaluated via model simulations. The risk of PK-DDIs was found to be low for combinations of these compounds. A strategy of using PBPK modeling for optimizing the development of antimalarial combinations is presented.

In conclusion, PBPK models for antimalarial drugs can be used to predict PK-DDIs for all potential combinations between these compounds, and help evaluating whether, how and when clinical DDI studies and/or dose adjustments are required. Such models are currently available for 3 development compounds, and the short-term goal is to provide them for all antimalarial compounds.

References:

1. WHO. World Malaria Report 2017. Geneva, World Health Organization, 2017
2. Burrows JN, Duparc S, Gutteridge WE, et al. New developments in anti-malarial target candidate and product profiles. *Malar J.* 2017 Jan 13;16(1):26

P157 - PREDICTIVE PERFORMANCE OF SIMCYP DEFAULT MODELS OF 8 CYTOCHROME P450 MODULATORS IN DIFFERENT CLINICAL SENARIOS.

Caroline Samer, Youssef Daali, Niloufar Marsousi, and Jules Alexandre Desmeules
Clinical Pharmacology and Toxicology, Geneva University Hospitals

Physiologically Based Pharmacokinetics modeling (PBPK) use in clinical setting has become an important challenge to help clinicians tailoring medication based on genetic, environmental as well as patients' characteristics. Validated models, exhaustive drugs database and multiple patients scenarios are needed to improve the predictability of Model-Informed Precision Dosing approach (MIPD). Drug-drug interactions (DDIs) prediction represents one of the most promising domains for a successful use of PBPK. The goal of this work was to evaluate the predictive performances of the default models of Simcyp® (version 15, release 1) (a Certara company, UK, Sheffield) for 5 competitive inhibitors of CYP1A2 (ciprofloxacin), CYP2C9/2C19 (fluconazole), CYP2D6 (quinidine), CYP3A (ketoconazole and itraconazole), 2 mechanism-based inhibitors of CYP2D6 (paroxetine) and CYP3A (clarithromycin), and finally 1 inducer of CYP3A (rifampicin).

Concentration-time profiles of all drugs were simulated using perfusion-limited minimal-PBPK distribution models encompassing liver, gut and central compartments, except for rifampicin single dose and repaglinide, for which full PBPK distribution was considered by the software. Accordingly, absorption was described by the first order absorption sub-model for all compounds except for rifampicin single dose and omeprazole for which advanced dissolution, absorption, and metabolism (ADAM) sub-model was taken into account. All compound PBPK models, namely the victim drugs, inhibitors, and rifampicin were used without modification of software default parameters.

Concerning ketoconazole model, 85% (number of clinical studies = 26) of generated AUC ratios were within the

commonly used 2-fold range interval, and 50% of these results were within 1.25-fold error range. Regarding other modulators, results were within 2-fold range interval for 81% (n = 16), 100% (n=7), 100% (n=11), 28% (n=18), 75% (n=8), 100% (n=4), and 65% (n=23) for itraconazole, clarithromycin, ciprofloxacin, quinidine, paroxetine, fluconazole and rifampicin, respectively.

In conclusion, the tested PBPK models present in Simcyp® can be successfully used to evaluate DDIs in untested scenarios except for quinidine inhibitor model that requires further improvement.

P158 - REDUCED PARENT-METABOLITE(S) PHYSIOLOGICALLY-BASED PHARMACOKINETIC MODEL: APPLICATION TO MYCOPHENOLIC ACID

Norikazu Matsunaga, Adam Darwich, Kayode Ogungbenro, and Aleksandra Galetin
University of Manchester

Mycophenolic acid (MPA) is an inosine-5'-monophosphate dehydrogenase (IMPDH) inhibitor widely used for immunosuppressive therapy after renal transplantation. MPA is usually administered as a prodrug mycophenolate mofetil (MMF), and carboxylesterases are involved in its hydrolysis to MPA. MPA is subsequently metabolised in the intestine, liver, and kidney to phenol-glucuronide (MPAG) which is inactive against IMPDH. MPAG is a substrate of several hepatic transporters, e.g. OATP1B1/1B3, MRP2, and MRP3, and undergoes enterohepatic circulation as MPA. Physiologically-based pharmacokinetic (PBPK) modelling is increasingly applied for the prediction of enzyme-transporter-mediated pharmacokinetics. The aim of the present study was to develop a reduced PBPK model to describe complex interplay between MMF (prodrug), MPA (active form), and MPAG (inactive metabolite). The model was developed in MATLAB (2015a) and consisted of gut lumen, gut wall, portal vein, liver, kidney, systemic blood, and rest of the body compartments. For MPAG, liver compartment was further separated into vascular and liver tissue to include hepatic transporter function. Transit compartment that allows a time delay for emptying of the bile into the gut lumen was included to capture enterohepatic circulation of MPAG. Metabolic clearances of intestinal hydrolysis of MMF and MPA glucuronidation in the intestine, liver, and kidney were scaled from *in vitro* microsomal data¹). *In vitro* hepatic transporter-mediated clearance and passive diffusion of MPAG previously reported²) were used in the model. Renal clearances (CL_R) of MPA and MPAG and total clearance of MMF were cited from clinical data in healthy subjects³). Tissue-plasma concentration ratio (K_p) were predicted by *in silico* method. The developed PBPK model accurately described the observed plasma concentration-time profiles of MMF, MPA, and MPAG in healthy subjects following a single oral administration of MMF. Further verification of the model was performed against clinical data reported in renal transplant patients; good agreement between the model predicted and observed C_{max} and C_{trough} of MPA and MPAG in renal transplant patients was achieved. The present study illustrates development of a parent-metabolite(s) PBPK model and its application to predict complex enzyme-transporter interplay associated with MPA.

References:

1. Gill KL, Houston JB, Galetin A. Drug Metab Dispos. 2012;40(4):825-35.
2. Matsunaga N, Wada S, Nakanishi T, Ikenaga M, Ogawa M, Tamai I. Mol Pharm. 2014;11(2):568-79.
3. Bullingham R, Monroe S, Nicholls A, Hale M. J Clin Pharmacol. 1996;36(4):315-24.

P159 - SEMI-PHYSIOLOGICALLY BASED PHARMACOKINETIC MODEL ALLOWS PREDICTION OF CNS DISPOSITION OF ONO-2333MS IN HUMANS

Norikazu Matsunaga, Takeshi Fukuda, and Haruo Imawaka
Ono Pharmaceutical Co., Ltd.

Drug development for central nervous system (CNS) disorders is challenging because of uncertainties and complications to mechanistically understand the drug acts. Adequate drug exposure is essential for the action, however, the brain is isolated from the blood circulation by physiological barriers, such as blood-brain-barrier. Therefore, accurate measurement or prediction of drug exposure in the CNS is important to understand the PK-PD relationship of CNS drugs. The physiological-based pharmacokinetic (PBPK) model is now commonly used in the drug development and allows prediction of drug exposure in inaccessible tissues where the drug acts. The aim of the present study was to develop a semi-PBPK model of ONO-2333Ms, a corticotropin releasing-factor 1 (CRF1) receptor antagonist, in rats and humans. In addition, predicted brain extracellular fluid (Brain_{ECF}) exposure by semi-PBPK model was compared with *in vitro* inhibition constant (K_i) value against CRF1 receptor. Plasma and brain concentrations of ONO-2333 following oral administrations from 0.3 to 10 mg/kg were used for rat semi-PBPK model. In human model, plasma ONO-2333 concentrations following oral administrations from 1 to 100 mg were used with allometrically scaled drug-specific CNS parameters (clearance from plasma to Brain_{ECF}, intercompartmental clearance between Brain_{ECF} and brain, and diffusion rate in the brain and cerebrospinal fluid) from rats. The model consisted of empirical three compartments for the systemic (V_c, V₁, and V₂) and physiologically-based compartments for the CNS (Brain, Brain_{ECF}, and cerebrospinal fluid in lateral ventricle, third and fourth ventricle, cisterna magna, and subarachnoid space). The developed semi-PBPK models accurately described the observed concentrations of ONO-2333 in rats (plasma and brain) and humans (plasma). In rats, simulated Brain_{ECF}

exposure at doses showing significant *in vivo* efficacy was greater than *in vitro* K_i against rat CRF1 receptor. In contrast, predicted human Brain_{ECF} exposure at the maximum dose in clinical proof-of-concept study did not reach *in vitro* K_i for human CRF1 receptor, consistent with the results in clinical trial. The present study illustrates the usefulness of PBPK modelling to mechanistically understand the PK-PD relationship of CNS drugs and discrepancy between nonclinical and clinical results.

P160 - PHYSIOLOGICALLY BASED PHARMACOKINETIC MODEL PREDICTIONS OF IVOSIDENIB (AG-120) AS A VICTIM AND PERPETRATOR OF DRUG-DRUG INTERACTIONS

Chandra Prakash¹, Yue Chen¹, Bin Fan¹, David Dai¹, Kha Le¹, Alice Ke², Eyal Attar¹, Hua Yang¹

¹Agios, ²Simcyp

Ivosidenib (IVO; AG-120) is an oral, potent, targeted, small molecule inhibitor of mutant isocitrate dehydrogenase 1 (mIDH1) in development for the treatment of mIDH1 cancers including acute myeloid leukemia (AML). IVO is readily and well absorbed after single and multiple doses in both healthy volunteers (HVs) and AML patients across the dose range of 100 mg BID to 1200 mg QD. *In vitro* studies suggest that IVO is a substrate for and an inducer of CYP3A4, and may also induce CYP2B6, 2C8 and 2C9. The effects of the strong CYP3A inhibitor, itraconazole, on IVO pharmacokinetics (PK) in HVs were previously evaluated in a drug-drug interaction (DDI) study. The main objectives of this study were to: 1) develop a physiologically based pharmacokinetic (PBPK) model of IVO using *in vitro* and clinical PK data from HVs; 2) verify and refine the model using IVO single-dose DDI results after coadministration with itraconazole; and 3) develop and apply the IVO PBPK model in AML patients to predict IVO multiple-dose DDI outcomes. A PBPK model for IVO was developed for HVs in Simcyp Population-Based Simulator (V15.1) using data from *in vitro* studies and phase 1 clinical trials. The assigned CYP3A4 component was verified and refined based on an itraconazole clinical DDI study. CYP3A4 induction potential based on *in vitro* data was optimized using 4 β -hydroxy-cholesterol biomarker data from IVO clinical trials. A separate model was developed for AML patients to account for the reduced systemic clearance in these patients. The AML model was applied in subsequent simulations to assess the DDI potential of IVO as both the victim (with CYP3A4 inhibitors/inducers) and perpetrator (with CYP2B6, CYP2C8, CYP2C9 and CYP3A4 sensitive substrates). For a single dose of IVO 500 mg, the HV model predicted a geometric mean AUC_(0-∞) ratio of 2.14 and C_{max} ratio of 1.04 with the strong CYP3A4 inhibitor, itraconazole, which were within 1.26-fold of the observed values (2.69 and 1.0, respectively). The predicted IVO 500 mg QD steady-state geometric mean AUC and C_{max} ratios were 1.44 and 1.29 in the presence of itraconazole. The predicted IVO geometric mean steady-state AUC_(0-∞) and C_{max} ratios were 1.90 and 1.52, respectively, in the presence of a moderate CYP3A4 inhibitor (fluconazole), while negligible DDI effects on IVO were predicted with a weak CYP3A4 inhibitor (flvoxamine). Co-administration of the strong CYP3A4 inducer, rifampin, predicted a greater DDI effect on the kinetics of a single dose of IVO (AUC and C_{max} ratios 0.35 and 0.91) than that of multiple doses of IVO (AUC and C_{max} ratios 0.67 and 0.81). For the sensitive CYP3A4 substrate midazolam, the model predicted a reduction in AUC by 83% and C_{max} by 74% with IVO (500 mg for 19 days), but no clinically relevant impact of IVO on the exposure of CYP2B6, CYP2C8 and CYP2C9 sensitive substrates. Considering the challenges in conducting multiple dose clinical DDI studies of IVO in patients, this PBPK-based DDI approach to assess IVO as either perpetrator or victim is valuable to examine various clinical scenarios with reasonable accuracy.

P161 - QUALITY-BY-DESIGN (QBD) APPROACH TO ADDRESS RIGOR AND REPRODUCIBILITY IN DMET QUANTITATIVE PROTEOMICS

Bhagwat Prasad

University of Washington

Background: Quantification of drug metabolizing enzyme and transporter (DMET) proteins in tissues and cells are useful in predicting interindividual variability of drug disposition as well as *in vitro* to *in vivo* extrapolation (IVIVE) of drug metabolism and transport. Targeted quantitative proteomics is an emerging technique for quantification of DMET proteins but the execution of this methodology involves significant technical challenges (1-2). Therefore, it is important to thoroughly address the critical variables that could affect DMET protein quantification by using a quality-by-design (QbD) approach, especially when the methodology is applied to analyze a big cohort of samples over a long period.

Method: LC-MS/MS proteomics was used to quantify various DMET proteins using multiple surrogate peptides in various biological matrices. Effect of variables such as type of samples (tissue homogenate, cell lysate, S9 fractions, microsomes, and cytosol preparations), type of surrogate peptides, membrane isolation method, use of surfactant during sample preparation, multiple trypsin digestion protocols, desalting methods, peptide vs. protein internal standards, and various data analysis methodologies was evaluated on peptide recovery, signal intensity and data reproducibility. We then devised various control experiments to address the critical variables as discussed below.

Results: We found that quality and reproducibility of peptide signal depend on issues such as surrogate peptide, sample loss during processing, incomplete or inconsistent protein digestion, ion suppression in MS source, and artifacts in data analysis. For example, protein enrichment (e.g., in membrane or microsome preparation) is the major technical variable which could be resolved by using a protein marker of target subcellular fraction. Consistent trypsin digestion was ensured

by using an internal or external protein standard. When two surrogate peptides were used for quantification, the absolute quantification could vary from 0.3-3 fold, but the data reproducibility can be examined by correlation analysis of the two peptides. Pre-column and on-column desalting significantly decreased ion suppression thus improving data quality. We also proposed reanalysis of samples on three-different days rather than consecutive replicate analysis to better differentiate biological vs. technical variability. Inter-day variability can be addressed by repeated analysis of representative pooled samples on different days as quality controls. Although absolute protein quantification can only be confirmed when purified protein standard is available, surrogate peptide method generates precise and reproducible data. Such quantitative data can be used for IVIVE and physiologically based pharmacokinetic (PBPK) modeling as long as the other technical variables that affect precision are adequately addressed.

Conclusions: Although DMET protein quantification is emerging as an invaluable tool for predicting interindividual variability and IVIVE of drug disposition during drug development, a robust QbD approach is essential for generating reliable data.

References:

1. Bhatt and Prasad, Clin Pharmacol Therap, 2017.
2. Prasad and Unadkat, AAPS J, 2014.

P162 - A NOVEL 'BOTTOM-UP' PHYSIOLOGICALLY BASED PHARMACOKINETIC (PBPK) MODEL OF ITRACONAZOLE AND ITS METABOLITES: THE IMPORTANCE OF ENZYME KINETICS AND PROTEIN BINDING

Luna Prieto Garcia¹, David Janzén¹, Kajsa Kanebratt¹, Hans Ericsson¹, Hans Lennernäs², and Anna Lundahl¹
¹AstraZeneca, ²Uppsala University

An accurate physiologically-based pharmacokinetic (PBPK) model that simultaneously predicts the PK profiles of itraconazole and two of its main metabolites: OH-itraconazole and keto-itraconazole has been developed. The model also predicts, within 2-fold, 100% of the drug-drug interaction (DDI) studies with midazolam as the victim (substrate) drug. A bottom-up mechanistic PBPK model for itraconazole is clearly beneficial for both DDI risk assessment and optimization of clinical trial design. However, the development of such a model is challenging, given the complexity of a parent compound and two sequential metabolites, which all are both substrates and inhibitors of CYP3A4. In order to remove uncertainties caused by variability in model input data, key parameters were simultaneously experimentally determined for the parent compound and the metabolites including not only IC₅₀ for CYP3A4, but also enzyme kinetics: V_{max} and K_m and protein binding in plasma and microsomes. Besides, specifically for keto-itraconazole an *in vivo* pharmacokinetic experiment was performed to determine the V_{ss} and CL_{renal}. All generated data for the parent, OH- and keto-itraconazole were included in the PBPK model that was built upon the existing Simcyp library file. In addition, an exhaustive sensitivity analysis was performed to gain further insights on the relative importance of key parameters towards changes in plasma exposure for itraconazole and its metabolites. Performance of the model was validated using pre-specified acceptance criteria against different dosing regimens and formulations for 21 PK and DDI studies with midazolam. The main outcome is an accurate PBPK that successfully predicted the CYP3A4 DDI risk. Furthermore, in the case of itraconazole and clinical study designs for DDI, the most critical data is the steady-state prediction, where our model showed more accurate performance with 80% of these studies within the more strict criteria of 1.25-fold error. Prediction precision and bias of DDI expressed as geometric mean fold error were for the area under the concentration- time curve and peak concentration, 1.12 and 0.94, respectively. Thus, the predictive DDI risk capability of the developed model is improved compared to previously published models [1, 2]. In summary, our observations suggest that this novel PBPK model built for itraconazole and two of its main metabolites can be successfully used to both evaluate DDI involving new victim compounds and to facilitate optimal study design.

References:

1. Chen Y, Ma F, Lu T, Budha N, Jin JY, Kenny JR, Wong H, Hop CE, and Mao J (2016) Development of a physiologically based pharmacokinetic model for itraconazole pharmacokinetics and drug-drug interaction prediction. Clin Pharmacokinet 55: 735-49.
2. Marsousi N, Desmeules JA, Rudaz S, and Daali Y (2017) Prediction of drug-drug interactions using physiologically-based pharmacokinetic models of CYP450 modulators included in Simcyp software. Biopharm Drug Dispos 39: 3-17.

P163 - QUANTITATIVE PREDICTION OF DRUG INTERACTION POTENTIAL BETWEEN COBICISTAT AND RUZASVIR USING A PHYSIOLOGICAL BASED PHARMACOKINETIC MODELING APPROACH

Ying-Hong Wang, Shiyong Chen, and Wei Gao
 Merck & Co., Inc

Coinfection with HIV and HCV is common among HIV-infected injection drug users. Drug interactions between HIV and HCV drugs are of concern. Ruzasvir is a HCV NS5A inhibitor being developed as part of combination regimens for the

treatment of chronic HCV infection and is primarily metabolized by CYP3A. Cobicistat is one of the components of HIV combination regimens and is a strong CYP3A inhibitor. The objective of this study is to prospectively predict the magnitude of interaction between cobicistat and ruzasvir. PBPK models of cobicistat and ruzasvir were developed. The ability of the cobicistat PBPK model to predict its effects on CYP3A were qualified with clinical drug interaction of cobicistat with CYP3A substrates, midazolam and elbasvir. The effect of cobicistat on ruzasvir PK was simulated. Drug interactions of cobicistat with midazolam and elbasvir were reasonably predicted; the simulated fold changes in AUC and C_{max} of midazolam and elbasvir were within 20% of the observed values. The model prospectively predicts that co-administration of 150-mg cobicistat and 180-mg ruzasvir once daily for seven days would increase ruzasvir plasma AUC by 1.7-fold, which is similar to the observed effect of cobicistat on ruzasvir. In conclusion, the PBPK model predicts that the magnitude of drug interaction between cobicistat and ruzasvir is approximately 2-fold, and this result was confirmed by clinical DDI study.

P164 - THE PHENOTYPING OF SOLUTE CARRIER TRANSPORTERS IN HUMAN PRIMARY HEPATOCYTES

Yi-an Bi, Sumathy Mathialagan, Laurie Tylaska, Sarah Lazzaro, Chester Costales, Emi Kimoto, Anna Vildhede, Wenyi Hua, David Rodrigues, Larry Tremaine, and Manthena V Varma
Pfizer Inc.

Purpose: Hepatic elimination of xenobiotics and endogenous compounds usually involves sequential events in hepatocytes – including uptake from the blood compartment across the sinusoidal membrane, followed by intracellular metabolism and/or biliary excretion into the bile. Hepatic (sinusoidal) uptake is the first step and often considered as rate-determining in the hepatic elimination of drugs. Such uptake is mediated by various combinations of different solute carriers (SLCs); e.g., sodium-independent organic anion transporting polypeptides (OATP1B1/1B3/2B1), organic anion transporter 2 (OAT2), organic cation transporter 1 (OCT1), and sodium-dependent taurocholate co-transporting polypeptide (NTCP). Therefore, quantitative delineation of active uptake clearance (versus passive) *in vitro*, as well as the contribution of individual SLCs to total active uptake (SLC phenotype), is critical when modeling hepatic drug clearance and drug-drug interactions (DDI). However, challenges and controversies still remain regarding the most appropriate methods and the tools to assess different SLC activities (and their contributions) in human primary hepatocytes are not well developed. In this presentation, the PHH (plateable human hepatocytes)-mediated uptake of various substrates was studied after the addition of different SLC inhibitors that presented as phenotyping tools.

Methods: PHH, HEK293-cell lines and a passive permeability assay (RRCK) were applied. The cells were preincubated for 10 min in HBSS buffer with or without a pan-SLC inhibitor (rifamycin SV) and selective inhibitors (low concentration of rifamycin SV and rifampicin, OATPs; ketoprofen, OAT2; quinidine, OCT1 and HBV seq1 peptide, NTCP) at target concentrations. The incubation conditions were optimized; uptake clearance (CL_{up}) and passive diffusion rate were determined. Samples were analyzed by LC/MS/MS and liquid scintillation counting.

Results: The results indicated that OATPs, but not other SLCs, were inhibited at a low concentration of RIFsv (20 μ M). OATP1B1 and 1B3 (not 2B1) were completely inhibited by 5 μ M rifampicin and the contribution by OATP2B1 was deduced by comparing 5 μ M rifampicin versus 20 μ M RIFsv. On the other hand, OAT2, OCT1 and NTCP activity was selectively inhibited by ketoprofen (100 μ M), quinidine (100 μ M) and HBV seq1 peptide (0.1 μ M) respectively. All transporters were inhibited in the presence of RIFsv at a high concentration (1 mM). Using the approach it was determined that for rosuvastatin active uptake is mediated by OATPs (~80%) and NTCP (~15%), with ~4% by passive diffusion. For cyclic guanosine monophosphate (cGMP), a very different SLC phenotype was obtained with PHH (OAT2 >80%; passive diffusion ~10%).

Conclusion: For a given substrate, hepatic phenotyping of OATPs, OAT2, OCT1, NTCP and passive diffusion can be achieved using a pan-SLC inhibitor and inhibitors selective for different SLCs, or combinations of SLCs, at the defined concentrations.

P165 - EQUILBRATIVE NUCLEOSIDE TRANSPORTER 1 (ENT1) FACILITATES TRANSFER OF THE ANTIRETROVIRAL DRUG ABACAVIR ACROSS THE PLACENTA

Lukas Cerveny¹, Zuzana Ptackova¹, Martina Ceckova¹, Lucie Jiraskova¹, Sara Karbanova¹, Rona Karahoda¹, Susan L. Greenwood², Jocelyn D. Glazier², and Frantisek Staud¹

¹Faculty of Pharmacy in Hradec Kralove, Charles University, ²Division of Developmental Biology and Medicine, The University of Manchester

Abacavir is a preferred antiretroviral drug for preventing mother-to-child HIV transmission; however, mechanisms of its placental transfer have not been satisfactorily described to date. Because abacavir is a nucleoside-derived drug, we hypothesized that the equilibrative nucleoside transporters (ENTs) ENT1 and/or ENT2 (encoded by *SLC29A1* and *SLC29A2*, respectively) may play a role in its transfer across the placenta. To test this hypothesis, we performed *in vitro/ex vivo* accumulation studies in BeWo cells, and fresh villous fragments/microvillous plasma membrane (MVM) vesicles prepared from human placentas suggesting that ENT1 mediates abacavir uptake into placental tissues. Subsequent experiments with dually perfused rat term placentas showed that ENT1 contributes significantly to overall

abacavir placental transport. Finally, we quantified the expression of *SLC29A* in first- and third-trimester placentas, revealing that *SLC29A1* is the dominant type. Neither *SLC29A1* nor *SLC29A2* expression changed over the course of placental development, but there was considerable inter-individual variability in their relative expression. Therefore, drug-drug interactions (e.g. with ribavirin) and the effect of inter-individual variability in placental ENT1 expression on abacavir disposition into fetal circulation should be further investigated to guarantee safe and effective abacavir-based combination therapies in pregnancy.

This project was financially supported by the Czech Science Foundation (GACR 17-16169S).

P166 - DEVELOPMENT AND VALIDATION OF AN LC-MS/MS METHOD FOR VESICLE ASSAY USING CORNING® TRANSPORTOCELLS™ HEK293-DERIVED ABC TRANSPORTER MEMBRANE VESICLES BCRP AND MRP2

Kirsten Cooper, Jie Wang, Joanne Bourgea, Sweta Parikh, Li Cao, and Rongjun Zuo
Corning

Traditionally, the characterization of drug interactions with ATP-binding cassette (ABC) transporters involves using inside-out membrane vesicles and either radioactive or fluorescent chemicals to measure uptake activities. However, with increased concern on cost and safety associated with radioactive compounds and limited usage of fluorescent compounds, there is a strong need to develop mass spectrometry based detection methods. The purpose of this study is to develop a robust non-radioactive assay method using mass spectrometry to characterize drug interactions with the two major human ABC transporters, BCRP and MRP2. Using the newly launched Corning® TransportoCells™ HEK293-derived ABC transporter vesicles which transiently overexpress human efflux transporters BCRP or MRP2, the uptake of radiolabeled chemicals or non-radiolabeled counterparts were compared. For BCRP, the radiolabeled and non-radiolabeled counterpart used was ³H-Estrone-3-Sulfate (E3S), and for MRP2, ³H-Estradiol-17-β-Glucuronide (E17βG) was used. For non-radiolabeled chemicals, the elution method was optimized by comparing different incubation times and elution buffer volumes following the standard assay protocol. The elution buffer was optimized by comparing solvent based elution buffers with aqueous based elution buffers following the standard assay protocol and the elution method previously determined. The kinetic profiles of E3S for BCRP and E17βG for MRP2, and IC₅₀ values of several inhibitors were determined using both radioactive and non-radioactive methods and were compared to published data. In conclusion, the LC-MS/MS assay method using a rapid filtration technique was optimized for the vesicle uptake assay using non-radiolabeled chemicals. With an optimized elution method and elution buffer, the kinetic characteristics and inhibitory profile is consistent between non-radiolabeled and radiolabeled substrates, and is aligned with literature data. Using selected probe substrates, the method was validated for HEK293-derived human BCRP and MRP2 transporter vesicles.

P167 - APPARENT NONCOMPETITIVE INHIBITION OF BSEP IN PRIMARY HUMAN HEPATOCYTES ASSOCIATED WITH SEVERE DRUG-INDUCED LIVER INJURY

Kan He, Emily Qian, Qin Shi, Thomas Woolf, and Lining Cai
Biotranex LLC

Hepatic Bile Salt Export Pump (BSEP, ABCB11) is primarily responsible for the transport of bile salts, while hepatic Multiple Drug Resistance Protein 3 (MDR3, ABCB4) for the transport of phosphatidylcholine. Bile salts and phosphatidylcholine form mixed micelles in bile flow, which are critical for solubilizing cholesterol and preventing highly concentrated bile salts from damaging biliary canaliculi epithelium cells. Inhibition of BSEP and/or MDR3 by drugs can lead to cholestasis and drug-induced liver injury (DILI), and in some cases the need for a liver transplant. However, not all potent BSEP inhibitors are associated with clinically concerned DILI. Several laboratories have attempted to incorporate other factors, such as inhibition of other hepatic transporters, to differentiate BSEP inhibitors associated with severe DILI from those with less DILI concern. One possible underline mechanism, which has not been successfully explored so far, is whether or not the DILI potential is related to the type of BSEP inhibition. In the present study, we investigated the type of BSEP inhibition in human primary hepatocyte using the BSEPCyte® assay format with four drugs: troglitazone, pioglitazone, flutamide and cyclosporine A. Troglitazone and flutamide are associated with severe DILI, while pioglitazone and cyclosporine A are associated with less DILI concern. Incubations were carried out for each drug at eight concentrations ranging from 0-10/30/100 μM with five substrate concentrations (3, 10, 30, 100 and 300 μM). Pre-incubation with inhibitors (30 min) was also carried out with substrate concentrations of 10 and 100 μM. The IC₅₀ values were calculated, and the data were further analyzed using Dixon and Cornish-Bowden plots. All four drugs showed potent concentration-dependent inhibition of BSEP activity in primary human hepatocytes. The IC₅₀ values ranged from 0.9 to 4.2 μM for troglitazone, 0.9 to 9.9 μM for pioglitazone, 14.7 to 24.5 μM for flutamide, and 0.4 to 6.6 μM for cyclosporine A. Further analysis showed that troglitazone and flutamide exhibited noncompetitive inhibition kinetics, while pioglitazone and cyclosporine did competitive inhibition kinetics. Pre-incubation with inhibitors did not show substantial effects on the IC₅₀ values of the four drugs. In conclusion, the implication of BSEP inhibition is not only related to the potency (IC₅₀ value), but also to the type of inhibition. Apparent noncompetitive BSEP inhibition in human hepatocytes is associated with severe drug-induced liver injury.

P168 - EFFECTS OF PEG200 AND PEG400 ON HUMAN RENAL UPTAKE/EFFLUX TRANSPORTERS**Robert Houle**¹, Yi-Zhong Gu², Frank D. Sistare², Kenneth Koeplinger¹, Kathleen Cox¹, Xiaoyan Chu¹¹Pharmacokinetics, Pharmacodynamics & Drug Metabolism (PPDM), Merck & Co. Inc, ²Safety Assessment and Laboratory Animal Resources (SALAR), Merck & Co. Inc

Some excipients, such as solubilizing agents and surfactants, have been broadly used in pharmaceutical formulation in the development of oral and parenteral dosage forms for many new molecular entities in clinical evaluation. However, interactions of excipients with drug metabolizing enzymes and transporters have been increasingly reported. Such interactions may alter drug disposition and drug induced toxicity. Merck Compound X, a substrate of human renal organic anion uptake transporter OAT3, showed high incidence of kidney toxicity using 10% PS80 as an oral dosing vehicle in a rat study, while exhibiting no toxicity when 100% PEG 200 was used as a vehicle. The plasma exposure of Compound X *in vivo* in rats was similar in the formulation with both vehicles. To explore the underlying mechanism, we conducted a series of *in vitro* studies to understand the potential interaction of PEG200 and PEG400, frequently used excipients, on major human renal uptake and efflux transporters, including OAT1, OAT3, organic cation transporter OCT2, multidrug and toxin exclusion proteins MATE1, MATE2K, and multidrug resistance proteins MRP2 and MRP4 using transporter transfected cells and membrane vesicles. Our studies indicated that PEG200 and PEG400 inhibited OAT3-mediated uptake of estrone sulfate, a prototypic substrate of OAT3, and of Compound X. Based on these *in vitro* observations, we hypothesized that PEG200 could reduce kidney toxicity of Compound X in rats by decreasing its intracellular concentrations in kidney cells via inhibition of OAT3-mediated uptake. Further investigation showed that PEG200 and PEG400 also inhibited renal uptake transporter OCT2, several efflux transporters, including MATE1, MATE2K, and MRP4 *in vitro* but did not inhibit, or showed very weak inhibition of OAT1 and MRP4, respectively. Additional *in vivo* studies in preclinical animal models are in progress to better understand the *in vivo* implications of inhibition of renal transporters by these dosing vehicles. However, based on these preliminary findings, investigators should consider the potential impact of solubilizing agents on transporter-related drug disposition and toxicity.

P169 - EXPRESSION OF CONCENTRATIVE NUCLEOSIDE TRANSPORTERS (SLC28A) IN THE HUMAN PLACENTA; EFFECTS OF GESTATION AGE AND PROTOTYPE DIFFERENTIATION-AFFECTING AGENTS**Lucie Jiraskova**, Sara Karbanova, Zuzana Ptackova, and Frantisek Staud
Charles University, Faculty in Pharmacy in Hradec Kralove

Equilibrative (*SLC29A*) and concentrative (*SLC28A*) nucleoside transporters contribute to proper placental development and mediate uptake of nucleosides/nucleoside-derived drugs. We analyzed placental expression of *SLC28A* mRNA during gestation and studied whether *SLC29A* and *SLC28A* mRNA levels can be modulated by activity of adenylate cyclase, retinoic acid receptor activation or CpG islands methylation/histone acetylation. We analyzed mRNA expression in the first-, third-trimester placenta and choriocarcinoma-derived BeWo cells exposed to forskolin, all-trans retinoic acid, sodium butyrate, sodium valproate, or 5-azacytidine. Accumulation study with [³H]-adenosine was employed to confirm changes at functional level. We determined that expression of *SLC28A* genes increased during gestation and revealed considerable inter-individual variability. *SLC28A2* was shown to be a dominant subtype of *SLC28A* genes exhibiting the highest propensity to regulation. We observed effect of 5-azacytidine, all-trans retinoic acid, sodium valproate, but not sodium butyrate, suggesting role of methylation and retinoic acid receptor activation in *SLC28A2* regulation. The highest increase in *SLC28A2* expression, reflected in elevated transport function, was detected in forskolin-treated cells. Subsequent experiments demonstrated role of cAMP/PKA pathway in *SLC28A2* regulation. On the other hand, *SL29A* genes exhibited constitutive expression. Based on this data, we suggest that in placentas with overactivated cAMP-PKA regulation pathway and likely in the third-trimester placenta substrates of concentrative nucleoside transporter 2 might be uptaken in higher extent.

This study was financially supported by the Czech Science Foundation (Grant No. 17-16169S) and by Grant Agency of Charles University (Grant No. 812216/C/2016 and SVV 2018/260-414).

P170 - AMILORIDE AS A PROBE SUBSTRATE FOR INVESTIGATION OF ORGANIC CATION TRANSPORT SYSTEM**Chisa Kaneko**, Tatsuya Kawasaki, Ryosuke Nakanishi, Yuichi Uwai, and Tomohiro Nabekura
Aichi Gakuin University

Introduction: Disposition and elimination of cationic drugs are governed by drug transporters, organic cation transporter 1 (OCT1, *SLC22A1*), OCT2 (*SLC22A2*), multidrug and toxin extrusion 1 (MATE1, *SLC47A1*), and MATE2-K (*SLC47A2*). Drug-drug interaction guidances from the regulatory agencies, Food and Drug Administration (USA) and Pharmaceuticals and Medical Devices Agency (Japan), have been updated that inhibition of OCT2, MATE1, and MATE2-K should be studied for all new investigational drugs. Amiloride is a potassium-sparing diuretic used for treatment of hypertension, and shows strong fluorescence in organic solvent or detergent solution. In this study, we investigated transport characteristics of amiloride by human OCT1, OCT2, MATE1, and MATE2-K. Methods: Cellular accumulation of amiloride was evaluated with mock or hOCT1, hOCT2, hMATE1, or hMATE2-K overexpressed HEK293 cells. Cells were lysed with 1% SDS and

fluorescence was measured with a microplate reader at 364 and 409 nm, excitation and emission wavelengths, respectively. Results and Discussion: Amiloride was taken up by OCT1 and OCT2 in time- and concentration-dependent manner. These uptake was linear until 5 min and inhibited by the known substrates and inhibitors tetraethylammonium (TEA) and verapamil. High potassium induced-membrane depolarization also decreased the uptake. OCT1 showed higher affinity than OCT2 (K_m of 42 and 253 μM ; V_{max} of 1.88 and 15.4 nmol/mg protein/3 min for OCT1 and OCT2, respectively). MATE1 and MATE2-K also transported amiloride. At extracellular pH 8.0, uptake was linear until 20 min. MATE1- and MATE2-K-mediated amiloride transport showed a bell-shaped pH profile and reached maximum at pH 8.0–8.5. At extracellular pH 7.4 and ammonium prepulse-induced intracellular acidification, uptake showed an overshoot phenomenon. In this condition, MATE1 showed higher affinity than MATE2-K (K_m of 21 and 40 μM ; V_{max} of 909 and 570 pmol/mg protein/min for MATE1 and MATE2-K, respectively). These transports were inhibited by TEA, metformin, verapamil, estrone-3-sulfate, and pyrimethamine. Conclusions: This study demonstrates that amiloride is a suitable fluorescent substrate of OCT1, OCT2, MATE1, and MATE2-K, and useful for investigating organic cation transport system.

Acknowledgements: We thank Dr. Ken-ichi Inui, Professor Emeritus of Kyoto University for providing expression plasmid vectors containing hOCT1 and hOCT2 and Dr. Yoshinori Moriyama of Okayama University for providing expression plasmid vectors containing hMATE1 and hMATE2-K.

P171 - ABC XENOBIOTIC TRANSPORTERS PLAY IMPORTANT ROLES IN SYSTEMIC EXPOSURE AND DERMAL DISTRIBUTION OF TYROSINE KINASE INHIBITOR REGORAFENIB AND ITS ACTIVE METABOLITES

Yukio Katov¹, Aya Hasan¹, Yusuke Masuo¹, Ken-ichi Fujita², Yutaro Kubota², and Yasutsuna Sasaki²

¹Kanazawa University, Faculty of Pharmacy; ²Showa University, Institute of Molecular Oncology

Purpose: Regorafenib is orally active multikinase inhibitor used for treatment of colorectal cancer and other tumors. Regorafenib exhibits a high rate of treatment-related dermal toxicity. Therefore, it is important to clarify the mechanism(s) involved in its systemic exposure and dermal distribution. The purpose of the present study was to clarify the role of P-glycoprotein (P-gp) and breast cancer resistance protein (Bcrp) in systemic exposure and dermal distribution of orally administered regorafenib, its active metabolites M2 and M5, and regorafenib *N*- β -D-glucuronide (M7).

Methods: Regorafenib was orally administered at a dose of 2 or 10 mg/kg once a day for 5 days in wild-type (WT) and *Abcb1a/1b/bcrp*^{-/-} (TKO) mice. Plasma and tissue concentrations were measured by LC-MS/MS.

[Results and Discussion] After single oral administration of regorafenib, plasma concentration of regorafenib was almost similar between WT and TKO mice, whereas that of M2 and M5 in TKO was much higher, and that of M7 was slightly lower than those in WT mice. The difference in systemic exposure of the active metabolites was more obvious after repeated oral administration, and AUC of M5 after 5th administration in TKO was more than 100 times that in WT mice. The dermal concentration of regorafenib in TKO mice at 24 hr after the 5th oral dose was also much higher than that in WT mice. Considering our previous report indicating that both M2 and M5 are substrates of these two ABC transporters (1), these results suggest that P-gp and/or Bcrp play important roles in systemic exposure and dermal distribution of these active metabolites. Since the biliary excretion is the major elimination pathway for M5, this process could be primarily mediated by these transporters. The accumulation ratio (ratio of AUC after 5th dose to that after single dose) of M5 was 8 and 13 in WT and TKO mice, respectively, whereas that of regorafenib was almost unity in both strains. This phenomenon was similar to that in humans. Since dose-normalized AUC of M5 tended to be higher at the higher dose, nonlinear pharmacokinetic behavior may be associated with such unusual accumulation of M5.

Conclusion: P-gp and/or BCRP may exert large impact on systemic exposure and dermal distribution of active metabolites of regorafenib after repeated oral administration. The relevance of these ABC transporters to dermal toxicity is now under investigation.

Reference:

1. Fujita K et al. Involvement of the transporters P-gp and BCRP in dermal distribution of the multi-kinase inhibitor regorafenib and its active metabolites. *J Pharm Sci* 106: 2632-2641, 2017.

P172 - INVESTIGATION OF HUMAN ORGANIC ANION TRANSPORTING POLYPEPTIDE 2B1 USING FLUORESCENT ANIONS

Tatsuya Kawasaki, Naoki Nomura, Yuichi Uwai, and Tomohiro Nabekura
Aichi Gakuin University

Introduction: Human organic anion transporting polypeptide 2B1 (OATP2B1, *SLCO2B1*) are expressed at the brush-border membrane of the small intestine and the sinusoidal membrane of hepatocytes. OATP2B1 transports diverse organic anions, including fexofenadine, lipid lowering statins, and pemetrexed. Therefore, it plays important roles in absorption, distribution and elimination of anionic drugs. Hence species difference between human and rodents in localization and substrates and/or inhibitors profiles are reported, *in vitro* assay is useful for understanding physiological and pharmacological importance of human OATP2B1. Fluorescent anions such as fluorescein analogues were recently

used for study of organic anion transporters such as OATP1B1 and OATP1B3. In this study, we investigated OATP2B1-mediated transport of fluorescent anions to identify better substrates for *in vitro* assays. Methods: OATP2B1- or empty vector-transfected HEK293 cells were used to evaluate the OATP2B1 function. The cellular accumulation of fluorescent anions was determined with a microplate reader at 485 and 535 nm, excitation and emission wavelengths, respectively. Results and Discussion: Among tested 9 fluorescein analogues, two type derivatives were found as OATP2B1 substrates: heavy halogenated (bromine and iodine) derivatives such as 4', 5'-dibromofluorescein (DBF) and 2', 4', 5', 7'-tetrabromofluorescein; and carboxylated derivatives such as 5-carboxyfluorescein (5-CF) and 6-carboxyfluorescein (6-CF). DBF and 5-CF were transported in a time- and concentration-dependent manner (V_{max} of 42.1 and 25.3 pmol/mg/5 min and K_m of 0.89 and 6.02 μ M for DBF and 5-CF, respectively). OATP2B1 inhibitors, such as estrone-3-sulfate and bromosulphophthalein, inhibited DBF and 5-CF transport. Pravastatin and penicillin G also inhibited 5-CF transport while they didn't affect DBF transport. DBF was transported in neutral pH (pH6.5-8.0), while 5-CF was transported in acidic pH (pH5.5-6.5). These results suggest that DBF and 5-CF transport are mediated by different mechanisms. Kinetic comparisons of fluorescein analogues suggested that 2', 7'-fluorine decreases affinity, 4', 5'-bromine drastically increases affinity, about 5Å transfer of carboxylate decreases affinity, and lactone form microspecies and 2', 7'-dichloro substitution are negligible effects on interactions with OATP2B1. Conclusions: We found two type fluorescent anions DBF and 5-CF as OATP2B1 substrate. DBF and 5-CF are useful for further study to reveal accurate binding sites and transport mechanism of OATP2B1.

P173 - QUANTITATION OF PLASMA MEMBRANE DRUG TRANSPORTERS ENABLES BOTTOM-UP PBPK MODELING OF TRANSPORTER SUBSTRATES

Ryota Kikuchi¹, William Chiou¹, Kenneth Durbin¹, Junli Ma¹, Arian Emami Riedmaier¹, Sonia de Morais², Gary Jenkins¹, and Daniel Bow¹

¹AbbVie Inc., ²SdM Biopharma Consultants

Quantitative proteomics has been widely used to quantify transporters in both *in vitro* and *in vivo* systems in order to determine the scaling factors needed to extrapolate *in vitro* kinetics to *in vivo*. However, no methodology to correct for the loss of membrane proteins during sample preparation has been reported, which could lead to underestimation of transporter abundances. In this study, a novel approach was developed to improve the accuracy of transporter quantitation using OCT2, MATE1 and MATE2K as examples. Plasma membrane fractions were prepared from both HEK293 cells overexpressing individual transporters and human kidney cortex, and processing recovery was determined by quantitating the plasma membrane marker Na⁺/K⁺-ATPase in both lysate and plasma membrane fractions. The recovery varied significantly between independent experiments (e.g. 6.9% to 35% for HEK-OCT2), indicating that the correction for the loss of membrane proteins in each preparation is necessary to accurately determine the transporter abundance. The plasma membrane expression of OCT2, MATE1 and MATE2K were quantitated and corrected for plasma membrane recovery, resulting in values of 4050, 4280 and 5690 fmol/10⁶ cells in transfected cells, and 37300, 58800 and 6920 fmol/10⁶ proximal tubule cells in human kidney cortex, respectively. Accordingly, their relative expression factors (REFs) were determined to be 9.2, 14 and 1.2, respectively. *In vitro* kinetics of metformin were determined and extrapolated to *in vivo* using the corresponding REFs in a physiologically-based pharmacokinetic model. Metformin exposures simulated at two different doses (250 and 500 mg) were within 2-fold of the actual clinical exposures. These results demonstrate that the accurate quantitation of transporter proteins in the plasma membrane can enable accurate predictions of drug disposition for transporter substrates.

Disclosures: AbbVie Inc. funded this study. AbbVie was responsible for the study design, research, analysis, data collection, interpretation of data, and writing, reviewing, and approving of the abstract. All authors are employees, former employees, or retirees of AbbVie.

P174 - SIMULTANEOUS MEASUREMENTS OF N1-METHYLNICOTINAMIDE, CREATININE, ISOBUTYRYL-L-CARNITINE BY LIQUID CHROMATOGRAPH WITH HIGH RESOLUTION MASS SPECTROMETRY FOR ASSESSING THE ACTIVITIES OF MULTIPLE RENAL CATIONIC TRANSPORTERS IN FIRST-IN-HUMAN CLINICAL TRIAL

Lina Luo, A. David Rodrigues, Jared Kay, and Ragu Ramanathan

Pfizer Inc.

Renal cation transporters are responsible for the disposition of various endogenous and therapeutic agents in humans. There is increased interest in utilizing endogenous probes, in conjunction with drug-drug interaction (DDI) decision trees from the regulatory agencies, to discharge DDI risk quickly in Phase 1 studies. Recommended organic cation transporter 2 (OCT2) and multidrug and toxin extrusion proteins (MATEs) DDI risk thresholds are known to be conservative, and high false positive rates are reported. Therefore, it is important to deploy a simple, reliable, and sensitive assay for incorporation in first-in-human (FIH) clinical studies for early discharge of renal transporter DDI risks. Here we present a robust UPLC-HRMS method for simultaneous quantitation of N¹-methylnicotinamide (1-NMN), creatinine, isobutyryl-L-carnitine in FIH study plasma and urine samples. A highly sensitive hydrophilic interaction chromatography (HILIC)-tandem mass spectrometry (HRMS/MS) assay was developed and fit-for-purpose validated, with HRMS confirmation of 1-

NMN and numerous isobaric compounds in biofluids. The surrogate matrix approach avoided the interference from endogenous analytes and ensured good accuracy and precision for the assay, parallelism to native plasma and urine were established. The assay performed accurately with all accuracies and precisions were within $\pm 10\%$ of their nominal values, also was successfully transferred to our CRO partner for more portfolio clinical study support. The basal 1-NMN levels respectively were 4-120 ng/mL and 2000-15000 ng/mL in human plasma and urine. 1-NMN plasma AUCs increased 2- to 4-fold versus placebo following the administration of a drug candidate, which *in vitro* experiments indicated to be an OCT2 inhibitor. Dose dependent 1-NMN changes were observed in the high and mid treatment groups with the single/ multiple ascending dose (SAD/MAD) study. These results support that 1-NMN may be a useful endogenous biomarker of OCT2 or MATEs mediated DDIs, which offers options for earlier characterization and clinical safety projections along with pharmacokinetic analyses of a new chemical entity (NCE) as part of FIH clinical studies. Such efforts will also support physiologically based pharmacokinetic (PBPK) model development and validation.

P175 - LST-3TM12 IS PART OF THE FXR MODULATED GENE NETWORK IN HEPATOCYTES

Vanessa Malagnino, Henriette Meyer zu Schwabedissen, Janine Hussner, and Ali Issa
University of Basel, Pharmaceutical Sciences, Biopharmacy

We have recently, reported that LST-3TM12 is a functional transporter and a member of the OATP1B (*SLCO1B*) –family, which transports estradiol 17 β -glucuronide and dehydroepiandrosterone sulfate [1]. A particularity of LST-3TM12 is, that *SLCO1B3* (OATP1B3) encodes for its initial 333 base pairs while the rest of the mRNA originates from the gene locus *SLCO1B7*, whereby suggesting that transcription of LST-3TM12 is controlled by the promoter of OATP1B3. One transcription factor shown to modulate OATP1B3 transcription and expression is the bile acid sensor farnesoid X receptor (FXR, *NR1H4*) [2]. FXR is a nuclear receptor, which functions after ligand activation as transcription factor of multiple genes involved in bile acid homeostasis [3]. It was aim of this study to elucidate whether LST-3TM12 is a splice variant of OATP1B3 and whether it has an active role in bile acid homeostasis.

For the investigation of the transcriptional regulation of LST-3TM12 the Huh-7 hepatoma cell line was used, which we showed to express both LST-3TM12 and OATP1B3 mRNA. To test whether LST-3TM12 transcription depends on OATP1B3, Huh-7 cells were transfected with a siRNA designed to interfere with exon 4 of *SLCO1B3*. Notably, this particular sequence is part of LST-3TM12 and of *SLCO1B3*. Silencing of *SLCO1B3* by this particular siRNA not only lowered the amount of *SLCO1B3* mRNA, but also that of LST-3TM12 in transfected cells. Furthermore, it was tested whether FXR a known regulator of OATP1B3 transcription also modifies expression of LST-3TM12. Thus, cells were treated with the bile acid chenodeoxycholic acid, which is a commonly used FXR ligand [4], and it was found that LST-3TM12 mRNA transcription was augmented to a similar extend as *SLCO1B3*. Finally, the observed interaction of primary and secondary bile acids with LST-3TM12 transport suggested that this transporter takes part in bile acid homeostasis, which is further supported by our findings showing direct transport of taurocholic acid by LST-3TM12.

Taken together our data suggest that LST-3TM12 is splice variant of OATP1B3 that is regulated by FXR. Furthermore, LST-3TM12 transports taurocholate. We have previously reported that LST-3TM12 is localized in the endoplasmic reticulum. Thus, we hypothesize that LST-3TM12 facilitates access of bile acids to enzymes exerting their metabolic function in the lumen of the ER, such as the UDP-glucuronosyltransferases.

References:

1. Malagnino V, Hussner J, Seibert I, Stolzenburg A, Sager CP and Meyer Zu Schwabedissen HE (2017) LST-3TM12 is a member of the OATP1B family and a functional transporter. *Biochemical pharmacology* 148: 75-87.
2. Jung D, Podvinec M, Meyer UA, Mangelsdorf DJ, Fried M, Meier PJ and Kullak-Ublick GA (2002) Human organic anion transporting polypeptide 8 promoter is transactivated by the farnesoid X receptor/bile acid receptor. *Gastroenterology* 122(7): 1954-1966.
3. Wang H, Chen J, Hollister K, Sowers LC and Forman BM (1999) Endogenous Bile Acids Are Ligands for the Nuclear Receptor FXR/BAR. *Molecular cell* 3(5): 543-553.
4. Makishima M, Okamoto AY, Repa JJ, Tu H, Learned RM, Luk A, Hull MV, Lustig KD, Mangelsdorf DJ and Shan B (1999) Identification of a nuclear receptor for bile acids. *Science* 284(5418): 1362-1365.

P176 - LST-3TM12 IS A MEMBER OF THE OATP1B-FAMILY AND A FUNCTIONAL TRANSPORTER INFLUENCED BY GENETIC VARIANTS

Henriette Meyer zu Schwabedissen, Vanessa Malagnino, Janine Hussner, and Isabell Seibert
University of Basel; Department of Pharmaceutical Sciences, Biopharmacy

It is widely accepted that OATP1B-transporters, which are highly expressed in the sinusoidal membrane of hepatocytes, impact pharmacokinetics of their substrates. Both OATP1B3 and OATP1B1 are encoded by the genes *SLCO1B3* and *SLCO1B1*, respectively, which are located on chromosome 12. In between those genes, an area annotated as *SLCO1B7* is located. This particular region is assumed to be a pseudogene, as no functional protein has been reported [1]. However, in 2005 Mizutamari and Abe filed a mRNA sequence labelled as *LST-3TM12* (AY257470.1), which is linked to

this particular region on chromosome 12. Intrigued by findings of genome wide association studies, where phenotypes such as clozapine-induced neutropenia [2] or total serum bilirubin levels [3] were shown to be associated with genetic polymorphisms located in the region annotated as *SLCO1B7*, we further investigated the published mRNA sequence. *In silico* analyses, comparing the LST-3TM12 mRNA to that of *SLCO1B1*, *SLCO1B3* and *SLCO1B7* suggested that *LST-3TM12* is a splice variant of *SLCO1B3* and *SLCO1B7*. Indeed, the first part of LST-3TM12 is identical to *SLCO1B3*, while the last part of the mRNA derives from *SLCO1B7*. The expression of *LST-3TM12* mRNA was verified in human liver. Further, quantitative analysis of human liver showed mRNA expression in tissue and in isolated human hepatocytes. Furthermore, immunohistochemical staining revealed that LST-3TM12 is expressed in hepatocytes, where it is located in intracellular vesicular structures, which are most likely part of the smooth endoplasmic reticulum. In accordance with this assumption is the finding that LST-3TM12 is enriched in liver microsomes, when compared to liver homogenate. For functional analyses, a vTF-7 based heterologous expression system was applied. Overexpression of LST-3TM12, but not OATP1B7 significantly enhanced cellular accumulation of dehydroepiandrosterone sulfate. Importantly, in transfected HeLa cells the transporter was present at the plasma membrane and in intracellular vesicular structures as determined by immunofluorescence and biotinylation assays. During cloning we observed previously reported single nucleotide polymorphisms. Testing the influence of these variants on transport activity *in vitro* revealed significant changes in presence of rs11045689, rs188817665, and rs1546308. The latter being the variant previously associated with clozapine-induced neutropenia. Taken together, LST-3TM12 is a functional protein expressed in human liver, where it is localized in intracellular vesicular structures. We identified dehydroepiandrosterone sulfate as substrate of the transporter, and were able to show the impact of genetic polymorphisms on transport function.

References:

1. Stieger, B. and B. Hagenbuch, *Organic anion-transporting polypeptides*. Current topics in membranes, 2014.
2. Legge, S.E., et al., *Genome-wide common and rare variant analysis provides novel insights into clozapine-associated neutropenia*. Molecular Psychiatry, 2016.
3. Johnson, A.D., et al., *Genome-wide association meta-analysis for total serum bilirubin levels*. Human Molecular Genetics, 2009.

P177 - UTILITY AND LIMITATIONS OF DUAL CHOLATE SHUNT ASSAY IN PRECLINICAL SPECIES

Vijay More¹ and Kara Pearson²

¹Celgene, ²Merck

Quantitative liver function tests utilize chemicals that are excellent substrates for hepatic clearance through uptake, metabolism and excretion. 'Dual cholate shunt' was a method utilized for assessment of hepatic function in patients with fibrosis in clinical trial for hepatitis C intervention. The assay uses oral (PO) and intravenous (IV) administration of stable labeled cholic acid tracers monitored over period of three hours. Here, we translated the assay in a rodent model of hepatic fibrosis, and healthy dogs, and describe the utility and the limitations of the assay in preclinical species. Four week treatment of 1ml/kg carbon tetrachloride (CCl₄) was used for inducing advanced fibrosis in rats, which was confirmed by shear wave elastography and histology. During multiple stages of fibrosis development, dual cholate shunt assay was performed using a modified protocol for rats. After fibrosis development, CCl₄ treatment was stopped, and animals were allowed to recover from hepatocellular injury, and dual cholate shunt was repeated.

After one week of CCl₄ treatment, severe hepatocellular injury was induced with 10-fold elevation in serum aminotransferases, however no fibrosis was evident. Plasma concentration- time curve for both PO and IV cholate were significantly altered in CCl₄-treated groups, with much higher areas under the curve (AUC) compared to vehicle group. However, shunt value remained unchanged with one week of CCl₄ treatment. After 4-weeks of CCl₄ treatment, hepatocellular injury was accompanied by advanced fibrosis, and even higher plasma aminotransferase levels. AUC values increased for both PO and IV cholate in CCl₄-treated groups, however, shunt remained unchanged. One week after CCl₄ treatment stopped, aminotransferase levels returned to normal; however, fibrosis scores remained severe. Interestingly, AUC change in PO cholate was higher than IV cholate at this time, and shunt value increased by >60% in fibrotic rodents.

Overall, it was demonstrated that 'dual cholate shunt' assay can be translated to preclinical species. Hepatic fibrosis increased shunt in rats; however, co-presence of hepatocellular injury, or hepatocellular injury alone masked shunt changes.

P178 - SUBSTRATE-DEPENDENT INTERACTIONS BETWEEN NATURAL FLAVONOIDS AND DRUG TRANSPORTER OATP2B1

Tomohiro Nabekura, Tatsuya Kawasaki, Kumi Kawai, Ken-ichi Nakashima, Makoto Inoue, and Yuichi Uwai
Aichi Gakuin University

Introduction: Organic anion transporting polypeptide 2B1 (OATP2B1, *SLCO2B1*) plays important roles in drug absorption, distribution and elimination. Recently, substrate-dependent food—drug interactions mediated by OAT2B1 have been

reported. For example, grapefruits juice component inhibits OATP2B1-mediated transport of fexofenadine, talinolol, aliskiren, and sulfasalazine but does not affect transport of pitavastatin and glibenclamide. Therefore, determinations of OATP2B1 transport function using different substrates are required for predicting food–drug interactions. In our previous study, we found two fluorescent anions 5-carboxyfluorescein (5-CF) and 4', 5'-dibromofluorescein (DBF) as substrate of OATP2B1 with different transport characteristics. 5-CF is low affinity substrate and transported in acidic pH while DBF is high affinity substrate and transported in neutral pH. In this study, we evaluated the effects of flavonoid aglycones and their glycosides, food components which can reach high concentrations in the gut lumen, on OATP2B1 transport activity using 5-CF and DBF. Methods: OATP2B1- or empty vector-transfected HEK293 cells were used to evaluate the OATP2B1 function. The cellular accumulation of fluorescent anions was determined with a microplate reader at 485 and 535 nm, excitation and emission wavelengths, respectively. Results and Discussion: Several flavonoid aglycones (quercetin, naringenin, hesperetine, nobiletin, tangeretin, and sudachitin) showed substrate-dependent effects on OATP2B1. Their concentration-effect curves showed non-sigmoidal curves with both inhibitory and stimulatory effects on OATP2B1 function. One of them, naringenin stimulated 5-CF transport at low concentrations (1-10 μM) while it inhibited at high concentration (100 μM). On the other hand, naringenin inhibited DBF transport at any tested concentrations (1-100 μM) with IC_{50} of 10.1 μM . Furthermore, its glycoside naringin inhibited both 5-CF and DBF transport with IC_{50} of 10.3 and 30.0 μM , respectively. Naringenin altered the maximal velocity without affecting the affinity of substrates, suggesting that naringenin is an allosteric modulator and does not share the binding site with DBF nor 5-CF. Conclusions: This study demonstrates that several flavonoids modulate OATP2B1 function with substrate- and concentration-dependent manner, suggesting the importance of using multiple substrates to predict food–drug interactions mediated by OATP2B1. Flavonoid aglycones and their glycoside are useful for further study to reveal accurate binding sites and transport mechanism of OATP2B1.

P179 - ESTABLISHED CHEMICAL KNOCKOUT CONDITION FOR P-GP MEDIATED EFFLUX AT THE BLOOD-BRAIN-BARRIER IN CYNOMOLGUS MONKEY

Masanori Nakakariya, Li Yang, Ron Chen, Angie Fenton, and Natalie Hosea
Takeda California

Purpose: To understand drug candidate disposition in brain is essential for drug discovery and development in CNS disease area. Since P-gp could be a barrier for drug candidates to penetrate at the blood brain barrier (BBB), clarification and deprioritization of P-gp substrates from *in vitro* and *in vivo* experiments is key factor to select best candidates in CNS disease area. Cynomolgus is well known as non-human primate species to predict human PK profile and to assess PD and efficacy in CNS disease area. To date there is no established *in vivo* approach to evaluate P-gp function for drug disposition at the BBB in monkey. Therefore, the purpose of the study is to validate *in vivo* condition where P-gp function is inhibited chemically with elacridar, a P-gp substrate and potent efflux transporter inhibitor.

Methods: Plasma and CSF concentrations of elacridar were evaluated after intravenous administration of elacridar at a dose of 5 mg/kg to monkey to set chemical knockout condition by elacridar. Drug-drug interaction study was conducted using P-gp substrates in the presence of elacridar to clarify whether the combination with elacridar could function as chemical knockout for P-gp activity. Verapamil, quinidine, loperamide, and topotecan were selected as a P-gp substrate. Carbamazepine and antipyrine which are P450 substrates not transporter substrates were selected as negative controls for P-gp chemical knockout. Protein binding of test compounds in monkey plasma was evaluated with RED device with a cut-off mass of 8000 Da. Test compound concentration in *in vitro* and *in vivo* samples were analyzed by liquid chromatography with tandem mass spectrometry.

Results and discussion: Free plasma concentrations of elacridar were comparable with CSF concentration after intravenous administration of elacridar at a dose of 5 mg/kg, suggesting that P-gp could be completely inhibited since CSF concentration should be much lower than free plasma concentration if P-gp function is maintain at the BBB. Moreover, the CSF concentration and free systemic exposure of elacridar exceeded the *in vitro* P-gp K_i value for 8h after elacridar administration. These results suggest that elacridar after intravenous dosing at 5 mg/kg could work for chemical knockout condition of P-gp at the BBB in monkey. CSF concentrations divided by free plasma concentration ($\text{K}_{p,u}$) of P-gp substrates except topotecan in the presence of elacridar were higher than those without elacridar by 2.6- to 5.4-fold, while the $\text{K}_{p,u}$ values of the negative control compounds carbamazepine and antipyrine were unchanged in the presence of elacridar. These results suggest that the combination with elacridar could inhibit P-gp function and have no effect for P450 activity. However, BCRP activity may not be inhibited fully by elacridar since no increase in the $\text{K}_{p,u}$ of topotecan, a dual substrate of P-gp and BCRP, was observed in the presence of elacridar.

Conclusion: We established chemical knockout condition of P-gp at the BBB in monkey. The experimental design of pre-treatment with elacridar at 5 mg/kg IV could be utilized to assess whether P-gp would be a barrier for the BBB penetration of drug candidates.

P180 - HEPATOBIILIARY TRANSPORTER EXPRESSION AND FUNCTIONAL UPTAKE OF SUBSTRATES IN 2D SANDWICH CULTURES USING UPCYTE® HEPATOCYTES

Astrid Noerenberg, Timo Johannssen, and Nikolett Nagy
upcyte technologies

Isolated hepatocytes are frequently used for hepatotoxicity studies. However, large-scale cultures of primary hepatocytes demanded by high throughput approaches face obstacles such as a limited lifetime and rapid dedifferentiation *in vitro*. Thus, it leads to often compromised reproducibility not only because of inhomogeneous cultures but also due to large donor-to-donor differences. upcyte technologies has previously described the expansion of primary hepatocytes after lentiviral transduction (upcyte® hepatocytes) for large-scale production and their subsequent use in hepatotoxicity screenings [1]. However, upcyte® hepatocytes have previously not been tested for the expression of hepatobiliary transporters. Widely used hepatic cell lines lack drug transporter expression, making them unsuitable for the evaluation of possible interaction between investigational new molecular entities and drug transporters in early drug development. Therefore, functional expression of drug transporters in recently described upcyte® hepatocytes was investigated in comparison to primary human hepatocytes [2]. To address this, mRNA and protein levels of key hepatobiliary transporters of upcyte® and primary hepatocytes were quantified as well as the associated uptake function in 2D sandwich culture was investigated. As a result, upcyte® hepatocytes were found to exhibit key attributes of mature hepatic cells in long-term culture compared to primary hepatocytes. OATP2B1-mediated uptake of Rosuvastatin (rosuvastatin), NTCP-mediated uptake of Taurocholate (taurocholic acid) as well as OCT1-mediated uptake of MMP+ (1-methyl-4-phenylpyridinium) were relatively well-preserved in upcyte® hepatocytes. Additionally, functional AhR-, CAR-, and PXR- mediated P450 regulation was also retained in these expanded cells as well as functional epithelial polarization and bile flow. Furthermore, upcyte® hepatocytes in a 2D collagen/Matrigel sandwich configuration were able to restore membrane proteins, and exhibit considerable expression of OATP1B1, OATP2B1, NTCP, and OCT1 after 5–7 days [2]. In conclusion, it is suggested that upcyte® hepatocytes may serve as a good *in vitro* tool for drug-drug interactions and hepatotoxicity assessment in preclinical drug development due to their well-preserved drug transporters and the nature of its reproducible and standardized profile. Additionally, these cells could also be used in NTCP-, OATP2B1- and OCT1-mediated uptake studies as well as during intrinsic clearance determinations of slowly metabolized drugs.

References:

1. Levy, G. et al. Long-term culture and expansion of primary human hepatocytes. *Nature Biotechnology*, 1264-1271, 33(12), 2015.
2. Schaefer, M. et al. Quantitative Expression of Hepatobiliary Transporters and Functional Uptake of Substrates in Hepatic Two-Dimensional Sandwich Cultures: A Comparative Evaluation of Upcyte and Primary Human Hepatocytes. *Drug Metabolism and Disposition*, 166-177, 46(2), 2018.

P181 - A DIRECT COMPARISON OF ASSAY DETECTION METHODS FOR THE ASSESSMENT OF TRANSPORTER-MEDIATED DRUG INTERACTIONS

Rachel Sayer, Thomas Heeley, Scott Willox, John Kendrick, and Anthony Glazier
Covance Laboratories Limited

Transporters are membrane-bound proteins which facilitate the movement of substances across biological membranes. These transporters regulate the absorption, distribution and elimination of many xenobiotic compounds and may have clinically relevant effects on the pharmacokinetics of a compound, including the potential to cause drug-drug interactions. Regulatory agencies have issued guidance identifying P-gp, BCRP, OATP1B1, OATP1B3, OAT 1, OAT 3, OCT2 and more recently MATE 1 and MATE-2K as key transporters with potential clinical implications. The purpose of these investigations was to directly compare the benefits and limitations of the assay detection methods used in the assessment of a platform of regulatory recommended transporters.

To evaluate potential substrates or inhibitors of ABC efflux transporters, Caco 2 or C2BBE1 cells were plated onto transwell® permeable supports and the bidirectional permeability was measured. Probe substrates in the presence and absence of inhibitors were added to either the apical (A-B) or basolateral (B-A) compartments. Following incubation at 37°C, 5% CO₂ for 2 hours, aliquots were sampled for analysis by either liquid scintillation counting (LSC) or LC-MS. Digoxin and BCRP probe substrates produced efflux ratios >4 and this ratio was abolished to <1 in the presence of prototypical inhibitors. Mannitol and Caffeine were incubated concurrently as paracellular and transcellular permeability markers and produced P_{app} values of <1x10⁻⁶ cm/s and >20 x10⁻⁶cm/s respectively.

To evaluate potential substrates and inhibitors of SLC uptake transporters, Corning® HEK293 TransportoCells™ which transiently overexpress various human SLC transporters were plated onto 24-well poly-lysine coated plates. The novel "thaw and use" model of TransportoCells™ generates results within 48 hours of plating which permits rapid data delivery using LSC or LC-MS endpoints. Uptake assays were performed using probe substrates in the presence and absence of inhibitors and incubated for the required time followed by aspiration of the substrate and washing the cells with ice cold HBSS buffer. Aliquots of the cell lysates were sampled for analysis by LSC or LC-MS. The kinetic (K_m) parameters for the

SLC uptake transporter probe substrates Estrone-3-sulphate, Estradiol-17 β -glucuronide, p-aminohippuric acid, Metformin and Cholecystokinin, together with the IC₅₀ values for prototypical inhibitors were comparable with literature values. A comparison of both LSC and LC-MS detection methods indicated both analyses produce robust, reliable and reproducible results for investigating whether a compound is a substrate or inhibitor of a transporter. In conclusion, cell-based systems used in conjunction with appropriately selected detection methods for either radiolabelled or non-radiolabelled compounds are effective *in vitro* tools to assess the potential for drug interactions for a platform of clinically relevant transporters.

P182 - CHARACTERIZATION OF GCDC TRANSPORT BY HUMAN HEPATIC UPTAKE TRANSPORTERS FOR *IN VITRO* TESTING PURPOSES

Beata Toth, Zoltan Timar, Viktoria Velky, Zsuzsanna Gaborik, Emese Kis, Joseph Zolnerciks, and Peter Krajcsi
Solvo Biotechnology

Background information: Bile acids and bile salts (BAs/BSs) contribute in several physiological processes including signaling pathways, absorption of fat, or elimination of cholesterol. Primary bile acids and their conjugates are formed in the hepatocytes, then excreted into the bile. Bile is depleted in the intestine where bacterial dehydroxylation and unconjugation occur, and the majority of the bile salt species gets reabsorbed into the blood and circulates back to the liver. Giving their detergent nature, high concentration of BAs/BSs intracellularly or in the circulation system can lead to cytotoxicity. Therefore, testing the effect of drug candidates with high hepatic clearance on the transport of BAs/BSs is an issue of critical importance. The most commonly used probe substrate in *in vitro* test systems is taurocholate (TC), although the concentration of taurine-conjugated bile salts in human is two/three-fold lower than that of glycine-conjugated species, whereas taurine conjugation is the main modification in rats. Hypothesis: Using glycochenodeoxycholate (GCDC), one of the most relevant conjugated bile salt in human, as probe substrate in *in vitro* test systems might provide better prediction on the effect on enterohepatic circulation of bile salts. Methods: HEK293 cells transduced with OATP1B1 and OATP1B3, as well as NTCP expressing CHO and HEK293 cells were used in uptake assay format. Proof of concept (POC) experiments were carried out with radiolabeled TC and unlabeled GCDC, sulfated GCDC and chenodeoxycholate-sulfate (3S-CDC) at two concentrations and two timepoints. Results and conclusion: All bile salts were transported by OATP1B1 and 1B3 in a time- and concentration-dependent manner, while only TC and GCDC was picked up as substrates for NTCP. Since GCDC was efficiently transported by all three transporters, full transport characterization on OATP1B1, 1B3 and NTCP were conducted with tritiated TC and GCDC as probe substrates. Michaelis-Menten constants (Km) were around three-fold lower for GCDC than TC, showing higher affinity for that bile salt. Inhibitory effect of known substrates and inhibitors (atorvastatin, CCK8, diclofenac, pravastatin, telmisartan and troglitazone) on both probes was also tested. Based on the obtained data, and the higher *in vivo* relevance, the authors suggest replacing TC to GCDC for human *in vitro* test systems.

P183 - SIMULTANEOUS ASSESSMENT OF TRANSPORTER DRUG-DRUG INTERACTIONS USING A PROBE DRUG COCKTAIL IN CYNOMOLGUS MONKEY

Manthena Varma, Rachel Kosa, Sarah Lazzaro, Yi-an Bi, Chester Costales, David Rodrigues, and Larry Tremaine
Pfizer Inc.

On the basis of established evidences P-glycoprotein (P-gp), breast cancer resistance protein (BCRP), organic anion transporting polypeptides (OATPs), organic anion and cation transporters (OATs and OCTs) and Multidrug And Toxic Compound Extrusion (MATE) transporters are suggested to be of clinical relevance. We aim to establish an *in vivo* preclinical model to enable simultaneous assessment of inhibition potential of an investigational drug on these clinically relevant drug transporters. Pharmacokinetics of substrate cocktail consisting of pitavastatin (OATP1B substrate), rosuvastatin (OATP1B/BCRP/OAT3), sulfasalazine (BCRP) and talinolol (P-gp) were obtained in cynomolgus monkey—alone or in combination with transporter inhibitors, a single dose oral treatment of an OATP inhibitor (rifampicin), P-gp and BCRP inhibitor (elacridar) or OAT1/3 inhibitor (probenecid). *In vitro* transport (substrate and inhibition) studies were carried out using membrane vesicle systems and primary monkey and human hepatocytes to corroborate the interaction mechanisms. Single dose rifampicin (30 mg/kg) significantly ($p < 0.01$) increased the plasma exposure of all four drugs, with a marked effect on pitavastatin and rosuvastatin (AUC ratio ~34-43). Elacridar, BCRP/P-gp inhibitor, increased the AUC of sulfasalazine, talinolol, as well as rosuvastatin and pitavastatin. An OAT1/3 inhibitor (probenecid) significantly ($p < 0.05$) impacted the renal clearance of rosuvastatin (~8-fold). Unbound plasma concentrations of the inhibitor drugs are in the range of human levels reported with clinically recommended doses. *In vitro*, rifampicin (10 μ M) inhibited uptake of pitavastatin and rosuvastatin, but not others, by monkey and human primary hepatocytes. Transport studies using membrane vesicles suggested that all probe substrates, except talinolol, are transported by cynoBCRP; while talinolol is a cynoP-gp substrate. Elacridar and rifampicin inhibited both cynoBCRP and cynoP-gp *in vitro*, indicating potential for *in vivo* intestinal efflux inhibition. In conclusion, a probe substrate cocktail was validated to simultaneously evaluate perpetrator impact on multiple clinically relevant transporters using the cynomolgus monkey. The results support the use of the cynomolgus monkey as a model that could enable drug-drug interaction risk assessment, before advancing a new

molecular entity into clinical development, as well as providing mechanistic insights in support of *in vitro-in vivo* extrapolation exercises.

P184 - INHIBITION OF SOLUTE CARRIER (SLC) TRANSPORTER PROTEINS USING CORNING® TRANSPORTOCELLS™ FOR DDI ASSESSMENT

Guy Webber

ENVIGO

Solute-carrier (SLC) transporter proteins facilitate the uptake of anionic and cationic molecular species in mammalian tissues and organs. They are increasingly being implicated in pharmacokinetic drug-drug interactions (DDI) and regulatory authorities require an assessment to be undertaken on new drug candidates to inhibit these transporters. The SLC transporters currently listed by regulatory authorities for inhibition testing are: Organic Anion Transporter Proteins OATP1B1 and OATP1B3 (both liver), Organic Anion Transporters OAT1 (kidney) and OAT3 (kidney), Organic Cation Transporter OCT2 (Kidney) and Multi-Drug and Toxin Extrusion Proteins MATE1 (Liver) and MATE2-K (kidney). In addition to these, we have also included an assay for OCT1 which is often conducted if hepatic uptake of a cationic molecule is suspected. We have completed assay validations for these transporters to complete our DDI assessment programme using Corning® TransportoCells™ as the *in vitro* test system. These novel cells transfected with the transporter proteins were used to test known inhibitors of these transporters and IC₅₀ values for each transporter-substrate-inhibitor combination was determined at 37°C under cell culture conditions. Results obtained were: IC₅₀ values of: OATP1B1-mediated Estradiol 17β-glucuronide uptake vs Rifampicin IC₅₀ = 2.4 μM, OATP1B3-mediated Estradiol 17β-glucuronide uptake vs Rifampicin IC₅₀ = 0.95 μM, OAT1-mediated Tenofovir uptake vs Probenecid IC₅₀ = 4.8 μM, OAT3-mediated Estrone 3-sulfate uptake vs Probenecid IC₅₀ = 14.9 μM, OCT1-mediated Metformin uptake vs Quinidine IC₅₀ = 57 μM, OCT2-mediated Metformin uptake vs Quinidine IC₅₀ = 65 μM, MATE1-mediated uptake of Metformin uptake vs Pyrimethamine IC₅₀ = 57 μM, MATE2-K-mediated uptake of Metformin vs Pyrimethamine IC₅₀ = 35 μM.

P185 - TANSHINONE IIA REVERSES RIFAMPICIN-INDUCED LIVER INJURY VIA ACTIVATING NRF2-MEDIATED REGULATION OF HUMAN NTCP TRANSPORTER EXPRESSION

Yujie Yang, Xuehua Jiang, and Ling Wang

West China School of Pharmacy, Sichuan University

Rifampicin (RFP) is one of recommended drug for Tuberculosis (TB) by the World Health Organization (WHO). Owing to long duration of RFP therapy, adverse effects can not be ignored. However, the pathogenesis of RFP -induced liver injury (DILI) is complicated and treating DILI remains uncharacterized. One proposed mechanism of liver injury is inhibition of bile acid transport.

Na⁺/taurocholate cotransporter (NTCP, SLC10A1) is the major transporter of bile acids and is involved in the enterohepatic circulatory system through Na⁺-mediated bile acids reuptake from hepatic portal vein to hepatocytes. So inhibition of NTCP further destroys of the enterohepatic circulation, which has been hypothesized to play a role in the development of liver injury. We have demonstrated that RFP dramatically inhibited the mRNA and protein levels of NTCP in L02 cells. NTCP gene expression is regulated by some nuclear factors, involving Nuclear factor erythroid 2-related factor 2 (NRF2), which plays a major role in response to inflammatory damage and oxidative stress. In this study, we found one NRF2 binding site musculo-aponeurotic fibrosarcoma (Maf) recognition element (MARE) in human NTCP proximal promoter region using computer software analysis. Then we assessed whether NRF2 played a role in human NTCP expression and relied on the putative MARE. Tanshinone IIA (the main fat-soluble component of *Salvia miltiorrhiza*), is a potent activator of NRF2, and we demonstrated that TAN IIA increased NTCP mRNA and protein expression in human hepatocytes. What's more, NRF2 knockdown remarkably reduced the gene expression of NTCP using small interfering RNA (siRNA), and abrogated the significant induction of NTCP by TAN IIA. Human NTCP promoter luciferase reporter gene plasmid containing MARE motif was stimulated by NRF2. Interestingly, mutation of MARE motif completely eliminated NRF2-inducible promoter activity in NTCP promoter. As expected, chromatin immunoprecipitation assays also demonstrated that NRF2 was specifically recruited and bound to the MARE in the NTCP proximal promoter in L02 cells, compared with IgG. Besides, TAN IIA significantly increased the direct binding of NRF2 to the MARE motif. These results indicated that Nrf2 activation is mediated by the MARE in the NTCP promoter.

In summary, TAN IIA possesses the ability to reverse the inhibition of NTCP expression by RFP, which is possibly mediated via NRF2 activation, so pharmacological activation of NRF2 by TAN IIA may be beneficial for RFP -induced liver injury.

P186 - UP-REGULATION OF ATP-BINDING CASSETTE TRANSPORTERS IN THE PLACENTA DURING PRE-ECLAMPSIA AND THE POTENTIAL ROLE OF NRF2

Lu Yu, Xuehua Jiang, and Ling Wang
West China School of Pharmacy, Sichuan University

The placenta is the protective barrier between maternal and fetal circulation, and it prevents exposure of the fetus to maternally delivered toxins and xenobiotics. This important function of the placental barrier depends considerably on ATP-binding cassette (ABC) transporters, which allow efflux of substances across a concentration gradient. These essential components of the placental barrier, however, are altered under some disease, e.g. Preeclampsia (PE). Nuclear factor (erythroid-derived 2)-like 2 (Nrf2) is an antioxidant transcription factor that plays a crucial role in the induction of phase II antioxidant enzymes. Diverse studies provided subsequent evidence for the protective role of Nrf2 in PE via increased Nrf2 activity within cytotrophoblastic nuclei. Although Nrf2 often binds to the AREs of some ABC transporters genes, the correlation between Nrf2 and ABC transporters in the placenta under PE has not been investigated. We investigated changes in crucial ATP-binding cassette transporters in the placenta under PE and examined the correlation between Nrf2 and some ABC transporters. Fresh, term placental tissues were selected to measure the mRNA and protein expression levels of BCRP, MRP1, MRP2, MRP4, P-gp, and Nrf2. Cellular models of JEG-3, with or without NRF2 gene knockdown, were established to simulate the inflammatory condition of human preeclamptic placentas and to verify the presence of altered ATP-binding cassette transporters in clinical samples. Pearson's correlation coefficient was used to investigate the relationships between Nrf2 and these ABC transporters. The PE model was induced in mice using an ultra-low-dose injection of LPS. This model was also used to further confirm the results of the cellular models. Twelve fresh, term placentas were collected, including 6 from normal pregnancies and 6 from patients with PE. The transcriptional and translational levels of BCRP, MRP1, MRP2, MRP4, P-gp, and NRF2 in term placental tissues of the PE women were significantly increased compared to those in the healthy subjects' tissues. Cellular inflammation models and rodent models of PE exhibited similar results, but only the mRNA and protein expression levels of P-gp were highly correlated with Nrf2 in both models. The expression of some ABC transporters increased in term placentas under PE, suggesting a potential target for clinical therapy for mothers and fetuses. Nrf2 could be the main factor mediating the up-regulation of ABC transporters.

P187 - ASSOCIATION OF GLUTATHIONE S-TRANSFERASE GENES (GSTM1 AND GSTT1) WITH BLOOD LEAD LEVELS IN OCCUPATIONALLY LEAD-EXPOSED WORKERS

Himani¹, Sudip Datta², Jamal Akhtar Ansari³, Dilutpal Sharma³, Abbas Ali Mahdi³

¹SGT University, Gurgaon, ²All India Institute of Medical Sciences, ³KGMU, Lucknow

Polymorphisms in several genetic loci including glutathione S-transferase (GST) supergene family (GSTP1, GSTT1, GSTM1) are believed to alter the toxicokinetics and/or toxicodynamics of lead (1). This may potentially lead to accumulation of lead within the body. In this study we investigate the association of *GST-mu1* (*GSTM1*) and *GST-theta1* (*GSTT1*) insertion-deletion (InDel) gene polymorphisms with blood lead levels. For this cross-sectional study we recruited 100 adult males who were apparently healthy after informed consent. 50 of them occupationally exposed to lead as they worked in battery industry (OEx) and 50 not occupationally exposed (NOEx). Routine biochemical parameters were analyzed for screening along with serum vitamin D, calcium and phosphorous using Modular P biochemistry auto-analyzer (Roche diagnostics, USA). *GSTT1* and *GSTM1* gene polymorphisms were studied using multiplex polymerase chain reaction with *CYP1A1* as internal control. Blood lead levels (BLL) were determined using microwave digestion followed by estimation by inductively coupled plasma optical emission spectrometry (ICP-OES). Data was analyzed statistically using the GraphPad prism 5.0 software. The distribution of InDel polymorphisms did not reveal any significant differences in distribution between the OEx and NOEx groups. BLL were found to have non-gaussian distribution and hence were compared between the genotypes by Mann Whitney U test. *GSTT1*- genotypes were observed to have significantly higher BLL compared to *GSTT1*+ ($p=0.024$). However, *GSTM1* InDel polymorphisms did not reveal significant differences in contrary to a previous study (2). Besides no difference was observed in our subjects in vitD, Calcium and phosphates between the genotypic groups. Summarily, *GSTT1* null genotypes were found to be associated with significantly higher BLL.

References:

1. Ding N, Wang X, Weisskopf MG, Sparrow D, Schwartz J, Hu H, et al. Lead-Related Genetic Loci, Cumulative Lead Exposure and Incident Coronary Heart Disease: The Normative Aging Study. *PLoS One*. 2016;11(9):e0161472.
2. Kim JH, Lee K-H, Yoo DH, Kang D, Cho S-H, Hong Y-C. GSTM1 and TNF-alpha gene polymorphisms and relations between blood lead and inflammatory markers in a non-occupational population. *Mutat Res*. 2007 Apr 20;629(1):32-9.

- , Himani, P30, P141, P187
 Abaji, R., S16
 Abla, Nada, P156
 Abouda, Arsany, P21
 Abu-Yousif, Adnan, P3
 Adedoyin, Adedayo, P63
 Agrawal, Nancy, P54
 Ahn, Jin Hee, P48
 Ahn, Sunjoo, P48
 Akhtar, Jamal, P30
 Alam, Novera, P85, P90
 Albaugh, Daniel, P127
 Alcorn, Jane, P43
 Allain, Eric, P31
 Almond, Lisa, P156
 Almousa, Ahmed, P43, P142
 Amaike, Yuto, P99
 Amaral, Kirsten, P85, P90
 Amin, Jakal, P103
 Andersson, Tommy, S36
 Ando, Yasuhiko, P2
 Ansari, Jamal Akhtar, P187
 Aponick, Aaron, P131
 Aratsu, Yusuke, P73
 Arguelles, Nicole, P32
 Arman, Tarana, P151
 Armstrong, Lyle, P104
 Artursson, Per, Sc3.2
 Aslamkhan, Amy, P54
 Attar, Eyal, P160
 Audet-Delage, Yannick, P33
 Auger, Patrice, P63

 B Wadji, Fariba, A2
 Badwaik, Vivek, P36
 Bae, Myung Ae, P48
 Baghai Wadji, Fariba, P32
 Bailey, Wendy, P54
 Baillie, Tom, S19, P45
 Banerjee, Basu Dev, A10
 Banijamali, Ali, P118
 Bansal, Sumit, P81
 Barden, Timothy, P118
 Barlow, Deborah, P38
 Barnette, Dustyn, P119
 Barter, Zoe, P156
 Bartonkova, Iveta, P64, P69
 Basit, Abdul, P14
 Baumgardner, Matthew, P56
 Bedwell, David, P92
 Bender, Steve, P153
 Benet, Dr. Leslie Z., P12
 Benkovic, Goran, P19
 Benmaouche, Meriem, P121
 Berger, Scott, P148
 Bertin, John, P148
 Bhadra, Aritra, P27
 Bhatt, Deepak Kumar, A4, P14
 Bi, Yi-An, P164, P183
 Black, Christopher, P50
 Bleicher, Kimberly, P72

 Bojic, Mirza, P19
 Bolger, Michael, Sc3.4
 Bolla, Lavanya, P111
 Bolleddula, Jayaprakasam, P3, P120, P122
 Borel, Anthony, P92
 Bouaita, Belkacem, P28
 Bourgea, Joanne, P166
 Bow, Daniel, Sc1.2, P173
 Bowlin, Steve, P34
 Bowman, Christine, P89
 Bradbury, Margaret, S19
 Bradley, Jenifer, P59
 Brauer, Dana, P100
 Braun, Marie-Gabrielle, P56
 Bree, Françoise, P23
 Brockman, Adam, P98
 Brouwer, Kenneth, P50
 Brouwer, Kim, S4
 Brown, Colin, P104, P105
 Buchholz, Lisa, P36
 Buckley, David, P65, P78
 Bunger, Maureen, P14
 Buonadonna, Angela, P143
 Burrows, Jeremy, S40, P156
 Burt, Howard, Sc3.5

 Cabalu, Tamara, P54
 Caculitan, Niña G., S43
 Cai, Lining, P167
 Calafat, Antonia, P130
 Calhoun, Michael, P37
 Callegari, Ernesto, P15
 Callies, Sophie, P139
 Cancilla, Mark, S41
 Cao, Li, P53, P166
 Cao, Yanshan, P1
 Carlson, Timothy, P134
 Caron, Patrick, P31
 Carvalho, Andrew, P118
 Cassidy, Kenneth, P139
 Cecchin, Erika, P143
 Ceckova, Martina, P68, P165
 Cerveny, Lukas, P66, P68, P165, P169
 Chae, Jin Sil, P48
 Chan, Edwin H.Y., P62
 Chang, Jae, P55
 Chappell, Jill, P139
 Charman, Susan A., P156
 Chawla, Diwesh, A10
 Chen, Buyun, S43, P89
 Chen, Eugene, P89
 Chen, Hao, P120
 Chen, Jenny, P150
 Chen, Jie, P150
 Chen, John, P55
 Chen, Laigao, A6, P11
 Chen, Liangfu, P78
 Chen, Liuxi, P89
 Chen, Qing, P72

 Chen, Ron, P179
 Chen, Shiyong, P163
 Chen, Yan, P42
 Chen, Yuan, P89
 Chen, Yue, P160
 Cheong, Jonathan, P56
 Chesne, Christophe, P23, P28
 Chiou, William, P173
 Cho, Tiffany, A3
 Choi, Seon Hee, P46, P47, P88
 Choi, Tae Hyun, P39
 Choughule, Kanika, P80
 Chow, Timothy, A11
 Chowdhury, Swapam K., P3, P120, P122
 Chu, Xiaoyan, A6, P11, P168
 Chuh, Joseha, S43
 Chung, Git, P104
 Chung, Michael, P150
 Clark, Robert. J, P80
 Clarke, John, P151
 Coe, Kevin, P135
 Cohen, Lawrence H., P120
 Collinge, Mark, Sc4.1
 Colombo, Federico, P10
 Comstock, Kate, P42
 Connolly, Michael, P93, P116
 Cooper, Kirsten, P53, P166
 Costales, Chester, P183
 Couture, Felix, P143
 Cox, Kathleen, P54, P168
 Craft Reich, Sessaly, P16
 Cravatt, Benjamin, S46
 Creegan, Timothy, P82
 Crickard, Lindsay, P150
 Cui, Xiaoming, P153
 Cunico, Katherine, P55
 Currie, Mark, P118
 Czerwinski, Maciej, P20

 Daali, Youssef, P70, P157
 Dai, David, P160
 Dallas, Shannon, P65, P78, P102
 Daly, Ann, S7
 D'andrea, Mario, P143
 Dang, Lena, P119
 Danks, Anne, P150
 Darwich, Adam, P158
 Datta, Sudip Kumar, P30, P141, P187
 Daublain, Pierre, P54
 Davis, Mary, P119
 De Mattia, Elena, P143
 De Morais, Sonia, P173
 De Silva, Franklyn, P43
 Dearborn, Susan, P103
 Debiasio, Richard, P97
 Dekeyser, Josh, P65, P78
 Delannoy, Ines, P144
 Denny, Joshua, S9
 Desino, Kelly, P77
 Desmeules, Jules, P70, P157

- Di, Li, P136
Dickins, Maurice, P156
Dillon, Greg, P37
Ding, Caroline, P42
Dolezel, Petr, P6
Dragovich, Peter S., S21, P43
Driscoll, James P, P134
Driscoll, Monica, P35
Durbin, Kenneth, P173
Dvorak, Zdenek, P64, P69, P140
- Edgar, Kyle, P56
Einolf, Heidi, P65, P78
Ekena, Joanne, P16
El Gaaloul, Myriam, P156
Emami Riedmaier, Arian, P173
Ensom, Mary Hh, P146, P147
Ericsson, Hans, P162
Erpelinck, Steven, P114
Erpelinck, Steven L.A., P91
Evers, Raymond, P54, P149
Ewy, Bill, P20
- Fairman, Andrew, P106
Fan, Bin, P160
Fancourt, Craig, P63
Fantaneanu, Tadeu, S15
Fantegrossi, William, P29
Faux, Laura, P86
Fenton, Angie, P179
Ferguson, Stephen, Sc2.3
Fisher, Ciarán, Sc3.6
Fitzgerald, Maria, P78
Fogueri, Uma, P92
Fox, Lisa, P80
Fox-Bosetti, Sabrina, P63
Fraczkiewicz, Grazyna, Sc3.4
Friedman, Lori, P56
Fujita, Ken-Ichi, P171
Fujiwara, Ryoichi, P29
Fukuda, Takeshi, P159
Fung, Conrad, P78
- Gaborik, Zsuzsanna, P182
Gagné, Sébastien, P9
Gagné, V., S16
Galetin, Aleksandra, P158
Gan, Jinping, S26
Gao, Wei, P163
Gardner, Iain, Sc3.1
Gastecki, Michelle, P151
Gatineau, Eva, P20
Geib, Timon, P106
Germano, Peter, P118
Ghosh, Dipayan, P44, P45
Giacomini, Kathy, S37
Gijzen, Linda, P113
Gil Berglund, Eva, S32
Glaab, Warren, P54
Glazier, Anthony, P181
Glazier, Jocelyn D., P165
- Gobeau, Nathalie, P156
Goldstein, Keith, P92
Golonzhka, Olga, P37
Gonzales, Frank, A2
Goodman, Andrew, S30
Goosen, Theunis, P15, P65, P78
Gordon, Kacy, P35
Goto, Motohito, P2
Gough, Albert, P97
Grater, Richard., P37
Greenwood, Susan L., P165
Gregoire, Jean, P33
Griffiths, Thomas, P72
Grime, Ken, S31
Groessler, Todd, P153
Grollers, Mariska, P114
Gruber, Michaela, P31
Gu, Guibao, P150
Gu, Yi-Zhong, P168
Guengerich, F.Peter, P25
Guesmi, Amal, P121
Guillemette, Chantal, P31, P33, P143
Guillet, Fabrice, P28
- Hammer, Helen, P26
Hanan, Emily, P56
Hao, Ming-Hung, P10
Hariparsad, Niresh, S33, P65, P78
Harris, Phil, P148
Harris, Stephen, P41
Hartman, Jessica, P35
Hasan, Aya, P171
Hasegawa, Hiroshi, P133
Hatfield, Nicholas, P20
Haugabook, Sharie, P60
Hawsawai, Ahlam, P43
He, Kan, P167
Heeley, Thomas, P181
Heim, David, P49
Hein, David W, A7
Helen, Walker, P58
Hellriegel, Edward, S19
Henderson, Jeffrey, A3
Henson, Claire, P41
Heyward, Scott, A6, P11, P22, P137
Higuchi, Yuichiro, P79
Hilborn, Elizabeth, P96
Hiratsuka, Masahiro, P138
Ho, David, P85, P90, P94, P95
Ho, Thuy, P80
Hoffmann, Matthew, P71
Hofman, Jakub, P68
Hollenbaugh, Diane, S1
Hop, Cornelis E. C. A., S21, S43, A6, A11, P11
Hosaka, Takuomi, P76, P99
Hosea, Natalie, P179
Houle, Robert, P168
Houseknecht, Karen, P38
Hu, Yue, P62
Hughes, Emma, P60
- Hui, Yu-Hua, P123
Humphreys, W. Griffith, A6, P11, P126
Hussner, Janine, P175, P176
- Ikemura, Noriaki, P84
Illes, Peter, P140
Im, So Hee, P48
Imawaka, Haruo, P159
Imperio, Jose, P55
Inoue, Makoto, P178
Isbell, John, P153
Ishigai, Masaki, P5, P74
Issa, Ali, P175
Ito, Shinya, S12
Iwamoto, Marian, P63
Iyer, Ramaswamy, P126
Izumi, Saki, A12
- Jackson, Jonathan, P50
Jackson, Klarissa, P21
Jacob, Lisa, P82
Jaligama, Shreelekha, P27
James, Margaret, P86
Janzén, David, P162
Jaochico, Allan, P56
Jee, Alison, P101
Jenkins, Gary, P173
Jeon, Yong Hyun, P46, P47, P88
Jerath, Angela, P155
Jia, Lily, P130
Jia, Yong, P153
Jian, Wenying, S44
Jiang, Xuehua, P185, P186
Jiraskova, Lucie, P165, P169
Jiskrova, Eva, P69
Johannssen, Timo, P100, P180
Johnson, Debra L., P93, P116
Johnson, Timothy, P54, P72
Jones, Barry, P65
Jonker, Derek, P143
Joore, Jos, P113
Joos, Thomas O, P26
Ju, Cynthia, Sc4.3
Juhasz, Viktoria, P11
- Kamali, Afrand, P3
Kamel, Amin, P34
Kamijo, Shinobu, P84
Kanda, Katsuhiko, P107
Kanebratt, Kajsa, P162
Kaneko, Chisa, P170
Kang, Joo Hyun, P39
Kang, Wen, P72
Kano, Makoto, P99
Kapadnis, Sudarshan, P112
Karahoda, Rona, P165
Karb, Mike, P108
Karbanova, Sara, P66, P165, P169
Karunanand, Busi, P30
Kato, Motohiro, P74

- Kato, Suguru, P122
 Kato, Yukio, P171
 Katyayan, Kishore, P123
 Kawai, Kumi, P178
 Kawasaki, Tatsuya, P170, P172, P178
 Kay, Jared, P174
 Kazmi, Faraz, P102
 Ke, Alice, P160
 Kelly, Edward J., S25
 Kendrick, John, P181
 Kennedy, Mark, P93, P116
 Kenny, Jane, Sc2.4, P65, P78
 Khaniya, Bina, P93, P116
 Khojasteh, S. Cyrus, S21, P43
 Kiang, Tony Kl, P145, P146, P147
 Kikuchi, Ryota, P173
 Kim, Byoung Soo, P39
 Kim, Dongkyu, P47
 Kim, Geum Ran, P48
 Kim, Hyoung Rae, P48
 Kim, Kil Soo, P47
 Kim, Phiho, P48
 Kim, Sang Kyoong, P46, P47, P88
 Kim, Seong Soon, P48
 Kim-Kang, Heasook, P49
 King, Kristopher, P37
 King, Tamara, P38
 Kis, Emese, P182
 Klatt, Nichole, S29
 Klein, Kathrin, P26
 Klett, Maren, P100
 Knemeyer, Ian, P72
 Kobayashi, Chinatsu, P84
 Koeplinger, Kenneth, P168
 Kogayu, Motohiro, P73
 Koh, Woo Suk, P47
 Komori, Takafumi, A12
 Koneti, Geervani, P44, P45, P51, P52
 Konrath, Kylie M., P60
 Korpala, Manav, P10
 Kortagere, Sandhya, P69
 Kosa, Rachel, P183
 Koudriakova, Tatiana, P135
 Kozak, Kathy, S43
 Kozminski, Kirk, P34, P137
 Krajcsi, Peter, P182
 Krajinovic, Maja, S16
 Krol, Edward, P128
 Kubota, Yutaru, P171
 Kucera, Radim, P68
 Kuhls, Matthew, P72
 Kumar, Amit, P141
 Kumar, Raman, P30
 Kumar, Vineet, A6, P11
 Kuramoto, Shino, P74
 Kurek, Dorota, P109
 Kusano, Kazutomi, P13
 Kustermann, Stefan, P109
 Kusuhara, Hiroyuki, S38, A12
 Kwan, Kin Ming, P62
 Labriet, Adrien, P143
 Ladumor, Mayurbhai Kathadbhai, A4
 Lahiri, Sujoy, P93, P116
 Lai, Weidong, P124
 Lai, Yurong, Sc1.1, A6, P11
 Lanz, Henriette, P109, P113
 Lapham, Kimberly, P15
 Laranjeiro, Ricardo, P35
 Lasker, Jerome, P94
 Lau, Aik Jiang, A8, P81
 Laverdière, C., S16
 Laws, George, P72
 Lazzaro, Sarah, P183
 Le, Kha, P160
 Le, Trang, P31
 Leal, Mauricio, S23
 Lebron, Jose, P72
 Leclerc, J.M., S16
 Lecluyse, Edward, S34
 Lee, Byung Hoi, P48
 Lee, Deborah, P127
 Lee, Dong, Sc4.2
 Lee, Kyeong-Ryoon, P48
 Lee, Yu-Ri, P48
 Leitz, Sara, P127
 Lelais, Gerald, P153
 Lennernäs, Hans, P162
 Lépine, Maggy, P9
 Lerman, Caryn, A5
 Lesage, Jacques, P9
 Leslie, Elaine, S5
 Lesniak, Paul, P77
 Lester, Cathy, P108
 Levesque, Eric, P31, P143
 Lewia, Allison, P103
 Li, Albert P., P75, P85, P90, P94, P95
 Li, Chun, P153
 Li, Feng, P53
 Li, Jie, P153
 Li, Linhao, P22
 Li, Ruoya, P28
 Li, Wenying, P126
 Li, Yu-Wen, P150
 Li, Zhihui, P22
 Liang, Xiaorong, P89
 Liao, Mingxiang, A6, P11
 Lin, Ge, P125
 Lin, Jian, P15
 Liu, Fang, P63
 Liu, Ning, P56
 Liu-Kreyche, Peggy, P126
 Loretz, Carol, P85, P94, P95
 Lowman, John, P109, P110
 Luethcke, Katherine Ros, P16
 Lukacova, Viera, Sc3.4
 Lundahl, Anna, P162
 Luo, Gang, P127
 Luo, Lina, P174
 Ly, Justin, P55
 Lynch, Donna, P54
 Ma, Junli, P173
 Ma, Li, P126
 Ma, Mingming, P36
 Ma, Shuguang, P42, P56
 Ma, Yong, S21, P43
 Macha, Sreeraj, P63
 Machotka, Sam, P54
 Mackowiak, Bryan, P22
 Maeda, Kazuya, A12
 Mahajan, Mukesh, P148
 Mahajan, Sandeep, P141
 Mahdi, Abbas Ali, P30, P187
 Mahony, Catherine, P108
 Malagnino, Vanessa, P175, P176
 Males, Zeljan, P19
 Mani, Sridhar, P69
 Mann, Sarah, P16
 Mao, Jialin, P89
 Marantz, Yael, S19
 Marinis, Jill, P148
 Marquis, Robert, P148
 Marsh, Donald, P72
 Marsousi, Niloufar, P157
 Martin, Solenne, P23
 Martineau, Mitchell, P17
 Masereeuw, Rosalinde, S3
 Masferrer, Jaime, P118
 Masuo, Yusuke, P171
 Mathialagan, Sumathy, P164
 Mathias, Anita, A6, P11
 Matsuda, Akihiro, P133
 Matsunaga, Norikazu, P158, P159
 Mayo, Patrick, P146
 Mccrea, Jacqueline, P63
 Mckenzie, Donald, P127
 Mei, Hong, P149
 Menzel, Karsten, P63
 Meyer, Joel, P35
 Meyer Zu Schwabedissen, Henriette, P175, P176
 Michelle, Whirl-Carillo, S10
 Miksys, Sharon, A2, P32
 Milan-Segovia, Rosa C, A7
 Miller, Grover, P119
 Miller, Randall, P149
 Miller, Randy, P54
 Milne, Todd, P118
 Mirzac, Angela, P63
 Mitchell, Walter, P85
 Mitra, Kaushik, P54, P72
 Miyake, Taiji, P5
 Miyata, Yoshinari, P122
 Mizuno, Kunihiko, P24
 Mlejnek, Petr, P6
 Moehrle, Joerg, P156
 Mohutsky, Michael, P65, P78, P92
 Moisan, Annie, P109
 Moniz, George, P124
 Monroe, James, P54, P72
 More, Vijay, P177
 Morita, Kenji, P73

- Moseley, Caroline, P50
Motyl, Katherine, P38
Moulton, Richard, P92, P139
Mullin, Jim, Sc3.4
Murayama, Norie, P25
- Nabekura, Tomohiro, P170, P172, P178
Nagai, Mika, P76
Nagano, Aiko, P133
Nagy, Nikolett, P180
Nakakariya, Masanori, P179
Nakakuki, Komei, P138
Nakanishi, Ryosuke, P170
Nakashima, Ken-Ichi, P178
Nanjappan, Satheeshkumar, P111
Naumovska, Elena, P109
Negishi, Masahiko, Sc2.2
Neuberg, D., S16
Ng, Yvonne Wan Xin, A8
Nguyen, Truyen, P54
Nicholds, Mike, P104
Nicolas, Arnaud, P109
Nicoll-Griffith, Deborah, P54
Niosi, Mark, P15
Nix, Darrel, P10
Noerenberg, Astrid, P100, P180
Noh, Keumhan, A9, P144
Nomura, Naoki, P172
Nomura, Yukihiko, P73
Nooijen, Irene H.G., P91, P114
Novalen, Maria, P32
Nozaki, Yoshitane, A12
Nulick, Kelly, P65
Nwabufo, Chukwunonso, P128
Nyagode, Beatrice, P108
- O'Brien, Molly, P20
Obach, Ronald Scott, P114
Oberheide, Brian, P20
Obringer, Cindy, P108
Offringa, Emma, P91
Ogilvie, Brian, P20
Ogungbenro, Kayode, P158
Ohlund, Leanne, P121
Ohmori, Shigeru, P84
Ohnishi, Shuichi, P133
Orozco, Christine, P15
O'shea, Morgan, P10
- Pacchione, Stephen, P54, P72
Paine, Mary, P151
Palamanda, Jairam, P54, P65
Palandra, Joe, S42
Palmer, Matthew, P50
Pan, Rui Sophie, P144
Panebianco, Deborah, P63
Pang, Jodie, P55, P56
Pang, K. Sandy, A9, P144, P155
Parikh, Sweta, P53, P166
Patel, Gaurang, P103
- Patilea-Vrana, Gabriela, A1, P129
Pearson, Kara, P177
Peng, Annie R., A5
Peng, Hao Benson, P144
Penketh, Sara, P115
Perrine-Faller, Susan, P60
Phipps, Colin, S22
Pietrasiewicz, Alicia, P112
Pillow, Thomas H., S21, P43
Pippert, Todd, P54
Piquette-Miller, Micheline, S13
Plante, Marie, P33
Plesa, M., S16
Plise, Emile, P56
Plourde, David, P103
Podtelezhnikov, Alexei, P54, P72
Polson, Andrew G., S21, P43
Portales-Perez, Diana P, A7
Pötz, Oliver, P26
Poulin, Dominic, P57
Powell, Francoise, P103
Prajapati, Sudeep, P10
Prakash, Chandra, P160
Prasad, Bhagwat, A4, P14, P87, P161
Prather, Paul, P29
Preau, James, P130
Prieto Garcia, Luna, P162
Proctor, William, S27
Profy, Albert, P118
Ptackova, Zuzana, P165, P169
Pusalkar, Sandeep, P120
- Qian, Emily, P167
Qiu, Jiabin, S18
Quach, Holly P., A9
- Raccor, Brianne, P27
Radomska-Pandya, Anna, P29
Raizada, Alpana, A10
Ralston-Hooper, Kimberly, P36
Ramamurthi, Narayanan, P44, P45, P51, P52
Ramanathan, Ragu, P174
Ramsden, Diane, P65, P78, P80
Reddy, Guru, P127
Reilly, Michael, P148
Reinen, Jelle, P67
Ren, Jia, P89
Ribadeneira, Maria, P118
Richardson, Vicki, P96
Richards-Peterson, Lauren, P148
Rioux, Nathalie, P10
Rodrigues, A. David, P164, P174, P183
Roe, Amy, P108
Rondel, Karine, P28
Rong, Haojing, P132
Rong, Yan, P145, P146, P147
Rooney, Michael, P37
Ross, Colin, S17
Roth, Adrian, P109
- Routier, Sylvain, P23
Rowbottom, Christopher, A6, P11, P37, P112
Rowland-Yeo, Karen, P156
Roychowdhury, Shantanu, P8, P17
Ruzickova, Eliska, P6
- Sacco, James, P16
Sadowsky, Jack D., S21, P43
Sakurai, Yuji, P5
Salazar-Gonzalez, Raul A., A7
Saldiva, Victor, P144
Saleh, Anthony, P97, P113
Sallan, S.E., S16
Salphati, Laurent, A6, P11, P56
Samadfam, Rana, P57
Samandar, Ella, P130
Samer, Caroline, P157
Sansoucy, Maxime, P18
Santora, Vinny, P150
Sasaki, Takamitsu, P99, P171
Satonin, Darlene, P139
Satsukawa, Masahiro, P76
Sayer, Rachel, P181
Schicker, Michael, P127
Schmidt, Felix, P26
Schmidt, Stephen, P56
Schnoll, Robert, A5
Schober, Andreas, P100
Scholes, Peter, P58
Schuren, Frank, P114
Scott, Trevor, P150
Sedarati, Farhad, P120
Seib, Christopher, P20
Seibert, Isabell, P176
Sekiguchi, Kazutaka, P133
Sensenhauser, Carlo, P102
Serson, Sylvia, P144
Shadid, Mohammad, P3
Shah, Abhi, P3, P122
Shah, Dhaval, S20
Shapiro, Michael, P153
Sharma, Anup, P97
Sharma, Ashwani, P23, P28
Sharma, Dilutpal, P30, P187
Sharma, Raman, P15
Sharma, Seema, P42
Shaw, Iain, P58
Sheldon, Adrian, P103
Shen, Hong, S39
Sherwood, David, P35
Shi, Qin, P167
Shimizu, Mai, P73
Shimizu, Makiko, P138
Shin, Dae-Seop, P48
Shindoh, Hidetoshi, P74
Shizu, Ryota, P99
Shuldiner, Alan, S8
Siddarth, Manushi, A10
Sierra, Teresa, P59, P98
Sikka, Meera, A10

- Silva, Manori, P130
 Silverman, L.B., S16
 Simonyan, David, P31, P143
 Singh, Archana, P141
 Singh, Ritu, P82
 Singh, Saranjit, A4
 Singleton, Marc D., P60
 Sinnott, D., S16
 Sinz, Michael, Sc2.1
 Sistare, Frank D., P54, P72, P168
 Siu, Amy, P65, P78, P124
 Skoupa, Nikola, P6
 Slatter, Greg, S48
 Sleno, Lekha, P9, P106, P121
 Smeltz, Marci, P86
 Smit, Martijn, P67
 Smith, Dennis, S2
 Smith, Latasha, P35
 Smith, Mike, P3
 Smith, Peter, P10
 Smith, Sherri, P10
 Sodhi, Jasleen K., P12
 Song, Ivy, P132
 Song, Jin Sook, P48
 Song, Kyung, P56
 Sorf, Ales, P68
 Spencer, Elizabeth, P40
 Speulman, Angelique E.A.M., P91, P114
 Spijkers, Xandor, P110
 Squirewell, Edwin, P86
 Srivastava, Pratima, P111
 Staben, Steve, P56
 Stacpoole, Peter, P86, P131
 Stamler, David, S19
 Stauber, Kathe, P150
 Staud, Frantisek, P66, P68, P165, P169
 Stepankova, Martina, P69
 Stevens, Lianne, P114
 Stevens, Lianne J., P91
 Stocco, Marlaina, A2
 Stoffolano, Peter, P108
 Storelli, Flavia, P70
 Strasser, Joseph, P96
 Stresser, David, P77
 Strock, Christopher, P59, P98
 Su, Dian, S21, P43
 Su, Ming, P72
 Suemizu, Hiroshi, P2, P79
 Sugiyama, Yuichi, Sc1.3, A12
 Sun, Jun, P77
 Sun, Kefeng, P132
 Surapaneni, Sekhar, P71
 Surendradoss, Jayakumar, P92
 Swamidass, S. Joshua, P119
 Tabatabaei, Ali, P150
 Takahashi, Riichi, P2
 Taniguchi, Toshio, P73
 Tanis, Keith, P54, P72
 Taunton, Jack, S47
 Taylor, D. Lansing, S24, P97
 Teo, Josephine Si Min, P81
 Thakkar, Himani, P141
 Thomas, Jennifer, P57, P67
 Thomas, Kevin, P8, P17
 Thomas, Steven, P148
 Tieberg, Deborah K., P93, P116
 Timar, Zoltan, P182
 Toffoli, Giuseppe, P143
 Tolledo, Edgor Cole, A2
 Tomek, Charles, P63
 Tomic, Sinisa, P19
 Tompkins, Celin, P153
 Tompson, Debbie, P148
 Tong, Zeen, P71
 Toscan, Anja, P144
 Tóth, Beáta, P11, P182
 Tremaine, Larry, P183
 Trepanier, Lauren, P16
 Trietsch, Sebastiaan, P109, P110, P113
 Trisdale, Sarah, P80
 Troutman, John, P108
 Trullinger, Tony, P36
 Tsuruta, Satoshi, P99
 Tuntland, Tove, P153
 Turcotte, Veronique, P31
 Turijan-Espinoza, Eneida, A7
 Turnbaugh, Peter, S28
 Tweedie, Donald, P65, P78
 Tyndale, Rachel F., A2, A5, P32
 Uehara, Shotaro, P2, P79
 Utrecht, Jack, A3, P1, P101
 Unadkat, Jashvant, S14, A1, A6, P11, P129
 Uwai, Yuichi, P170, P172, P178
 Vaes, Wouter H.J., P91, P114
 Vaillancourt, Mei-Ting, P153
 Van De Steeg, Evita, P91, P114
 Van Der Plaats, Arjan, P91
 Van Koppen, Arianne, P91
 Van Vught, Remko, P109, P110, P113
 Vanura, Katrina, P31
 Varma, Manthena, Sc3.3, P164, P183
 Veizaj, Elvana, P112
 Velky, Viktoria, P182
 Venkatakrisnan, Karthik, P120
 Venzl, Karin, P31
 Vernetti, Lawrence, P97
 Villeneuve, Lyne, P33, P143
 Vivian, Jef, P150
 Vormann, Marianne, P113
 Vrana, Marc, P87
 Vrzal, Radim, P69
 Vulto, Paul, P97, P109, P110, P113
 Wakefield, James, P118
 Walker, Gregory, P114
 Walsky, Robert, P78
 Walton, Patty, P103
 Wang, Amy Q., P60
 Wang, Evan, S18
 Wang, Hongbing, P22
 Wang, Jie, P166
 Wang, John, P10
 Wang, Kai, P135
 Wang, Ling, P185
 Wang, Ling, P186
 Wang, Peter, P61
 Wang, Qianwen, P62
 Wang, Shuai, S43
 Wang, Ying-Hong, P163
 Wang, Zhibin, P72
 Wąowicz, Marcin, P155
 Warmuth, Markus, P10
 Watari, Ryosuke, P133
 Watari, Ryuji, P13
 Webber, Guy, P83, P115, P184
 Webster, Yue, S18
 Wehmeyer, Ken, P108
 Welty, Devin, P132
 Wenker, Mira, P67
 Wesche, David, P156
 Westlin, William, S11
 Wevers, Nienke, P110
 Wheeler, Jennifer, Sc4.4
 Whicke, Andrew, P41
 Wierk, Antonia, A3
 Willox, Scott, P181
 Willy, Jeffrey, S18
 Wilschut, Karlijn, P97, P109, P110
 Wilson, Derek, P106
 Wines, Kahari, P21
 Wisniewski, Jessica, P122
 Witek, Rafal, P93, P116
 Wong, Chun-Ho, P62
 Wong, Harvey, A11
 Wong, Siew Ying, A8
 Wong, Simon, P65
 Woo, Jae Chun, P48
 Woolf, Thomas, P167
 Wright, Matthew R., A11, P89
 Wu, Jiejun, P135
 Wyglinski, Joanne, P59
 Xia, Cindy, P3
 Xiao, Guangqing, A6, P11
 Xu, Xin, P60
 Yadav, Aprajita, P134
 Yamamoto, Masafumi, P2
 Yamaori, Satoshi, P84
 Yamazaki, Hiroshi, P25, P79, P138
 Yang, Hua, P160
 Yang, Jung Yoon, P48
 Yang, Li, P179
 Yang, Mengbi, P125
 Yang, Qi Joy, A9, P155

Yang, Qian, P85	Yoshinari, Kouichi, P76, P99	Zhao, Jianwei, P61
Yang, Xiaolei, P43	Yu, Lu, P186	Zhao, Ping, S35
Yang, Yujie, P185	Yu, Robert, P124	Zhao, Tian, P63
Yarbrough, Azure, P29	Yu, Shang-Fan, S21, P43	Zhou, Lian, P139
Yates, Phillip, P65	Yun, Chang Soo, P48	Zhou, Xiao, P36
Ye, Qing, P61		Zhou, Xiaofei, P120
Ye, Xiaoyun, P130	Zamek-Glisczynski, Maciej J., Sc1.4	Zhu, Xiaochun/Sean, P49
Yerramilli, Usha, P71	Zanger, Ulrich M, P26	Zientek, Michael, P24, P137
Yi, Ping, P139	Zhang, David, P148	Zimmer, Daniel, P118
Yiannikouris, Frederique, P20	Zhang, Donglu, S21, P43	Zolnerciks, Joseph, P182
Yoda, Hiromi, P138	Zhang, George, P65, P78, P80, P82	Zook, Doug, P150
Yoneda, Nao, P2, P79	Zhang, Haeyoung, P14	Zuo, Rongjun, P53, P166
Yoon, Doo Hyun, P39	Zhang, Shu, P89	Zuo, Zhong, P62
Yoshimaru, Shohei, P99	Zhao, Bin, A2	

- ACYL GLUCURONIDE, P135
ADME, P49
ADVERSE DRUG REACTIONS, P1
ANIMAL MODEL, P2
ANTIBODY DRUG CONJUGATES (ADCS), S21, S43, P3

BIOAVAILABILITY, SC3.2, P5, P6, P8
BIOLOGICAL MONITORING, BIOMARKER, MASS SPECTROMETRY, P9
BLOOD LEAD, P187
BONE MARROW, P38

CATABOLISM, P3
CERENKOV LUMINESCENT IMAGING, P88
CHEMICAL DERIVATIZATION, P135
CLEARANCE PREDICTION, A1, P10, P11, P12, P13, P14, P28, P91, P139
CONJUGATION REACTIONS AND ENZYMES, A8, P10, P15, P16, P17, P18, P121, P127
CRISPR/CAS9, S18
CRUSHED GOLD SHELLS, P88
CYTOCHROME P450, S36, A2, P19, P20, P21, P22, P23, P24, P25, P26, P27, P28, P29, P32, P67, P70, P74, P78, P81, P84, P94, P119

DIFFERENCES IN METABOLISM (SPECIES, GENDER, AGE, DISEASES), S15, A9, P20, P30, P31, P32, P33, P34, P35, P36, P37, P122, P126, P133, P155, P161
DISPOSITION, S2, S5, A4, P38, P39, P40, P41, P55, P118, P129, P144, P169, P171, P174
DRIED BLOOD SPOT, P123
DRUG DISCOVERY AND DEVELOPMENT, SC4.1, SC4.2, S2, S11, S19, S23, S27, S40, S45, S47, S48, P15, P39, P41, P42, P43, P44, P45, P46, P47, P48, P49, P50, P51, P52, P53, P54, P55, P56, P57, P58, P59, P60, P61, P62, P63, P72, P76, P109, P110, P116, P128, P136
DRUG INTERACTION, SC2.1, S3, S29, S31, S32, S36, S38, S39, A1, A3, P2, P63, P64, P65, P66, P67, P68, P69, P70, P71, P77, P83, P111, P113, P120, P147, P156, P160, P162, P163, P165, P170, P172, P178, P183, P184
DRUG-INDUCED LIVER INJURY, SC4.3, P72

ENVIRONMENTAL POLLUTANTS, A10

ENZYMES
ENZYME INDUCTION, SC2.1, SC2.2, SC2.3, SC2.4, S31, S32, S33, S34, S35, P22, P25, P26, P64, P69, P73, P79, P80
ENZYME INHIBITION/INACTIVATION, S45, S47, A2, A7, A8, P81, P82, P83, P84, P86, P92, P134
EXPOSURE ASSESSMENT, P130
EXTRAHEPATIC METABOLISM, S30, P27, P85, P86, P87, P137

GOLD NANOPARTICLES, P88

HEPATIC UPTAKE, P89, P90, P91, P96, P149, P176, P177, P180
HEPATOCYTES, SC2.2, SC2.3, A3, P53, P79, P90, P92, P93, P94, P95, P96, P97, P98, P99, P102, P107, P164, P167, P185
HEPATOTOXICITY, P100

IMMUNOLOGY, SC4.3
IMMUNO-ONCOLOGY, S1
IMMUNOTOXICOLOGY, SC4.1, SC4.4, P101
IN SILICO, P23, P44, P45, P51, P52
IN VITRO IN VIVO EXTRAPOLATION (IVIVE), SC1.3, SC3.1, SC3.3, SC3.4, SC3.5, SC3.6, A6, A10, A12, P12, P14, P36, P80, P102, P112, P173
IN VITRO TECHNIQUES, SC3.1, S27, P13, P75, P82, P85, P97, P103, P104, P105, P106, P107, P108, P109, P110, P111, P112, P113, P114, P115, P116, P181

KIDNEY FIBROSIS, A10

LC-MS, P135
LIVER SINUSOIDAL ENDOTHELIAL CELLS, P100

MASS SPECTROMETRY, P61
MEDICATION ADHERENCE, A5
METABOLISM, S26, S41, S44, P1, P17, P19, P24, P29, P31, P35, P42, P43, P95, P103, P114, P115, P118, P119, P120, P121, P123, P124, P125, P126, P127, P128, P129, P130, P131, P132, P133, P134, P148
METABOLISM-INDUCED HEPATOTOXICITY, P125
METABOLITE IDENTIFICATION, P135
MILD CONDITIONS, P135
MS IMAGING, P47

NON-P450 PHASE I ENZYMES, A4, P18, P34, P87, P136, P137, P138, P139
NUCLEAR MEDICINE IMAGING, P88
NUCLEAR RECEPTORS, P99, P140

ORGANS-ON-CHIPS, S25

PASSIVE TARGETING, P88
PEPTIDE, S41
PESTICIDES AND RENAL CLEARANCE, P141
PHARMACOGENETICS, S7, S8, S9, S10, S16, S17, S28, A5, A7, P16, P21, P142, P143
PHARMACOKINETIC PREDICTION, SC3.6, S4, S20, S22, P37, P48, P144, P145, P146, P147, P148, P149, P153, P158, P159
PHARMACOKINETICS AND PHARMACODYNAMICS, S12, S23, S40, S42, S48, P60, P104, P105, P150, P151, P153, P155
PHYSIOLOGICALLY-BASED PHARMACOKINETIC (PBPK), SC3.4, S14, A11, P6, P89, P156, P157, P158, P159, P160, P161, P162, P163
PRECLINICAL RISK ASSESSMENT, P54
PREGNANCY AND EPILEPSY, S15
PROTEIN BIOTRANSFORMATION, S44
PROTEOMICS, S46
PYRROLIZIDINE ALKALOIDS, P108

RADIOACTIVE IODINE-124, P88
REACTIVE INTERMEDIATE, P124
RENAL TRANSPORTERS INHIBITION, P168

SPHEROID, 3D, P93

TOXICITY, SC4.2
TOXICOGENOMICS, S18
TRACER, P150
TRANSPORTERS, SC1.1, SC1.2, SC1.3, SC1.4, S3, S4, S5, S13, S37, S38, S39, A6, A9, A12, P5, P8, P11, P46, P50, P62, P66, P68, P71, P132, P142, P151, P164, P165, P166, P167, P168, P169, P170, P171, P172, P173, P174, P175, P176, P177, P178, P179, P180, P181,
TUMOR IMAGING, P88

VOLUME PREDICTION, S24

XENOBIOTIC METABOLISING ENZYME POLYMORPHISM, P187

